RICE UNIVERSITY

Harmonic Wavelets Procedures and Wiener Path Integral Methods for Response Determination and Reliability Assessment of Nonlinear Systems/Structures

by

Ioannis A. Kougioumtzoglou

A THESIS SUBMITTED
IN PARTIAL FULFILLMENT OF THE
REQUIREMENTS FOR THE DEGREE

Doctor of Philosophy

APPROVED, THESIS COMMITTEE:

Pol D. Spanos, L. B. Ryon Professor
of Mechanical Eng. and Civil Eng.

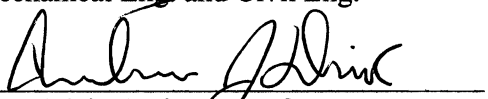

Andrew Dick, Assistant Professor
Mechanical Eng. and Materials Science

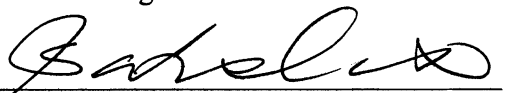

Satish Nagarajaiah, Professor
Civil Eng. and Mechanical Eng.

Ilinca Stanciulescu, Assistant Professor
Civil and Environmental Eng.

Houston, Texas
May, 2011

Abstract

Harmonic Wavelets Procedures and Wiener Path Integral Methods for Response Determination and Reliability Assessment of Nonlinear Systems/Structures

by

Ioannis A. Kougioumtzoglou

In this thesis a novel approximate/analytical approach based on the concepts of stochastic averaging and of statistical linearization is developed for the response determination of nonlinear/hysteretic multi-degree-of-freedom (MDOF) systems subject to evolutionary stochastic excitation. The significant advantage of the approach relates to the fact that it is readily applicable for excitations possessing even non-separable evolutionary power spectra (EPS) circumventing ad hoc pre-filtering and pre-processing excitation treatments associated with existing alternative schemes of linearization. Further, the approach can be used, in a rather straightforward manner, in conjunction with recently developed design spectrum based analyses for obtaining peak response estimates without resorting to numerical integration of the nonlinear equations of motion.

Furthermore, a novel approximate/analytical Wiener path integral based solution (PIS) is developed and a numerical PIS approach is extended to determine the response and first-passage probability density functions (PDFs) of nonlinear/hysteretic systems subject to evolutionary stochastic excitation.

Applications include the versatile Preisach hysteretic model, recently applied in modeling systems equipped with smart material (shape memory alloys) devices used for seismic hazard risk mitigation. The approach is also applied to determine the capsizing probability of a ship, whose rolling dynamics is captured by a softening Duffing oscillator.

Finally, novel harmonic wavelets based joint time-frequency response analysis and identification approaches are developed capable of determining the time-varying frequency content of non-stationary complex stochastic phenomena encountered in engineering applications. Specifically, a harmonic wavelets based statistical linearization approach is developed to determine the EPS of the response of nonlinear/hysteretic systems subject to stochastic excitation. In a similar context, an identification approach for nonlinear time-variant systems based on the localization properties of the harmonic wavelet transform is also developed. It can be construed as a generalization of the well established reverse multiple-input/single-output (MISO) spectral identification approach to account for non-stationary inputs and time-varying system parameters. Several linear and nonlinear time-variant systems are used to demonstrate the reliability of the approach.

Acknowledgements

There are those advisors who pre-determine the research topic for their students, depriving them of the pleasure of creativity. And, there are those who guide their students into conducting trivial research, depriving them of the pleasure of originality. And then there is *Professor Pol D. Spanos*; my advisor and thesis committee chair, who simply generates enthusiasm for scientific inquiry through his inspiring mentorship. He always makes sure to relieve the student from the "ordinary" so that there is time for the "extraordinary". I am honestly grateful to him for the "scientific freedom" he provided, as well as for "protecting and mentoring my dreams".

Moreover, I would like to express my thanks to the committee members, *Professor Satish Nagarajaiah*, *Assistant Professor Ilinca Stanciulescu and Assistant Professor Andrew Dick*, for participating in the committee, reviewing the manuscript, and providing valuable suggestions. I deeply appreciate their encouragement and interest in my work.

Finally, I would like to express my gratitude to my family for their encouragement, and trust in my skills, but mostly for their unconditional love. Specifically, I am indebted to my father, *Athanasios Kougioumtzoglou*, for encouraging me to embrace a mathematical way of thinking; and to my mother, *Vasiliki Liggri*, for urging me to make this thinking more colorful.

Table of contents

List of figures

Chapter 1

Introduction

1.1 Motivation and objectives

Since the invention of modern calculus, differential and integral equations have been used in applied sciences, engineering, economics, and even social sciences, to describe the current state of a system and predict its evolution in time. A simplified approach suggests that the coefficients and the input to these equations are known quantities. In other words, when the level of uncertainty related to these systems is relatively small, the associated problems may be formulated in terms of averages. Nevertheless, the aforementioned deterministic approach cannot be expected to describe realistically systems in which the level of uncertainty is severe.

Over the past decades it has been realized that loads caused by earthquakes, sea waves, blast events, and winds may be adequately described on a stochastic basis. For instance, most contemporary aseismic code provisions tend to incorporate a stochastic/probabilistic framework for the design of structured facilities. In fact, insufficient information, poor interpretation of underlying mechanisms, and inherent randomness of the system result in defining problems which possess random coefficients and input. In such cases, a stochastic approach constitutes a rational basis for system analysis and design.

The scientific branches of physics and astronomy benefited greatly from the incorporation of stochastic approaches during the first half of the twentieth century (e.g. Chandrashekhar, 1943). Engineering applications first occurred in the area of communication theory to address the problem of noisy signals (e.g. Rice, 1944; Middleton, 1960). The analysis and design of structural systems followed which led to the birth of the new scientific discipline of random vibrations (e.g. Crandall, 1958; Crandall, 1963; Crandall and Mark, 1963; Robson, 1963; Lin, 1967; Soong, 1973; Nigam, 1983; Ibrahim, 1985; Kree and Soize, 1986; Newland, 1993a; Soong and Grigoriu, 1993; Preumont, 1994; Lin and Cai, 1995; Solnes, 1997; Elishakoff, 1999; To, 2000; Grigoriu, 2002; Roberts and Spanos, 2003; Lutes and Sarkani, 2004; Socha, 2008; Li and Chen, 2009).

Over the past fifty years considerable interest has been developed in random vibration analysis of dynamic systems used as models in structural engineering. In general, the use of the term random vibration analysis suggests the determination of the response statistics of a system subjected to stochastic loads. Further, a persistent challenge in the area of modern stochastic dynamics, known as the first-passage problem, is the determination of the probability the response of the system reaches, and possibly crosses, a predetermined barrier level for the first time. Such a reliability-based analysis can be beneficial in terms of safety or risk assessments.

Moreover, if the system under consideration is linear, the general methodology developed for treating deterministically posed problems can be readily extended and applied to random vibration analysis. Linear dynamic

models are appealing for many structural engineering applications. Nevertheless, in several cases structural components are expected to exhibit nonlinear behavior associated, in general, either with material or geometrical aspects. For instance, structural systems can become nonlinear and inelastic with restoring forces depending on the response history under severe earthquake excitations. This kind of behavior is generally described in the literature by the term hysteresis.

The number of nonlinear random vibration problems which lend themselves to exact solutions is strikingly limited. Thus, the predominant approach for determining, with any preselected reliability, the response statistics of nonlinear structural systems under stochastic excitation is the Monte Carlo simulation (MCS) method (e.g. Rubinstein, 1981; Spanos and Zeldin, 1998; Schueller and Spanos, 2000; Proppe et al., 2003; Gamerman, 2006; Rubinstein and Kroese, 2008; Rubino and Tuffin, 2009). This approach involves purely numerical random experiments. Specifically, a large number of time history samples are numerically simulated and considered representative of an infinite ensemble of possible time histories. Clearly, the computational cost increases almost linearly with the number of records, compared to the accuracy which increases with the square root of the number of records simulated. Hence, there are cases, especially for nonlinear multi-degree-of-freedom (MDOF) systems, where the MCS method can be computationally prohibitive. Thus, several approximate analytical or numerical approaches have been developed over the years (e.g. Schueller et al., 1997; Kougioumtzoglou, 2009; Li and Chen, 2009). Among these approaches, the method of statistical linearization is considered,

perhaps, the most versatile one (e.g. Proppe et al., 2003; Roberts and Spanos, 2003; Socha, 2005; Socha, 2008).

In this context, an approximate analytical stochastic framework will be developed in this thesis for response and reliability analysis of nonlinear (hysteretic) systems. To this aim the localization properties and the joint time-frequency representation capabilities of the orthogonal wavelet transform (e.g. Daubechies, 1992; Young, 1993; Newland, 1993a; Hussaini, 1996; Koornwinder, 1998; Vidakovich, 1999; Mallat, 1999; Qian, 2002; Keinert, 2004; Nason, 2008; Radunovic, 2009) as well as the accuracy of the Wiener path integral method (e.g. Feynman and Hibbs, 1965; Schulman, 1981; Chachian and Demichev, 2001; Kleinert, 2009) will be utilized to model and analyze structural systems under non-stationary excitations with physically realistic time-varying frequency contents.

1.2 Organization of the thesis

The thesis consists of ten chapters followed by the list of cited references. Excluding chapter 1, which plays an introductory role, and chapter 10, which contains the concluding remarks, each of the remaining chapters presents an independent research topic. Therefore, they are self-contained and include an introductory section followed by the analytical derivations, verified by digital simulations.

Chapter 1 serves as an introduction to the thesis presenting the motivation and objectives of the current research effort. Moreover, the contents of the thesis are briefly outlined.

Chapter 2 focuses on an approximate formula which utilizes the concept of conditional power spectral density (PSD) and has been employed by several investigators to determine the response PSD of stochastically excited nonlinear systems in numerous applications. However, its derivation has been treated to date in a rather heuristic, even "unnatural" manner, and its mathematical legitimacy has been based on loosely supported arguments. In this chapter, a perspective on the veracity of the formula is provided by utilizing spectral representations both for the excitation and for the response processes of the nonlinear system; this is done in conjunction with a stochastic averaging treatment of the problem. Then, the orthogonality properties of the monochromatic functions which are involved in the representations are utilized. Further, not only stationarity but ergodicity, as well, of the system response are invoked. In this context, the nonlinear response PSD is construed as a sum of the PSDs that correspond to equivalent response amplitude dependent linear systems. Next, relying on classical excitation-response PSD relationships for these linear systems leads, readily, to the derivation of the formula for the determination of the PSD of the nonlinear system.

In chapter 3 an approximate analytical approach based on the concepts of statistical linearization and of stochastic averaging is presented for determining the response of a MDOF nonlinear system subject to a stochastic excitation vector

with an evolutionary broad-band power spectrum matrix. Specifically, relying on an evolutionary spectral matrix analysis approach and on statistical linearization second order response statistics are derived. It is further shown that assuming the case of relatively stiff systems leads to a substantial reduction of computational effort and to a quasi-stationary approach which can be fairly accurate for a wide range of systems of practical interest. Further, a system dimension reduction approach is introduced by determining an effective linear time-variant (LTV) single-degree-of-freedom (SDOF) system corresponding to each degree of freedom. Then, relying on stochastic averaging the response amplitude probability density function (PDF) of the LTV SDOF system is determined. A significant advantage of the approach relates to the fact that it can be used in a rather straightforward manner in conjunction with recently developed design spectrum based analyses to obtain peak response estimates. This is done without resorting to numerical integration of the nonlinear equations of motion. The approach is readily applicable even for excitations possessing non-separable evolutionary power spectra. In this regard there is no need to resort to pre-processing treatments of the excitation, such as pre-filtering, commonly used in alternative linearization schemes. The nonlinearities could be either of the hysteretic or of the zero-memory kind. Numerical examples include MDOF systems possessing stiffness and damping nonlinearities as well as MDOF systems following the Bouc-Wen (hysteretic) model. The accuracy of the approach is demonstrated by pertinent Monte Carlo simulations.

In chapter 4 a numerical Wiener path integral solution (PIS) approach is developed to derive response and first-passage statistics of nonlinear oscillators subject to evolutionary broad-band stochastic excitation. Specifically, based on the concepts of stochastic averaging and of statistical linearization the response envelope is modeled as a one-dimensional Markov diffusion process. Further, relying on a discrete version of the Chapman-Kolmogorov (C-K) equation and on the associated first-order stochastic differential equation the response envelope and first-passage PDFs are obtained. The basic concept of the approach is that the evolution of the response PDF is computed in short time steps, assuming a Gaussian form for the conditional response PDF. The Van der Pol, the Duffing, and the Preisach (hysteretic) oscillators are considered in demonstrating the applicability of the approach. Its efficiency and reliability is verified by pertinent Monte Carlo simulations.

In chapter 5 a numerical Wiener PIS approach is developed for determining the response behavior of the softening Duffing oscillator under stochastic excitation. Specifically, introducing a special form for the conditional response PDF and relying on a discrete version of the C-K equation a rigorous analysis of the response amplitude process behavior is achieved, in contrast to previous heuristic treatments of the subject. Further, the softening Duffing oscillator with nonlinear damping that has been widely used to model the nonlinear ship roll motion in beam seas is considered. In this context, the developed approach is applied to determine the capsizing probability of a ship

subject to physically realistic non-white wave excitations. Pertinent Monte Carlo simulation data demonstrate the accuracy of the approach.

Chapter 6 contains an approximate analytical Wiener PIS approach for the determination of the non-stationary response PDF of a broad class of stochastically excited nonlinear oscillators. Specifically, relying on the notion of the Wiener path integral and adopting a variational formulation the non-stationary PDF of processes with nonlinear drift and constant diffusion coefficients is expressed in terms of the most probable path. Further, using the concepts of stochastic averaging and of statistical linearization it is shown that the response amplitude envelope of oscillators with nonlinear damping is governed by a first-order stochastic differential equation. The process possesses nonlinear drift and constant diffusion coefficients. Thus, the analytical Wiener PIS approach can be applied demonstrating its potential to address physically realistic problems. The significant advantage of the proposed approach relates to the determination of the non-stationary response PDF without the need to advance the solution in short time steps as it is required for the existing alternative numerical PIS approaches. The accuracy of the approach is demonstrated by pertinent Monte Carlo simulations.

In chapter 7 a novel harmonic wavelet-based statistical linearization approach is proposed for determining the evolutionary power spectrum (EPS) of the response of nonlinear oscillators subject to stochastic excitation. Specifically, first a mathematically rigorous wavelet-based representation of non-stationary stochastic processes is presented. Next, a representation of the process

corresponding to a specific scale and translation level is derived. This procedure leads to an EPS estimation approach which is applicable for estimating not only separable but non-separable in time and frequency EPS as well. Several numerical results are presented in this context. Next, focusing on the case of the stochastic response of a linear system and relying on the orthogonality properties of the developed representation an excitation-response EPS relationship is derived. It is further shown that the excitation-response EPS relationship is valid even for LTV systems since the approach possesses inherently the element of time-dependence. Further, an extension via statistical linearization of the input-output EPS relationship for the case of a nonlinear system is developed. The approach involves the concept of assigning optimal and response dependent equivalent stiffness and damping elements corresponding to the specific frequency and time bands. This leads to an iterative determination of the EPS of the oscillator response. Pertinent Monte Carlo simulations establish the reliability and versatility of the approach.

In chapter 8 the harmonic wavelet-based statistical linearization method developed in chapter 7 is modified and extended to determine the EPS of the response of a SDOF Bouc-Wen hysteretic oscillator subject to stochastic excitation. Specifically, optimal and response dependent equivalent linear elements corresponding to the specific frequency and time bands are assigned, leading to an iterative determination of the response EPS. Thus, a joint time-frequency response analysis is achieved, which is readily applicable even for

cases of physically realistic non-separable excitation EPS. Pertinent Monte Carlo simulations demonstrate the reliability and accuracy of the approach.

Further, structural systems subject to severe excitations, such as seismic motions, winds, and ocean waves can often exhibit time-varying nonlinear behavior. In this regard, a reliable identification approach is crucial in performing effective structural health monitoring (SHM). In chapter 9, an identification approach for nonlinear time-variant systems based on the localization properties of the harmonic wavelet transform is developed. Specifically, utilizing measured excitation-response (non-stationary) data and recasting the original single-input/single-output (SISO) system into an equivalent multiple-input/single-output (MISO) system in the wavelet domain the unknown time and frequency dependent generalized harmonic wavelet-based frequency response functions (GHW-FRFs) are identified. To this aim, a conditioning procedure is applied to decouple the resulting sub-systems of the MISO system. The developed approach can be viewed as a generalization of the well established reverse MISO spectral identification approach to account for non-stationary inputs and time-varying system parameters. Several linear and nonlinear time-variant systems are used to demonstrate the reliability of the approach. The approach is shown to behave satisfactorily as well even in the case of noise corrupted data.

Concluding remarks along with suggestions for future work are provided in chapter 10; and a list of cited references follows.

Chapter 2

On the determination of the power spectrum of randomly excited oscillators via stochastic averaging: An alternative perspective

2.1 Preliminary remarks

Popular random vibration techniques, such as the statistical linearization (e.g. Roberts and Spanos, 2003; Socha, 2005), have been proven quite successful in determining approximately the response statistics, such as the variance, of nonlinear systems (e.g. Caughey, 1963; Kougioumtzoglou and Spanos, 2009). However, this is not the case for quantities such as the response power spectral density (PSD). In fact, response PSD estimation applications that utilize a statistical linearization technique may reflect a significant discrepancy from the correct result. Specifically, while the technique yields the right resonance frequencies, it may overestimate the peak values and underestimate the bandwidths (e.g. Bouc, 1994).

In Miles (1989) an improved linearization technique was proposed, where the stiffness element of the oscillator was treated as a random variable. In Miles (1993) the form of the conditional PSD was presented for the first time and was used to derive an approximate formula for the response PSD. However, the term conditional PSD had not been introduced until Bouc (1994) first suggested the terminology and derived an approximate formula for computing the nonlinear

PSD by resorting to the stochastic averaging method (e.g. Roberts and Spanos, 1986; Zhu, 1996). In general, the technique developed by Miles (1993) and by Bouc (1994) utilizes a family of equivalent linear systems whose elements are response amplitude envelope dependent. Specifically, the response PSD is estimated as a weighted sum of the response PSDs of the linear systems. The weight function is merely the PDF of the amplitude process. In Spanos et al. (2004a) the response amplitude PSD of a stochastically excited Preisach system was computed accurately using the discussed formula. This kind of approach was also adopted and applied in the context of nonlinear system identification (e.g. Bellizzi and Defilippi 2003; Soize, 1995). Moreover, in Krenk and Roberts (1999) and subsequent papers (Rudinger and Krenk, 2003a; 2003b) an alternative formulation was presented relying on equivalent linear systems whose elements are response energy envelope dependent. In this manner, additional information related to the occurrence of higher harmonics was captured.

Taking into account the versatility and the accuracy of this technique as it has been reported in a large number of applications, it is desirable to attempt to establish its veracity on a rigorous mathematical basis; thus, the derivation of a concrete proof and the presentation of an alternative perspective on the veracity of the technique constitute this chapter. To this aim, spectral representations (e.g. Grigoriu, 1993; Shinozuka and Deodatis, 1991) for both the stochastic excitation and the response processes, the orthogonality conditions of the monochromatic functions and stochastic averaging are combined to derive the discussed formula.

2.2 Mathematical formulation

2.2.1 Equivalent linear system interpretation

Consider a nonlinear single degree of freedom system whose motion is governed by the differential equation

$$\ddot{x} + \beta\dot{x} + z(t, x, \dot{x}) = w(t). \tag{2.1}$$

In this equation a dot over a variable denotes differentiation with respect to time (t); $(z(t,x,\dot{x}))$ is the restoring force which can be either hysteretic or depend only on the instantaneous values of (x) and $(\dot{x})$; (β) is a linear damping coefficient; and $(w(t))$ represents a zero-mean stationary random process possessing a broad-band power spectrum $S_w(\omega)$. It is further assumed that the system is lightly damped and thus the response can be treated as a narrow-band process with slowly varying effective amplitude (A), and frequency $(\omega(\mathrm{A}))$.

A statistical linearization/stochastic averaging technique may be adopted to determine response amplitude dependent equivalent damping and stiffness elements. In fact, several different implementations of the linearization technique exist in the literature, which are presented and discussed in Roberts and Spanos (2003) and in Socha (2005). Following the technique developed in Goto and Iemura (1983), the linearized counterpart of Eq.(2.1) becomes

$$\ddot{x} + \beta(\mathrm{A})\dot{x} + \omega^2(\mathrm{A})x = w(t), \tag{2.2}$$

where the equivalent damping element and natural frequency are taken to be functions of the amplitude (A) of the response to account for the effect of the nonlinearity. Due to the overall light damping of the system, the amplitude (A) is

a slowly varying function with respect to time and, therefore, is treated as a constant over one cycle of oscillation. Specifically, defining the error between Eq.(2.1) and Eq.(2.2) as

$$\varepsilon = z(t,x,\dot{x}) + [\beta - \beta(\mathrm{A})]\dot{x} - \omega^2(\mathrm{A})x, \tag{2.3}$$

the expressions

$$\beta(\mathrm{A}) = \beta + \frac{\oint \dot{x}z dt}{\oint \dot{x}^2 dt}, \tag{2.4}$$

and

$$\omega^2(\mathrm{A}) = \frac{\oint xz dt}{\oint x^2 dt}, \tag{2.5}$$

are derived. Eqs.(2.4) and (2.5) are obtained by applying an error minimization procedure in the mean square sense, where $\left(\oint\ \right)$ can be interpreted as 'an average over one cycle' operator. Due to the narrow-band attribute of the response Eqs.(2.4) and (2.5) yield, respectively,

$$\beta(A) = \beta + \frac{S(A)}{A\omega(A)}, \tag{2.6}$$

and

$$\omega^2(A) = \frac{C(A)}{A}, \tag{2.7}$$

where

$$C(A) = \frac{1}{\pi}\int_0^{2\pi} \cos[\psi] z(t, A\cos\psi, -\omega(A)A\sin\psi) d\psi, \tag{2.8}$$

and

$$S(A) = -\frac{1}{\pi}\int_0^{2\pi} \sin[\psi] z(t, A\cos\psi, -\omega(A)A\sin\psi)d\psi \,. \tag{2.9}$$

Considering the aforementioned derivation of the equivalent linear system, it can be argued that the PSD of the response process is likely to lend itself to an equivalent amplitude dependent "linearized" representation. Since for a fixed value of the amplitude, i.e. $(A = A^*)$, the oscillator of Eq.(2.2) takes the form of a linear oscillator with fixed damping and stiffness elements, the PSD of the response is expected to be

$$S_x(\omega) = \frac{S_w(\omega)}{\left(\omega^2(A^*) - \omega^2\right)^2 + \left(\beta(A^*)\omega\right)^2}. \tag{2.10}$$

Therefore, an intuitive estimate of the expression of the response PSD would be a weighted sum of the "linear" PSD components of the form of Eq.(2.10) for $(A^* \in [0,\infty])$. Furthermore, considering a long time interval, the weighting factors of this sum would be the ratios of the time the process spends at amplitude (A^*) over the total period of time. In mathematical terms, one can set as an approximation for the system response PSD the expression

$$S_x(\omega) = \lim_{\substack{T\to\infty \\ M\to\infty \\ \Delta A\to 0}} \left[\sum_{k=0}^{M} \left(\frac{T_k}{T} \frac{S_w(\omega)}{\left(\omega^2(k\Delta A) - \omega^2\right)^2 + \left(\beta(k\Delta A)\omega\right)^2} \right) \right]. \tag{2.11}$$

Note that inherent in the derivation of Eq.(2.11) is the consideration of two different time scales. Specifically, a short time scale (t_s) is associated with the rapid fluctuations induced by the dynamics of the model, and a relatively long

time scale (t_l) is associated with the low variations of the amplitude. In an attempt to confirm the reliability of Eq.(2.11), a Duffing oscillator of the form

$$\ddot{x}+2\zeta_0\omega_0\dot{x}+\omega_0^2x+\varepsilon\omega_0^2x^3=w(t), \qquad \varepsilon>0, \tag{2.12}$$

is considered, where (ζ_0) is the ratio of critical damping. Using Eq.(2.6) and Eq.(2.7), the amplitude-dependent equivalent natural frequency and damping term are found to be, respectively,

$$\beta(A)=2\zeta_0\omega_0, \tag{2.13}$$

and

$$\omega^2(A)=\omega_0^2(1+\frac{3}{4}\varepsilon A^2). \tag{2.14}$$

Choosing the values $(S_w(\omega)=S_0=0.3)$, $(\zeta_0=0.01,\omega_0=3.612rad/\sec)$, $(\varepsilon=0.2,M=300)$ and utilizing Eq.(2.11), the response PSD of the Duffing oscillator is estimated in Fig.(2.1). For this, an adequately long time interval is considered and the time portions the response spends at each amplitude level are determined and substituted into Eq.(2.11). The derived result is compared with a direct estimation of the response PSD using the Welch method (e.g. Bendat and Piersol, 1971; Welch, 1967). An identical procedure is also applied to a linear oscillator possessing the same values for the natural frequency, and the ratio of critical damping. Examining Eq.(2.1) the numerical results clearly support the interpretation suggested by Eq.(2.11). Furthermore, the presented PSD estimations are in agreement with the conclusions drawn in Bouc (1994), in Miles (1989) and in Reinhall and Miles (1989). Specifically, it can be readily seen that

the nonlinear stiffness induces a significant broadening and a shift in resonance peaks in the response PSD.

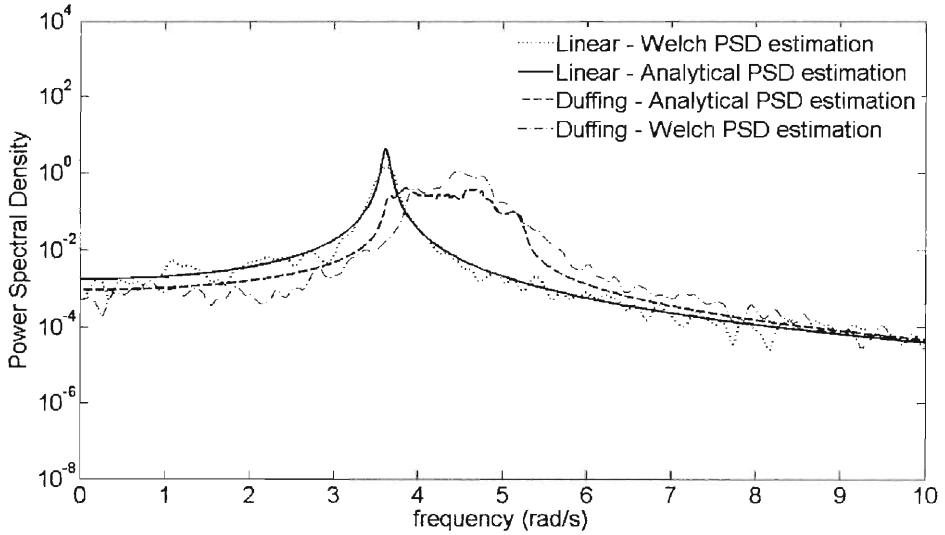

Fig.(2.1). Response PSD estimation of a Duffing $\left(S_w(\omega)=S_0=0.3\right)$, $\left(\zeta_0=0.01,\omega_0=3.612 rad/\sec,\varepsilon=0.2\right)$, and of a linear oscillator $\left(S_w(\omega)=S_0=0.3\right)$, $\left(\zeta_0=0.01,\omega_0=3.612 rad/\sec,\varepsilon=0\right)$; comparison between PSD direct estimation using Welch method and Eq.(2.11) $\left(M=300\right)$.

Returning to Eq.(2.11), the ergodicity property for the response will be invoked to proceed. Specifically, the response displacement $\left(x\right)$, the response velocity $\left(\dot{x}\right)$ and the response amplitude $\left(A\right)$ processes will be treated as ergodic in the second order sense. Thus, the term $\left(\lim_{T\to\infty}\frac{T_k}{T}\right)$ may be interpreted as the probability the process maintains the specific amplitude level $\left(A=k\Delta A\right)$. Specifically, it can be argued that

$$\lim_{T\to\infty}\frac{T_k}{T}=p(k\Delta A)\Delta A, \tag{2.15}$$

where $(p(.))$ represents the probability density function of the response amplitude envelope. Substituting Eq.(2.15) into Eq.(2.11) leads to the formula

$$S_x(\omega)=\int_0^\infty \frac{S_w(\omega)}{\left(\omega^2(A)-\omega^2\right)^2+\left(\beta(A)\omega\right)^2}p(A)dA \tag{2.16}$$

for the response PSD as reported in Miles (1993). Then, the conditional PSD is introduced as

$$S_x(\omega|A)=\frac{S_w(\omega)}{\left(\omega^2(A)-\omega^2\right)^2+\left(\beta(A)\omega\right)^2}. \tag{2.17}$$

2.2.2 Response power spectral density determination

In context with the developments of the preceding sections, several efforts have been made in the literature to determine the response power spectrum of a nonlinear system by resorting to the concept of the conditional PSD. For this purpose, the formula

$$S_x(\omega)=\int_0^\infty S_x(\omega|A)p(A)dA, \tag{2.18}$$

which is equivalent to Eq.(2.16), has been extensively used by various researchers (e.g. Bouc, 1994; Krenk and Roberts, 1999; Miles, 1993; Spanos et al., 2004a) to derive an approximate estimation of the response PSD of nonlinear oscillators of the form of Eq.(2.1). In Eq.(2.18) the variable $(p(A))$ represents the PDF of the response amplitude envelope, whereas the variable $(S_x(\omega|A))$ may be viewed as

the response PSD of a linear oscillator possessing natural frequency equal to $(\omega(A))$ and damping element equal to $(\beta(A))$. Taking into account the preceding analysis, Eq.(2.11) can be recast into the form of Eq.(2.16), or equivalently in the form

$$S_x(\omega) = S_w(\omega) E\left[\frac{1}{\left(\omega^2(A)-\omega^2\right)^2+\left(\beta(A)\omega\right)^2}\right]. \tag{2.19}$$

Despite the fact that Eq.(2.18) has been applied extensively, no concrete proof of this formula has been reported. In fact, the available treatments vary from the rather heuristic ones to those with indisputable mathematical rigor, which, however, lack proper perspective. In this section, a proof of Eq.(2.18) is attempted based on a spectral representation (e.g. Shinozuka and Jan, 1972; Shinozuka and Deodatis, 1991; Shinozuka and Deodatis, 1996; Spanos and Zeldin, 1998) of the excitation and of the response processes.

To proceed, adopt spectral representations for the processes $(x(t))$ and $(w(t))$ which utilize monochromatic functions of random amplitude (e.g. Grigoriu, 1993). Specifically, set

$$x(t) = \sum_{n=0}^{N-1} A_n \cos\left[(n\Delta\omega)t\right] + \sum_{n=0}^{N-1} B_n \sin\left[(n\Delta\omega)t\right], \tag{2.20}$$

and

$$w(t) = \sum_{n=0}^{N-1} C_n \cos\left[(n\Delta\omega)t\right] + \sum_{n=0}^{N-1} D_n \sin\left[(n\Delta\omega)t\right], \tag{2.21}$$

where

$$\Delta\omega = \frac{\omega_u}{N}, \tag{2.22}$$

and (A_n), (B_n) and (C_n), (D_n) are random amplitudes associated with $(x(t))$ and $(w(t))$, respectively.

In Eq.(2.22), (ω_u) represents an upper cut-off frequency beyond which the corresponding PSD can be assumed to be zero. The sequences of the random variables $\{A_0, A_1, ..., A_n\}, \{B_0, B_1, ..., B_n\}$, $\{C_0, C_1, ..., C_n\}, \{D_0, D_1, ..., D_n\}$ can be shown (e.g. Shinozuka and Deodatis, 1991) to be statistically independent with mean value equal to zero and variance equal to

$$\sigma_n^2 = 2S(n\Delta\omega)\Delta\omega. \tag{2.23}$$

Moreover, Eqs.(2.20) and (2.21) yield stochastic processes which are ergodic in the mean, mean square, correlation function, and first order distribution in the weak sense. A more global and detailed treatment of the properties which are implied by this kind of representation may be found in Grigoriu (1993) and in Shinozuka and Deodatis (1991). Note that the approximating processes are periodic with period

$$T_0 = \frac{2\pi}{\Delta\omega} = \frac{2\pi N}{\omega_u}. \tag{2.24}$$

Taking the first and second derivatives of Eq.(2.20) with respect to time yields

$$\dot{x}(t) = \sum_{n=0}^{N-1} -(n\Delta\omega) A_n \sin\left[(n\Delta\omega)t\right] + \sum_{n=0}^{N-1} (n\Delta\omega) B_n \cos\left[(n\Delta\omega)t\right], \tag{2.25}$$

and

$$\ddot{x}(t) = \sum_{n=0}^{N-1} -(n\Delta\omega)^2 A_n \cos\left[(n\Delta\omega)t\right] + \sum_{n=0}^{N-1} -(n\Delta\omega)^2 B_n \sin\left[(n\Delta\omega)t\right]. \tag{2.26}$$

Considering next the orthogonality conditions of monochromatic functions leads to

$$\int_0^{T_0} \cos[(l\Delta\omega)t]\cos[(n\Delta\omega)t]dt = \begin{cases} \frac{1}{2}T_0 & l = n \\ 0 & l \neq n \end{cases}, \tag{2.27}$$

$$\int_0^{T_0} \sin[(l\Delta\omega)t]\sin[(n\Delta\omega)t]dt = \begin{cases} \frac{1}{2}T_0 & l = n \\ 0 & l \neq n \end{cases}, \tag{2.28}$$

and

$$\int_0^{T_0} \sin[(l\Delta\omega)t]\cos[(n\Delta\omega)t]dt = 0. \tag{2.29}$$

Substituting Eqs.(2.20), (2.21), (2.25) and (2.26) into Eq.(2.2) and exploiting Eqs.(2.27-2.29) yields

$$\begin{cases} -(n\Delta\omega)^2 A_n + \beta(A)(n\Delta\omega)B_n + \omega^2(A)A_n = C_n \\ -(n\Delta\omega)^2 B_n - \beta(A)(n\Delta\omega)A_n + \omega^2(A)B_n = D_n \end{cases}. \tag{2.30}$$

In producing Eq.(2.30), it was assumed that the equivalent damping element and natural frequency are constant over the period (T_0). Further manipulation of Eq.(2.30) yields

$$A_n^2 + B_n^2 = \frac{C_n^2 + D_n^2}{\left[\omega^2(A) - (n\Delta\omega)^2\right]^2 + \left[(n\Delta\omega)\beta(A)\right]^2}. \tag{2.31}$$

The PSD estimation for the stationary processes $\left(w(t)\right)$ and $\left(x(t)\right)$ is given (e.g. Bendat, 1998; Newland, 1993) by the equations

$$S_w(\omega) = \lim_{T\to\infty} \frac{1}{T} E\left[\left|\int_0^T w(t)e^{-i\omega t}dt\right|^2\right], \tag{2.32}$$

and

$$S_x(\omega) = \lim_{T\to\infty} \frac{1}{T} E\left[\left|\int_0^T x(t)e^{-i\omega t}dt\right|^2\right]. \tag{2.33}$$

Substituting Eq.(2.21) into Eq.(2.32), taking into account the orthogonality conditions of Eqs.(2.27-2.29) and assuming a fixed value for the frequency (ω), i.e. $(\omega = \omega^*)$ yields

$$\begin{aligned}
&S_w(\omega^*) = \lim_{T\to\infty} \frac{1}{T} E\left[\left|\int_0^T w(t)e^{-i\omega^* t}dt\right|^2\right] = \ldots \\
&\lim_{T\to\infty} \frac{1}{T} E\left[\left|\int_0^T w(t)\cos(\omega^* t)dt - i\int_0^T w(t)\sin(\omega^* t)dt\right|^2\right] = \ldots \\
&\lim_{T\to\infty} \frac{1}{T} E\left[\left|\frac{T}{2}C_* - i\frac{T}{2}D_*\right|^2\right] = \ldots \\
&\lim_{T\to\infty} \frac{1}{T} E\left[\frac{T^2}{4}\left(C_*^2 + D_*^2\right)\right].
\end{aligned} \tag{2.34}$$

In this equation the term $\left(C_*^2 + D_*^2\right)$ is interpreted as the squared amplitude of the process which corresponds to the fixed frequency $(\omega = \omega^*)$. Applying a similar procedure for $S_x(\omega^*)$ yields

$$\begin{aligned}
&S_x(\omega^*) = \lim_{T\to\infty} \frac{1}{T} E\left[\left|\int_0^T x(t)e^{-i\omega^* t}dt\right|^2\right] = \ldots \\
&\lim_{T\to\infty} \frac{1}{T} E\left[\left|\int_0^T x(t)\cos(\omega^* t)dt - i\int_0^T x(t)\sin(\omega^* t)dt\right|^2\right] = \ldots \\
&\lim_{T\to\infty} \frac{1}{T} E\left[\left|\frac{T}{2}A_* - i\frac{T}{2}B_*\right|^2\right] = \ldots \\
&\lim_{T\to\infty} \frac{1}{T} E\left[\frac{T^2}{4}\left(A_*^2 + B_*^2\right)\right].
\end{aligned} \tag{2.35}$$

Further, combining Eqs.(2.31) and (2.35) gives

$$S_x(\omega^*) = \lim_{T\to\infty}\frac{1}{T}E\left[\frac{T^2}{4}\left(A_*^2 + B_*^2\right)\right] = \ldots$$

$$\lim_{T\to\infty}\frac{1}{T}E\left[\frac{T^2}{4}\left(\frac{C_*^2 + D_*^2}{\left(\omega^2(A) - (\omega^*)^2\right)^2 + \left((\omega^*)\beta(A)\right)^2}\right)\right] = \ldots \tag{2.36}$$

$$\lim_{T\to\infty}\frac{1}{T}E\left[\frac{T^2}{4}\left(C_*^2 + D_*^2\right)\right]E\left[\frac{1}{\left(\omega^2(A) - (\omega^*)^2\right)^2 + \left((\omega^*)\beta(A)\right)^2}\right].$$

Obviously, Eq.(2.36) can be recast in the form

$$S_x(\omega^*) = S_w(\omega^*)E\left[\frac{1}{\left(\omega^2(A) - (\omega^*)^2\right)^2 + \left((\omega^*)\beta(A)\right)^2}\right]. \tag{2.37}$$

Since Eq.(2.19) is proven for an arbitrary value of the frequency, i.e. $(\omega = \omega^*)$, it holds true for any value of (ω). Therefore, the validity of Eq.(2.18) is proven. Nevertheless, note that deriving Eq.(2.36) independence has been assumed between $\left(C_*^2 + D_*^2\right)$ and the amplitude (A). Considering the correlation time $\left(\tau_{cor}^w\right)$ of the excitation process, it can be argued that for a stationary broad-band random process it is approximately equal to

$$\tau_{cor}^w \simeq \frac{2\pi}{\omega_u}. \tag{2.38}$$

A similar approximation can be assumed for the response process (x). Taking into account the assumption of light damping, it can be deduced that the main part of the energy of the process is concentrated in a small frequency band around the dominant frequency $(\omega(A))$. Therefore, the correlation time $\left(\tau_{cor}^x\right)$ of the response process can be approximated as

$$\tau_{cor}^{x} \simeq \frac{2\pi}{\omega(A)}. \tag{2.39}$$

Due to the slowly-varying nature of the amplitude process (A) it is safe to assume that the correlation time $\left(\tau_{cor}^{A}\right)$ of the response amplitude is greater than $\left(\tau_{cor}^{x}\right)$. This argument together with Eqs.(2.38) and (2.39) yields

$$\tau_{cor}^{A} > \tau_{cor}^{x}. \tag{2.40}$$

Thus,

$$\frac{\tau_{cor}^{w}}{\tau_{cor}^{A}} < \frac{\tau_{cor}^{w}}{\tau_{cor}^{x}}, \tag{2.41}$$

which leads to

$$\frac{\tau_{cor}^{w}}{\tau_{cor}^{A}} < \frac{\omega(A)}{\omega_{u}} \ll 1. \tag{2.42}$$

This implies that the terms $\left(C_{*}^{2} + D_{*}^{2}\right)$ and (A) in Eq.(2.36) are uncorrelated, and therefore independence can be assumed.

Chapter 3

A dimension reduction approach for MDOF nonlinear system response determination under evolutionary stochastic excitation

3.1 Preliminary remarks

Structural and mechanical systems of engineering interest are often subject to stochastic excitations which are evolutionary in nature such as seismic motions, winds, and ocean waves. Thus, a realistic system analysis and design necessitates the representation of this kind of loading by non-stationary stochastic processes.

Research efforts towards determining evolutionary response statistics of linear systems were initiated by the pioneering work of Caughey and Stumpf (1961) who studied the transient response of a single-degree-of-freedom (SDOF) oscillator under stationary stochastic excitation. Subsequently, Hammond (1968, 1973) derived expressions for the response of SDOF and MDOF systems subject to excitations possessing evolutionary power spectra (EPS) as defined by Priestley (1965, 1967). Further, Spanos and Lutes (1980) determined the response amplitude probability density function (PDF) of a linear oscillator by modeling the response amplitude as a Markov process and relying on stochastic averaging. Moreover, Sun and Kareem (1989) computed the response of a MDOF linear system under evolutionary excitation utilizing a modal time domain approach. In Di Paola and Elishakoff (1996) approaches for obtaining response statistics of

MDOF linear systems under Gaussian and non-Gaussian evolutionary excitations were reviewed. Lin et al. (1994) proposed a pseudo-excitation algorithm for evolutionary response determination, whereas Tootkaboni and Graham-Brady (2010) constructed a stochastic version of direct integration schemes for second-order response statistics of MDOF linear systems under evolutionary excitation. Further discussions related to evolutionary excitation response relationships can be found in the papers by Jangid and Datta (1999) and by Gupta and Trifunac (2000).

Notably, limited progress has been made in terms of determining the evolutionary stochastic response of nonlinear systems. Muscolino et al. (1997) computed the response PDF of nonlinear oscillators by utilizing a Gram-Charlier kind series expansion and by applying a weighted residual approach. Further, Schenk et al. (2005) presented a numerical approach for computing second-order response statistics of nonlinear finite element systems based on a Karhunen-Loeve expansion, whereas Smyth and Masri (2002) combined statistical linearization and decomposition of the covariance matrix of the input stochastic process. Spanos et al. (2007) used a Galerkin approach to compute the non-stationary response of oscillators with stiffness and damping nonlinearities. Moreover, combining the concepts of statistical linearization and stochastic averaging Kougioumtzoglou and Spanos (2009) derived evolutionary response statistics for a broad class of nonlinear oscillators.

In this chapter, an approximate analytical approach based on the concepts of statistical linearization and of stochastic averaging is presented for determining

the evolutionary stochastic response of a MDOF nonlinear system. The nonlinearities could be either of the hysteretic or of the zero-memory kind. A system dimension reduction approach yields the non-stationary response amplitude PDF corresponding to each degree of freedom. Numerical examples include MDOF systems with stiffness and damping nonlinearities as well as MDOF systems following the Bouc-Wen (hysteretic) model. The accuracy of the approach is demonstrated by pertinent Monte Carlo simulations.

3.2 Mathematical formulation

3.2.1 Statistical linearization

Consider next the d-degree-of-freedom nonlinear system defined as

$$M\underline{\ddot{q}}+C\underline{\dot{q}}+K\underline{q}+\underline{g}(\underline{q},\underline{\dot{q}})=\underline{F}(t), \tag{3.1}$$

where (M), (C) and (K) denote the $(d\times d)$ mass, damping and stiffness matrices, respectively; $(\underline{g}(\underline{q},\underline{\dot{q}}))$ is an arbitrary nonlinear $(d\times 1)$ vector function of the variables $(\underline{q}^T=[q_1,...,q_d])$ and $(\underline{\dot{q}}^T=[\dot{q}_1,...,\dot{q}_d])$; and $(\underline{F}(t)^T=[f_1(t),...,f_d(t)])$ is a $(d\times 1)$ zero-mean, non-stationary stochastic vector process possessing an EPS matrix

$$S_F(\omega,t)=\begin{bmatrix} S_{f_1f_1}(\omega,t) & S_{f_1f_2}(\omega,t) & \cdots & S_{f_1f_d}(\omega,t) \\ S_{f_2f_1}(\omega,t) & S_{f_2f_2}(\omega,t) & & \vdots \\ \vdots & & \ddots & S_{f_{d-1}f_d}(\omega,t) \\ S_{f_df_1}(\omega,t) & \cdots & S_{f_df_{d-1}}(\omega,t) & S_{f_df_d}(\omega,t) \end{bmatrix}. \tag{3.2}$$

Note that the non-stationary stochastic process $\left(f_i(t)\right)$ is regarded to be a filtered stationary stochastic process according to the concept proposed by Priestley (1965, 1967). The idea was generalized for the case of bivariate processes (Priestley and Tong, 1973) and was later refined by Dahlhaus (1997) who introduced the class of locally stationary processes. In this manner, the excitation EPS matrix (Eq.(3.2)) can be written as

$$S_F(\omega,t) = A(\omega,t) S_{\tilde{F}}(\omega) A(\omega,t)^{T*}, \tag{3.3}$$

where the superscripts $\left(^T\right)$ and $\left(^*\right)$ denote matrix transposition and complex conjugation, respectively; $\left(A(\omega,t)\right)$ is the modulating matrix which serves as a time-variant filter; and $\left(S_{\tilde{F}}(\omega)\right)$ is the power spectrum matrix corresponding to the stationary stochastic vector process $\left(\underline{\tilde{F}}(t)\right)$. Both separable and non-separable EPS can be defined considering Eq.(3.3). Thus, realistic excitations with both time and frequency varying content can be considered.

Next, focusing on the frequency domain, the response determination problem is defined as seeking the response EPS matrix of the form

$$S_q(\omega,t) = \begin{bmatrix} S_{q_1q_1}(\omega,t) & S_{q_1q_2}(\omega,t) & \cdots & S_{q_1q_d}(\omega,t) \\ S_{q_2q_1}(\omega,t) & S_{q_2q_2}(\omega,t) & & \vdots \\ \vdots & & \ddots & S_{q_{d-1}q_d}(\omega,t) \\ S_{q_dq_1}(\omega,t) & \cdots & S_{q_dq_{d-1}}(\omega,t) & S_{q_dq_d}(\omega,t) \end{bmatrix}. \tag{3.4}$$

Following a statistical linearization approach (e.g. Roberts and Spanos, 2003) and adopting the standard Gaussian assumption for the response processes, an equivalent linear system is given in the form

$$M\underline{\ddot{q}}+\left(C+C_e\right)\underline{\dot{q}}+\left(K+K_e\right)\underline{q}=\underline{F}(t), \tag{3.5}$$

where the time-dependent elements of the matrices $\left(C_e\right)$ and $\left(K_e\right)$ are given by the expressions

$$c_{i,j}^{e}=E\left[\frac{\partial g_i}{\partial \dot{q}_j}\right], \tag{3.6}$$

and

$$k_{i,j}^{e}=E\left[\frac{\partial g_i}{\partial q_j}\right], \tag{3.7}$$

respectively. In the general case of a linear MDOF system under evolutionary excitation a matrix input-output spectral relationship of the form

$$S_q\left(\omega,t\right)=H_{gen}\left(\omega,t\right)S_{\tilde{F}}\left(\omega\right)H_{gen}^{T*}\left(\omega,t\right), \tag{3.8}$$

can be derived (e.g. Gupta and Trifunac, 2000; Li and Chen, 2009), where

$$H_{gen}\left(\omega,t\right)=\int_0^t h\left(t-\tau\right)A\left(\omega,\tau\right)e^{-i\omega\left(t-\tau\right)}d\tau, \tag{3.9}$$

in which $\left(h(t)\right)$ denotes the impulse response function matrix. Moreover, the time-dependent cross-variance of the response can be evaluated by the expression

$$E\left[q_i(t)q_j(t)\right]=\int_{-\infty}^{\infty}S_{q_iq_j}\left(\omega,t\right)d\omega. \tag{3.10}$$

Eqs.(3.5-3.10) establish a nonlinear system of equations which can be solved iteratively. Specifically, for each time instant initial values are assumed for the elements of the equivalent linear system. Then, the response power spectrum matrix is calculated using Eqs.(3.8-3.9). Note that the impulse response function matrix $\left(h(t)\right)$ needs also to be updated. Next, the values of the equivalent linear

elements (Eqs.(3.6-3.7)) are updated taking into account Eq.(3.10). The iterative scheme is repeated until convergence is reached.

Focusing on the relationship for the response EPS (Eq.(3.8)) it can be argued that the convolution operation involved in the derivation of the evolutionary frequency response matrix (Eq.(3.9)) renders the linearization approach computationally demanding. Although Eq.(3.9) has been analytically computed for special cases of time-dependent only modulating function $\left(i.e., A(\omega,t)=A(t)\right)$ for SDOF systems (e.g. Zembaty, 1988; Jangid and Datta, 1999) analytical computation of the convolution operation (Eq.(3.9)) is in general intractable. In fact, omitting the convolution of the impulse response function matrix with the modulating matrix can lead to substantial reduction of computational effort, especially for the case of MDOF systems. In this manner, Eq.(3.9) takes the form

$$H_{gen}(\omega,t)=H(\omega)A(\omega,t), \tag{3.11}$$

where $\left(H(\omega)\right)$ is the matrix of the frequency response functions defined as

$$H(\omega)=\left(-\omega^2 M+i\omega\left(C+C_e\right)+\left(K+K_e\right)\right)^{-1}. \tag{3.12}$$

Consequently, Eq.(3.8) becomes

$$S_q(\omega,t)=H(\omega)A(\omega,t)S_{\bar{F}}(\omega)A^{T^*}(\omega,t)H^{T^*}(\omega), \tag{3.13}$$

or, equivalently

$$S_q(\omega,t)=H(\omega)S_F(\omega,t)H^{T^*}(\omega), \tag{3.14}$$

where Eq.(3.3) was taken into account. It can be readily seen that the spectral input-output relationship (Eq.(3.14)) is exact for the case of stationary processes.

Indeed, Eq.(3.14) is a straightforward generalization of the celebrated spectral relationship based on stationarity and on the Wiener-Khinchin theorem. Thus, the aforementioned approximation can be viewed as a quasi-stationary approach which can be quite accurate for a wide range of systems of practical interest. In fact, it has been shown in Hammond (1968, 1973) that the use of Eq.(3.14) can be a satisfactory approximation for relatively stiff systems. Indeed, in cases where the system natural period is small compared to the duration of the evolutionary excitation Eq.(3.14) can yield satisfactory results. In other words, a small natural period implies the system impulse response function is short lived, and thus Eq.(3.14) becomes more accurate. Further, comparisons in terms of computational time were made in Jangid and Datta (1999) between Eq.(3.8) and Eq.(3.14) demonstrating the efficiency of Eq.(3.14). Furthermore, even for cases where Eq.(3.14) deviated considerably from the exact value it was shown that the quasi-stationary approach provides always a conservative estimate of the peak values of the response.

3.2.2 System dimension reduction

Without loss of generality, consider the case where $\left(f_i(t) = f(t),\ \ i = 1,..,d\right)$ such that the stochastic vector process $\left(\underline{F}(t)\right)$ has an EPS matrix

$$S_F(\omega,t) = \begin{bmatrix} S_f(\omega,t) & 0 & \cdots & 0 \\ 0 & S_f(\omega,t) & & \vdots \\ \vdots & & \ddots & 0 \\ 0 & \cdots & 0 & S_f(\omega,t) \end{bmatrix}. \tag{3.15}$$

This form of EPS matrix can be used, for instance, to model the earthquake excitation of a multi-story shear kind building structure assuming equal masses for all stories. Focusing next on Eq.(3.10) and using Eqs.(3.14) and (3.15) it can be readily seen that for the i-th degree of freedom yields

$$E\left[q_i^2(t)\right]=\int_{-\infty}^{\infty}\left(\left|\mathrm{H}_{i1}(\omega)\right|^2+\left|\mathrm{H}_{i2}(\omega)\right|^2+..+\left|\mathrm{H}_{id}(\omega)\right|^2\right)S_f(\omega,t)\,d\omega\,. \tag{3.16}$$

Moreover, adopting the aforementioned quasi-stationary approach the equation

$$E\left[\dot{q}_i^2(t)\right]=\int_{-\infty}^{\infty}\omega^2\left(\left|\mathrm{H}_{i1}(\omega)\right|^2+\left|\mathrm{H}_{i2}(\omega)\right|^2+..+\left|\mathrm{H}_{id}(\omega)\right|^2\right)S_f(\omega,t)\,d\omega\,. \tag{3.17}$$

holds true in the approximate sense discussed in section 3.2.1. Focusing on the integrand of Eq.(3.16) the term in the parenthesis can be viewed as the transfer function of an effective LTV system. This observation leads to defining an auxiliary effective LTV system corresponding to each degree of freedom, namely

$$\ddot{q}_i+\beta_{au,i}(t)\dot{q}_i+\omega_{au,i}^2(t)q_i=f(t)\,, \tag{3.18}$$

where $\left(\beta_{au,i}(t)\right)$ and $\left(\omega_{au,i}^2(t)\right)$ account for the effective time-varying damping and stiffness elements, respectively. Then, the equations

$$E\left[q_i^2(t)\right]=\int_{-\infty}^{\infty}\left(\frac{1}{\left(\omega_{au,i}^2(t)-\omega^2\right)^2+\left(\beta_{au,i}(t)\omega\right)^2}\right)S_f(\omega,t)\,d\omega\,, \tag{3.19}$$

and

$$E\left[\dot{q}_i^2(t)\right]=\int_{-\infty}^{\infty}\omega^2\left(\frac{1}{\left(\omega_{au,i}^2(t)-\omega^2\right)^2+\left(\beta_{au,i}(t)\omega\right)^2}\right)S_f(\omega,t)\,d\omega\,, \tag{3.20}$$

hold true in a quasi-stationary sense. Combining Eqs.(3.16-3.17) and Eqs.(3.19-3.20) it can be readily seen that a nonlinear system of two algebraic equations is

formed for the stiffness and damping elements of the auxiliary LTV system for each time instant. Thus, based on the concept of equation of second moments, a system dimension reduction approach is introduced since the response determination problem of the initial MDOF system reduces to the solution of the effective LTV SDOF system of Eq.(3.18).

Note that in the case of stationary stochastic processes Eqs.(3.14), (3.16-3.17) and (3.19-3.20) are exact and the effective linear system (Eq.(3.18)) is time-invariant. In this manner, the developed system dimension reduction approach can be used in conjunction with design spectrum based analyses which utilize the concept of a design spectrum compatible stationary excitation power spectrum. For instance, a relatively straightforward generalization of the approach recently proposed by Giaralis and Spanos (2010) is possible for MDOF systems. Specifically, the original nonlinear d-degree-of-freedom system is replaced by (d) effective linear systems of the form of Eq.(3.18) corresponding to each degree of freedom. Then, the derived damping and stiffness coefficients of the effective linear systems can be used in conjunction with the design spectrum to obtain peak response estimates (see Giaralis and Spanos, 2010) without resorting to numerical integration of the governing nonlinear equations of motion.

3.2.3 Stochastic averaging

Focusing on Eq.(3.18) and assuming the case of a lightly damped system, it can be argued that the oscillator exhibits a pseudo-harmonic behavior described by the equations

$$q_i(t) = A_i(t)\cos\left(\omega_{au,i}(t)t + \phi_i(t)\right), \tag{3.21}$$

and

$$\dot{q}_i(t) = -\omega_{au,i}(t)A_i(t)\sin\left(\omega_{au,i}(t)t + \phi_i(t)\right), \tag{3.22}$$

in which the response amplitude envelope (A_i) is a slowly varying function with respect to time and is defined as

$$A_i^2(t) = q_i^2(t) + \left(\frac{\dot{q}_i(t)}{\omega_{au,i}(t)}\right)^2. \tag{3.23}$$

Relying further on a combination of deterministic and stochastic averaging (e.g. Roberts and Spanos, 1986; Kougioumtzoglou and Spanos, 2009) a first-order (Ito) stochastic differential equation of the form

$$\dot{A}_i = -\frac{1}{2}\beta_{au,i}(t)A_i + \frac{\pi S_f(\omega_{au,i}(t),t)}{2A_i\omega_{au,i}^2(t)} + \frac{\left(\pi S_f(\omega_{au,i}(t),t)\right)^{1/2}}{\omega_{au,i}(t)}\eta(t), \tag{3.24}$$

is derived which governs approximately the evolution in time of the amplitude $(A_i(t))$. In Eq.(3.24), $(\eta(t))$ is a zero mean and delta correlated process of intensity one, i.e., $E(\eta(t)) = 0$; and $E(\eta(t)\eta(t+\tau)) = \delta(\tau)$, with $(\delta(\tau))$ being the Dirac delta function. It can be readily seen that Eq.(3.24) is decoupled from the phase $(\phi_i(t))$. Thus, it is feasible to model the amplitude process $(A_i(t))$ as a one-dimensional Markov process.

The Fokker-Planck equation that corresponds to Eq.(3.24) is (e.g. Arnold 1974)

$$\frac{\partial p(A_i,t)}{\partial t} = -\frac{\partial}{\partial A_i}\left\{\left(-\frac{1}{2}\beta_{au,i}(t)A_i + \frac{\pi S_f(\omega_{au,i}(t),t)}{2A_i\omega_{au,i}^2(t)}\right)p(A_i,t)\right\} + \ldots$$
$$\frac{\pi S_f(\omega_{au,i}(t),t)}{2\omega_{au,i}^2(t)}\frac{\partial^2 p(A_i,t)}{\partial A_i^2}. \tag{3.25}$$

Following a similar approach as the one described in Spanos and Lutes (1980) and in Kougioumtzoglou and Spanos (2009), a solution of Eq.(3.25) is attempted in the form

$$p(A_i,t) = \frac{A_i}{c_i(t)}e^{\frac{A_i^2}{2c_i(t)}}. \tag{3.26}$$

Substituting Eq.(3.26) into Eq.(3.25) and manipulating yields

$$\dot{c}_i(t) = -\beta_{au,i}(t)c_i(t) + \frac{\pi S_f\left(\omega_{au,i}(t),t\right)}{\omega_{au,i}^2(t)}. \tag{3.27}$$

Eq.(3.27) constitutes a first-order nonlinear ordinary differential equation which can be solved by standard numerical schemes such as the fourth order Runge-Kutta. Thus, the response amplitude non-stationary PDF corresponding to the i-th degree of freedom is determined approximately combining the concepts of statistical linearization and of stochastic averaging and assuming a time-dependent Rayleigh response amplitude PDF.

3.3 Numerical Examples

3.3.1 Stiffness and damping nonlinearities

To demonstrate the accuracy of the proposed approach a 2-DOF nonlinear system modeling a shear kind building structure is considered. Specifically, introducing the coordinates transformations

$$y_1 = q_1, \tag{3.28}$$

and

$$y_2 = q_2 - q_1, \tag{3.29}$$

Eq.(1) becomes

$$M\underline{\ddot{y}} + C\underline{\dot{y}} + K\underline{y} + \underline{g}(\underline{y}, \underline{\dot{y}}) = \underline{F}(t), \tag{3.30}$$

where

$$M = \begin{bmatrix} 1 & 0 \\ 1 & 1 \end{bmatrix}, \tag{3.31}$$

$$C = \begin{bmatrix} c_1 & -c_2 \\ 0 & c_2 \end{bmatrix}, \tag{3.32}$$

$$K = \begin{bmatrix} k_1 & -k_2 \\ 0 & k_2 \end{bmatrix}, \tag{3.33}$$

and

$$\underline{g}(\underline{y}, \underline{\dot{y}}) = \begin{pmatrix} \varepsilon_1 k_1 y_1^3 + \varepsilon_2 c_1 \dot{y}_1^3 \\ \varepsilon_1 k_2 y_2^3 + \varepsilon_2 c_2 \dot{y}_2^3 \end{pmatrix}. \tag{3.34}$$

The above defined 2-DOF nonlinear system represents a building structure where the coordinates (y_1, y_2) monitor the relative displacements of the stories and the masses of the stories are assumed to be equal to unity. Examining further Eq.(3.34), it can be readily seen that nonlinear springs, of the linear-plus-cubic kind, connect the first story to the ground and the first to the second story. Similarly, nonlinear dampers, of the linear-plus-cubic kind, connect the first story to the ground and the first to the second story. Next, applying Eqs.(3.6) and (3.7) the equivalent linear matrices (C_e) and (K_e) become

$$C_e = \begin{bmatrix} 3\varepsilon_2 c_1 E\left[\dot{y}_1^2\right] & 0 \\ 0 & 3\varepsilon_2 c_2 E\left[\dot{y}_2^2\right] \end{bmatrix}, \tag{3.35}$$

and

$$K_e = \begin{bmatrix} 3\varepsilon_1 k_1 E\left[y_1^2\right] & 0 \\ 0 & 3\varepsilon_1 k_2 E\left[y_2^2\right] \end{bmatrix}, \tag{3.36}$$

respectively. Further, the excitation EPS $\left(S_f(\omega,t)\right)$ of Eq.(3.15) is assumed to have the form

$$S_f(\omega,t) = |w(t)|^2 S_v(\omega), \tag{3.37}$$

where

$$w(t) = k(e^{-at} - e^{-bt}), \tag{3.38}$$

in which $(a = 0.1)$ and $(b = 0.3)$; (k) is a normalization constant so that $(w_{\max} = 1)$, and

$$S_v(\omega) = S_1 \frac{(\omega/\omega_f)^4}{\left(1-(\omega/\omega_f)^2\right)^2 + 4(\zeta_f)^2(\omega/\omega_f)^2} \frac{(\omega_g)^4 + 4(\zeta_g)^2(\omega_g)^2\omega^2}{\left((\omega_g)^2 - \omega^2\right)^2 + 4(\zeta_g)^2(\omega_g)^2\omega^2}, \tag{3.39}$$

in which $(\omega_g = 4 rad/\sec)$, $(\zeta_g = 0.5)$, $(\omega_f = 15 rad/\sec)$ and $(\zeta_f = 1)$. The aforementioned form of Eq.(3.39) represents a Clough-Penzien (C-P) stationary power spectrum (Clough and Penzien, 1993), commonly used in earthquake engineering applications. In essence, it constitutes a modified Kanai-Tajimi power spectrum (Kanai 1957; Tajimi 1960). Specifically, the C-P spectrum incorporates a second-order high-pass filter to eliminate the presence of low-frequency content

allowed by the K-T form. For the case $(S_1 = 1)$ the C-P EPS is plotted in Fig.(3.1).

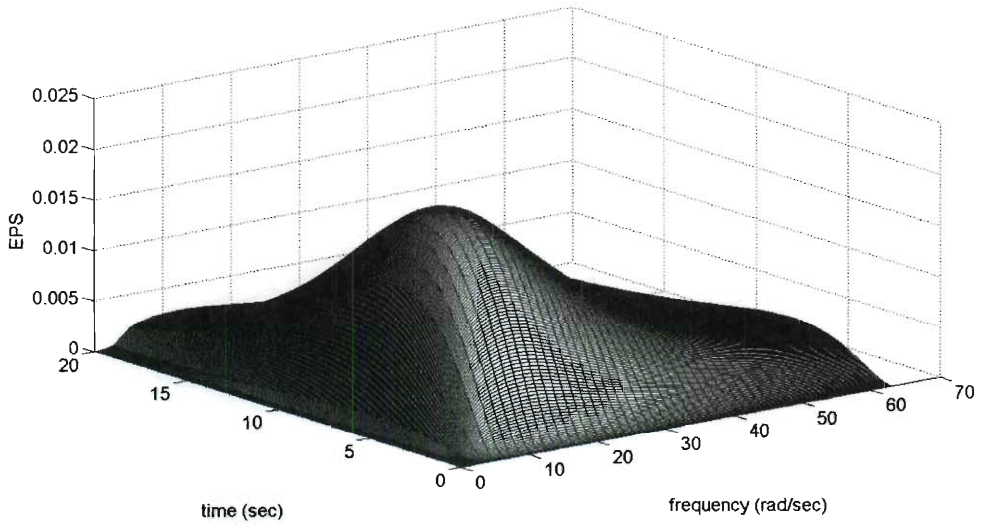

Fig.(3.1). Time-modulated Clough-Penzien power spectrum: $(a = 0.1, b = 0.3)$ and $(\omega_g = 4 rad/\sec)$, $(\zeta_g = 0.5)$, $(\omega_f = 15 rad/\sec)$, $(\zeta_f = 1)$ and $(S_1 = 1)$.

In Spanos and Zeldin (1998) the most common approaches for producing PSD compatible signals are reviewed. Realizations of the process characterized by Eq.(3.37) can be produced generating first stationary time histories $(v(t))$ compatible with $(S_v(\omega))$. In this manner, the autoregressive moving average (ARMA) method is employed to generate realizations of the stationary process $(v(t))$ as the response of a linear time-invariant digital filter subjected to clipped white noise input. The n-th sample of an ARMA(p,q) process is calculated recursively by using the equation

$$v_n = \sum_{l=0}^{q} c_l s_{n-l} - \sum_{k=1}^{p} b_k v_{n-k} \,, \tag{3.40}$$

where (c_l, b_k) are the coefficients of the ARMA filter; and (s) represents a band-limited white noise process. The ARMA filter coefficients are determined by the power order matching (POM) method (e.g. Spanos and Mignolet 1986). To this aim, linear prediction theory is used to construct an autoregressive (AR) digital filter as a first approximation. Then, the ARMA representation is deduced by equating the transfer functions of the AR and ARMA filters.

Next, the parameters values to be used in the numerical examples are chosen to be $(k_1 = k_2 = 1600, c_1 = c_2 = 4, \varepsilon_1 = 2, \varepsilon_2 = 0.5)$. To demonstrate the reliability of the approach different excitation magnitude levels are chosen, namely $(S_1 = 50, 100, 200)$. In Fig.(3.2) the evolutionary response variance is plotted for the (y_1) coordinate. Comparisons with Monte Carlo simulations show that it captures successfully the time-dependent behavior for the different excitation magnitude levels. Similarly, in Fig.(3.3) the evolutionary response variance of the (y_2) coordinate is in good agreement with the Monte Carlo data. In Figs.(3.4) and (3.5) the damping elements and the natural frequencies of the effective LTV SDOF systems are plotted, respectively. Further, in Figs.(3.6) and (3.7) the non-stationary response amplitude PDF (Eq.(3.26)) is plotted for different time instants for the coordinates (y_1) and (y_2), respectively. The excitation magnitude is equal to $(S_1 = 50)$. Comparisons with Monte Carlo simulation data demonstrate the satisfactory accuracy of the approach. In the same

manner, in Figs.(3.8) and (3.9) the non-stationary response amplitude PDF is plotted for the coordinates (y_1) and (y_2), respectively, whereas the excitation magnitude is equal to $(S_1 = 100)$. Finally, in Figs.(3.10) and (3.11) the non-stationary response amplitude PDF is plotted for the coordinates (y_1) and (y_2), respectively, whereas the excitation magnitude is equal to $(S_1 = 200)$. In any case, comparisons with Monte Carlo simulation data demonstrate the accuracy for all the different excitation magnitude levels.

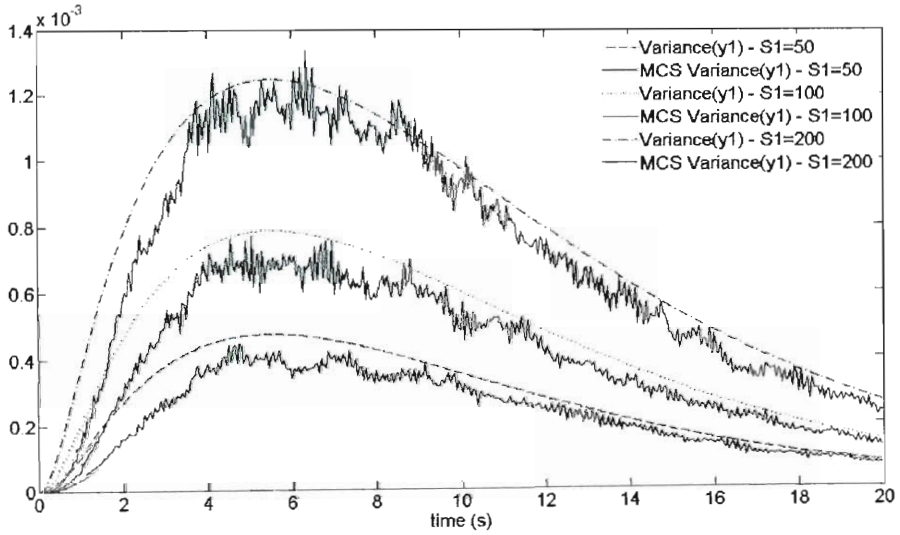

Fig.(3.2). Response variance of the coordinate (y_1) of a 2-DOF structure $(k_1 = k_2 = 1600, c_1 = c_2 = 4, \varepsilon_1 = 2, \varepsilon_2 = 0.5)$ with stiffness and damping nonlinearities. Comparison with Monte Carlo data (500 realizations).

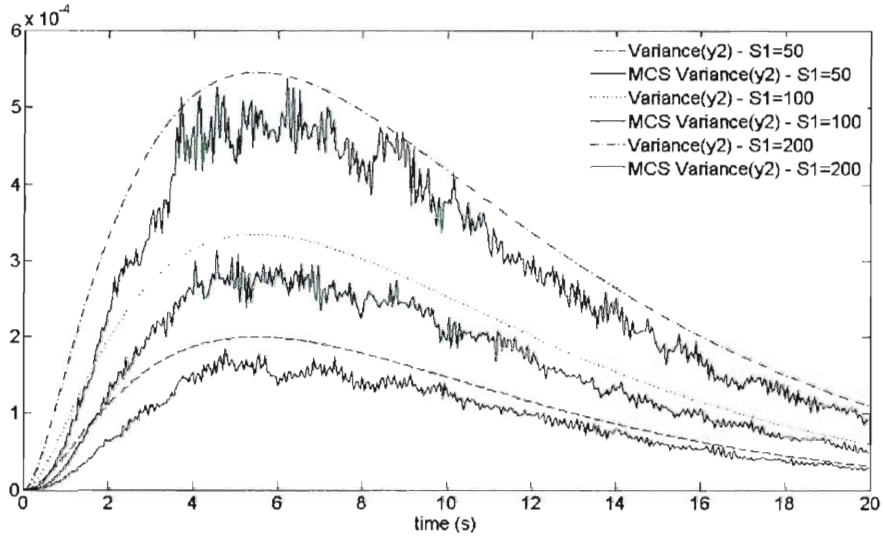

Fig.(3.3). Response variance of the coordinate (y_2) of a 2-DOF structure $(k_1 = k_2 = 1600, c_1 = c_2 = 4, \varepsilon_1 = 2, \varepsilon_2 = 0.5)$ with stiffness and damping nonlinearities. Comparison with Monte Carlo data (500 realizations).

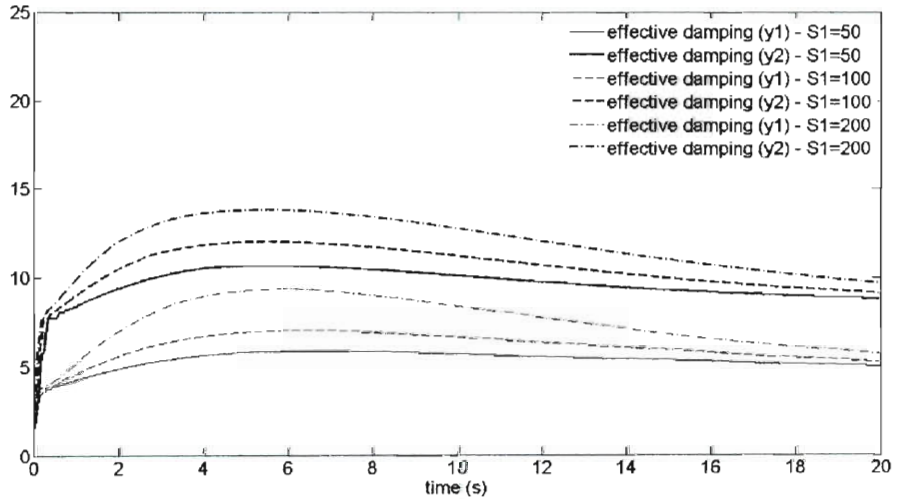

Fig.(3.4). Damping values of the effective LTV SDOF systems corresponding to the 2-DOF structure $(k_1 = k_2 = 1600, c_1 = c_2 = 4, \varepsilon_1 = 2, \varepsilon_2 = 0.5)$ with damping and stiffness nonlinearities.

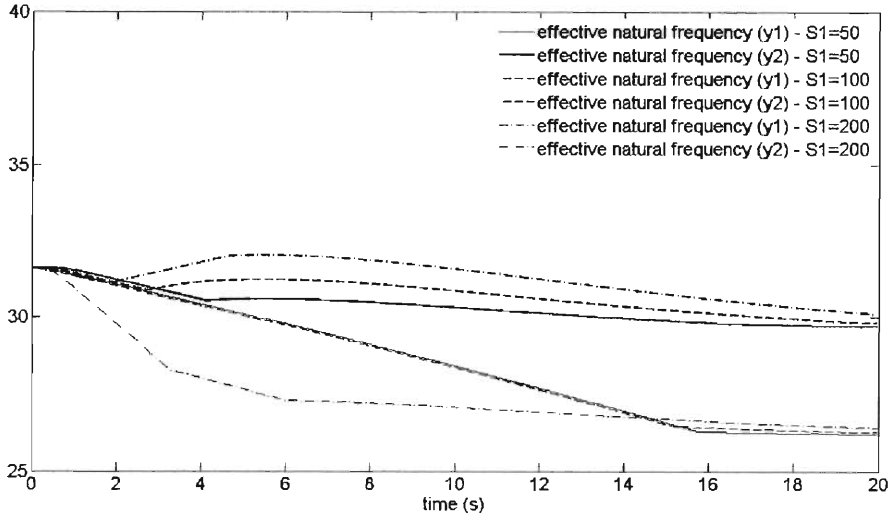

Fig.(3.5). Natural frequency values of the effective LTV SDOF systems corresponding to the 2-DOF structure $\left(k_1 = k_2 = 1600, c_1 = c_2 = 4, \varepsilon_1 = 2, \varepsilon_2 = 0.5\right)$ with damping and stiffness nonlinearities.

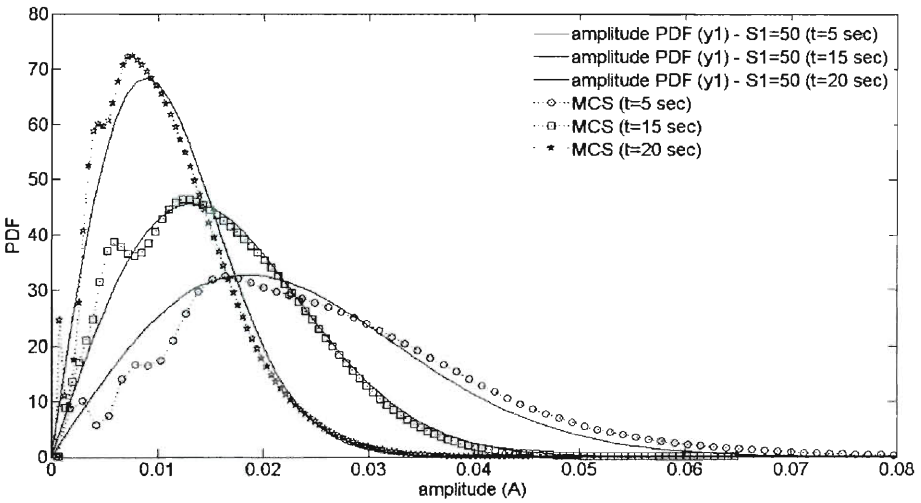

Fig.(3.6). Non-stationary response amplitude PDF of the coordinate $\left(y_1\right)$ of the 2-DOF structure $\left(k_1 = k_2 = 1600, c_1 = c_2 = 4, \varepsilon_1 = 2, \varepsilon_2 = 0.5, S_1 = 50\right)$ with damping and stiffness nonlinearities. Comparison with Monte Carlo data (5000 realizations).

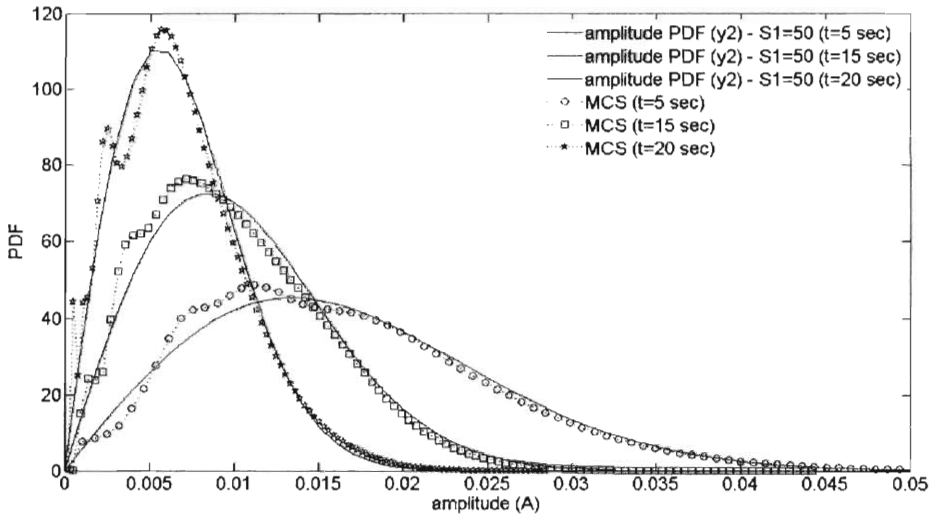

Fig.(3.7). Non-stationary response amplitude PDF of the coordinate (y_2) of the 2-DOF structure $(k_1 = k_2 = 1600, c_1 = c_2 = 4, \varepsilon_1 = 2, \varepsilon_2 = 0.5, S_1 = 50)$ with damping and stiffness nonlinearities. Comparison with Monte Carlo data (5000 realizations).

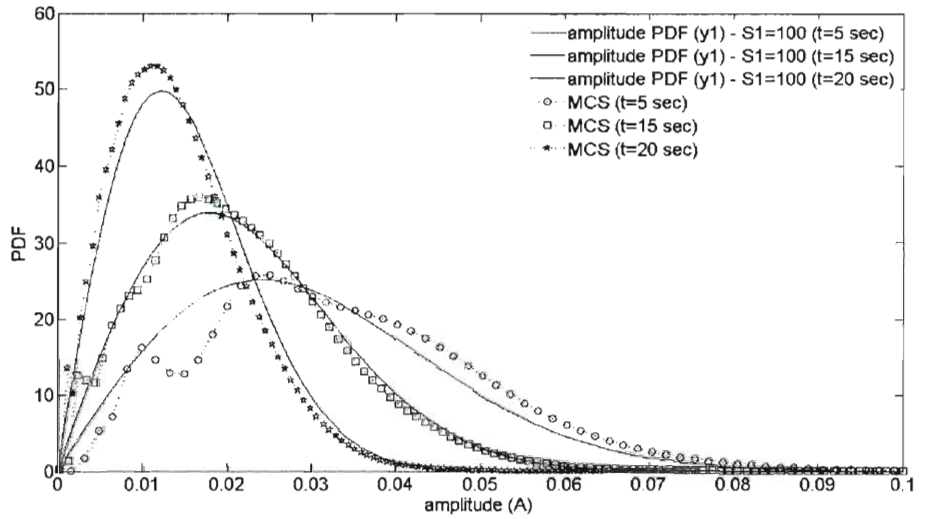

Fig.(3.8). Non-stationary response amplitude PDF of the coordinate (y_1) of the 2-DOF structure $(k_1 = k_2 = 1600, c_1 = c_2 = 4, \varepsilon_1 = 2, \varepsilon_2 = 0.5, S_1 = 100)$ with damping and stiffness nonlinearities. Comparison with Monte Carlo data (5000 realizations).

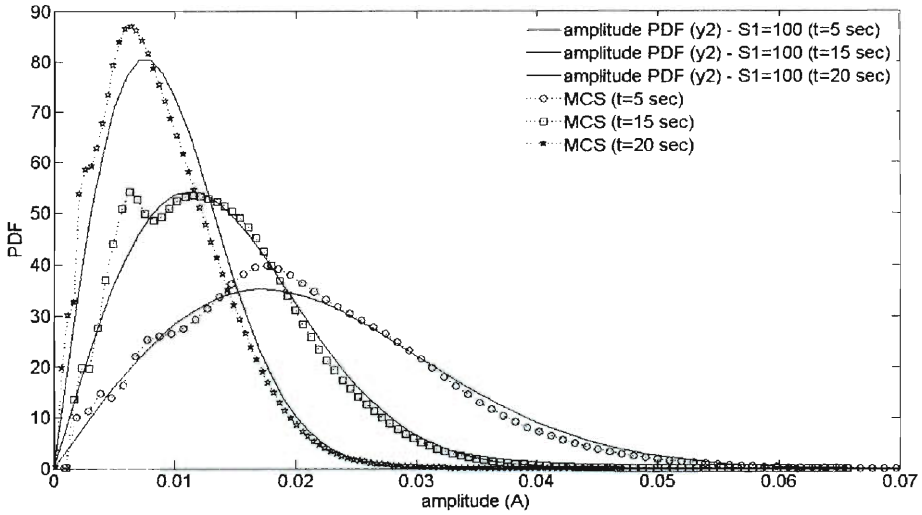

Fig.(3.9). Non-stationary response amplitude PDF of the coordinate (y_2) of the 2-DOF structure $(k_1 = k_2 = 1600, c_1 = c_2 = 4, \varepsilon_1 = 2, \varepsilon_2 = 0.5, S_1 = 100)$ with damping and stiffness nonlinearities. Comparison with Monte Carlo data (5000 realizations).

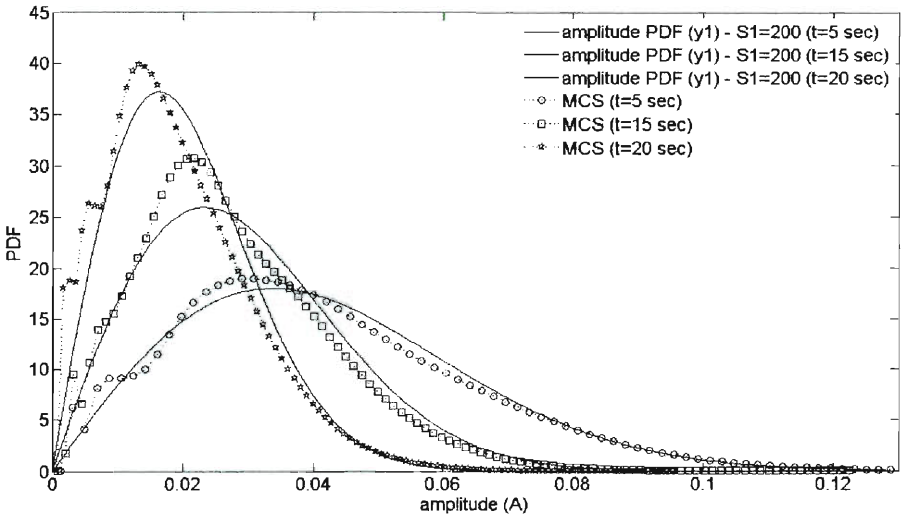

Fig.(3.10). Non-stationary response amplitude PDF of the coordinate (y_1) of the 2-DOF structure $(k_1 = k_2 = 1600, c_1 = c_2 = 4, \varepsilon_1 = 2, \varepsilon_2 = 0.5, S_1 = 200)$ with damping and stiffness nonlinearities. Comparison with Monte Carlo data (5000 realizations).

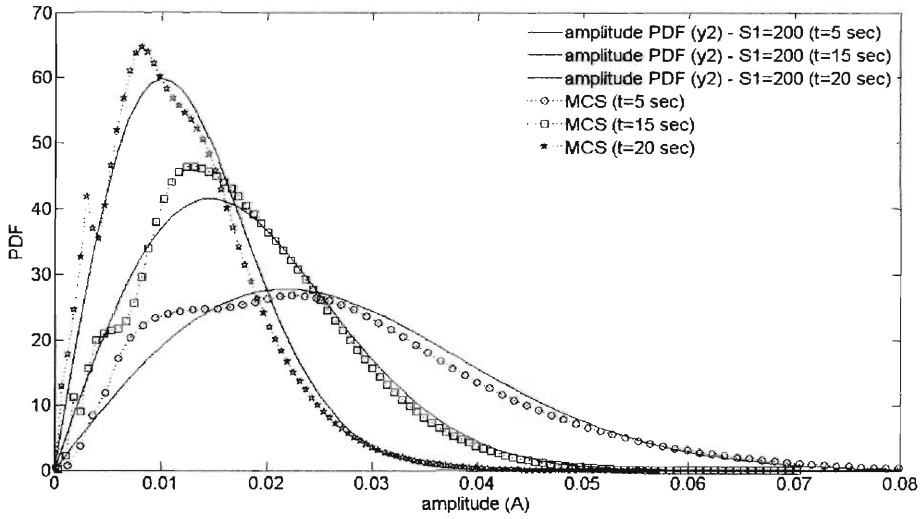

Fig.(3.11). Non-stationary response amplitude PDF of the coordinate (y_2) of the 2-DOF structure $(k_1 = k_2 = 1600, c_1 = c_2 = 4, \varepsilon_1 = 2, \varepsilon_2 = 0.5, S_1 = 200)$ with damping and stiffness nonlinearities. Comparison with Monte Carlo data (5000 realizations).

3.3.2 Hysteretic nonlinearities

Under severe earthquake excitations structures become nonlinear and inelastic with restoring forces depending on the time history of the response. This memory-dependent relationship between force and deformation is generally described in the literature by the term hysteresis. A mathematical description of various existing models of hysteresis can be found in Macki et al. (1993) and in Bertotti and Mayergoyz (2003). The introduction of the smooth and versatile Bouc-Wen hysteretic model (Bouc, 1967; Wen, 1976) was followed by its successful application to numerous structural dynamics related fields. Besides its versatility in efficiently capturing a broad range of hysteretic behaviors, the model is also capable of explicitly computing equivalent linear elements. Specifically, a statistical linearization method (e.g. Roberts and Spanos, 2003) was proposed by

Wen (1980) where closed form expressions were derived for the equivalent linear elements of the Bouc-Wen model. A detailed presentation of the applications and the extensions of the Bouc-Wen model can be found in Ikhouane and Rodellar (2007, 2009) and in review articles such as the ones by Wen (1986, 1989).

Consider next the 2 DOF building model introduced in section 3.3.1. In this case the nonlinearity consists of the hysteretic restoring forces described by the Bouc-Wen model. Introducing the same coordinates transformations as in Eqs.(3.28-3.29), Eq.(3.1) becomes (e.g. Roberts and Spanos, 2003)

$$M\underline{\ddot{y}} + C\underline{\dot{y}} + K\underline{y} + \underline{g}(\underline{y}, \underline{\dot{y}}) = \underline{F}(t), \tag{3.41}$$

where

$$\underline{y} = \begin{pmatrix} y_1 \\ y_2 \\ z_1 \\ z_2 \end{pmatrix}, \tag{3.42}$$

$$M = \begin{bmatrix} 1 & 0 & 0 & 0 \\ 1 & 1 & 0 & 0 \\ 0 & 0 & 0 & 0 \\ 0 & 0 & 0 & 0 \end{bmatrix}, \tag{3.43}$$

$$C = \begin{bmatrix} c_1 & -c_2 & 0 & 0 \\ 0 & c_2 & 0 & 0 \\ 0 & 0 & 1 & 0 \\ 0 & 0 & 0 & 1 \end{bmatrix}, \tag{3.44}$$

$$K = \begin{bmatrix} ak_1 & -ak_2 & (1-a)k_1 & -(1-a)k_2 \\ 0 & ak_2 & 0 & (1-a)k_2 \\ 0 & 0 & 0 & 0 \\ 0 & 0 & 0 & 0 \end{bmatrix}, \tag{3.45}$$

$$\underline{F}(t)=\begin{pmatrix} f(t) \\ f(t) \\ 0 \\ 0 \end{pmatrix}, \tag{3.46}$$

and

$$\underline{g}(\underline{y},\underline{\dot{y}})=\begin{pmatrix} 0 \\ 0 \\ -g_1(\dot{y}_1,z_1) \\ -g_2(\dot{y}_2,z_2) \end{pmatrix}. \tag{3.47}$$

where (a) represents the "rigidity ratio" and can be viewed as a form of post-yield to pre-yield stiffness ratio. It can be readily seen that in the Bouc-Wen model the additional state (z_i) is related to the displacement (y_i) via the differential equation

$$\dot{z}_i = g_i(\dot{y}_i, z_i), \tag{3.48}$$

where

$$g_i(\dot{y}_i, z_i) = -\gamma|\dot{y}_i|z_i|z_i|^{n-1} - \beta\dot{y}_i|z_i|^n + A\dot{y}_i, \tag{3.49}$$

where the constant parameters (γ), (β), (A) and (n) are capable of representing a wide range of hysteresis loops, including softening and hardening behaviors. Following a statistical linearization approach (Wen, 1980; Roberts and Spanos, 2003) the equivalent linear matrices (C_e) and (K_e) become

$$C_e=\begin{bmatrix} 0 & 0 & 0 & 0 \\ 0 & 0 & 0 & 0 \\ c_{e1} & 0 & 0 & 0 \\ 0 & c_{e2} & 0 & 0 \end{bmatrix}, \tag{3.50}$$

and

$$K_e = \begin{bmatrix} 0 & 0 & 0 & 0 \\ 0 & 0 & 0 & 0 \\ 0 & 0 & k_{e1} & 0 \\ 0 & 0 & 0 & k_{e2} \end{bmatrix}, \tag{3.51}$$

respectively. For the special case of $(n=1)$, the elements (c_{ei}) and (k_{ei}) are given by the expressions

$$c_{ei} = \sqrt{\frac{2}{\pi}} \left[\gamma \frac{E(\dot{y}_i z_i)}{\sqrt{E(\dot{y}_i^2)}} + \beta \sqrt{E(z_i^2)} \right] - A, \tag{3.52}$$

and

$$k_{ei} = \sqrt{\frac{2}{\pi}} \left[\gamma \sqrt{E(\dot{y}_i^2)} + \beta \frac{E(\dot{y}_i z_i)}{\sqrt{E(z_i^2)}} \right]. \tag{3.53}$$

Note that more complicated expressions can be derived for the equivalent linear elements for the case of $(n \neq 1)$ (e.g. Wen, 1980). Further, the excitation EPS $(S_f(\omega,t))$ of Eq.(3.15) is assumed to have the non-separable form

$$S(\omega,t) = S_2 \left(\frac{\omega}{15\pi} \right)^2 e^{-0.2t} t^2 e^{-\left(\frac{\omega}{15\pi}\right)^2 t}, \quad t \geq 0, \quad -\infty < \omega < \infty. \tag{3.54}$$

This spectrum comprises some of the main characteristics of seismic shaking, such as decreasing of the dominant frequency with time (e.g. Liu, 1970; Spanos and Solomos, 1983). Realization records compatible with Eq.(3.54) are produced using the concept of spectral representation of a stochastic process (e.g. Shinozuka and Deodatis, 1991; Liang et al., 2007). For the case $(S_1 = 1)$ the non-separable EPS is plotted in Fig.(3.12).

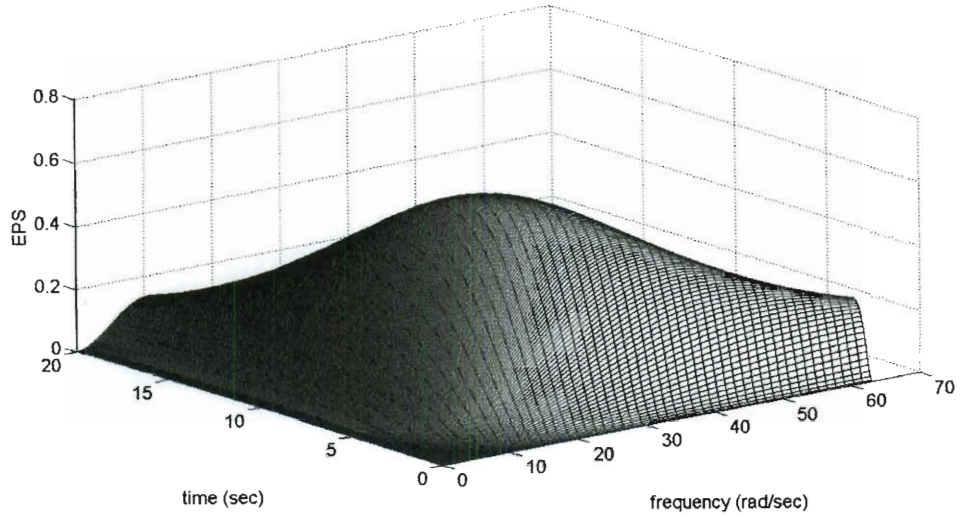

Fig.(3.12). Non-separable evolutionary power spectrum $(S_2 = 1)$.

Further, the parameters values to be used in the numerical examples are chosen to be $(k_1 = k_2 = 1600, c_1 = c_2 = 4, \gamma = \beta = 0.5, A = 1, a = 0.1)$. To demonstrate the reliability of the approach, various excitation magnitude levels are chosen, namely $(S_2 = 50, 100, 200)$. In Figs.(3.13-3.14) it is shown that the evolutionary response variances for the (y_1) and (y_2) coordinates, respectively, capture successfully the time-dependent behavior for the different excitation magnitude levels. Comparisons with Monte Carlo data verify the above argument. In Figs.(3.15) and (3.16) the damping elements and the natural frequencies of the effective LTV SDOF systems are plotted, respectively. In Figs.(3.17) and (3.18) the non-stationary response amplitude PDF (Eq.(3.26)) is plotted for different time instants for the coordinates (y_1) and (y_2), respectively, and for an excitation magnitude equal to $(S_2 = 50)$. Similarly, in Figs.(3.19) and (3.20) the

non-stationary response amplitude PDF is plotted for the coordinates (y_1) and (y_2), respectively, whereas the excitation magnitude is equal to $(S_2 = 100)$. Finally, in Figs.(3.21) and (3.22) the non-stationary response amplitude PDF is plotted for the coordinates (y_1) and (y_2), respectively, whereas the excitation magnitude is equal to $(S_2 = 200)$.

Evidently, comparisons with Monte Carlo simulation data demonstrate an adequate degree of accuracy for all the various excitation magnitude levels. In fact, the accuracy achieved justifies the choice of the time-dependent Rayleigh PDF (Eq.(3.26)) to approximate the non-stationary response amplitude PDF and renders the approach suitable even for cases of excitations possessing non-separable EPS, such as the one given by Eq.(3.54).

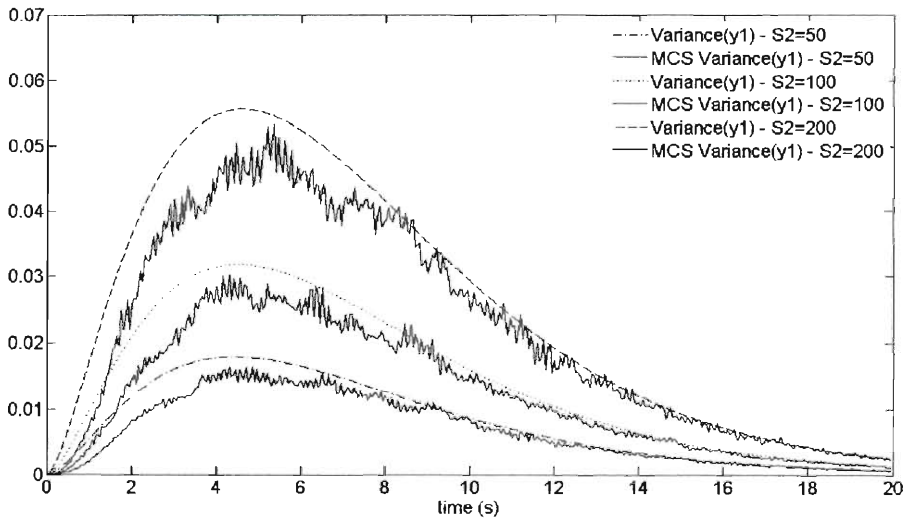

Fig.(3.13). Response variance of the coordinate (y_1) of a 2-DOF structure $(k_1 = k_2 = 1600, c_1 = c_2 = 4, \gamma = \beta = 0.5, A = 1, a = 0.1)$ with hysteretic (Bouc-Wen) nonlinearities. Comparison with Monte Carlo data (500 realizations).

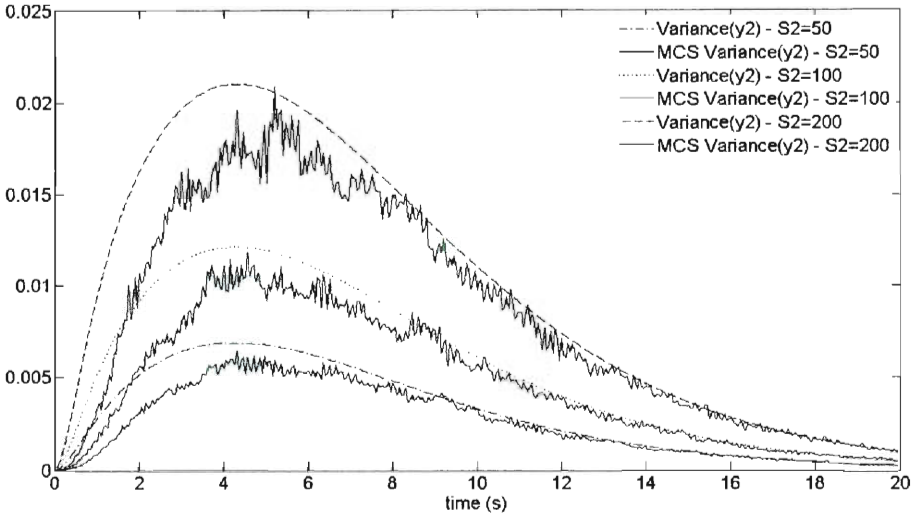

Fig.(3.14). Response variance of the coordinate (y_2) of a 2-DOF structure $(k_1 = k_2 = 1600, c_1 = c_2 = 4, \gamma = \beta = 0.5, A = 1, a = 0.1)$ with hysteretic (Bouc-Wen) nonlinearities. Comparison with Monte Carlo data (500 realizations).

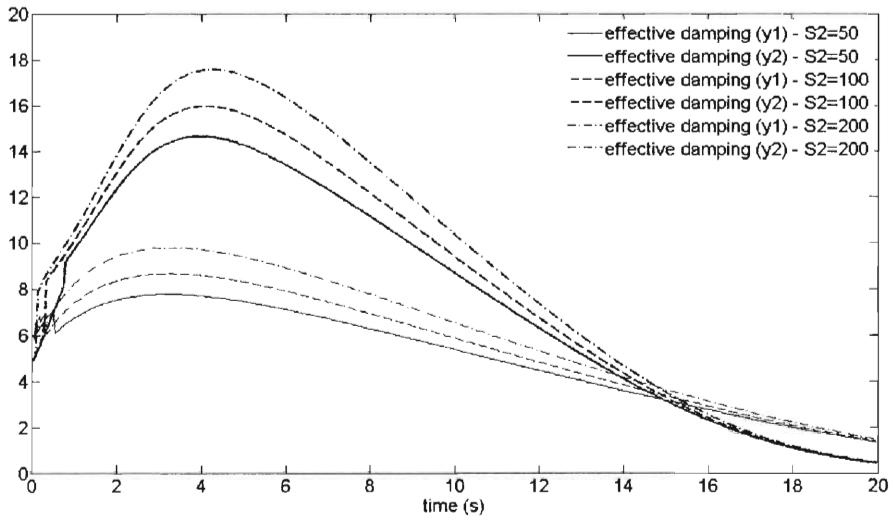

Fig.(3.15). Damping values of the effective LTV SDOF systems corresponding to the 2-DOF structure $(k_1 = k_2 = 1600, c_1 = c_2 = 4, \gamma = \beta = 0.5, A = 1, a = 0.1)$ with hysteretic (Bouc-Wen) nonlinearities.

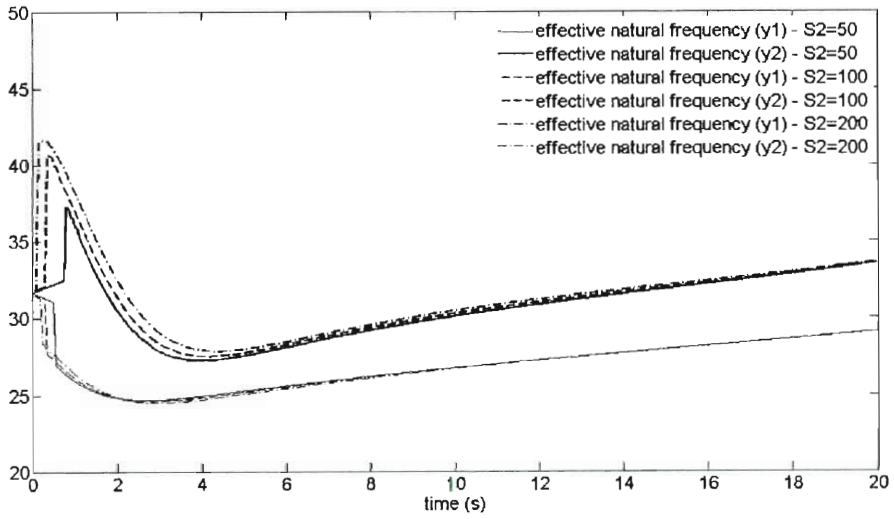

Fig.(3.16). Natural frequency values of the effective LTV SDOF systems corresponding to the 2-DOF structure $\left(k_1 = k_2 = 1600, c_1 = c_2 = 4, \gamma = \beta = 0.5, A = 1, a = 0.1\right)$ with hysteretic (Bouc-Wen) nonlinearities.

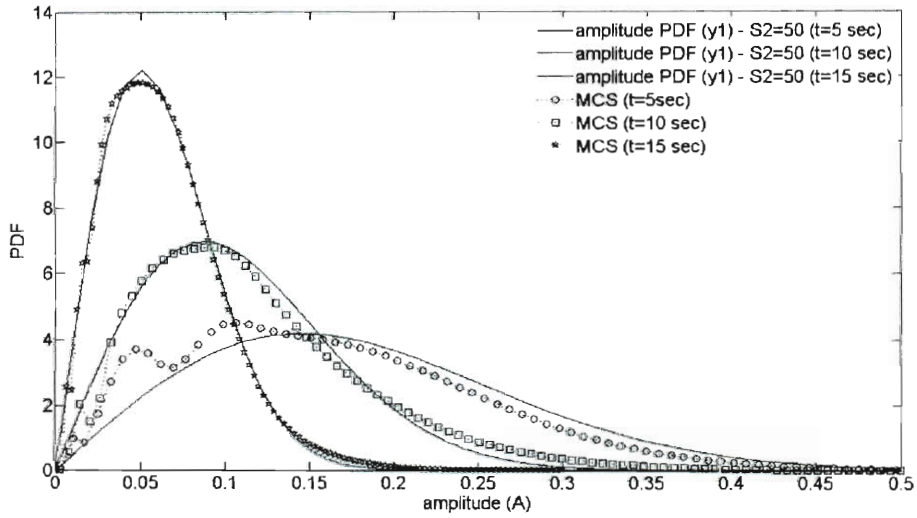

Fig.(3.17). Non-stationary response amplitude PDF of the coordinate $\left(y_1\right)$ of the 2-DOF structure $\left(k_1 = k_2 = 1600, c_1 = c_2 = 4, \gamma = \beta = 0.5, A = 1, a = 0.1\right)$ with hysteretic (Bouc-Wen) nonlinearities. Comparison with Monte Carlo data (5000 realizations).

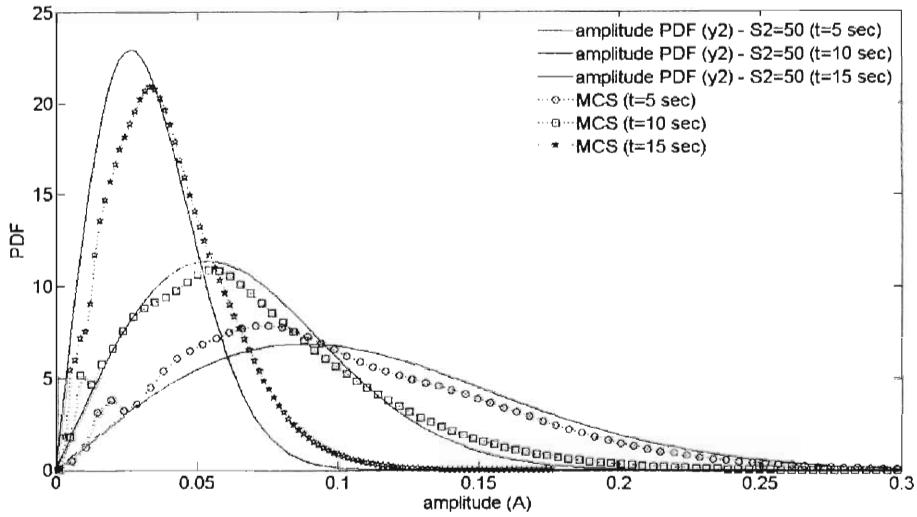

Fig.(3.18). Non-stationary response amplitude PDF of the coordinate (y_2) of the 2-DOF structure $(k_1 = k_2 = 1600, c_1 = c_2 = 4, \gamma = \beta = 0.5, A = 1, a = 0.1)$ with hysteretic (Bouc-Wen) nonlinearities. Comparison with Monte Carlo data (5000 realizations).

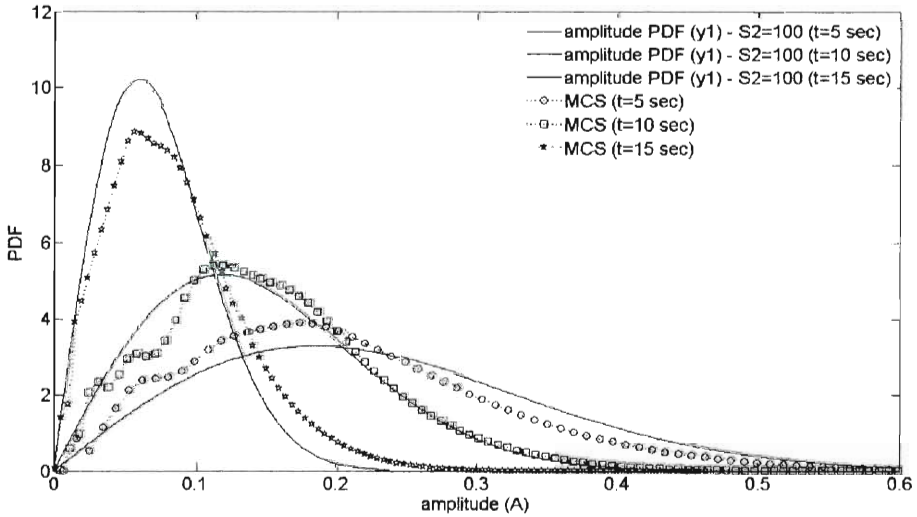

Fig.(3.19). Non-stationary response amplitude PDF of the coordinate (y_1) of the 2-DOF structure $(k_1 = k_2 = 1600, c_1 = c_2 = 4, \gamma = \beta = 0.5, A = 1, a = 0.1)$ with hysteretic (Bouc-Wen) nonlinearities. Comparison with Monte Carlo data (5000 realizations).

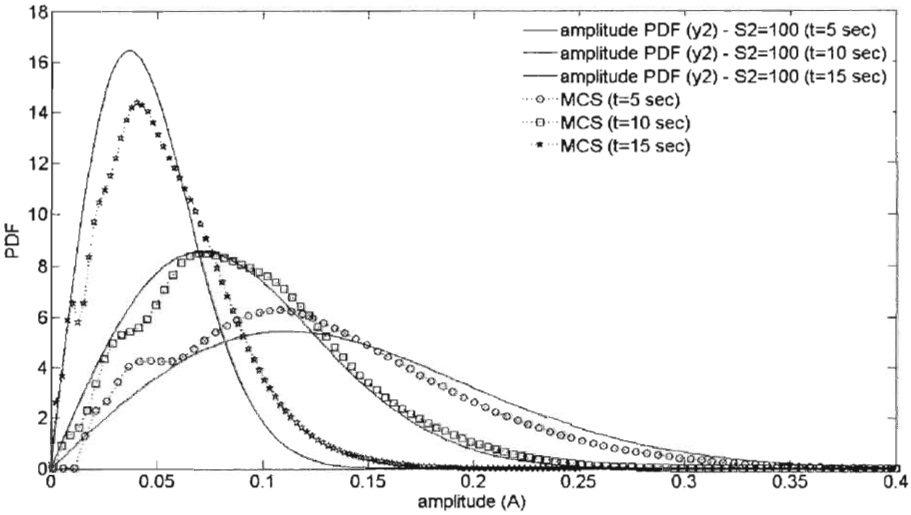

Fig.(3.20). Non-stationary response amplitude PDF of the coordinate (y_2) of the 2-DOF structure $(k_1 = k_2 = 1600, c_1 = c_2 = 4, \gamma = \beta = 0.5, A = 1, a = 0.1)$ with hysteretic (Bouc-Wen) nonlinearities. Comparison with Monte Carlo data (5000 realizations).

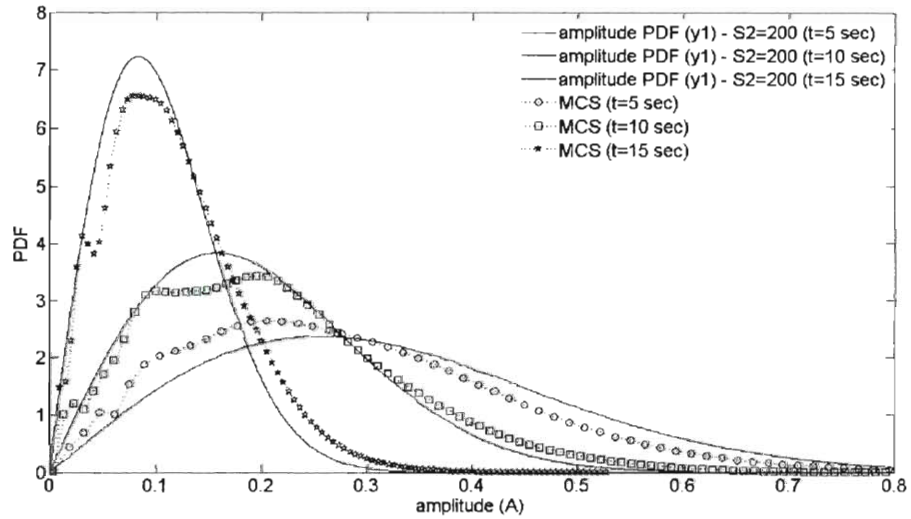

Fig.(3.21). Non-stationary response amplitude PDF of the coordinate (y_1) of the 2-DOF structure $(k_1 = k_2 = 1600, c_1 = c_2 = 4, \gamma = \beta = 0.5, A = 1, a = 0.1)$ with hysteretic (Bouc-Wen) nonlinearities. Comparison with Monte Carlo data (5000 realizations).

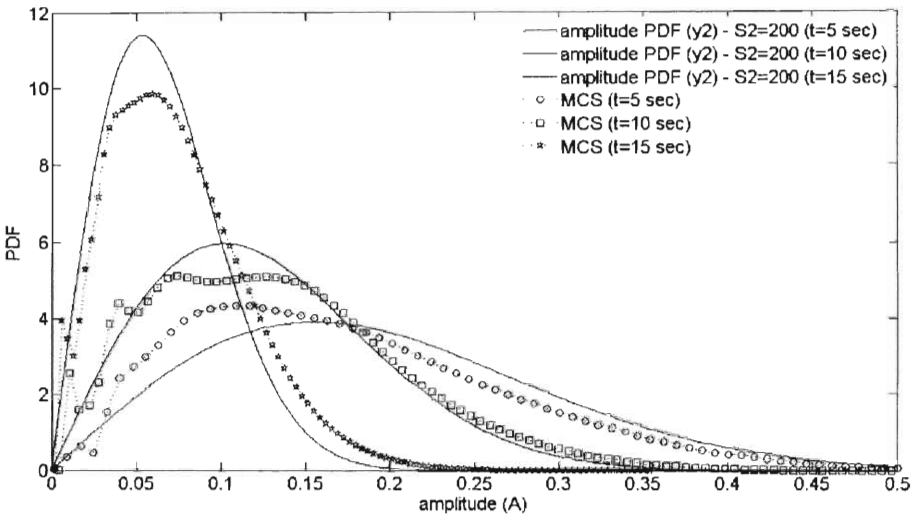

Fig.(3.22). Non-stationary response amplitude PDF of the coordinate (y_2) of the 2-DOF structure $(k_1 = k_2 = 1600, c_1 = c_2 = 4, \gamma = \beta = 0.5, A = 1, a = 0.1)$ with hysteretic (Bouc-Wen) nonlinearities. Comparison with Monte Carlo data (5000 realizations).

Chapter 4

Response and first-passage analysis via a numerical Wiener path integral approach – Classical oscillators

4.1 Preliminary remarks

A persistent challenge in the area of modern stochastic dynamics is the determination of the probability that the system response stays within a prescribed domain within a specified time interval. Such a reliability-based analysis can be beneficial in terms of safety or risk assessment. An alternative equivalent definition of the aforementioned question, known as the first-passage problem, is the evaluation of the probability the response of the system reaches, and possibly crosses, a predetermined level for the first time. Attempts to address the first-passage problem range from the ones which include derivation of exact solutions (e.g. Kovaleva, 2009) to the more numerical ones (e.g. Pichler and Pradlwarter, 2008).

Recently, numerical approaches based on the concept of the Wiener path integral have emerged in the area of engineering mechanics. The notion of path integral was introduced by Wiener (1930) as an approach to solve problems in the theory of Brownian motion. A numerical version of the path integral solution (PIS) has been used in engineering applications to derive response and reliability statistics of nonlinear oscillators. Most of the developed PIS approaches constitute, in essence, a discrete version of the well-known Chapman-

Kolmogorov (C-K) equation which is associated with Markov processes (e.g. Arnold, 1974; Gardiner, 1985). The basic feature of the approach is that the evolution of the response probability density function (PDF) is computed in short time steps, assuming a Gaussian form for the conditional response PDF. Although it was shown in Dekker (1976) that the Gaussian distribution leads to the original Fokker-Planck (F-P) equation in an exact manner, this choice is not restrictive (e.g. Langouche et al., 1979; Risken, 1984; Naess and Moe, 1996). It was Wehner and Wolfer (1983a, 1983b, 1987) who first developed certain numerical aspects of the approach and established it as a robust numerical tool. A PIS approach was employed in Naess and Johnsen (1993) to yield response statistics of nonlinear offshore structures and was further used in Naess and Moe (1996) to determine the non-stationary response of a hysteretic bilinear oscillator subject to time-modulated white noise excitation. Lin and Yim (1996) employed a PIS approach to derive rocking responses of rigid bodies. Moreover, the Gauss-Legendre integration scheme developed in Yu et al. (1997) was applied in Xie et al. (2005) to study a Rayleigh-Duffing oscillator under harmonic and stochastic excitation. Recently, Mamontov and Naess (2009) developed the successive-transition method, essentially a PIS approach based on an analytical approximation of the conditional PDF. Futher, Di Paola and Santoro (2008) extended the approach to cope with Poisson white noise excitation (see also Pirrotta and Santoro, 2010). Note that the great accuracy achieved at the tails of the computed response PDF (e.g. Naess and Moe, 2000) indicates the suitability of the approach for reliability-

based analyses (e.g. Grigoriu, 1990; Cai and Lin, 1998; Iourtchenko et al., 2008; Naess et al., 2010).

In this chapter, a general PIS framework is developed based on statistical linearization and on stochastic averaging to perform response and reliability analyses of a broad class of nonlinear oscillators. Specifically, relying on the Markov properties of the response process and on a discrete version of the C-K equation, response envelope and first-passage PDFs are derived. This is done for the Van der Pol, the Duffing, and the Preisach oscillators under broad-band evolutionary excitation. The validity of the proposed approach in the case where the excitation deviates from being white noise is discussed and its accuracy is demonstrated by comparisons to Monte Carlo data.

4.2 Mathematical formulation

Consider a nonlinear single-degree-of-freedom system whose motion is governed by the differential equation

$$\ddot{x} + \beta\dot{x} + z(t, x, \dot{x}) = w(t), \tag{4.1}$$

where a dot over a variable denotes differentiation with respect to time (t); $(z(t, x, \dot{x}))$ is the restoring force which could be either hysteretic or depend only on the instantaneous values of (x) and $(\dot{x})$; (β) is a linear damping coefficient; and $(w(t))$ represents a Gaussian, zero-mean non-stationary random process possessing an evolutionary broad-band power spectrum, $S(\omega,t)$.

Adopting the assumption of a lightly damped system, it can be argued that the nonlinear oscillator (Eq.(4.1)) exhibits a pseudo-harmonic behavior described by the equations

$$x(t) = A(t)\cos\left[\omega(A)t + \phi(t)\right], \tag{4.2}$$

and

$$\dot{x}(t) = -\omega(A)A(t)\sin\left[\omega(A)t + \phi(t)\right], \tag{4.3}$$

in which the response amplitude envelope (A) is a slowly varying function with respect to time and, thus, can be treated as a constant over one cycle of oscillation.

Further, following an statistical linearization approach discussed in Kougioumtzoglou and Spanos (2009) and in Roberts and Spanos (2003), a linearized counterpart of Eq.(4.1) is

$$\ddot{x} + \beta(\mathrm{A})\dot{x} + \omega^2(\mathrm{A})x = w(t), \tag{4.4}$$

where the equivalent damping element and the natural frequency are given by the expressions

$$\beta(\mathrm{A}) = \beta + \frac{\oint \dot{x}z dt}{\oint \dot{x}^2 dt}, \tag{4.5}$$

and

$$\omega^2(\mathrm{A}) = \frac{\oint xz dt}{\oint x^2 dt}. \tag{4.6}$$

Substituting Eq.(4.2) and Eq.(4.3) into Eq.(4.5) and Eq.(4.6) and considering $\left(A(t)\right)$ and $\left(\phi(t)\right)$ constant over one cycle yields

$$\beta(A) = \beta + \frac{S(A)}{A\omega(A)}, \tag{4.7}$$

and

$$\omega^2(A) = \frac{C(A)}{A}, \tag{4.8}$$

where

$$C(A) = \frac{1}{\pi}\int_0^{2\pi} \cos[\psi] z(t, A\cos\psi, -\omega(A)A\sin\psi) d\psi\,, \tag{4.9}$$

and

$$S(A) = -\frac{1}{\pi}\int_0^{2\pi} \sin[\psi] z(t, A\cos\psi, -\omega(A)A\sin\psi) d\psi\,. \tag{4.10}$$

Focusing on Eq.(4.2) and Eq.(4.3), the amplitude (A) and phase (ϕ) can be expressed by the equations

$$A^2(t) = x^2(t) + \left(\frac{\dot{x}(t)}{\omega(A)}\right)^2, \tag{4.11}$$

and

$$\phi(t) = -\omega(A)t - \tan^{-1}\left(\frac{\dot{x}(t)}{\omega(A)x(t)}\right). \tag{4.12}$$

Differentiating Eq.(4.2) and Eq.(4.3) and taking into account Eq.(4.1) yields

$$\dot{A}(t) = -\beta(A)A(t)\sin^2[\omega(A)t + \phi(t)] - \frac{w(t)}{\omega(A)}\sin[\omega(A)t + \phi(t)]\,. \tag{4.13}$$

Relying once more on the assumption of light damping, further simplification of Eq.(4.13) is achieved by a combination of deterministic and stochastic averaging (e.g. Roberts and Spanos, 1986; Zhu, 1988). This yields the (Ito) stochastic differential equation

$$\dot{A} = K_1(A,t) + K_2(A,t)\eta(t)\,, \tag{4.14}$$

where

$$K_1(A,t) = -\frac{1}{2}\beta(A)A(t) + \frac{\pi S(\omega(A),t)}{2A(t)\omega^2(A)}, \tag{4.15}$$

and

$$K_2(A,t) = \frac{\left(\pi S(\omega(A),t)\right)^{1/2}}{\omega(A)}, \tag{4.16}$$

which governs approximately the evolution in time of the amplitude $(A(t))$. In Eq.(4.14), $\eta(t)$ is a zero mean and delta correlated process of intensity one, i.e., $E(\eta(t)) = 0$; and $E(\eta(t)\eta(t+\tau)) = \delta(\tau)$, with $(\delta(\tau))$ being the Dirac delta function. The Fokker-Planck (F-P) equation which corresponds to Eq.(4.14) takes the form (e.g. Arnold, 1974; Gardiner, 1985)

$$\begin{aligned}\frac{\partial}{\partial t}p(A,t\,|\,A',t') &= -\frac{\partial}{\partial A}\left[K_1(A,t)\,p(A,t\,|\,A',t')\right] + \ldots \\ &\frac{1}{2}\frac{\partial^2}{\partial A^2}\left[K_2^2(A,t)\,p(A,t\,|\,A',t')\right].\end{aligned} \tag{4.17}$$

The importance of Eq.(4.14) relates to the fact that it is decoupled from the phase $(\phi(t))$. Thus, it is feasible to model the amplitude process $(A(t))$ as a one-dimensional Markov diffusion process (e.g. Arnold, 1974; Gardiner, 1985; Soong and Grigoriu, 1993). Therefore, since the response amplitude of the oscillator (Eq.(4.1)) is treated as a Markov process, the C-K equation

$$p(A,t+2\Delta t\,|\,A'',t) = \int_0^\infty p(A,t+2\Delta t\,|\,A',t+\Delta t)\,p(A',t+\Delta t\,|\,A'',t)\,dA', \tag{4.18}$$

is satisfied (e.g. Soong, 1973), where $\left(p(A,t+\Delta t\,|\,A',t)\right)$ represents the conditional PDF of the response amplitude process. Next, following a procedure described in Iourtchenko et al. (2008) the evaluation of the reliability function $\left(R_B(T)\right)$ is possible. This is defined as the probability the system response

amplitude stays below the threshold (B) over the time interval $[t_0, T]$. Further, the corresponding first-passage time PDF, namely the time at which the response amplitude crosses the prescribed boundary for the first time, is obtained as

$$p_B(T) = -\frac{dR_B(T)}{dT}. \tag{4.19}$$

Specifically, assuming that the time interval $[t_0, T]$ under consideration is discretized such as $t_j = t_0 + (j-1)\Delta t, \quad j = 1,..,n$ and $\Delta t = (T - t_0)/(n-1)$, and considering an initial PDF $(p(A_1, t_1))$, the reliability function $(R_B(t_j))$ becomes

$$R_B(t_j) = \int_0^B p(A_j, t_j \mid A_{j-1}, t_{j-1}) \ldots \int_0^B p(A_2, t_2 \mid A_1, t_1)\, p(A_1, t_1) dA_2 \cdots dA_j \,. \tag{4.20}$$

It can be readily seen that knowledge of the conditional PDF is adequate to evaluate Eqs.(4.20) and (4.19) using Eq.(4.18). The interesting part about the F-P Eq.(4.17) is that the conditional PDF $p(A, t + \Delta t \mid A', t)$, often called short-time propagator, has been shown to follow a Gaussian distribution of the form

$$p(A, t + \Delta t \mid A', t) = \frac{1}{\sqrt{2\pi K_2^2(A', t)\Delta t}} \exp\left(-\frac{(A - A' - K_1(A', t)\Delta t)^2}{2K_2^2(A', t)\Delta t} \right). \tag{4.21}$$

In fact, in Dekker (1976) it was shown that Eq.(4.21) together with Eq.(4.18) lead in an exact manner to the general nonlinear F-P Eq.(4.17).

4.3 Numerical examples

In the numerical applications following, the evolutionary non-separable power spectrum of the form

$$S(\omega,t)=S_1\left(\frac{\omega}{5\pi}\right)^2 e^{-0.15t}t^2e^{-\left(\frac{\omega}{5\pi}\right)^2 t}, \quad t\geq 0, \quad -\infty<\omega<\infty, \tag{4.22}$$

is chosen to illustrate the ability of the PIS approach to cope with non-white excitations which, however, retain the attribute of being broad-band. This spectrum (Fig.(4.1)) comprises some of the main characteristics of seismic shaking, such as decreasing of the dominant frequency with time (Liu, 1970; Spanos and Solomos, 1983).

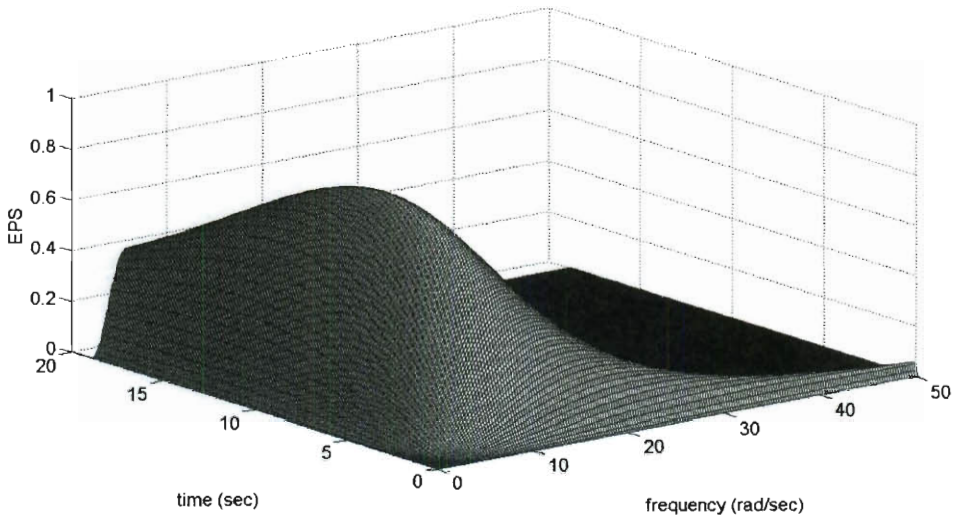

Fig.(4.1). Non-separable evolutionary excitation spectrum $(S_1=1)$

Realizations compatible with Eq.(4.22) are produced using the concept of spectral representation of a stochastic process. In this regard, a representation of

the non-stationary process $\left(z_{non}(t)\right)$ takes the form (Shinozuka and Deodatis, 1988; Spanos and Zeldin, 1998; Liang et al., 2007)

$$z_{non}(t)=\sum_{n=0}^{N-1}\sqrt{4S_{z_{non}}(n\Delta\omega,t)\Delta\omega}\cos\left(\left(n\Delta\omega\right)t+\phi_n\right), \tag{4.23}$$

where $\left(\phi_0,\phi_1,...\phi_{N-1}\right)$ are independent random phases which follow a uniform distribution over the interval $[0,2\pi]$; and $\left(S_{z_{non}}(\omega,t)\right)$ is the evolutionary power spectrum (EPS) of the non-stationary process $\left(z_{non}(t)\right)$.

As far as numerical implementation issues and convergence criteria are concerned, Wehner and Wolfer (1983a) provided an extended discussion on conditions to be satisfied for the values of the time increment and the grid size. Moreover, it can be readily seen that for the case of the response amplitude process, the origin is a reflecting boundary and the drift coefficient $K_1(A,t)$ experiences a singularity at $\left(A=0\right)$, namely a potential reason for numerical errors. The same situation was experienced in Naess and Moe (1996), where they tried to avoid the problem by exploiting the non-uniqueness of the conditional response PDF (e.g. Langouche et al., 1979; Risken, 1984). However, despite the singularity, the Gaussian conditional PDF (Eq.(4.21)) led to the same level of accuracy as the other alternatives.

In the following examples the value of 0.01 is chosen for the ratio of critical damping $\left(\zeta\right)$, whereas the barrier level value $\left(B\right)$ is expressed as a fraction of the maximum value of the non-stationary standard deviation of the response. Further, the initial distribution chosen for the response amplitude PDF

is the Dirac delta function, namely $\left(p(A,t=0)=\delta(A)\right)$, assuming that the system is initially at rest. For each Monte Carlo simulation, an ensemble average of 5000 realizations is used.

4.3.1 Van der Pol Oscillator

As a first application, a stochastically excited Van der Pol oscillator is considered whose equation of motion is given by

$$\ddot{x}+\beta\left(-1+\varepsilon x^2\right)\dot{x}+\omega_0^2 x=w(t), \qquad \varepsilon>0. \tag{4.24}$$

Then, using Eq.(4.7) and Eq.(4.8) yields

$$\beta(A)=\beta\left(-1+\varepsilon\frac{A^2}{4}\right), \tag{4.25}$$

and

$$\omega^2(A)=\omega_0^2. \tag{4.26}$$

In Fig.(4.2) and in Fig.(4.3) the response amplitude PDFs corresponding to the parameter values $\left(S_1=0.5,\omega_0^2=10,\varepsilon=2\right)$ and $\left(S_1=1,\omega_0^2=10,\varepsilon=2\right)$ respectively, are plotted for different time instants. It can be readily seen that the PIS approach yields quite accurate and reliable results for the two different excitation levels despite the non-white character of the excitation. Comparisons between the first-passage PDFs obtained via Monte Carlo simulation and the first-passage PDFs computed via the PIS approach for different barrier level values for the oscillator with parameter values $\left(S_1=1,\omega_0^2=10,\varepsilon=2\right)$ are shown in Fig.(4.4).

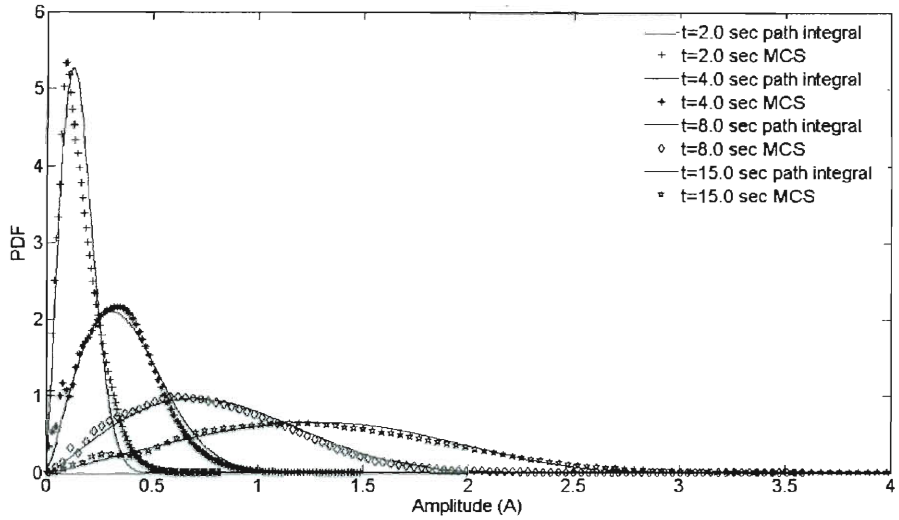

Fig.(4.2). Evaluation of $\left(p(A,t)\right)$ for a Van der Pol oscillator $\left(\varepsilon = 2, \omega_0^2 = 10\right)$ under the non-separable evolutionary excitation spectrum $\left(S_1 = 0.5\right)$. Comparison between MCS data (5000 realizations) and PIS approach.

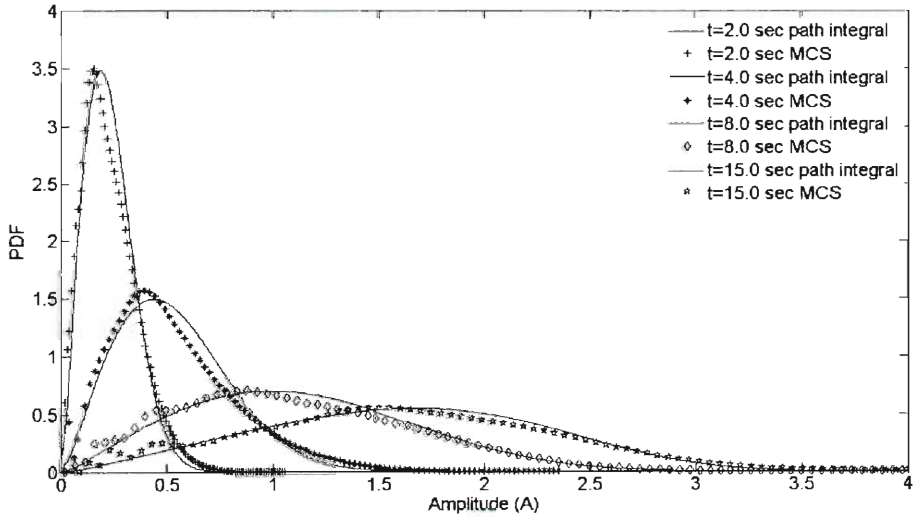

Fig.(4.3). Evaluation of $\left(p(A,t)\right)$ for a Van der Pol oscillator $\left(\varepsilon = 2, \omega_0^2 = 10\right)$ under the non-separable evolutionary excitation spectrum $\left(S_1 = 1\right)$. Comparison between MCS data (5000 realizations) and PIS approach.

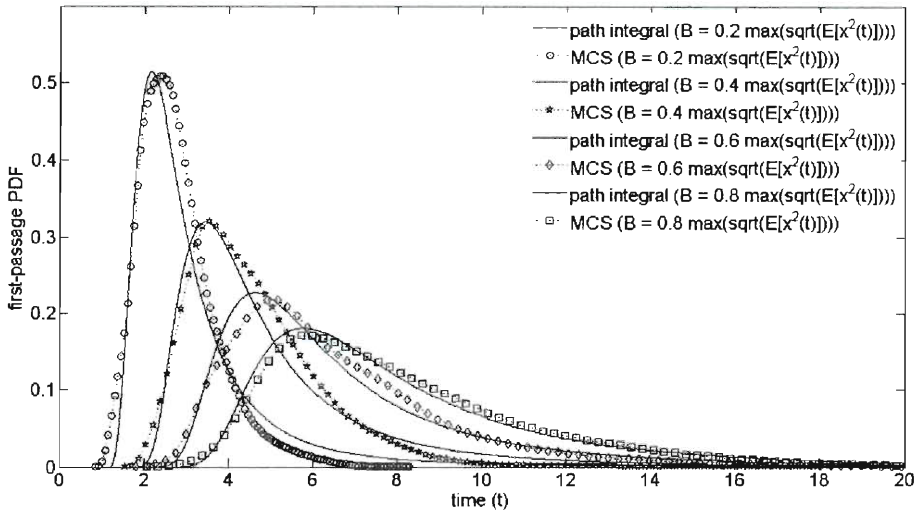

Fig.(4.4). First-Passage PDF for the Van der Pol oscillator $\left(\varepsilon = 2, S_1 = 1, \omega_0^2 = 10\right)$ under the non-separable evolutionary excitation spectrum. Comparison between MCS data (5000 realizations) and PIS approach.

4.3.2 Duffing Oscillator

Next, a stochastically excited Duffing oscillator is considered whose equation of motion is given by

$$\ddot{x} + \beta\dot{x} + \omega_0^2 x + \varepsilon\omega_0^2 x^3 = w(t), \quad \varepsilon > 0, \tag{4.27}$$

for which the function $(z(t, x, \dot{x}))$ is defined as

$$z(t, x, \dot{x}) = \omega_0^2 x + \varepsilon\omega_0^2 x^3 . \tag{4.28}$$

Then, using Eq.(4.7) and Eq.(4.8) yields

$$\beta(A) = \beta, \tag{4.29}$$

and

$$\omega^2(A) = \omega_0^2\left(1 + \frac{3}{4}\varepsilon A^2\right). \tag{4.30}$$

To illustrate the accuracy of the proposed approach the Duffing oscillator (Eq.(4.27)) subject to Gaussian white noise of the form

$$S(\omega,t)=S_0,\quad 0\le|\omega|\le\infty, \tag{4.31}$$

is considered. The purpose for this application is to compare the numerically evaluated stationary response amplitude PDF to the following analytical expression (Lin, 1967) for the stationary response amplitude PDF given by

$$p(A)=\frac{\left(A+\varepsilon A^3\right)}{\sigma^2}\exp\left(-\frac{\left(\frac{A^2}{2}+\varepsilon\frac{A^4}{4}\right)}{\sigma^2}\right),\quad \sigma^2=\frac{\pi S_0}{2\zeta\omega_0^3}. \tag{4.32}$$

In Fig.(4.5) and in Fig.(4.6) the response amplitude PDFs corresponding to the parameter values $\left(S_0=1,\omega_0^2=10,\varepsilon=0.5\right)$ and $\left(S_0=1,\omega_0^2=10,\varepsilon=1.5\right)$ respectively, are plotted for different time instants. It can be readily seen that the stationary PDF obtained by the path integral approach is in a quite good agreement with Eq.(4.32).

Advancing next to the case where the excitation power spectrum is assumed of the form of Eq.(4.22), the first-passage PDFs corresponding to parameter values $\left(S_1=1,\omega_0^2=10,\varepsilon=2\right)$ are plotted in Fig.(4.7) for various barrier level values. Comparisons with Monte Carlo simulations reveal a satisfactory level of accuracy.

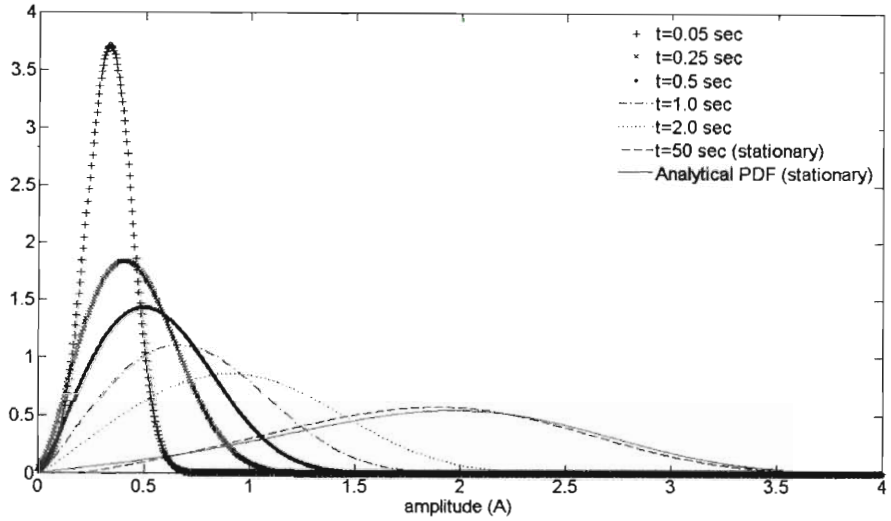

Fig.(4.5). Evaluation of $\left(p(A,t)\right)$ for a Duffing oscillator $\left(\varepsilon = 0.5, \omega_0^2 = 10\right)$ under Gaussian white noise $\left(S_0 = 1\right)$. Comparison to the analytical expression for the stationary PDF.

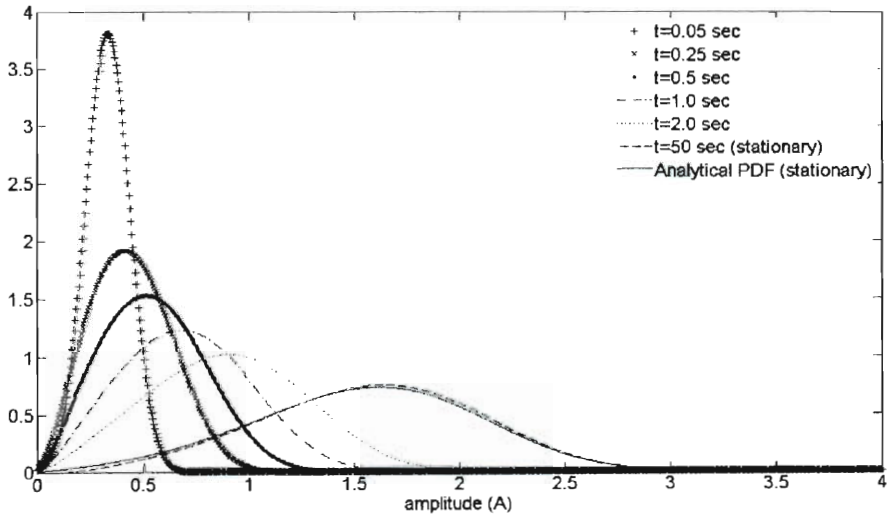

Fig.(4.6). Evaluation of $\left(p(A,t)\right)$ for a Duffing oscillator $\left(\varepsilon = 1.5, \omega_0^2 = 10\right)$ under Gaussian white noise $\left(S_0 = 1\right)$. Comparison to the analytical expression for the stationary PDF.

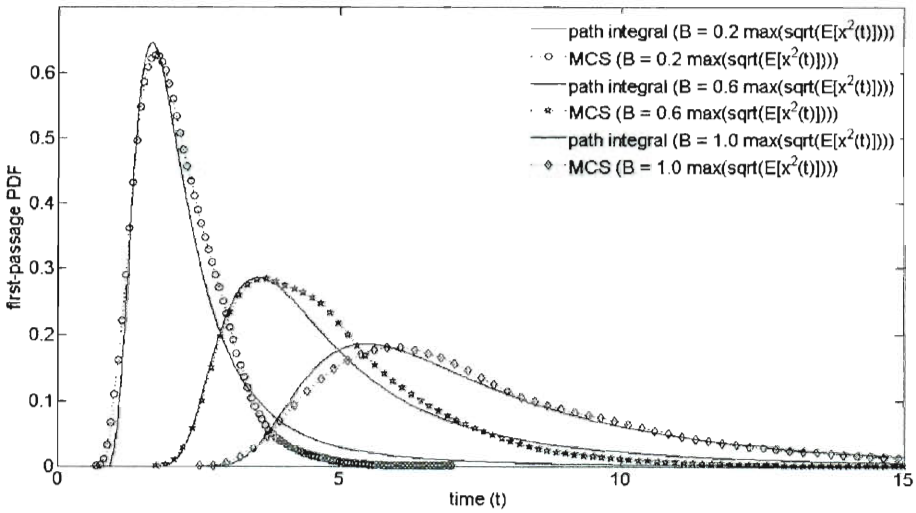

Fig.(4.7). First-Passage PDF for the Duffing oscillator $\left(\varepsilon = 2, S_1 = 1, \omega_0^2 = 10\right)$ under the non-separable evolutionary excitation spectrum. Comparison between MCS data (5000 realizations) and PIS approach.

4.3.3 Preisach Oscillator

Various kinds of hysteresis, such as magnetic, ferroelectric, mechanical and economic, encountered in a diverse range of scientific disciplines make hysteresis a ubiquitous phenomenon. In the field of earthquake engineering for instance, structures become nonlinear and inelastic with restoring forces depending on the time history of the response under severe earthquake excitation. This memory-dependent relationship between force and deformation is the essence of hysteresis. A mathematical description of various existing hysteretic models can be found in Macki et al. (1993) and in Bertotti and Mayergoyz (2003a). Naturally, several research attempts have focused on determining response statistics of hysteretic oscillators. For instance, a PIS approach was used

to study the response of a bilinear oscillator under time-modulated Gaussian white noise (Naess and Moe, 1996).

Recently, the Preisach model, extensively used in the area of ferromagnetism, has been adopted to describe the hysteretic behavior of smart materials, such as shape memory alloys (e.g. Ktena et al., 2001; Spanos et al., 2004b). It is a versatile model capable of representing diverse hysteretic behaviors and of capturing minor loops present in many physical phenomena. Applications of the Preisach formalism can be found in Bertotti and Mayergoyz (2003b). They include modeling of superconducting hysteresis and eddy current hysteresis, modeling of thermal relaxations (viscocity) in hysteretic materials as well as modeling of soil-moisture hysteresis.

A detailed presentation of this model can be found in Meyergoyz (2003), whereas a review of some of the approaches to obtain the stochastic response of a Preisach system can be found in Mayergoyz and Dimian (2005). Specifically, in Ni et al. (2002) stationary second order statistics were obtained for a Preisach oscillator under Gausian white noise. In Spanos et al. (2004a) stochastic averaging was applied to yield the response amplitude PDF of Preisach hysteretic systems under stationary Gaussian white noise excitation. Subsequently, the approach was modified to compute response energy envelope statistics and study the nonlinear stochastic optimal control of Preisach systems (Wang et al., 2009a; Wang et al., 2009b). Recently, an approach was developed by Kougioumtzoglou and Spanos (2009) to evaluate second-order response statistics of Preisach oscillators under evolutionary excitation.

Following the notation introduced in Spanos et al. (2004a), the Preisach hysteretic restoring force $\left(f(t)\right)$ is given by

$$f(t)=\iint_{\alpha\geq\beta}\mu(\alpha,\beta)\gamma_{\alpha,\beta}(x;t)d\alpha d\beta, \tag{4.33}$$

where $\left(\gamma_{\alpha,\beta}(x;t)\right)$ represents the hysteron, or relay operator. The model of Eq.(4.33) can represent various hysteretic phenomena by appropriately choosing weight functions $\left(\mu(\alpha,\beta)\right)$. Choosing the weight function which corresponds to the Iwan-Jenkins model and following the derivations suggested in Spanos et al. (2004a), the equation of motion (Eq.(4.1)) becomes

$$\ddot{x}+\beta\dot{x}+\bar{\omega}^2x+f_H(t)=w(t), \tag{4.34}$$

where

$$\bar{\omega}=\sqrt{\omega_0^2+\omega_j^2}=\omega_j\sqrt{1+\phi}, \tag{4.35}$$

$$\omega_j=\sqrt{k_j}, \tag{4.36}$$

and

$$\phi=\omega_0^2/\omega_j^2. \tag{4.37}$$

In Eqs.(4.34-4.37) it is suggested that the Preisach restoring force can be divided in two terms; a linear part (ω_j^2x) and a nonlinear one $(f_H(t))$ monitoring the memory of the system. Thus, (ϕ) quantifies the stiffness of the linear counterpart of the Preisach element compared to the linear stiffness (ω_0^2) contribution. Introducing next the parameter

$$\psi=\frac{\bar{\omega}^2}{f_y^*}, \tag{4.38}$$

Eq.(4.34) can be recast in the form

$$\ddot{x}+\beta\dot{x}+\bar{\omega}^2\left(x+\psi d_H(t)\right)=w(t), \tag{4.39}$$

where ($d_H(t)$) is the scaled hysteretic restoring force. Further,

$$f_y^*=\frac{f_{y,\max}+f_{y,\min}}{2}, \tag{4.40}$$

where (f_y) is the yielding force. Defining the non-dimensional parameter (ν) as

$$\nu=\frac{f_{y,\max}-f_{y,\min}}{2f_y^*}, \tag{4.41}$$

and applying Eqs.(4.7) and (4.8) for $\nu=1$ yields

$$\beta(A)=\beta+\frac{\psi\bar{\omega}^2}{3\pi(1+\phi)^2\sqrt{\bar{\omega}^2-\frac{\psi\bar{\omega}^2}{4(1+\phi)^2}A}}A, \tag{4.42}$$

and

$$\omega^2(A)=\bar{\omega}^2-\frac{\psi\bar{\omega}^2}{4(1+\phi)^2}A. \tag{4.43}$$

For the special case where the excitation is modeled as white noise and $\left(\frac{\pi S_0}{\beta\bar{\omega}^2}=1\right)$ Spanos et al. (2004a) determined the stationary response amplitude PDF. It takes the form

$$\begin{aligned} p(A,\lambda)&=C(\lambda)A\left(\frac{\beta}{(1-A\lambda)\bar{\omega}}\right)^{-1/2}\\ &\times\exp\left(-\frac{A^2}{2}+\frac{A^3\lambda}{12}+\frac{2\bar{\omega}\left(128+48A\lambda+15A^2\lambda^2\right)(4-A\lambda)^{3/2}}{630\beta\pi\lambda^2}\right), \end{aligned} \tag{4.44}$$

where the dimensionless parameter (λ) is defined as

$$\lambda = \frac{\psi}{(1+\phi)^2}, \tag{4.45}$$

and $(C(\lambda))$ is a normalization constant. To verify the accuracy of the PIS approach a Preisach oscillator $(\bar{\omega}^2 = 10, \phi = 0.5, \psi = 1)$ under Gaussian white noise $\left(\frac{\pi S_0}{\beta \bar{\omega}^2} = 1\right)$ is considered. In Fig.(4.8) the numerically evaluated stationary response amplitude PDF is compared to the analytical expression of Eq.(4.44), whereas in Fig.(4.9) the first-passage PDFs for the oscillator with parameter values $(\bar{\omega}^2 = 10, \phi = 2, \psi = 1)$ and $\left(\frac{\pi S_0}{\beta \bar{\omega}^2} = 1\right)$ are compared with Monte Carlo simulations.

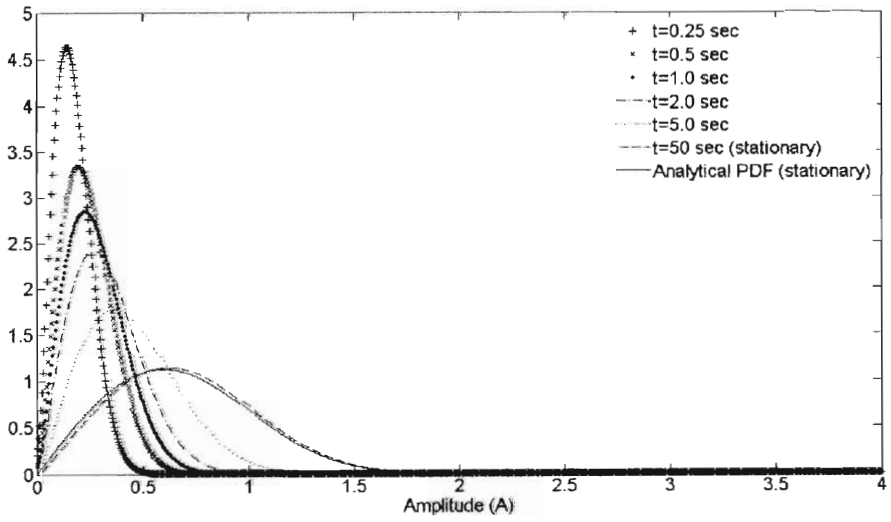

Fig.(4.8). Evaluation of $(p(A,t))$ for a Preisach oscillator $(\bar{\omega}^2 = 10, \phi = 0.5, \psi = 1)$ under Gaussian white noise $(\pi S_0 / \beta \bar{\omega}^2 = 1)$. Comparison to the analytical expression for the stationary PDF.

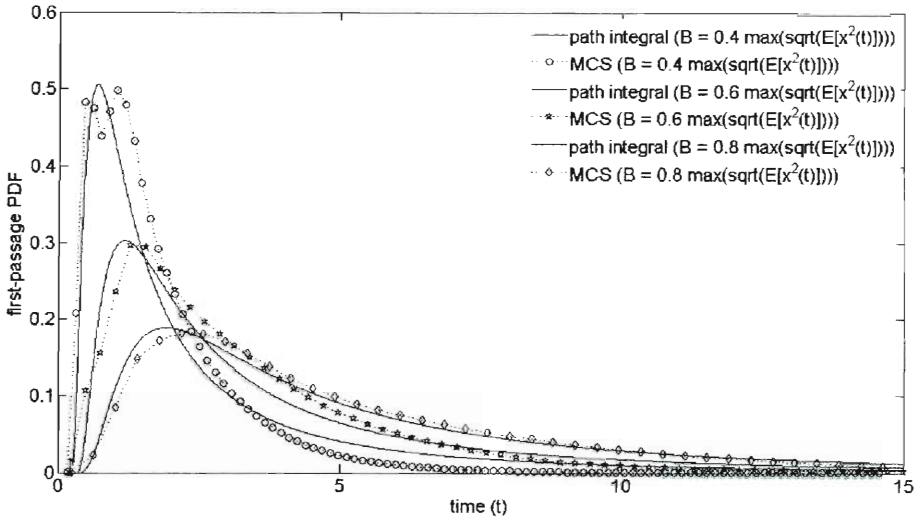

Fig.(4.9). First-Passage PDF for the Preisach oscillator $\left(\bar{\omega}^2 = 10, \phi = 2, \psi = 1\right)$ under Gaussian white noise $\left(\frac{\pi S_0}{\beta \bar{\omega}^2} = 1\right)$. Comparison between MCS data (5000 realizations) and PIS approach.

As far as the numerical implementation of the Preisach model is concerned, a standard fourth order Runge-Kutta integration scheme is used with a time step equal to $\left(\Delta t = 0.005\right)$. The wiping-out property of the Preisach model (e.g. Mayergoyz, 2003) is taken into account to update the current response maxima and minima at each time step of the integration scheme (Spanos et al., 2004a).

Next, the case of the evolutionary excitation of Eq.(4.22) is considered. In Figs.(4.10) and (4.11) the non-stationary response amplitude PDFs for the oscillators with parameter values $\left(\bar{\omega} = 10, \phi = 2, \psi = 1, S_1 = 2\right)$ and $\left(\bar{\omega} = 10, \phi = 2, \psi = 1, S_1 = 5\right)$ are shown, respectively and compared with Monte Carlo data. In Fig.(4.12) comparisons between the first-passage PDFs obtained

via Monte Carlo simulation and the first-passage PDFs computed via the PIS approach for the oscillator $\left(\varpi = 10, \phi = 2, \psi = 1, S_1 = 5\right)$ are plotted.

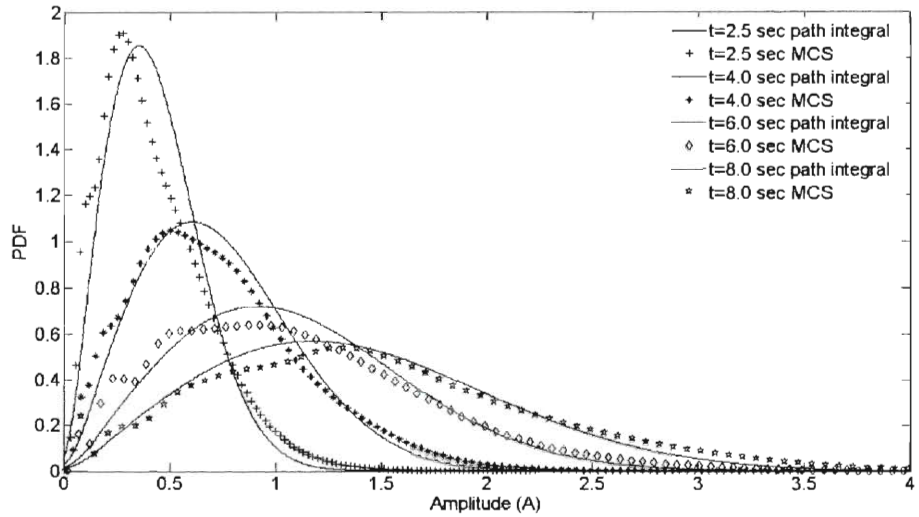

Fig.(4.10). Evaluation of $\left(p(A,t)\right)$ for a Preisach oscillator $\left(\varpi^2 = 10, \phi = 2, \psi = 1\right)$ under the non-separable evolutionary excitation spectrum $\left(S_1 = 2\right)$. Comparison between MCS data (5000 realizations) and PIS approach.

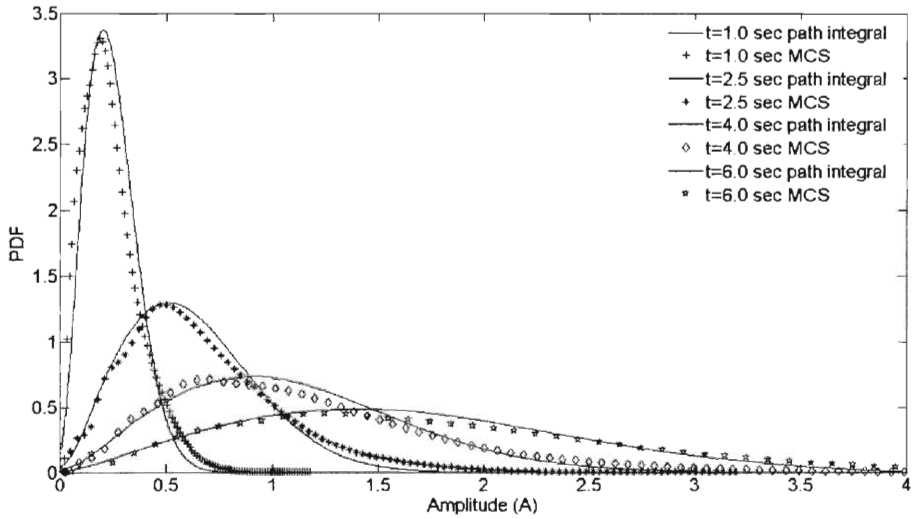

Fig.(4.11). Evaluation of $\left(p(A,t)\right)$ for a Preisach oscillator $\left(\varpi^2 = 10, \phi = 2, \psi = 1\right)$ under the non-separable evolutionary excitation spectrum $\left(S_1 = 5\right)$. Comparison between MCS data (5000 realizations) and PIS approach.

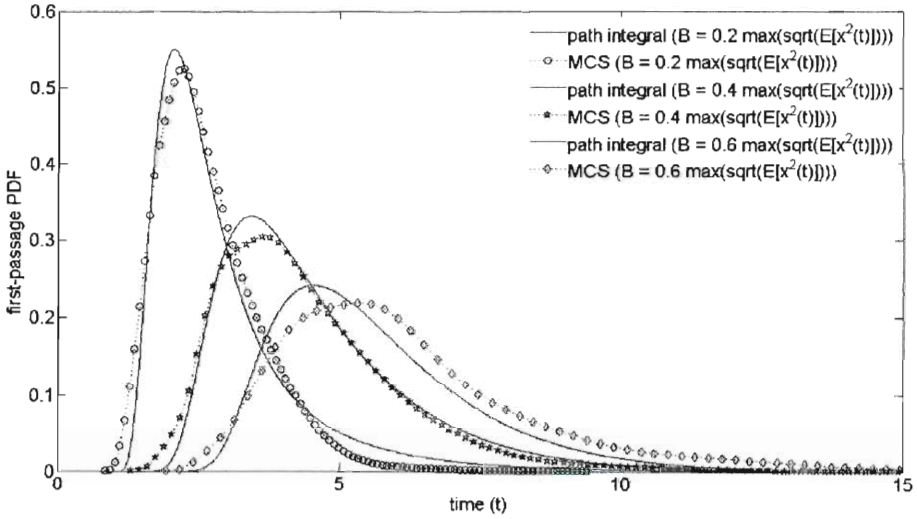

Fig.(4.12). First-Passage PDF for the Preisach oscillator $\left(\overline{\omega}^2 = 10, \phi = 2, \psi = 1\right)$ under the non-separable evolutionary excitation spectrum $\left(S_1 = 5\right)$. Comparison between MCS data (5000 realizations) and PIS approach.

It can be argued that the high accuracy observed in the case of white noise excitation is slightly decreased when evolutionary non-white excitation is considered. Undoubtedly, one of the reasons is the kind of the excitation power spectrum used and the effect it has on the Markovian character of the response process. In Figs.(4.8-4.9) Gaussian white noise was used to represent the excitation, whereas in Figs.(4.10-4.12) the evolutionary power spectrum of Eq.(4.22) was employed. Clearly, the Markovian assumption of the response process which is needed for Eq.(4.18) to be valid is better justified in the former case rather than the latter one. Nevertheless, the level of accuracy achieved in the latter case is deemed adequate and supports using the PIS approach in conjunction with realistic versions of excitation spectra, such as the non-separable one of Eq.(4.22).

Chapter 5

Response and first-passage analysis via a numerical Wiener path integral approach – Softening Duffing oscillator and ship capsizing application

5.1 Preliminary remarks

In addressing the first-passage problem beyond approaches applicable to classical oscillators such as the ones considered in the preceding chapter, a generalized version of the numerical Wiener path integral approach is developed, herein, which is also applicable to non-classical oscillators (i.e. oscillators possessing negative stiffness).

A potent paradigm of the usefulness of the first-passage problem relates to the ship rolling motion. Indeed, the large annual number of ship losses in world's oceans and the economical and environmental cost implied necessitate the development of reliable frameworks for capsizing probability determination. For this a softening Duffing oscillator, namely a nonlinear oscillator possessing a linear-plus-cubic negative kind of stiffness element will be used. Under certain assumptions, it can be shown that this third order polynomial approximates satisfactorily the restoring moment in rolling (e.g. Belenky and Sevastianov, 2007). Note that besides the importance of the softening Duffing model in nonlinear ship dynamics, applications can be found, as well, in other diverse scientific fields. For instance, in von Wagner (2004) the longitudinal vibrations of

piezoceramic rods under weak electric field were found to follow the softening Duffing model, whereas in Miller (2005) the same softening nonlinear model was used in plant biomechanics to describe the structural dynamics of plant stems. Although the aforementioned softening Duffing oscillator has received considerable attention in terms of response and stability analysis in the context of deterministic dynamics (e.g. Szemplinska – Stupnicka, 1988; Nayfeh and Sanchez, 1989; Virgin and Cartee, 1991; Lu and Evan-Iwanowski, 1994; Brennan et al., 2008), the stochastic analysis has been so far based on rather heuristic approaches. For instance, in Roberts (1986a) and in Roberts and Vasta (2000) the response was treated as a stationary diffusion process, although it is evident from the form of the softening Duffing equation that the response trajectories eventually depart from the region of stability in the phase plane, since the restoring force becomes negative. Nevertheless, considering a low level of excitation magnitude the authors computed response statistics assuming that the probability the response leaves the stable region is extremely small.

In this chapter, response and first-passage PDFs are derived for a softening Duffing oscillator under stochastic loading via a PIS approach. Specifically, relying on the Markov properties of the response process and on a discrete version of the C-K equation, first-passage statistics are derived assuming a special form for the conditional PDF of the response amplitude. Further, the developed approach is applied to a softening Duffing oscillator with nonlinear damping subject to realistic non-white wave excitation to derive capsizing probability estimates. This model has been widely used to approximate the uncoupled

nonlinear rolling motion of ships in beam seas (e.g. Ibrahim et al. 2007). The accuracy and reliability of the approach is demonstrated by comparisons to pertinent Monte Carlo data.

5.2 Softening Duffing oscillator stochastic response analysis

5.2.1 Mathematical formulation

Consider the following softening Duffing oscillator whose motion is governed by the differential equation

$$\ddot{x}+2\zeta_0\omega_0\dot{x}+\omega_0^2x+\varepsilon\omega_0^2x^3=w(t),\quad \varepsilon<0, \tag{5.1}$$

where (ε) is a negative constant representing the magnitude of the nonlinearity degree; (ζ_0) is the ratio of critical damping; (ω_0) is the natural frequency of the corresponding linear oscillator; and $(w(t))$ represents a Gaussian, zero-mean white noise random process possessing a power spectral density equal to (S_0).

Examining Eq.(5.1), it can be readily seen that there exist values of the response displacement (x) for which the stiffness element of the oscillator reaches zero and even negative values. This leads to an unstable behavior of the system, since the negative stiffness component forces the response to exhibit an unbounded behavior and asymptotically reach infinity. Bearing this qualitative picture in mind, let (a) denote the response amplitude envelope process, and (a_{cr}) denote the amplitude value for which the stiffness of the oscillator (Eq.(5.1)) becomes zero. Next, the conditional PDF of the response amplitude process $(p(a,t+\Delta t\,|\,a',t))$ is introduced such that

$$p(a,t+\Delta t \mid a',t)=\begin{cases} p_G(a,t+\Delta t \mid a',t), & 0 \le a' < a_{cr} \\ \delta(a-a_{\inf}), & a_{cr} \le a' \end{cases}, \tag{5.2}$$

where $(\delta(.))$ denotes the Dirac delta function and $(a_{\inf} \gg a \in [0,a_{cr}])$. The introduction of this form of the conditional PDF incorporates clearly the very realistic assumption that if the oscillator is in a state where it possesses a zero or a negative stiffness value, then its response at the next time instant will exhibit a tendency towards infinity, portraying the unbounded character of the system response.

In stochastic dynamics, the response of a nonlinear system under Gaussian white noise excitation can be described as a Markov process (e.g. To, 2000). Thus, the response amplitude of the oscillator (Eq.(5.1)) can be regarded as a Markov process, and thus, the C-K equation

$$p(a,t+2\Delta t \mid a'',t)=\int_0^{\infty} p(a,t+2\Delta t \mid a',t+\Delta t)\, p(a',t+\Delta t \mid a'',t)\, da', \tag{5.3}$$

is satisfied (e.g. Soong, 1973; Soong and Grigoriu, 1993). Taking into consideration Eq.(5.2), Eq.(5.3) becomes

$$\begin{aligned} p(a,t+2\Delta t \mid a'',t)=&\int_0^{a_{cr}} p_G(a,t+2\Delta t \mid a',t+\Delta t)\, p(a',t+\Delta t \mid a'',t)\, da' + \ldots \\ &\int_{a_{cr}}^{\infty} \delta(a-a_{\inf})\, p(a',t+\Delta t \mid a'',t)\, da', \end{aligned} \tag{5.4}$$

or, equivalently

$$\begin{aligned} p(a,t+2\Delta t \mid a'',t)=&\int_0^{a_{cr}} p_G(a,t+2\Delta t \mid a',t+\Delta t)\, p(a',t+\Delta t \mid a'',t)\, da' + \ldots \\ &\delta(a-a_{\inf}) \int_{a_{cr}}^{\infty} p(a',t+\Delta t \mid a'',t)\, da'. \end{aligned} \tag{5.5}$$

Obviously, Eq.(5.5) is subject to the condition

$$\int_0^{\infty} p(a,t+2\Delta t \mid a'',t)\,da = 1, \tag{5.6}$$

or, equivalently

$$\begin{aligned} &\int_0^{\infty}\int_0^{a_{cr}} p_G(a,t+2\Delta t \mid a',t+\Delta t)\,p(a',t+\Delta t \mid a'',t)\,da'da + \ldots \\ &\int_{a_{cr}}^{\infty} p(a',t+\Delta t \mid a'',t)\,da' = 1, \end{aligned} \tag{5.7}$$

where Eq.(5.5) and the properties of the Dirac delta function have been considered. Examining the right hand side of Eq.(5.5), it can be argued that it is composed by two conceptually different terms. The first one represents a distribution of the probability over different amplitude values according to the common PDF concept, whereas the factor $\left(\int_{a_{cr}}^{\infty} p(a',t+\Delta t \mid a'',t)\,da'\right)$ in the second term represents the probability the response grows unbounded, namely the system response asymptotically approaches infinity.

Considering the next time step $(t+3\Delta t)$ and exploiting Eq.(5.5) yields

$$\begin{aligned} &p(a,t+3\Delta t \mid a'',t) = \ldots \\ &\int_0^{a_{cr}} p_G(a,t+3\Delta t \mid a',t+2\Delta t)\,p(a',t+2\Delta t \mid a'',t+\Delta t)\,da' + \ldots \\ &\delta(a-a_{\inf})\int_{a_{cr}}^{\infty} p(a',t+2\Delta t \mid a'',t+\Delta t)\,da', \end{aligned} \tag{5.8}$$

or, equivalently

$$\begin{aligned} &p(a,t+3\Delta t \mid a''',t) = \ldots \\ &\int_0^{a_{cr}} p_G(a,t+3\Delta t \mid a',t+2\Delta t)\left(\int_0^{a_{cr}} p_G(a',t+2\Delta t \mid a'',t+\Delta t)\,p(a'',t+\Delta t \mid a''',t)\,da''\right)da' + \ldots \\ &\int_0^{a_{cr}} p_G(a,t+3\Delta t \mid a',t+2\Delta t)\left(\delta(a'-a_{\inf})\int_{a_{cr}}^{\infty} p(a'',t+\Delta t \mid a''',t)\,da''\right)da' + \ldots \\ &\delta(a-a_{\inf})\int_{a_{cr}}^{\infty}\left(\int_0^{a_{cr}} p_G(a',t+2\Delta t \mid a'',t+\Delta t)\,p(a'',t+\Delta t \mid a''',t)\,da''\right)da' + \ldots \\ &\delta(a-a_{\inf})\int_{a_{cr}}^{\infty}\left(\delta(a'-a_{\inf})\int_{a_{cr}}^{\infty} p(a'',t+\Delta t \mid a''',t)\,da''\right)da' \end{aligned} \tag{5.9}$$

or, equivalently

$$
\begin{aligned}
&p(a,t+3\Delta t \mid a''',t) = ... \\
&\int_0^{a_{cr}} p_G(a,t+3\Delta t \mid a',t+2\Delta t)\left(\int_0^{a_{cr}} p_G(a',t+2\Delta t \mid a'',t+\Delta t)\, p(a'',t+\Delta t \mid a''',t)\, da''\right) da' + ... \\
&\delta(a-a_{\inf})\int_{a_{cr}}^{\infty}\left(\int_0^{a_{cr}} p_G(a',t+2\Delta t \mid a'',t+\Delta t)\, p(a'',t+\Delta t \mid a''',t)\, da''\right) da' + ... \\
&\delta(a-a_{\inf})\int_{a_{cr}}^{\infty} p(a'',t+\Delta t \mid a''',t)\, da''.
\end{aligned}
\tag{5.10}
$$

The reliability function $(R_B(T))$ is defined next as the probability the system response amplitude stays below the threshold (B) over the time interval $[t_0,T]$. Further, the corresponding first-passage time PDF, namely the time at which the response amplitude crosses the prescribed boundary for the first time, is obtained as

$$
p_B(T) = -\frac{dR_B(T)}{dT}. \tag{5.11}
$$

Specifically, assuming the time interval $[t_0,T]$ under consideration, discretized such as $t_j = t_0 + (j-1)\Delta t, \quad j = 1,..,n$ and $\Delta t = (T-t_0)/(n-1)$, and considering an initial PDF $(p(a_1,t_1))$, the reliability function $(R_B(t_j))$ becomes

$$
R_B(t_j) = \int_0^B p(a_j,t_j \mid a_{j-1},t_{j-1}) \ldots \int_0^B p(a_2,t_2 \mid a_1,t_1)\, p(a_1,t_1) da_2 \cdots da_j . \tag{5.12}
$$

Attention is focused now on the conditional PDF $(p_G(a,t+\Delta t \mid a',t))$ which is defined for $(a' \in [0,a_{cr}))$. It is well known (e.g. Gihman and Skorohod, 1975) that for a Markov process the sample paths are continuous functions of (t) with probability one, if the Lindeberg condition holds true, namely for any $(k>0)$

$$\lim_{\Delta t\to 0}\frac{1}{\Delta t}\int_{|a-a'|>k} p_G\left(a,t+\Delta t\,|\,a',t\right)da'=0\,. \tag{5.13}$$

Interpreting Eq.(5.13), the probability for the position (a) to be different from (a') approaches zero faster than (Δt), as (Δt) approaches zero. Further, defining the drift $\left(K_1(a',t)\right)$ and diffusion $\left(K_2(a',t)\right)$ coefficients, respectively, as

$$K_1(a',t)=\lim_{\Delta t\to 0}\frac{1}{\Delta t}\int_{|a-a'|>k}(a-a')\,p_G\left(a,t+\Delta t\,|\,a',t\right)da', \tag{5.14}$$

and

$$K_2^2(a',t)=\lim_{\Delta t\to 0}\frac{1}{\Delta t}\int_{|a-a'|>k}(a-a')^2\,p_G\left(a,t+\Delta t\,|\,a',t\right)da', \tag{5.15}$$

it is possible for the C-K equation to be cast in the well-known F-P equation (e.g. Arnold, 1974; Gardiner, 1985) of the form

$$\begin{aligned}\frac{\partial}{\partial t}p_G\left(a,t\,|\,a',t'\right)&=-\frac{\partial}{\partial a}\left[K_1(a,t)\,p_G\left(a,t\,|\,a',t'\right)\right]+\ldots\\ &\frac{1}{2}\frac{\partial^2}{\partial a^2}\left[K_2^2(a,t)\,p_G\left(a,t\,|\,a',t'\right)\right].\end{aligned} \tag{5.16}$$

It can be readily seen that the assumptions (Eqs.(5.13-5.15)) involved in the derivation of the F-P equation are associated with continuity properties of the response amplitude process. In fact, the process (a) in Eq.(5.16) is mathematically known as a diffusion process (e.g. Arnold, 1974; Gardiner, 1985; Soong and Grigoriu, 1993). A probabilistic discussion of the general diffusion process in one dimension can be found in the authoritative paper by Feller (1954).

The interesting part about the F-P Eq.(5.16) is that the conditional PDF $p_G\left(a,t+\Delta t\,|\,a',t\right)$ has been shown to follow a Gaussian distribution of the form

$$p_G(a,t+\Delta t \mid a',t)=\frac{1}{\sqrt{2\pi K_2^2(a',t)\Delta t}}\exp\left(-\frac{\left(a-a'-K_1(a',t)\Delta t\right)^2}{2K_2^2(a',t)\Delta t}\right), \tag{5.17}$$

for $(\Delta t \to 0)$. In fact, in Dekker (1976) the concept of time-local Gaussian processes was introduced, and was shown that Eq.(5.17) together with Eq.(5.3) lead in an exact manner to the general nonlinear F-P Eq.(5.16).

Further, the relation between the F-P Eq.(5.16) for the diffusion process (a) and the corresponding first-order (Ito) stochastic differential equation (e.g. Soong, 1973; Gardiner, 1985; Oksendal, 2003) is such that

$$\dot{a}=K_1(a,t)+K_2(a,t)\eta(t), \tag{5.18}$$

where $\eta(t)$ is a zero mean and delta correlated process of intensity one, i.e., $E(\eta(t))=0$; and $E(\eta(t)\eta(t+\Delta t))=\delta(\Delta t)$.

Focusing on the softening Duffing oscillator (Eq.(5.1)), an averaging scheme (e.g. Roberts and Spanos, 1986; Zhu, 1988) is employed to yield a first-order (Ito) stochastic differential equation governing the response amplitude. This is based on the assumption of pseudo-harmonic behavior of the response. Following a statistical linearization approach as described in Roberts and Spanos (2003) and in Kougioumtzoglou and Spanos (2009), a linearized counterpart of Eq.(5.1) is

$$\ddot{x}+2\omega_0\zeta_0\dot{x}+\omega_{eq}^2(a)x=w(t), \tag{5.19}$$

where the equivalent natural frequency is assumed to be a function of the amplitude (a) of the response to partly account for the effect of the nonlinearity. Focusing on the case of a lightly damped system, it can be argued that the

amplitude (a) is a slowly varying function with respect to time and therefore can be treated as a constant over one cycle of oscillation. Thus, introducing the transformations

$$x(t) = a\cos\left[\omega_{eq}(a)t + \phi(t)\right], \tag{5.20}$$

and

$$\dot{x}(t) = -\omega_{eq}(a)a\sin\left[\omega_{eq}(a)t + \phi(t)\right], \tag{5.21}$$

and performing a mean square minimization procedure on the error between Eq.(5.1) and Eq.(5.19) the expression

$$\omega_{eq}^2(a) = \frac{\omega_0^2}{\pi a}\int_0^{2\pi}\cos\psi\left(\left(a\cos\psi\right) + \varepsilon\left(a\cos\psi\right)^3\right)d\psi = \omega_0^2\left(1 + \frac{3}{4}\varepsilon a^2\right), \tag{5.22}$$

is derived for the equivalent linear stiffness element. Examining Eqs.(5.20-5.21) it is readily seen that the amplitude (a) can be expressed as

$$a^2(t) = x^2(t) + \left(\frac{\dot{x}(t)}{\omega_{eq}(a)}\right)^2. \tag{5.23}$$

Combining Eqs.(5.19-5.21) and Eq.(5.23) and relying on the assumption of light damping, modeling the amplitude process $(a(t))$ as a one-dimensional Markov process is feasible by applying a combination of deterministic and stochastic averaging (e.g. Roberts and Spanos, 1986). This leads to the stochastic differential equation

$$\dot{a} = -\omega_0\zeta_0 a + \frac{\pi S_0}{2a\omega_0^2\left(1 + \varepsilon\frac{3}{4}a^2\right)} + \sqrt{\frac{\pi S_0}{\omega_0^2\left(1 + \varepsilon\frac{3}{4}a^2\right)}}\eta(t). \tag{5.24}$$

Comparing Eq.(5.24) to Eq.(5.18) yields

$$K_1(a,t) = -\omega_0\zeta_0 a + \frac{\pi S_0}{2a\omega_0^2\left(1+\varepsilon\frac{3}{4}a^2\right)}, \tag{5.25}$$

and

$$K_2^2(a,t) = \frac{\pi S_0}{\omega_0^2\left(1+\varepsilon\frac{3}{4}a^2\right)}. \tag{5.26}$$

It can be readily seen that in this case

$$a_{cr} = \sqrt{-\frac{4}{3\varepsilon}}, \tag{5.27}$$

and for $\left(a \in [0, a_{cr})\right)$ the conditional PDF (Eq.(5.17)) satisfies the conditions (Eqs.(5.13-5.15)).

5.2.2 Numerical examples

In this section, a softening Duffing oscillator under Gaussian white noise excitation is chosen for the numerical simulations. Different levels of nonlinearity magnitude (ε) are considered to illustrate the reliability and accuracy of the developed approach. Note that the value of (ε) relates to the value of critical amplitude (a_{cr}) through Eq.(5.27).

As far as numerical implementation issues and convergence criteria are concerned, Wehner and Wolfer (1983a) provided an extended discussion on conditions to be satisfied for the values of the time increment and the grid size. Further, it can be readily seen that for the case of the response amplitude process, the origin is a reflecting boundary and the drift coefficient $K_1(a,t)$ experiences a

singularity at $(a=0)$, namely a potential reason for numerical errors. The same situation was experienced in Naess and Moe (1996), where they tried to avoid the problem by exploiting the non-uniqueness of the conditional response PDF (e.g. Langouche et al., 1979). Nevertheless, the Gaussian conditional PDF led to the same level of accuracy as the other alternatives.

In Fig.(5.1) the component of the amplitude response PDF which depicts the bounded part of the motion for the softening Duffing oscillator $(\varepsilon=-2.08, a_{cr}=0.8, S_0=1, \omega_0^2=10, \zeta=0.05)$ is plotted. In Figs.(5.2-5.4) the response PDF components corresponding to the bounded motion for the oscillators with common parameters values $(S_0=1, \omega_0^2=10, \zeta=0.05)$ and critical amplitude values $(\varepsilon=-2.08, a_{cr}=0.8)$, $(\varepsilon=-1.33, a_{cr}=1)$, $(\varepsilon=-0.926, a_{cr}=1.2)$ and $(\varepsilon=-0.68, a_{cr}=1.4)$, are plotted, respectively. The initial distribution chosen is the Dirac delta function $(p(a,t=0)=\delta(a))$, assuming the system is initially at rest. In Fig.(5.5), the reliability functions $(R_B(t), B=a_{cr})$ for the aforementioned oscillators are plotted, whereas in Fig.(5.6) the corresponding first-passage PDFs are plotted. Comparisons with Monte Carlo simulations show that the PIS approach developed provides a reliable estimate of the first-passage PDF. The satisfactory accuracy of the approach for different levels of nonlinearity magnitude and of barrier value further confirms the reliability of the approach.

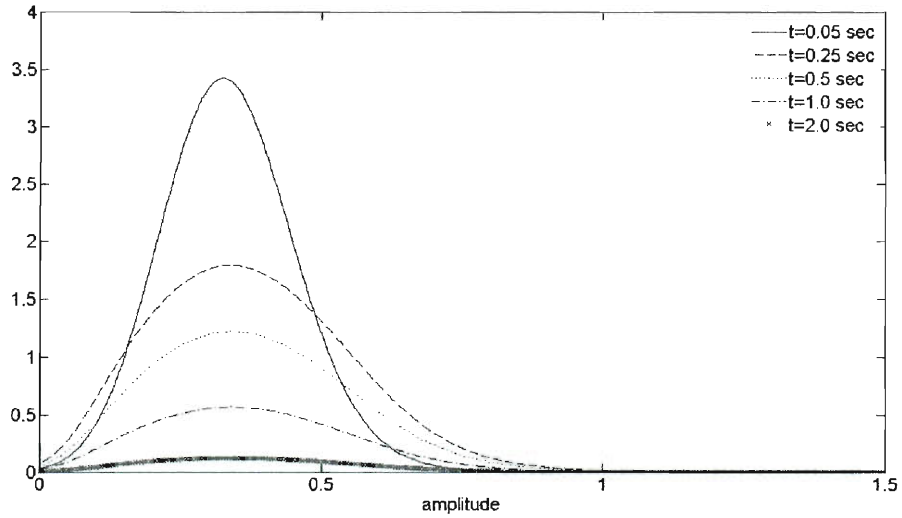

Fig.(5.1). Amplitude response PDF component corresponding to bounded motion for the softening Duffing oscillator $\left(\varepsilon = -2.08, a_{cr} = 0.8, S_0 = 1, \omega_0^2 = 10, \zeta = 0.05\right)$.

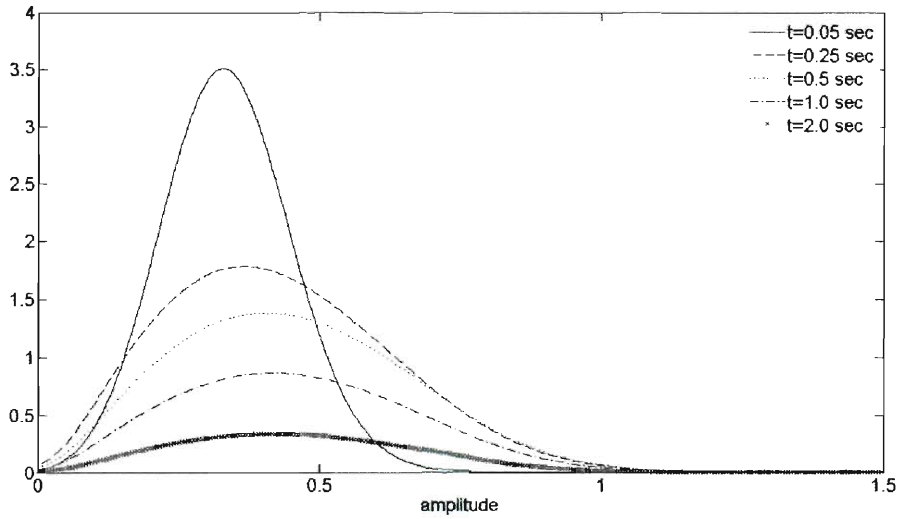

Fig.(5.2). Amplitude response PDF component corresponding to bounded motion for the softening Duffing oscillator $\left(\varepsilon = -1.33, a_{cr} = 1, S_0 = 1, \omega_0^2 = 10, \zeta = 0.05\right)$.

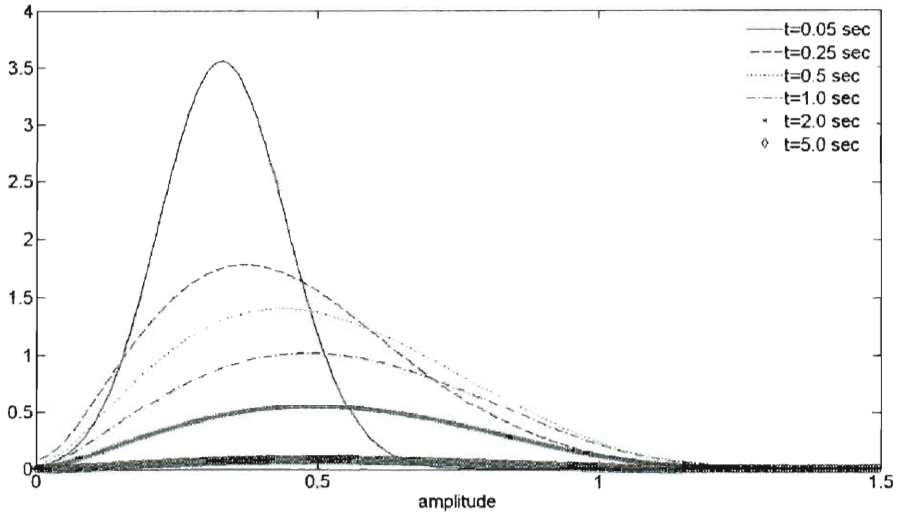

Fig.(5.3). Amplitude response PDF component corresponding to bounded motion for the softening Duffing oscillator $\left(\varepsilon = -0.926, a_{cr} = 1.2, S_0 = 1, \omega_0^2 = 10, \zeta = 0.05\right)$.

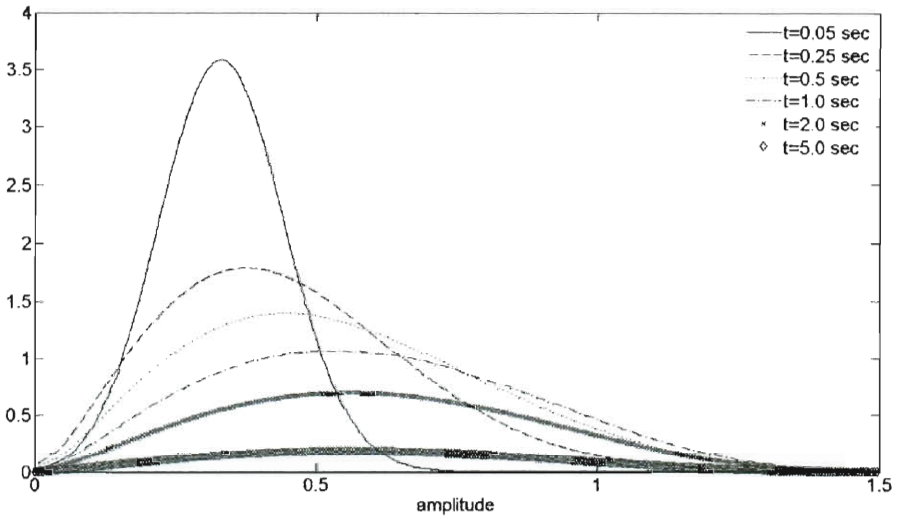

Fig.(5.4). Amplitude response PDF component corresponding to bounded motion for the softening Duffing oscillator $\left(\varepsilon = -0.68, a_{cr} = 1.4, S_0 = 1, \omega_0^2 = 10, \zeta = 0.05\right)$.

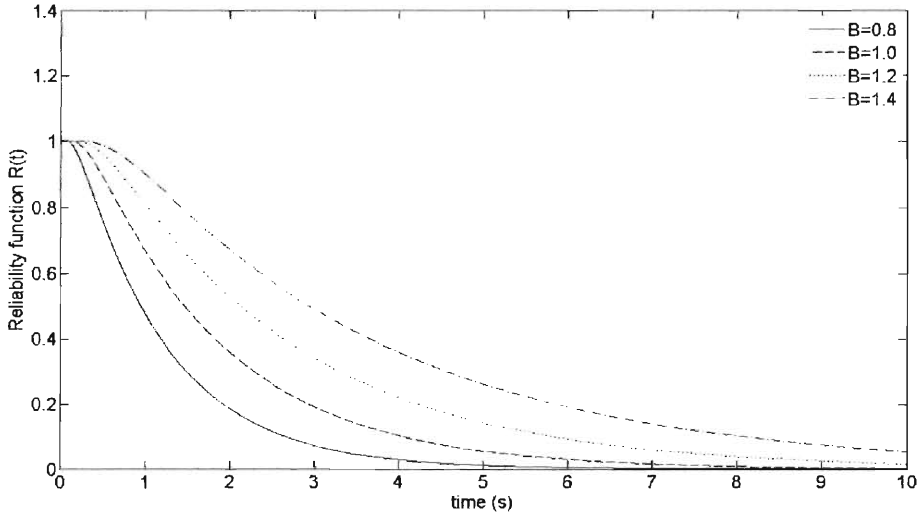

Fig.(5.5). Reliability functions $\left(R_B(t), B = a_{cr}\right)$ for the softening Duffing oscillators with common parameters values $\left(S_0 = 1, \omega_0^2 = 10, \zeta = 0.05\right)$ and critical amplitude values $\left(\varepsilon = -2.08, a_{cr} = 0.8\right)$, $\left(\varepsilon = -1.33, a_{cr} = 1\right)$, $\left(\varepsilon = -0.926, a_{cr} = 1.2\right)$ and $\left(\varepsilon = -0.68, a_{cr} = 1.4\right)$.

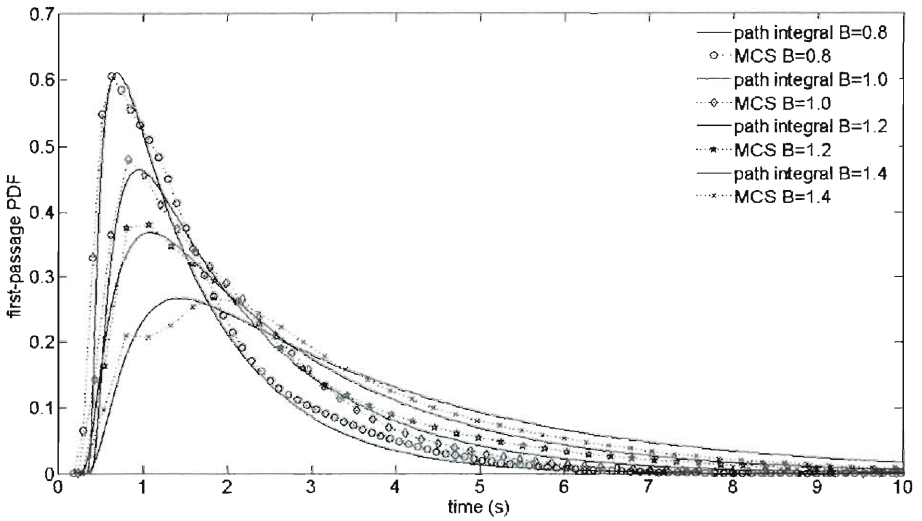

Fig.(5.6). First-passage PDFs $\left(B = a_{cr}\right)$ for the softening Duffing oscillators with common parameters values $\left(S_0 = 1, \omega_0^2 = 10, \zeta = 0.05\right)$ and critical amplitude values $\left(\varepsilon = -2.08, a_{cr} = 0.8\right)$, $\left(\varepsilon = -1.33, a_{cr} = 1\right)$, $\left(\varepsilon = -0.926, a_{cr} = 1.2\right)$ and $\left(\varepsilon = -0.68, a_{cr} = 1.4\right)$. Comparison between MCS data (5000 realizations) and PIS approach.

5.3 Ship capsizing probability determination

5.3.1 Mathematical formulation

Ship rolling motion is in general nonlinear and coupled with other motions, such as sway, pitch and heave. Nevertheless, considering the motion of a ship in unidirectional beam waves enables one to approximate reasonably well the roll motion as uncoupled (e.g. Arnold et al., 2004; Belenky and Sevastianov, 2007). Since the pioneering work by Froude (1861) both experimental and analytical results have been published addressing issues of ship roll motion instability and eventual capsizing. These range from those considering a deterministic framework and wavelet transforms (e.g. Yu et al., 2006) to cases where the excitation is regarded as a random process (e.g. Hsieh et al., 1994; Senjanovic et al., 2000; To and Chen, 2008). A detailed presentation of the subject can be found in review articles such as the ones by Spyrou and Thomson (2000), by Arnold et al. (2004) and by Ibrahim et al. (2007).

As it is pointed out in Belenky and Sevastianov (2007) a linear expression is adequate to describe wave damping for low magnitude motions. However, to take into account the viscous and vortex components of roll damping a nonlinear expression of the form

$$M_D = \beta\dot{\phi} + \delta_1\beta\left|\dot{\phi}\right|\dot{\phi}, \tag{5.28}$$

is usually adopted for the damping force. In general, several approximations exist in the literature. For instance, in Spanos and Chen (1980) the hydrodynamic drag force was accounted for by an equivalent viscous dashpot. Further, polynomial approximations of the form

$$M_D = \beta\dot{\phi} + \varepsilon_1\beta\dot{\phi}^3, \tag{5.29}$$

constitute common choices (e.g. Dalzell, 1978; Taylan, 2000; Yu et al., 2006). Alternatively, Mamontov and Naess (2009) used the expression

$$M_D = \beta\dot{\phi}\sqrt{1+\gamma_1\dot{\phi}^2}\,. \tag{5.30}$$

As far as the restoring moment is concerned, nonlinearity is mainly associated with the fact that the well-known GZ curve does not have an analytical form due to the difficulty in separating the Froude-Krylov part of the wave excitation and roll hydrostatic moment (e.g. Belenky and Sevastianov, 2007). Thus, an approximation is required for the restoring moment. A commonly used one (e.g. Taylan, 1999) is given by

$$M_R = k\phi + \varepsilon_2 k\phi^3, \quad \varepsilon_2 < 0\,. \tag{5.31}$$

This expression, although artificial to an extent, captures to an adequate degree the qualitative behavior and basic physics of nonlinear ship rolling motion under beam waves. Different representations of the restoring moment have been proposed in the literature including various degrees of odd-order polynomials such as fifth and seventh order expressions (e.g. Taylan, 2000; Senjanovic et al., 2000; Surendran et al., 2007).

Without loss of generality, consider the uncoupled ship roll motion given by the equation

$$\ddot{\phi} + \beta\dot{\phi} + \varepsilon_1\beta\dot{\phi}^3 + k\phi + \varepsilon_2 k\phi^3 = w(t), \quad \varepsilon_1 > 0, \quad \varepsilon_2 < 0\,, \tag{5.32}$$

where a dot over a variable denotes differentiation with respect to time (t); (ϕ) denotes the ship rolling angle; (β) and (k) are constants; (ε_1) and (ε_2)

represent the damping and stiffness nonlinearity degree respectively; and $(w(t))$ represents a Gaussian stationary random process possessing a power spectrum $(S(\omega))$. It can be readily seen that the restoring moment of the ship is of a softening kind such that as the roll angle increases from zero it increases with (ϕ), reaches a maximum value and then falls to zero at some critical value. Under these circumstances, the roll response cannot be treated as a stationary random process since sample paths will eventually reach the critical roll angle and capsizing will happen. Clearly, conventional statistical descriptions of the roll response are inappropriate and, thus, an approach such as the one developed in section 5.2 is next applied.

As far as the excitation spectrum is concerned, it can be related to the wave energy spectrum via the relationship (e.g. Jiang et al., 2000)

$$S(\omega)=\left|F_{roll}(\omega)\right|^2 S_w(\omega), \tag{5.33}$$

where $(S_w(\omega))$ represents the wave energy spectrum; and the function $(F_{roll}(\omega))$ relates the wave energy spectrum to the roll moment excitation spectrum $(S(\omega))$. In general, wave energy spectra, such as the JONSWAP (e.g. Hasselman et al., 1976), are narrow-band with a distinct peak. Nevertheless, it has been shown that the resulting roll moment excitation spectrum is significantly more broad-band than the corresponding wave energy spectrum (e.g. Roberts, 1986a; Senjanovic et al., 2000). Note that for the C-K equation (Eq.(5.3)) to be valid, the corresponding response process needs to be Markovian, which implies a white noise excitation. Deviation from white noise excitation such as in Eq.(5.32) leads to questions

regarding the validity of the C-K equation. Nevertheless, the aforementioned broad-band character of the excitation of Eq.(5.32) justifies to an extent the applicability of the approach developed in section 5.2.

Next, following a similar approach as in Kougioumtzoglou and Spanos (2009) and in section 5.2 yields the linearized equation of motion

$$\ddot{\phi} + \beta_{eq}(a)\dot{\phi} + k_{eq}(a)\phi = w(t), \tag{5.34}$$

where

$$\beta_{eq}(a) = \beta\left(1 + \varepsilon_1 \frac{3}{4} k_{eq}(a) a^2\right), \tag{5.35}$$

and

$$k_{eq}(a) = k\left(1 + \varepsilon_2 \frac{3}{4} a^2\right). \tag{5.36}$$

The drift and diffusion coefficients for the corresponding first-order stochastic differential equation to be used in Eq.(5.17) are, respectively,

$$K_1(a,t) = -\frac{1}{2}\beta_{eq}(a)a + \frac{\pi S\left(\sqrt{k_{eq}(a)}\right)}{2ak_{eq}(a)}, \tag{5.37}$$

and

$$K_2^2(a,t) = \frac{\pi S\left(\sqrt{k_{eq}(a)}\right)}{k_{eq}(a)}. \tag{5.38}$$

It can be readily seen that in this case the critical roll angle is given by

$$a_{cr} = \sqrt{-\frac{4}{3\varepsilon_2}}, \tag{5.39}$$

and for $\left(a \in [0, a_{cr})\right)$ the conditional PDF (Eq.(5.17)) satisfies the conditions (Eqs.(5.13-5.15)).

5.3.2 Numerical examples

In this section, the oscillator (Eq.(5.32)) subject to the non-white excitation of the form of Eq.(5.33) is considered. To this aim, a special case of the JONSWAP spectrum is chosen for the wave energy spectrum, namely the Pierson-Moskowitz (P-M) spectrum (e.g. Pierson and Moskowitz, 1964) of the form

$$S_w(\omega) = \frac{A}{\omega^5} \exp\left(-\frac{B}{\omega^4}\right), \tag{5.40}$$

where $\left(A = 8.1 \cdot 10^{-3} g^2, B = 0.74 (g/u)^4\right)$; (g) represents the gravitational acceleration; and (u) represents the wind velocity generating the waves. In the following, the value $(u = 10 m/s)$ is used. The P-M spectrum has received considerable attention in the literature in terms of employing signal processing techniques to produce spectrum compatible realizations efficiently. In fact, in Spanos (1983) the advantages of using a cascade of linear second-order filters to model the P-M spectrum were elucidated, whereas in Spanos and Mignolet (1986) the mathematical peculiarities associated with the P-M spectrum were addressed and techniques were described to derive efficient simulation algorithms which rely on a prior reasonably accurate autoregressive (AR) approximation.

Focusing next on Eq.(5.33), a rather general form for the roll moment excitation spectrum is given by the equation (e.g. Senjanovic et al., 2000)

$$S(\omega) = C\omega^4 S_w(\omega), \tag{5.41}$$

where the constant (C) is associated with beam sea and oscillator characteristics. In the following, the value $(C = 3)$ is used. Focusing on Eq.(5.41) it can be readily seen that the excitation spectrum is more broad-band than the related wave energy spectrum. This claim can be verified by examining Fig.(5.7) where both the wave energy and the excitation spectra are plotted.

First-passage PDFs are determined next for various levels of the nonlinearity magnitude (ε_2). Note that the value of (ε_2) relates to the value of critical amplitude (a_{cr}) through Eq.(5.39). In Fig.(5.8) the component of the amplitude response PDF which depicts the bounded part of the rolling motion with parameters values $(\varepsilon_1 = 0.1, \varepsilon_2 = -2.08, a_{cr} = 0.8, C = 3, k = 10, \beta = 0.32)$ is plotted. In Figs.(5.9-5.10) the response PDF components corresponding to the bounded motion for the oscillators with common parameters values $(\varepsilon_1 = 0.1, C = 3, k = 10, \beta = 0.32)$ and critical amplitude values $(\varepsilon_2 = -1.33, a_{cr} = 1)$ and $(\varepsilon_2 = -0.926, a_{cr} = 1.2)$, are plotted, respectively. The initial distribution chosen is the Dirac delta function $(p(a, t = 0) = \delta(a))$, assuming the system is initially at rest. In Figs.(5.11-5.12), the reliability functions $(R_B(t), B = a_{cr})$ and the corresponding first-passage PDFs for the aforementioned oscillators are plotted. Comparisons with Monte Carlo simulations show that the PIS approach developed provides a reliable estimate of the first-passage PDF. It can be argued that the high accuracy observed in the case

of white noise excitation is slightly decreased when non-white excitation is considered. Undoubtedly, one of the reasons for this feature is the kind of the excitation power spectrum used and the effect it has on the Markovian character of the response process. Nevertheless, the level of accuracy achieved in the latter case for various levels of nonlinearity magnitude and of barrier value is deemed adequate for using the PIS approach in conjunction with realistic versions of roll moment excitation spectra, such as the one given by Eq.(5.41).

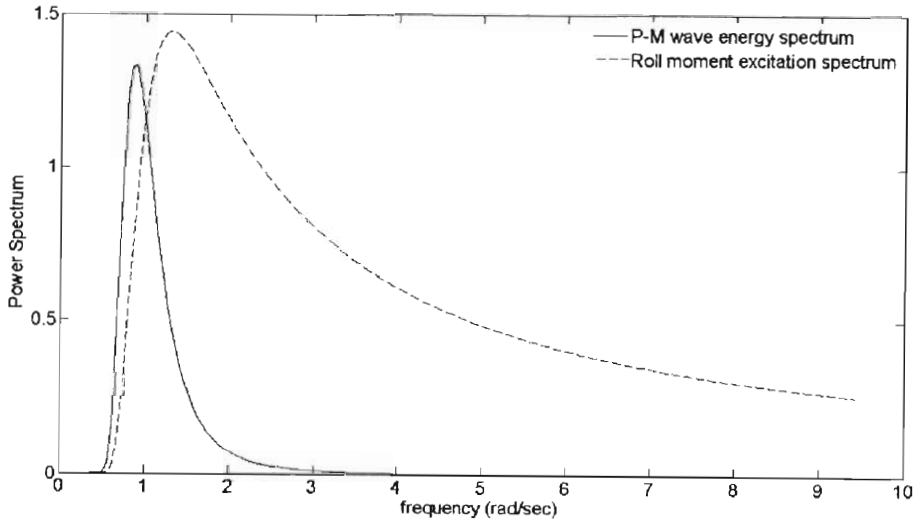

Fig.(5.7). Pierson-Moskowitz wave energy power spectrum $(u = 10m/s)$ and the corresponding roll moment excitation power spectrum $(C = 3)$.

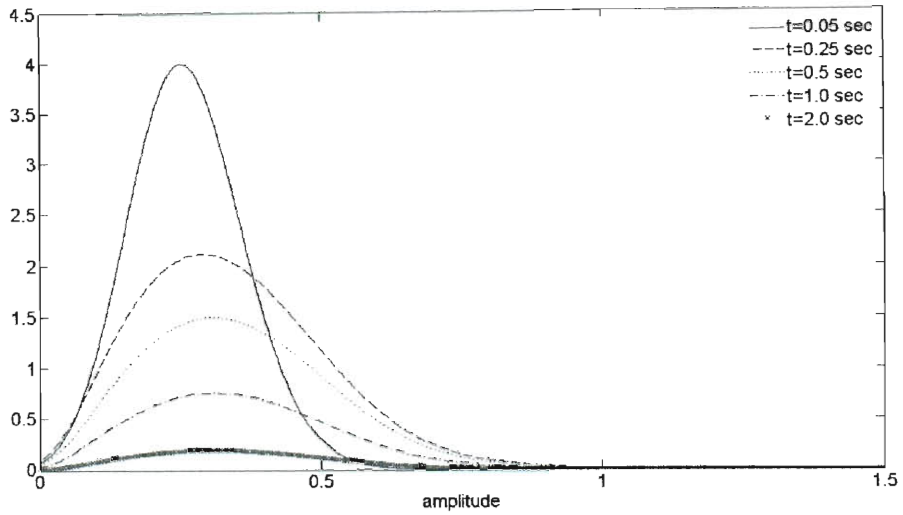

Fig.(5.8). Amplitude response PDF component corresponding to bounded motion for the ship rolling $\left(\varepsilon_1 = 0.1, \varepsilon_2 = -2.08, a_{cr} = 0.8, C = 3, k = 10, \beta = 0.32\right)$.

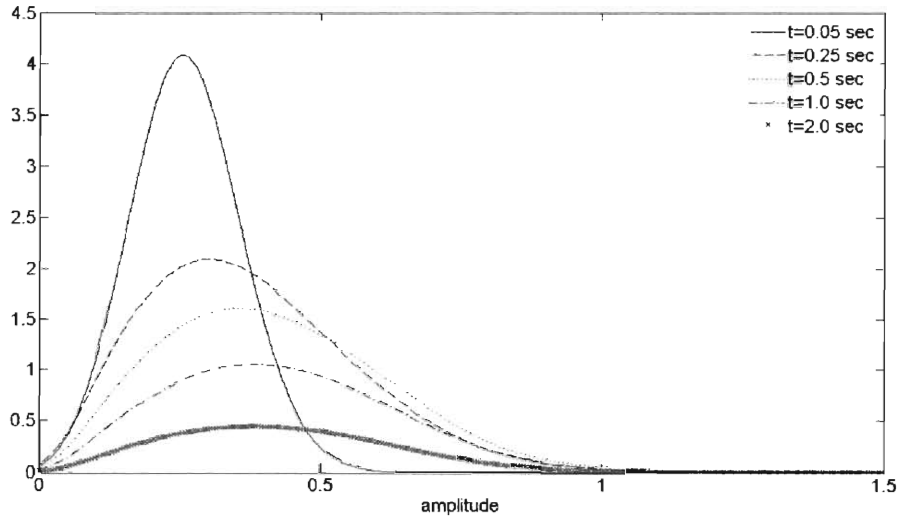

Fig.(5.9). Amplitude response PDF component corresponding to bounded motion for the ship rolling $\left(\varepsilon_1 = 0.1, \varepsilon_2 = -1.33, a_{cr} = 1, C = 3, k = 10, \beta = 0.32\right)$.

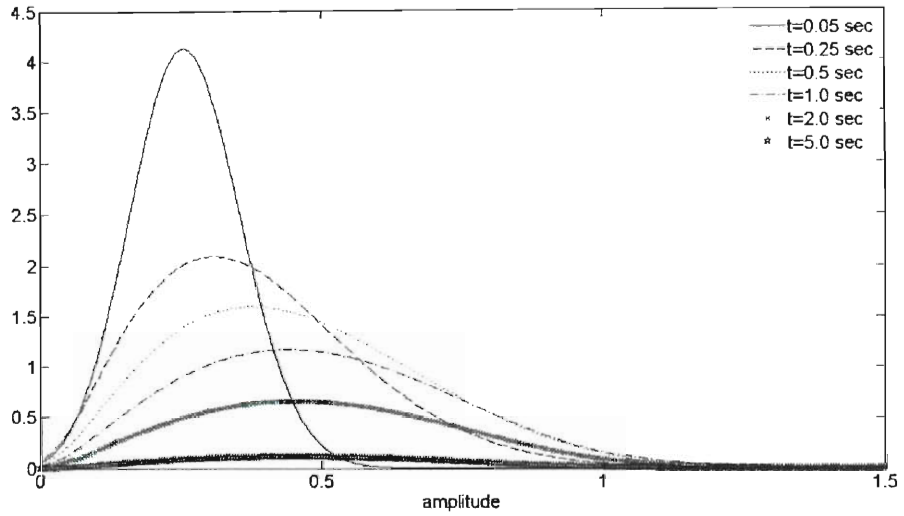

Fig.(5.10). Amplitude response PDF component corresponding to bounded motion for the ship rolling $(\varepsilon_1 = 0.1, \varepsilon_2 = -0.926, a_{cr} = 1.2, C = 3, k = 10, \beta = 0.32)$.

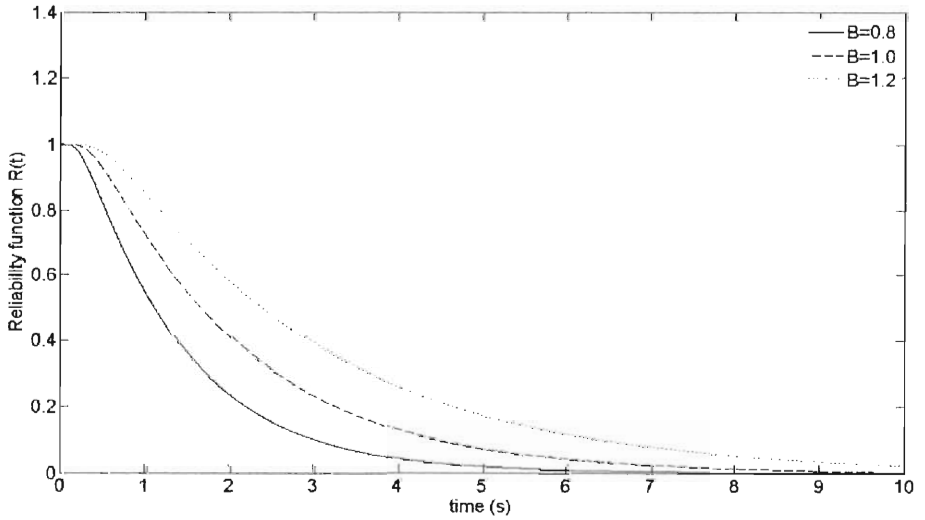

Fig.(5.11). Reliability functions $(R_B(t), B = a_{cr})$ for the ship rolling with common parameters values $(\varepsilon_1 = 0.1, C = 3, k = 10, \beta = 0.32)$ and critical amplitude values $(\varepsilon_2 = -2.08, a_{cr} = 0.8)$, $(\varepsilon_2 = -1.33, a_{cr} = 1)$ and $(\varepsilon_2 = -0.926, a_{cr} = 1.2)$.

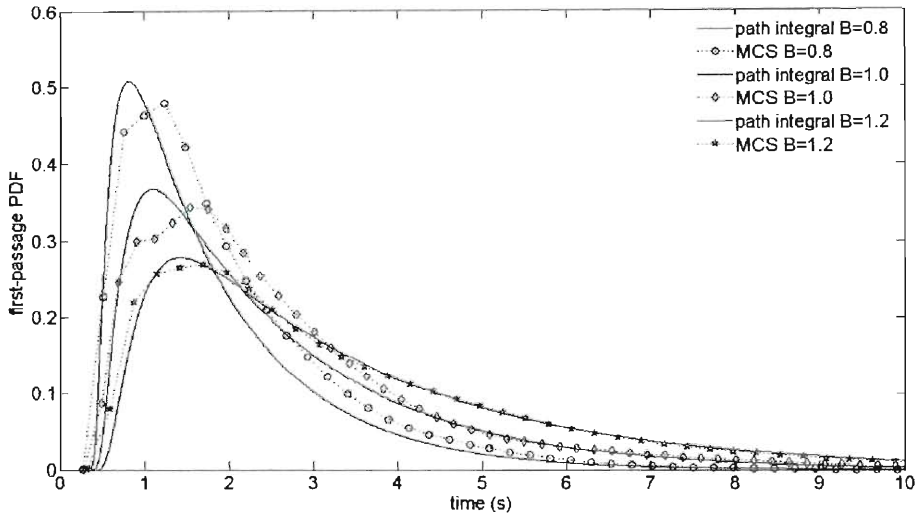

Fig.(5.12). First-passage PDFs $(B = a_{cr})$ for the ship rolling with common parameters values $(\varepsilon_1 = 0.1, C = 3, k = 10, \beta = 0.32)$ and critical amplitude values $(\varepsilon_2 = -2.08, a_{cr} = 0.8)$, $(\varepsilon_2 = -1.33, a_{cr} = 1)$ and $(\varepsilon_2 = -0.926, a_{cr} = 1.2)$. Comparison between MCS data (5000 realizations) and PIS approach.

Chapter 6

Response analysis via an analytical Wiener path integral approach – Arbitrarily large time step

6.1 Preliminary remarks

Despite the various approaches developed to address problems in nonlinear stochastic dynamics the engineering community seems to have neglected the potential of an analytical approach based on the concept of the Wiener path integral.

The notion of path integral was introduced by Wiener (1930) as an approach to solve problems in the theory of Brownian motion. It was reinvented in a different form by Feynman (1948) for the reformulation of quantum mechanics, known as the third formulation of quantum mechanics. The importance of path integral approaches in theoretical physics can hardly be disputed. Their applications in most branches of modern physics have proved extremely fruitful as a guide for the formulation and development of new ideas and approaches in the description of physical phenomena. For instance, path integrals were used extensively for the development of the theories of superfluidity, of unified electromagnetic and weak interactions, and of quantum chromodynamics. Early work includes the celebrated Feynman-Kac (F-K) formula (Feynman, 1948; Kac, 1949; Oksendal, 2003) which expresses the transition probability density function (PDF) for a wide class of stochastic

processes in terms of path integrals. Further, several analytical or approximate approaches to solve Wiener path integrals can be found in Gelfand and Yaglom (1960), Brush (1961), Wiegel (1975) and Feng et al. (1992). Recently, a fractional system subject to Gaussian white noise was studied by combining path integrals and the maximum entropy principle (Jumarie, 2007).

From a mathematical point of view the phrase 'path integral' simply refers to the generalization of integral calculus to functionals. It is noted that that the level of mathematical rigor is different for different kinds of path integral. While the Wiener path integral is based on a well-established mathematical background, the complex oscillatory Feynman path integral faces analytical difficulties in attempts of rigorous mathematical definition and justification. Roughly speaking, the Wiener path integral is based on a well-defined functional integral measure, while the Feynman path integral does not admit any strictly defined measure and should be understood as the limit of its finite-dimensional approximation (e.g. Chachian and Demichev, 2001). One of the reasons for this difference in mathematical rigor can be found in an essential distinction between the two kinds of path integral whose origin is the existence of a fundamental object in quantum mechanics, namely, the probability amplitude (e.g. Feynman, 1948).

Clearly, the similarities between Wiener and Feynman path integrals are adequate to reduce a broad range of quantum-mechanical problems to consideration of the corresponding Wiener path integral. In fact, the Feynman integrals can be converted into the form of Wiener integrals by a transition to purely imaginary time variables: $(t \to -it)$, and in many cases this transformation

can be mathematically justified. This enables a straightforward application of standard methods of classical stochastic processes to quantum mechanical problems (e.g. Rocandelli, 1989).

In general, a variety of approaches have been developed for the construction and calculation of path integrals such as operator symbol calculus, stochastic Ito calculus, coherent states, the semiclassical approximation, the perturbation expansion, the localization technique and path integration on group manifolds. A more detailed treatment of path integrals can be found in a number of books such as those by Feynman and Hibbs (1965), Schulman (1981), Chachian and Demichev (2001) and Kleinert (2009).

In this chapter, an approximate analytical approach is developed for the determination of the non-stationary response PDF of nonlinear oscillators based on the notions of the Wiener path integral and of the most probable path. To this aim, relying on the assumption of light damping and resorting to stochastic averaging and to statistical linearization the response amplitude is modeled as a one-dimensional Markov diffusion process. Then, a variational formulation, which utilizes the drift and diffusion coefficients of the associated stochastic differential equation, is employed to derive the non-stationary response amplitude PDF. The advantage of the approach relates to the use of an arbitrarily large time step for advancing the solution in contrast to the numerical path integral approaches developed in the preceding chapters. The accuracy of the approach is verified via pertinent Monte Carlo simulation data.

6.2 Mathematical formulation

6.2.1 Wiener path integral formulation

Consider a Markov stochastic process (a). Then, the Chapman-Kolmogorov (C-K) equation

$$p(a_f,t_f \mid a_{i-1},t_{i-1}) = \int_{-\infty}^{\infty} p(a_f,t_f \mid a_i,t_i)\, p(a_i,t_i \mid a_{i-1},t_{i-1})\, da_i \tag{6.1}$$

is satisfied (e.g. Soong, 1973; Soong and Grigoriu, 1993), where $\left(p(a_f,t_f \mid a_i,t_i)\right)$ denotes the transition PDF of the process (a); and $(t_f > t_i)$. For a Markov process the sample paths are continuous functions of (t) with probability one, if the Lindeberg condition (e.g. Gihman and Skorohod, 1975) holds true, namely for any $(k>0)$

$$\lim_{t_f - t_i \to 0} \frac{1}{t_f - t_i} \int_{|a_f - a_i| > k} p(a_f,t_f \mid a_i,t_i)\, da_i = 0. \tag{6.2}$$

Further, defining the drift $\left(K_1(a_i,t_i)\right)$ and diffusion $\left(K_2(a_i,t_i)\right)$ coefficients, respectively, as

$$K_1(a_i,t_i) = \lim_{t_f - t_i \to 0} \frac{1}{t_f - t_i} \int_{|a_f - a_i| > k} (a_f - a_i)\, p(a_f,t_f \mid a_i,t_i)\, da_i, \tag{6.3}$$

and

$$K_2^2(a_i,t_i) = \lim_{t_f - t_i \to 0} \frac{1}{t_f - t_i} \int_{|a_f - a_i| > k} (a_f - a_i)^2\, p(a_f,t_f \mid a_i,t_i)\, da_i, \tag{6.4}$$

it is possible for the C-K equation to be recast in the well-known Fokker-Planck (F-P) equation for the transition PDF $\left(p\left(a_f,t_f\,|\,a_i,t_i\right)\right)$ (e.g. Arnold, 1974; Gardiner, 1985) of the form

$$\frac{\partial p}{\partial t_f}=-\frac{\partial}{\partial a_f}\left[K_1\left(a_f,t_f\right)p\right]+\frac{1}{2}\frac{\partial^2}{\partial a_f{}^2}\left[K_2^2\left(a_f,t_f\right)p\right]. \tag{6.5}$$

The process (a) in Eq.(6.5) is known as a diffusion process (e.g. Feller, 1954; Gihman and Skorohod, 1975). Further, the connection between the F-P equation of the diffusion process (a) and the corresponding Ito stochastic differential equation (e.g. Soong, 1973; Gardiner, 1985; Oksendal, 2003) is such that

$$\dot{a}_f=K_1\left(a_f,t_f\right)+K_2\left(a_f,t_f\right)\eta(t_f), \tag{6.6}$$

where $\eta(t_f)$ is a zero mean and delta correlated process of intensity one, i.e., $E\left(\eta(t_f)\right)=0$; and $E\left(\eta(t_i)\eta(t_f)\right)=\delta\left(t_f-t_i\right)$. The interesting aspect about the F-P equation is that the transition PDF, often called short-time propagator, has been shown to follow a Gaussian distribution for $\left(t_f-t_i\to 0\right)$ of the form

$$p\left(a_f,t_f\,|\,a_i,t_i\right)=\frac{1}{\sqrt{2\pi K_2^2\left(a_f,t_f\right)\left(t_f-t_i\right)}}$$
$$\times\exp\left(-\frac{\left(a_f-a_i-K_1\left(a_f,t_f\right)\left(t_f-t_i\right)\right)^2}{2K_2^2\left(a_f,t_f\right)\left(t_f-t_i\right)}\right). \tag{6.7}$$

Note that in Dekker (1976) the concept of time-local Gaussian processes was introduced and was further shown that Eq.(6.7) together with Eq.(6.1) lead in an exact manner to the general nonlinear F-P Eq.(6.5). However, the choice of

Eq.(6.7) for the form of the transition PDF is not restrictive (e.g. Langouche et al., 1979; Risken, 1984; Naess and Moe, 1996).

Eq.(6.7) has been the starting point for the development of numerical path integral solution approaches which constitute, in essence, a discrete version of the C-K equation as it has been pointed out in the preceding chapters. The fact that the PDF is computed in short time steps can be regarded as a major shortcoming of the approach making it computationally inefficient. Thus, developing an approach which expresses the transition PDF as a Wiener path integral can be viewed as the analytical counterpart of the aforementioned numerical approach.

In general, the transition PDF $\left(p\left(a_f,t_f \mid a_i,t_i\right)\right)$ denotes the probability of a transition from a point in state space $\left(a_i\right)$ at time $\left(t_i\right)$ to a point in state space $\left(a_f\right)$ at time $\left(t_f\right)$ where $\left(t_f > t_i\right)$. Adopting the notation of Chachian and Demichev (2001), let $\left(C\left\{a_i,t_i;a_f,t_f\right\}\right)$, denote the set of trajectories starting at point $\left(a(t_i)=a_i\right)$ and having the endpoint $\left(a(t_f)=a_f\right)$. It is clear that to obtain the transition PDF that the particle starting at point $\left(a(t_i)=a_i\right)$ ends up at point $\left(a(t_f)=a_f\right)$, the probabilities over the set $C\left\{a_i,t_i;a_f,t_f\right\}$ of all the trajectories which have common starting and ending points must be summed. The symbol $\left(\int_{C\{a_i,t_i;a_f,t_f\}}\right)$ denotes the summation over a set of trajectories which are assumed to be continuous and is called the Wiener path integral. The Wiener path integral can be realized as a functional integral over the space of all paths possessing a

probability distribution on the path space as its integrand, which is denoted as $W[a(t)]$ and is called probability density functional. Then,

$$p\left(a_f,t_f\middle|a_i,t_i\right)=\int\limits_{C\{a_i,t_i;a_f,t_f\}} W[a(t)][da(t)]. \tag{6.8}$$

The approach to describe a stochastic process by its probability density functional was first considered by Wiener (1930) for the process with $\left(K_1\left(a_f,t_f\right)=0\right)$ and $\left(K_2\left(a_f,t_f\right)=1\right)$. In this case the Wiener path integral (Eq.(6.8)) can be evaluated directly from its definition (e.g. Chachian and Demichev, 2001). For a stochastic process with a linear drift and a constant diffusion coefficients, Onsager and Machlup (1953) pursued a similar idea which led Tisza and Manning (1957) to the determination of the probability density functional in the form

$$W[a(t)][da(t)]=C\exp\left\{-\int_{t_i}^{t_f} OM\left(a,\dot{a}\right)dt\right\}[da(t)], \tag{6.9}$$

where (C) is a normalization constant; and $\left(OM\left(a,\dot{a}\right)\right)$ is the Onsager-Machlup (O-M) function. Their approach, however, was restricted to processes with linear drift coefficient as was the work of Falkoff (1958) who considered the Onstein-Uhlenbeck process. Several attempts towards determining the O-M function for a stochastic process with nonlinear drift and diffusion coefficients resulted in controversial results in the 1970s. In Stratonovich (1971) a formula was provided for the probability density functional by invoking the Radon-Nikodym theorem (e.g. Grigoriu, 2002) and transforming the F-P equation in a manner that the F-K formula could be applied. In agreement with Stratonovich (1971) is the work by Graham (1977) who derived the O-M function by means of an operator calculus;

by Horsthemke and Bach (1975) and by Bach et al. (1977) who used Ito stochastic differential equations; and by Dekker (1977) who utilized a discretization rule. At variance with the aforementioned results was the work by Haken (1976) who also employed a discretization rule (see also Langouche et al., 1979). Further, several investigators, based on the idea of Tisza and Manning (1957), have tried to interpret the O-M function as a Lagrangian for determining the most probable path of the stochastic process by a variational principle (e.g. Graham, 1977). However, this cannot hold true for a path of the diffusion process since the solution of the variational principle should be twice differentiable and almost all paths of a diffusion process are nowhere differentiable as it is pointed out in Durr and Bach (1978). Instead, the O-M function can be defined as the Lagrangian giving the most probable tube if one seeks for the probability that a path lies within a certain region (e.g. tube) along a differentiable function. Further, a measure is required in function space to compare the probabilities of different tubes of the same 'thickness'. In this manner, in Durr and Bach (1978) the Girsanov formula (e.g. Gihman and Skorohod, 1972) was applied for measures induced by diffusion processes with constant diffusion and nonlinear drift coefficients. It was shown that the O-M function can be defined as the Lagrangian for the most probable tube around a differentiable function. It was further shown that in the case of a process dependent diffusion coefficient, the induced measure is not absolutely continuous with respect to a quasi translation invariant measure and was concluded that the O-M function cannot be defined as a Lagrangian for processes with process dependent diffusion coefficients. In this

manner, for the case of constant diffusion and nonlinear drift coefficients Eqs.(6.3) and (6.4) become

$$K_1(a,t) = f(a), \tag{6.10}$$

and

$$K_2(a,t) = c. \tag{6.11}$$

Further, the transition PDF expressed in terms of the Wiener path integral is given by Eq.(6.8), whereas Eq.(6.9) becomes

$$W[a(t)][da(t)] = C\exp\left\{-\int_{t_i}^{t_f} L(a,\dot{a})\,dt\right\}[da(t)], \tag{6.12}$$

where

$$L(a,\dot{a}) = \frac{1}{2}\left\{\frac{(\dot{a}-f(a))^2}{c^2} + f'(a)\right\}, \tag{6.13}$$

in which the dot denotes differentiation with respect to time; and $(')$ denotes differentiation with respect to the variable (a). It can be readily seen that the O-M function has been substituted by the Lagrangian $(L(a,\dot{a}))$ in Eq.(6.12) to provide a variational principle compatible solution approach.

6.2.2 Variational formulation

According to a variational approach (e.g. Feynman and Hibbs, 1965; Durr and Bach, 1978; Chachian and Demichev, 2001) the largest contribution to the Wiener path integral (Eq.(6.12)) comes from the trajectory for which the integral in the exponential becomes as small as possible. Variational calculus rules (e.g.

Ewing, 1985) dictate that this trajectory with fixed endpoints satisfies the extremality condition

$$\delta\int_{t_i}^{t_f} L(a,\dot{a})dt = 0\,. \tag{6.14}$$

This condition leads to the Euler-Lagrange (E-L) equation

$$\frac{\partial L}{\partial a} - \frac{\partial}{\partial t}\frac{\partial L}{\partial \dot{a}} = 0, \quad a(t_i) = a_i, \quad a(t_f) = a_f\,. \tag{6.15}$$

Substituting Eq.(6.13) in Eq.(6.15) yields

$$\ddot{a} = f(a)f'(a) + \frac{c^2}{2}f''(a), \quad a(t_i) = a_i, \quad a(t_f) = a_f\,, \tag{6.16}$$

or equivalently

$$(t+c_2)^2 = \left(\int_{a_i}^{a} \frac{1}{\sqrt{c_1 + f^2(x) + c^2 f'(x)}}dx\right)^2, \quad a(t_i) = a_i, \quad a(t_f) = a_f\,, \tag{6.17}$$

where (c_1) and (c_2) are integration constants to be determined from the conditions $(a(t_i) = a_i, a(t_f) = a_f)$; and (x) is an auxiliary integration variable. Solving Eq.(6.16), or equivalently Eq.(6.17), yields a solution for the transition PDF for the process (a) (e.g. Bach et al., 1978; Chachian and Demichev, 2001) in the form

$$p(a_f, t_f | a_i, t_i) = \phi(t_f - t_i)\exp\left\{-\int_{t_i}^{t_f} L(a_c, \dot{a}_c)dt\right\}, \tag{6.18}$$

where (a_c) is the solution of Eq.(6.16) representing the most probable trajectory. It can be seen that for fixed time points (t_i) and (t_f) the function $\phi(t_f - t_i)$ can be determined by simply applying the normalization condition

$$\int_{-\infty}^{\infty} p\left(a_f, t_f \middle| a_i, t_i\right) da_f = 1. \tag{6.19}$$

In Durr and Bach (1979) the aforementioned formulation was applied for the study of an anharmonic oscillator. As it is pointed out in Bach et al. (1978) the accuracy of the approximation increases as the diffusion coefficient (Eq.(6.11)) becomes smaller. Roughly summarized, this formulation yields the most probable path of a diffusion process, namely the trajectory which determines the most probable realizations of the process. This concept is analogous to the fact that the most probable value of a random variable is the one corresponding to the maximum value of the PDF.

6.2.3 Stochastic averaging

Consider a nonlinear single-degree-of-freedom system whose motion is governed by the differential equation

$$\ddot{x} + \beta\dot{x} + z(t, x, \dot{x}) = w(t), \tag{6.20}$$

where a dot over a variable denotes differentiation with respect to time (t); $(z(t, x, \dot{x}))$ is the restoring force which could be either hysteretic or depend only on the instantaneous values of (x) and $(\dot{x})$; (β) is a linear damping coefficient; and $(w(t))$ represents a Gaussian, zero-mean white noise process possessing a power spectrum (S_0).

Considering the case of a lightly damped system, it can be argued that the nonlinear oscillator (Eq.(6.20)) exhibits a pseudo-harmonic behavior described by the equations

$$x(t) = a\cos\left[\omega(a)t + \phi(t)\right], \tag{6.21}$$

and

$$\dot{x}(t) = -\omega(a)a\sin\left[\omega(a)t + \phi(t)\right], \tag{6.22}$$

in which (a) denotes the response amplitude envelope defined as

$$a = \sqrt{x^2 + \frac{\dot{x}^2}{\omega^2(a)}}. \tag{6.23}$$

Assuming that (a) is a slowly varying function with respect to time a statistical linearization method (e.g. Roberts and Spanos, 2003) can yield a linearized system of the form

$$\ddot{x} + \beta(a)\dot{x} + \omega^2(a)x = w(t), \tag{6.24}$$

where

$$\beta(a) = \beta + \frac{-\frac{1}{\pi}\int_0^{2\pi} \sin[\psi] z(t, a\cos\psi, -\omega(a)a\sin\psi)d\psi}{a\omega(a)}, \tag{6.25}$$

and

$$\omega^2(a) = \frac{\frac{1}{\pi}\int_0^{2\pi} \cos[\psi] z(t, a\cos\psi, -\omega(a)a\sin\psi)d\psi}{a}. \tag{6.26}$$

Further, resorting to stochastic averaging (e.g. Kougioumtzoglou and Spanos, 2009) yields a first order stochastic differential equation for the response amplitude envelope (a) of the form

$$\dot{a} = -\frac{1}{2}\beta(a)a + \frac{\pi S_0}{2a\omega^2(a)} + \frac{\sqrt{\pi S_0}}{\omega(a)}\eta(t). \tag{6.27}$$

As in Eq.(6.6), $\eta(t)$ is a zero mean and delta correlated process of intensity one, i.e., $E(\eta(t))=0$; and $E(\eta(t)\eta(t+\tau))=\delta(\tau)$, with $(\delta(\tau))$ being the Dirac delta function.

Obviously for a broad class of nonlinear oscillators, namely oscillators with nonlinear damping, Eq.(6.27) reduces to

$$\dot{a}=-\frac{1}{2}\beta(a)a+\frac{\pi S_0}{2a\omega_0^2}+\frac{\sqrt{\pi S_0}}{\omega_0}\eta(t), \tag{6.28}$$

where (ω_0) represents the natural frequency of the corresponding linear oscillator. Comparing Eq.(6.27) to Eq.(6.6) it can be deduced that Eq.(6.28) is a stochastic differential equation possessing nonlinear drift and constant diffusion coefficients. In fact, Eqs.(6.10) and (6.11) yield

$$f(a)=-\frac{1}{2}\beta(a)a+\frac{\pi S_0}{2a\omega_0^2}, \tag{6.29}$$

and

$$c=\frac{\sqrt{\pi S_0}}{\omega_0}. \tag{6.30}$$

Thus, it has been shown that the variational approach presented in section 6.2.2 can be applied to oscillators with nonlinear damping. In this manner, the potential of the Wiener path integral to address physically realistic problems has been demonstrated.

6.3 Numerical examples

In this section the versatility of the preceding approach is demonstrated by numerical examples. Specifically, a Van der Pol, a Rayleigh and a linear plus cubic damping oscillators are considered. The initial conditions assumed are $\left(a(t_i=0)=1, \dot{a}(t_i=0)=0\right)$. The most probable path $\left(a_c(t)\right)$ is determined by solving Eq.(6.16) numerically in conjunction with the conditions $\left(a(t_i=0)=a_i=1, a(t_f)=a_f\right)$. In this manner, for a given time instant (t_f) and a given amplitude value $\left(a_f\right)$ Eq.(6.18) yields a single point of the response amplitude PDF. Further, assuming an effective domain of values for the response amplitude PDF (i.e. $a_f \in \left[a_{f,\min}, a_{f,\max}\right]$), discretized such as $a_{f,j}=a_{f,\min}+(j-1)\Delta a_f$, $j=1,..,n$ and $\Delta a_f=\left(a_{f,\max}-a_{f,\min}\right)/(n-1)$, the response PDF at time instant (t_f) is determined by solving Eq.(6.16) (n) times. In the following, the value $(n=100)$ is used. The results of the approximate analytical approach are compared to pertinent Monte Carlo simulations. The ordinary differential equations involved in both the Wiener path integral approach and the Monte Carlo simulations are solved numerically by a standard fourth order Runge-Kutta scheme. The advantage of the proposed approach lies in the determination of the response PDF at a time instant (t_f) without the need of the existing alternative numerical path integral solution approaches to evaluate the response PDF at all the past time instants.

6.3.1 Van der Pol oscillator

Consider a Van der Pol oscillator of the form

$$\ddot{x}+\beta\left(-1+\varepsilon x^2\right)\dot{x}+\omega_0^2 x=w(t), \qquad \varepsilon>0. \tag{6.31}$$

Then, using Eq.(6.25) and Eq.(6.26) yields

$$\beta(a)=\beta\left(-1+\varepsilon\frac{a^2}{4}\right), \tag{6.32}$$

and

$$\omega^2(a)=\omega_0^2. \tag{6.33}$$

Further, substituting Eq.(6.32) in Eq.(6.29) yields

$$f(a)=-\zeta_0\omega_0\left(-a+\varepsilon\frac{a^3}{4}-\frac{\sigma^2}{a}\right), \tag{6.33}$$

and

$$c=\sqrt{2\zeta_0\omega_0\sigma^2}, \tag{6.34}$$

where

$$\sigma^2=\frac{\pi S_0}{2\zeta_0\omega_0^3}. \tag{6.35}$$

In Eq.(6.35) $\left(\sigma^2\right)$ represents the stationary response variance of a corresponding linear oscillator under a Gaussian, zero-mean white noise process possessing a power spectrum $\left(S_0\right)$; and $\left(\zeta_0\right)$ denotes the ratio of critical damping. The non-stationary response amplitude PDFs for the Van der Pol oscillators possessing the values $\left(\omega_0=1,\zeta_0=0.01,\varepsilon=2,\sigma^2=1\right)$ and $\left(\omega_0=1,\zeta_0=0.01,\varepsilon=2,\sigma^2=2\right)$ are plotted in Fig.(6.1) and in Fig.(6.2), respectively, for various time instants.

Comparison with Monte Carlo simulations reveals an adequate degree of accuracy. Further, the same level of accuracy is retained for various levels of excitation magnitude.

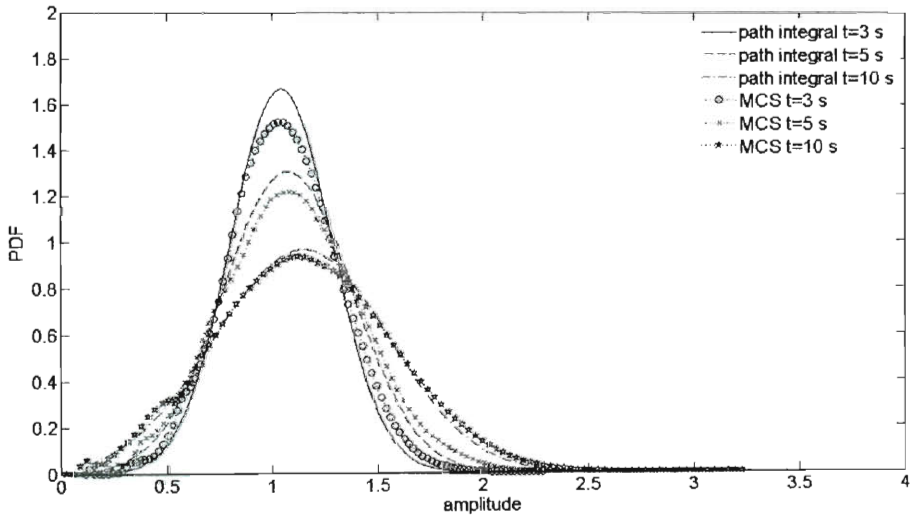

Fig.(6.1). Evaluation of $\left(p(a,t)\right)$ for a Van der Pol oscillator $\left(\omega_0 = 1, \zeta_0 = 0.01, \varepsilon = 2, \sigma^2 = 1\right)$. Comparison with Monte Carlo simulations (5000 realizations).

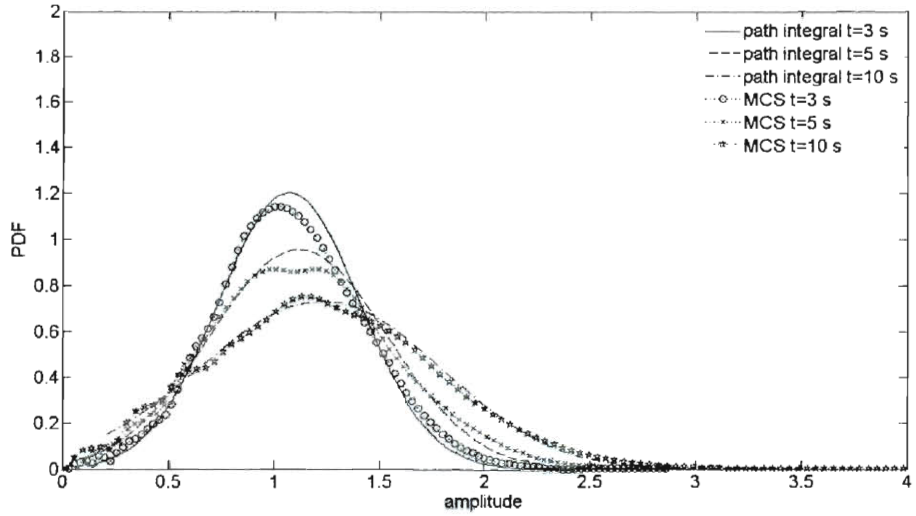

Fig.(6.2). Evaluation of $\left(p(a,t)\right)$ for a Van der Pol oscillator $\left(\omega_0 = 1, \zeta_0 = 0.01, \varepsilon = 2, \sigma^2 = 2\right)$. Comparison with Monte Carlo simulations (5000 realizations).

6.3.2 Rayleigh oscillator

A Rayleigh oscillator of the form

$$\ddot{x} + \beta\left(-1 + \varepsilon\dot{x}^2\right)\dot{x} + \omega_0^2 x = w(t), \qquad \varepsilon > 0, \tag{6.36}$$

is considered next. Further, using Eq.(6.25) and Eq.(6.26) yields

$$\beta(\alpha) = \beta\left(-1 + \varepsilon\frac{3}{4}\omega_0^2 a^2\right), \tag{6.37}$$

and

$$\omega^2(a) = \omega_0^2. \tag{6.38}$$

Further, substituting Eq.(6.37) in Eq.(6.29) yields

$$f(a) = -\zeta_0\omega_0\left(-a + \varepsilon\frac{3}{4}\omega_0^2 a^3 - \frac{\sigma^2}{a}\right), \tag{6.39}$$

and

$$c = \sqrt{2\zeta_0 \omega_0 \sigma^2} \,. \tag{6.40}$$

The non-stationary response amplitude PDFs corresponding to parameter values $\left(\omega_0 = 1, \zeta_0 = 0.01, \varepsilon = 3, \sigma^2 = 1\right)$ and $\left(\omega_0 = 1, \zeta_0 = 0.01, \varepsilon = 3, \sigma^2 = 3\right)$ are plotted in Fig.(6.3) and in Fig.(6.4), respectively, for various time instants. Comparisons between the response PDFs determined via the Wiener path integral approach and the response PDFs obtained via Monte Carlo simulations demonstrate reasonable accuracy for various excitation levels.

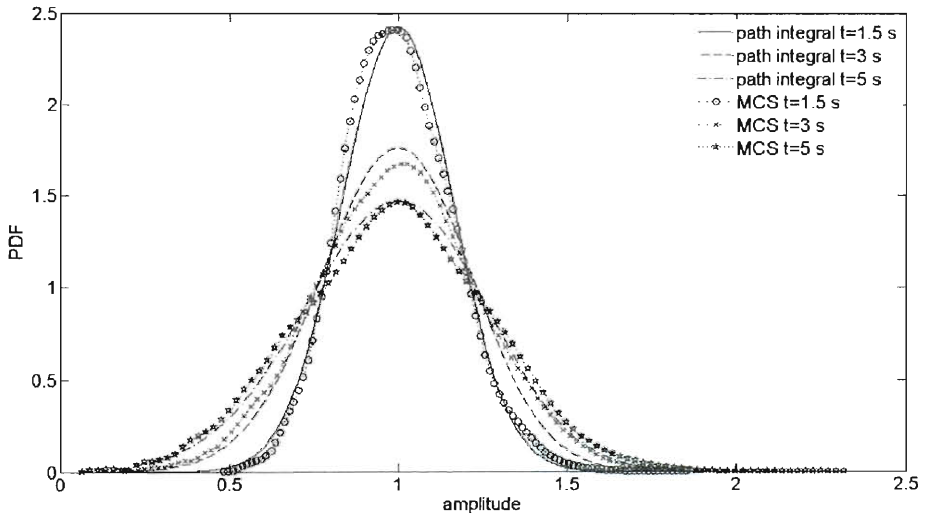

Fig.(6.3). Evaluation of $\left(p(a,t)\right)$ for a Rayleigh oscillator $\left(\omega_0 = 1, \zeta_0 = 0.01, \varepsilon = 3, \sigma^2 = 1\right)$. Comparison with Monte Carlo simulations (5000 realizations).

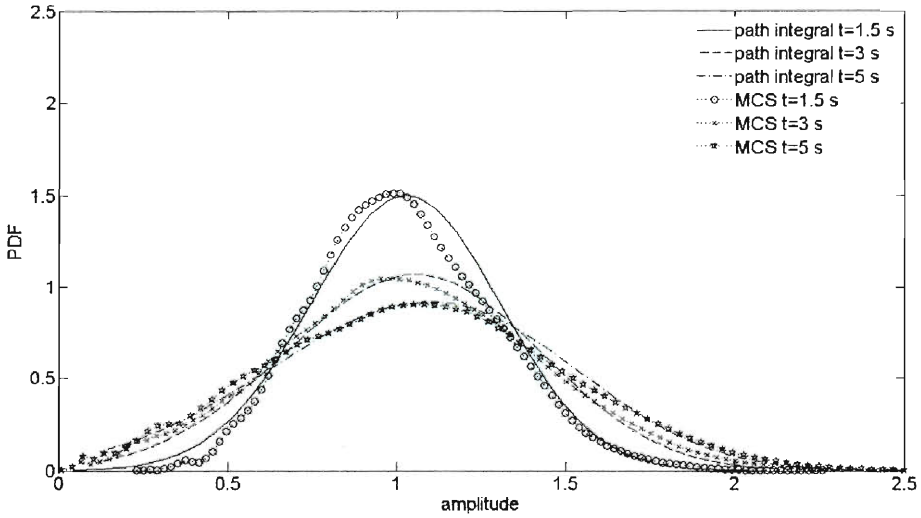

Fig.(6.4). Evaluation of $\left(p(a,t)\right)$ for a Rayleigh oscillator $\left(\omega_0 = 1, \zeta_0 = 0.01, \varepsilon = 3, \sigma^2 = 3\right)$. Comparison with Monte Carlo simulations (5000 realizations).

6.3.3 Linear plus cubic damping oscillator

As a final case, a linear plus cubic damping oscillator of the form

$$\ddot{x} + \beta\dot{x}\left(1 + \varepsilon\dot{x}^2\right) + \omega_0^2 x = w(t), \qquad \varepsilon > 0, \tag{6.41}$$

is considered next. Further, using Eq.(6.25) and Eq.(6.26) yields

$$\beta(\alpha) = \beta\left(1 + \varepsilon\frac{3}{4}\omega_0^2 a^2\right), \tag{6.42}$$

and

$$\omega^2(a) = \omega_0^2. \tag{6.43}$$

Further, substituting Eq.(6.42) in Eq.(6.29) yields

$$f(a) = -\zeta_0\omega_0\left(a + \varepsilon\frac{3}{4}\omega_0^2 a^3 - \frac{\sigma^2}{a}\right), \tag{6.44}$$

and

$$c = \sqrt{2\zeta_0 \omega_0 \sigma^2} \ . \tag{6.45}$$

The non-stationary response amplitude PDFs for the oscillators possessing the parameter values $\left(\omega_0 = 1, \zeta_0 = 0.01, \varepsilon = 2, \sigma^2 = 2\right)$ and $\left(\omega_0 = 1, \zeta_0 = 0.01, \varepsilon = 2, \sigma^2 = 3\right)$ are plotted in Fig.(6.5) and in Fig.(6.6), respectively, for various time instants. Comparison with Monte Carlo simulations indicates a satisfactory level of accuracy for various excitation magnitudes.

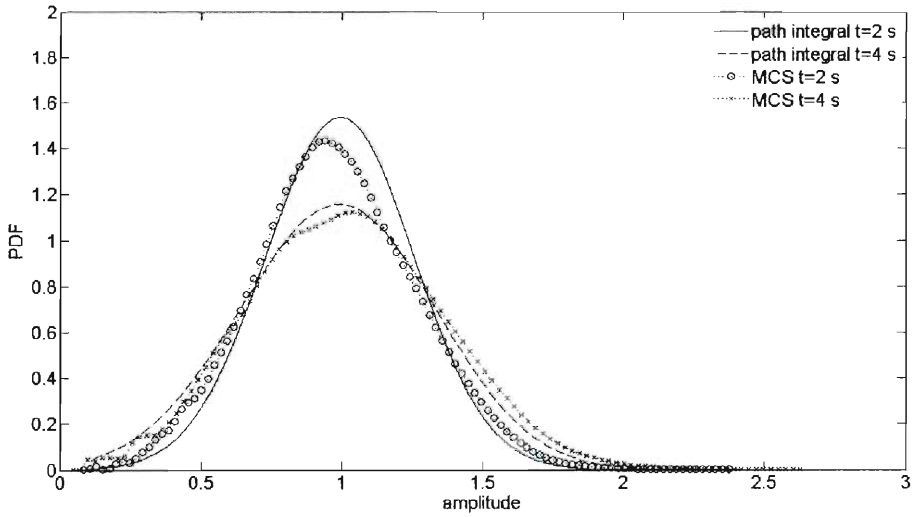

Fig.(6.5). Evaluation of $\left(p(a,t)\right)$ for a linear plus cubic damping oscillator $\left(\omega_0 = 1, \zeta_0 = 0.01, \varepsilon = 2, \sigma^2 = 2\right)$. Comparison with Monte Carlo simulations (5000 realizations).

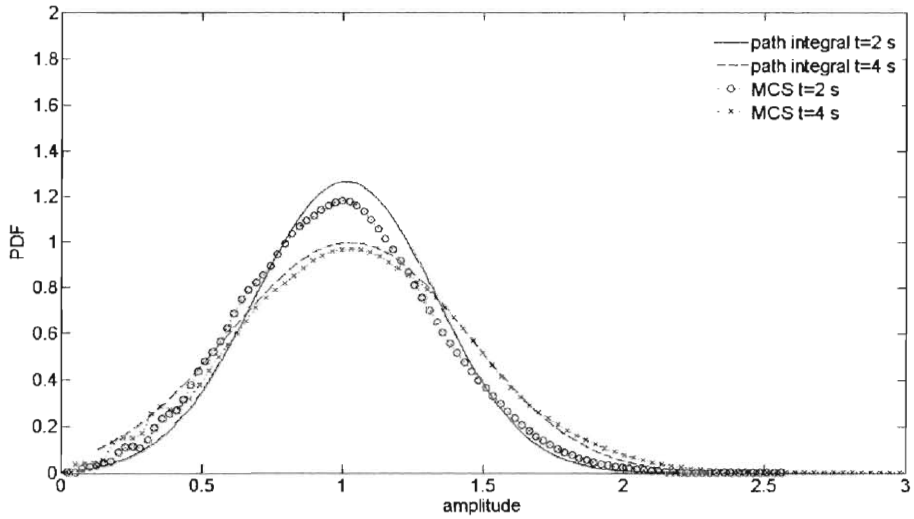

Fig.(6.6). Evaluation of the $\left(p(a,t)\right)$ for a linear plus cubic damping oscillator $\left(\omega_0 = 1, \zeta_0 = 0.01, \varepsilon = 2, \sigma^2 = 3\right)$. Comparison with Monte Carlo simulations (5000 realizations).

Chapter 7

Harmonic wavelets based statistical linearization for response evolutionary power spectrum determination

7.1 Preliminary remarks

Several research efforts have focused on determining the response of systems under evolutionary stochastic excitation; see Kougioumtzoglou and Spanos (2009) for a recent reference. Nevertheless, limited results exist in the context of a joint time-frequency response analysis.

Obviously, the time-dependent frequency content of a non-stationary signal cannot be adequately captured by applying ordinary Fourier analysis, since this transform provides only the average spectral decomposition of the signal. On the other hand, wavelet-based analysis can be employed to perform a joint time-frequency study of non-stationary signals, circumventing the limitations of traditionally used methods, such as the short-time Fourier transform (STFT) and the Wigner-Ville method (WVM) (e.g. Newland, 1997; Qian, 2002). The basic concept behind wavelet analysis is to represent a function in terms of simpler ones defined as both scaled and translated versions of an oscillatory function. The term 'wavelet' was first introduced by Morlet, a geophysical engineer, while attempting to analyze seismic signals. Since the rigorous mathematical formulation of the continuous wavelet transform (Grossmann and Morlet, 1984), wavelets have been used in a large number of diverse scientific fields.

As far as engineering mechanics related applications are concerned, wavelets have been successfully applied to study dynamic systems with time-varying characteristics (e.g. Newland, 1994a; Agrawal, 1998; Newland and Butler, 2000). Further, wavelets have been used in developing system identification approaches based on the localization properties of the wavelet transform (e.g. Stasjewski, 1998; Ghanem and Romeo, 2000; Ghanem and Romeo, 2001; Kijewski and Kareem, 2003; Chen et al., 2009). Further, the wavelet transform was employed in Mukherjee and Gupta (2002) and in Giaralis and Spanos (2009) to address the problem of synthesizing artificial seismic accelerograms compatible with a given design spectrum. A wavelet-based approach was developed in Phoon et al. (2002) to solve the Fredholm integral equation for Karhunen-Loeve expansion, whereas in McWilliam and Knappett (2000) a numerical solution of the Fokker-Planck (F-P) equation using Shannon wavelets was presented. Note that several damage detection applications have been based on wavelet analysis (e.g. Rucka and Wilde, 2006; Spanos et al., 2006; Lam and Ng, 2008). A more detailed presentation of engineering related applications can be found in review papers such as the one by Spanos and Failla (2005).

Harmonic wavelets have a critical presence in structural dynamics applications. In this chapter, relying on the properties of the generalized harmonic wavelets and on a mathematically rigorous approach to modeling non-stationary processes (Nason et al., 2000, Eckley et al., 2010), a representation of the process corresponding to a specific scale and translation level is derived. Relevant

numerical results demonstrate the applicability of the approach for both separable and non-separable EPS estimation. Further, the response EPS of a linear system is derived and a novel statistical linearization approach is developed for the nonlinear response EPS determination. The advantages of this approach vis-à-vis the existing linearization schemes are emphasized and its reliability is verified by pertinent Monte Carlo studies.

7.2 Harmonic wavelets based stochastic process representation

7.2.1 Harmonic wavelet transform

The family of generalized harmonic wavelets uses two parameters (m,n) for the definition of the bandwidth at each scale level; see Newland (1994b). The main advantage relates to the fact that these two parameters essentially decouple the time-frequency resolution achieved at each scale from the value of the central frequency, in contrast to other wavelet bases such as the Morlet and other families.

Generalized harmonic wavelets have a band-limited, box-shaped frequency spectrum. A wavelet of (m,n) scale and (k) position in time attains a representation in the frequency domain of the form (Newland, 1994b)

$$\Psi^{G}_{(m,n),k}(\omega)=\begin{cases}\dfrac{1}{(n-m)\Delta\omega}e^{-i\frac{\omega kT_o}{n-m}}, & m\Delta\omega\le\omega<n\Delta\omega\\ 0, & otherwise\end{cases}, \tag{7.1}$$

where (m), (n) and (k) are considered to be positive integers and

$$\Delta\omega = \frac{2\pi}{T_o}, \tag{7.2}$$

where (T_o) is the total time duration of the signal under consideration. The inverse Fourier transform of Eq.(7.1) yields the time-domain representation of the wavelet which is equal to

$$\psi^G_{(m,n),k}(t) = \frac{e^{in\Delta\omega\left(t-\frac{kT_0}{n-m}\right)} - e^{im\Delta\omega\left(t-\frac{kT_0}{n-m}\right)}}{i(n-m)\Delta\omega\left(t-\frac{kT_0}{n-m}\right)}, \tag{7.3}$$

and is in general complex-valued, with magnitude (Spanos et al., 2005)

$$\left|\psi^G_{(m,n),k}(t)\right| = \frac{\sin\left(\pi(n-m)\left(\frac{t}{T_o}-\frac{k}{n-m}\right)\right)}{\pi(n-m)\left(\frac{t}{T_o}-\frac{k}{n-m}\right)}, \tag{7.4}$$

and phase

$$\phi^G_{(m,n),k}(t) = \pi(n+m)\left(\frac{t}{T_o}-\frac{k}{n-m}\right). \tag{7.5}$$

It has been shown (Newland, 1994b) that a collection of harmonic wavelets spanning adjacent non-overlapping intervals at different scales forms an orthogonal basis. The continuous generalized harmonic wavelet transform (GHWT) is defined as (Newland, 1994b)

$$W^G_{(m,n),k} = \frac{n-m}{T_o}\int_{-\infty}^{\infty} f(t)\overline{\psi^G_{(m,n),k}(t)}dt, \tag{7.6}$$

and projects the $(f(t))$ on this wavelet basis; the bar over a symbol represents complex conjugation. Further, the orthogonality properties of such a basis allow

for perfect reconstruction of the original signal $(f(t))$ according to the equation (Newland, 1994b; Spanos et al., 2005)

$$f(t) = 2\,\mathrm{Re}\left[\sum_{m,n}\sum_{k}\left(W^{G}_{(m,n),k}\psi^{G}_{(m,n),k}(t)\right)\right], \tag{7.7}$$

where in Eq.(7.7) $(f(t))$ is assumed to be a zero-mean signal. Note that Eq.(7.7) represents a harmonic wavelet based representation of deterministic functions. In the next section, a harmonic wavelet based representation of non-stationary stochastic processes is developed based on the locally stationary wavelet (LSW) process representation introduced by Nason et al. (2000).

7.2.2 Locally stationary wavelet process representation

Most rigorous approaches to modeling non-stationary stochastic processes are based on extensions of the classical representation of stationary processes (e.g. Cramer and Leadbetter, 1967). Specifically, a zero mean stationary process $(f(t))$ can be represented as

$$f(t) = \int_{-\infty}^{\infty} A(\omega)e^{i\omega t}dZ(\omega), \tag{7.8}$$

where $(A(\omega))$ is a deterministic function and $(dZ(\omega))$ is a zero mean orthonormal increment stochastic process. The power spectrum of the process $(f(t))$ is then defined as $S_f(\omega) = |A(\omega)|^2$.

Next, to develop models whose spectral content changes with time one option is to replace the amplitude $(A(\omega))$ in Eq.(7.8) by a time-varying version $(A(t,\omega))$. This leads to the notion of slowly varying non-stationary processes as

defined by Priestley (1965, 1967, 1988). This concept was later refined by Dahlhaus (1997) who introduced the class of locally stationary processes. Intuitively, a stochastic process is considered locally stationary if an interval can be formed where the process is approximately stationary about each time point. In the Dahlhaus model the Fourier basis functions are used which are not localized in time. The localization is achieved by the time-varying function $\left(A(t,\omega)\right)$.

Another option involves replacing the Fourier basis functions by others which are localized both in the time and frequency domains. For this purpose, Ombao et al. (2002) developed a representation of the form of Eq.(7.8) in terms of the smooth localized complex exponential (SLEX) functions; they can be considered as localized versions of the Fourier complex exponential functions since they are obtained by applying two specially constructed windows on the Fourier vectors. The SLEX model, in contrast to the Dahlhaus model, provides an explicit segmentation of the time-frequency plane and, therefore, a time-varying spectrum which is piecewise constant along time segments of stationarity.

A similar framework developed by Nason et al. (2000) and by Eckley et al. (2010) introduced a novel representation of non-stationary stochastic processes in which the Fourier basis is replaced by a wavelet basis. The proposed process model is constructed to be locally stationary by imposing constraints on the model coefficients, resulting in what is known as a LSW process. This allows for defining a wavelet spectrum at a particular scale and location. According to the LSW process representation, the non-stationary process $\left(f(t)\right)$ can be represented as

$$f(t)=\sum_{j}\sum_{k} w_{j,k}\psi_{j,k}(t)\xi_{j,k}\,, \tag{7.9}$$

where $\left(\xi_{j,k}\right)$ is a stochastic orthonormal increment sequence; $\left(\psi_{j,k}(t)\right)$ is a non-decimated family of wavelets and $\left(\sum_{j}\right)$ and $\left(\sum_{k}\right)$ represent summations over the different scales and translation levels, respectively. According to the properties of the representation of Eq.(7.9), which are defined and proved in Nason et al. (2000), the local contribution to the variance of the process of Eq.(7.9) is given by the term $\left(\left|w_{j,k}\right|^2\right)$. Rewriting next Eq.(7.9) for the case of generalized harmonic wavelets yields

$$f(t)=\sum_{(m,n)}\sum_{k}\sqrt{S_{(m,n),k}\left(n-m\right)\Delta\omega}\,\psi^{G}_{(m,n),k}\left(t\right)\xi_{(m,n),k}\,, \tag{7.10}$$

where $\left(S_{(m,n),k}\right)$ is the evolutionary spectrum at scale $\left(m,n\right)$ and translation $\left(k\right)$. In conjunction with the preceding analysis consider a representation of a stochastic process $\left(f(t)\right)$ in the form

$$f(t)=\sum_{(m,n)}\sum_{k} f_{(m,n),k}(t)\,, \tag{7.11}$$

where $\left(f_{(m,n),k}(t)\right)$ represents the process at scale $\left(m,n\right)$ and translation $\left(k\right)$ defined in the intervals $\left(m\Delta\omega\le\omega<n\Delta\omega\right)$ and $\left(\frac{k}{n-m}T_o\le t<\frac{k+1}{n-m}T_o\right)$, and is given by

$$f_{(m,n),k}(t)=\sqrt{S_{(m,n),k}\left(n-m\right)\Delta\omega}\,\psi^{G}_{(m,n),k}\left(t\right)\xi_{(m,n),k}\,. \tag{7.12}$$

Taking into account Eq.(7.3) and noticing that

$$\int_{m\Delta\omega}^{n\Delta\omega} e^{i\omega\left(t-\frac{kT_0}{n-m}\right)} d\omega = \frac{e^{in\Delta\omega\left(t-\frac{kT_0}{n-m}\right)} - e^{im\Delta\omega\left(t-\frac{kT_0}{n-m}\right)}}{i(n-m)\Delta\omega\left(t-\frac{kT_0}{n-m}\right)}(n-m)\Delta\omega, \tag{7.13}$$

yields

$$\int_{m\Delta\omega}^{n\Delta\omega} e^{i\omega\left(t-\frac{kT_0}{n-m}\right)} d\omega = \psi^G_{(m,n),k}(t)\left((n-m)\Delta\omega\right). \tag{7.14}$$

Combining Eqs.(7.12) and (7.14) gives

$$f_{(m,n),k}(t) = \int_{m\Delta\omega}^{n\Delta\omega} e^{i\omega\left(t-\frac{kT_0}{n-m}\right)} dZ_{(m,n),k}(\omega), \tag{7.15}$$

with the properties

$$E\left(dZ_{(m,n),k}(\omega)\right) = 0, \tag{7.16}$$

and

$$E\left(\left|dZ_{(m,n),k}(\omega)\right|^2\right) = S_{(m,n),k}(n-m)\Delta\omega. \tag{7.17}$$

The similarity between Eq.(7.8) and Eq.(7.15) is obvious. This is not surprising considering the fact that the harmonic wavelet basis functions are essentially localized Fourier functions. Note that $\left(f_{(m,n),k}(t)\right)$ is real valued if and only if

$$f_{(m,n),k}(t) = \overline{f_{(m,n),k}}(t), \tag{7.18}$$

or, equivalently

$$dZ_{(m,n),k}(\omega) = \overline{dZ_{(m,n),k}}(-\omega). \tag{7.19}$$

Then, following a similar analysis as in Liang et al. (2007), and assuming that the frequency band $[m\Delta\omega, n\Delta\omega]$ is small enough a spectral representation of

$\left(f_{(m,n),k}(t)\right)$ of the form of Eq.(7.15) involving harmonics of random amplitudes (e.g. Shinozuka and Deodatis, 1991, Grigoriu, 1993) can be cast in the form

$$f^{RA}_{(m,n),k}(t) = A_{(m,n),k}\cos\left(\omega_{c,(m,n),k}\left(t-\frac{kT_0}{n-m}\right)\right)+... \\ B_{(m,n),k}\sin\left(\omega_{c,(m,n),k}\left(t-\frac{kT_0}{n-m}\right)\right). \tag{7.20}$$

Note that this representation is defined in the intervals $\left(m\Delta\omega \le \omega_l < n\Delta\omega\right)$ and $\left(\frac{k}{n-m}T_o \le t < \frac{k+1}{n-m}T_o\right)$ with

$$\omega_{c,(m,n),k} = \frac{(n+m)\Delta\omega}{2}, \tag{7.21}$$

and $\left(A_{(m,n),k}\right)$, $\left(B_{(m,n),k}\right)$ representing statistically independent random variables with mean value equal to zero and variance equal to

$$E\left(A^2_{(m,n),k}\right) = E\left(B^2_{(m,n),k}\right) = 2S_{(m,n),k}(n-m)\Delta\omega\,. \tag{7.22}$$

Alternatively, it can be shown (e.g. Shinozuka and Deodatis, 1991) that a spectral representation of $\left(f_{(m,n),k}(t)\right)$ of the form of Eq.(7.15) involving harmonics of constant amplitudes and of random phases can be cast in the form

$$f^{RP}_{(m,n),k}(t) = \sqrt{4S_{(m,n),k}(n-m)\Delta\omega}\cos\left(\omega_{c,(m,n),k}\left(t-\frac{kT_0}{n-m}\right)+\phi_{(m,n),k}\right), \tag{7.23}$$

where $\left(\phi_{(m,n),k}\right)$ are independent random variables following a uniform distribution over the interval $[0,2\pi]$. Taking the first and second derivatives of Eq.(7.20) yields

$$\dot{f}^{RA}_{(m,n),k}(t) = -\omega_{c,(m,n),k} A_{(m,n),k} \sin\left(\omega_{c,(m,n),k}\left(t - \frac{kT_0}{n-m}\right)\right) + \ldots$$
$$\omega_{c,(m,n),k} B_{(m,n),k} \cos\left(\omega_{c,(m,n),k}\left(t - \frac{kT_0}{n-m}\right)\right), \tag{7.24}$$

and

$$\ddot{f}^{RA}_{(m,n),k}(t) = -\left(\omega_{c,(m,n),k}\right)^2 A_{(m,n),k} \cos\left(\omega_{c,(m,n),k}\left(t - \frac{kT_0}{n-m}\right)\right) \ldots$$
$$-\left(\omega_{c,(m,n),k}\right)^2 B_{(m,n),k} \sin\left(\omega_{c,(m,n),k}\left(t - \frac{kT_0}{n-m}\right)\right), \tag{7.25}$$

respectively. Further, consider the term

$$E\left(f^{RA}_{(m,n),k}(t)\right) = E\left(A_{(m,n),k}\right)\cos\left(\omega_{c,(m,n),k}\left(t - \frac{kT_0}{n-m}\right)\right) + \ldots$$
$$E\left(B_{(m,n),k}\right)\sin\left(\omega_{c,(m,n),k}\left(t - \frac{kT_0}{n-m}\right)\right), \tag{7.26}$$

where $\left(E(.)\right)$ denotes the expectation operator. Since $E\left(A_{(m,n),k}\right) = E\left(B_{(m,n),k}\right) = 0$, Eq.(7.26) yields

$$E\left(f^{RA}_{(m,n),k}(t)\right) = 0. \tag{7.27}$$

For the same reason

$$E\left(\dot{f}^{RA}_{(m,n),k}(t)\right) = E\left(\ddot{f}^{RA}_{(m,n),k}(t)\right) = 0. \tag{7.28}$$

Further,

$$E\left(f^{RA}_{(m,n),k}(t)\dot{f}^{RA}_{(m,n),k}(t)\right)=...$$

$$-E\left(A^2_{(m,n),k}\right)\omega_{c,(m,n),k}\cos\left(\omega_{c,(m,n),k}\left(t-\frac{kT_0}{n-m}\right)\right)\sin\left(\omega_{c,(m,n),k}\left(t-\frac{kT_0}{n-m}\right)\right)+...$$

$$E\left(A_{(m,n),k}B_{(m,n),k}\right)\omega_{c,(m,n),k}\cos^2\left(\omega_{c,(m,n),k}\left(t-\frac{kT_0}{n-m}\right)\right)-... \tag{7.29}$$

$$E\left(A_{(m,n),k}B_{(m,n),k}\right)\omega_{c,(m,n),k}\sin^2\left(\omega_{c,(m,n),k}\left(t-\frac{kT_0}{n-m}\right)\right)+...$$

$$E\left(B^2_{(m,n),k}\right)\omega_{c,(m,n),k}\cos\left(\omega_{c,(m,n),k}\left(t-\frac{kT_0}{n-m}\right)\right)\sin\left(\omega_{c,(m,n),k}\left(t-\frac{kT_0}{n-m}\right)\right).$$

Taking next into account the independence of $\left(B_{(m,n),k}\right)$ and $\left(A_{(m,n),k}\right)$, and considering Eqs.(7.22) and (7.27) yields

$$E\left(f^{RA}_{(m,n),k}(t)\dot{f}^{RA}_{(m,n),k}(t)\right)=0. \tag{7.30}$$

Similarly,

$$E\left(\dot{f}^{RA}_{(m,n),k}(t)\ddot{f}^{RA}_{(m,n),k}(t)\right)=0. \tag{7.31}$$

Further, taking into account Eq.(7.22) and manipulating yields

$$E\left(\left(f^{RA}_{(m,n),k}(t)\right)^2\right)=2S_{(m,n),k}\left(n-m\right)\Delta\omega. \tag{7.32}$$

Similarly,

$$E\left(\left(\dot{f}^{RA}_{(m,n),k}(t)\right)^2\right)=2\omega^2_{c,(m,n),k}S_{(m,n),k}\left(n-m\right)\Delta\omega, \tag{7.33}$$

$$E\left(\left(\ddot{f}^{RA}_{(m,n),k}(t)\right)^2\right)=2\omega^4_{c,(m,n),k}S_{(m,n),k}\left(n-m\right)\Delta\omega, \tag{7.34}$$

and

$$E\left(f^{RA}_{(m,n),k}(t)\ddot{f}^{RA}_{(m,n),k}(t)\right)=-2\omega^2_{c,(m,n),k}S_{(m,n),k}\left(n-m\right)\Delta\omega. \tag{7.35}$$

7.3 Separable and Non-Separable EPS estimation

7.3.1 Spectral estimates via the harmonic wavelet transform

An early effort to estimate the power spectrum of non-stationary processes was made by Spanos et al. (1987). Early attempts of applications of wavelets in spectral estimation for vibration problems include the work by Basu and Gupta (1998, 2000) where they related the mean square value of the wavelet transform at different scales and the time-dependent spectral content of the process. Spanos and Failla (2004) followed an alternative approach developing relationships between the EPS and the wavelet coefficients in context with the theory of non-stationary processes as proposed by Priestley (1965, 1967). This approach was also adopted in the response analysis of long span bridges by Chakraborty and Basu (2008). In a recent paper by Huang and Chen (2009) the approach initially proposed by Spanos and Failla (2004) was extended to obtain EPS estimations of multivariate processes. In the same paper, the approach was also compared to direct estimates of the spectrum through wavelet coefficients (e.g. Basu and Gupta, 2000) illustrating higher accuracy. It can be argued that one of the obvious reasons for the low performance of the direct estimation approach relates to the manner in which the time-frequency plane is partitioned. In fact, this observation is highlighted in the paper by Spanos et al. (2005) where the performance of generalized harmonic wavelets (e.g. Newland, 1994b) over dyadic harmonic wavelets (e.g. Newland, 1993a; Newland, 1993b) in estimating separable EPS appears superior.

In the same context, the developments of the preceding section are used herein to derive a scheme for estimations of both separable and non-separable EPS for stochastic processes. In this sense, taking into account the fact that any two general harmonic wavelets are orthogonal if they are at different levels, and that they are also orthogonal if they are in the same level (m,n) and translated with respect to each other by any interval $\left(kT_o/(n-m)\right)$ (Newland, 1994b), the equation

$$\int_{-\infty}^{\infty}|f(t)|^2 dt = 2\sum_{m,n}\sum_{k}\left(\frac{T_o}{n-m}\left|W^G_{(m,n),k}\right|^2\right), \tag{7.36}$$

holds true. Moreover, according to Parseval's theorem,

$$2\pi\int_{-\infty}^{\infty}|F(\omega)|^2 d\omega = \int_{-\infty}^{\infty}|f(t)|^2 dt\,. \tag{7.37}$$

Taking expectations on both sides of Eq.(7.37) yields

$$2\pi\int_{-\infty}^{\infty}E\left[|F(\omega)|^2\right]d\omega = \int_{-\infty}^{\infty}E\left[|f(t)|^2\right]dt\,. \tag{7.38}$$

Combining Eqs.(7.36) and (7.38) and considering the non-overlapping character of the different energy bands, it can be argued that the estimation of the EPS $\left(S(\omega,t)\right)$ can be obtained as

$$S(\omega_i,t_i) = \frac{T_o}{2\pi(n-m)}E\left[\left|W^G_{(m,n),k}\right|^2\right], \quad m\Delta\omega \le \omega_i < n\Delta\omega, \quad \frac{kT_o}{n-m} \le t_i < \frac{(k+1)T_o}{n-m}\,. \tag{7.39}$$

Note that Eq.(7.39) is in agreement with the LSW process representation of section 7.2. In fact, it was shown in Nason et al. (2000) that the expectation of the squared amplitude of the wavelet coefficient corresponding to the specific

scale and translation level, computed using sample paths of the process of Eq.(7.9), converges to the target evolutionary spectrum.

7.3.2 Separable EPS estimation application

To demonstrate the accuracy of the proposed estimation the following form of a time-modulated Kanai-Tajimi (Kanai, 1957; Tajimi, 1960) spectrum is considered

$$S(\omega,t)=|g(t)|^2 S_v(\omega). \tag{7.40}$$

In this equation

$$g(t)=k(e^{-at}-e^{-bt}), \tag{7.41}$$

where $(a=0.1)$ and $(b=0.2)$; (k) is a constant so that $(g_{\max}=1)$; and

$$S_v(\omega)=S_1\frac{(\omega_g)^4+4(\zeta_g)^2(\omega_g)^2\omega^2}{\left((\omega_g)^2-\omega^2\right)^2+4(\zeta_g)^2(\omega_g)^2\omega^2},\quad -\infty<\omega<\infty, \tag{7.42}$$

in which $(\omega_g=20 rad/\sec)$, $(\zeta_g=0.24)$ and $(S_1=1)$. The Kanai-Tajimi spectrum (Eq.(7.42)) relates to the squared modulus of the frequency response function of a single-degree-of-freedom oscillator with prescribed stiffness and damping elements. Realizations of the process characterized by $S(\omega,t)$ can be produced generating first stationary time histories $(v(t))$ compatible with $(S_v(\omega))$. Next, the desired non-stationary records are obtained by multiplying the stationary $(v(t))$ realizations by the modulating function $(g(t))$.

For simulation purposes, the autoregressive moving average (ARMA) method is employed to generate realizations of the stationary process $(v(t))$ as the response of a linear time-invariant digital filter subjected to clipped white noise input; see for a review Spanos and Zeldin (1998). Specifically, the n-th sample of an ARMA(p,q) process is calculated recursively by using the equation

$$v_n = \sum_{l=0}^{q} c_l s_{n-l} - \sum_{k=1}^{p} b_k v_{n-k} \,, \tag{7.43}$$

where (c_l, b_k) are the coefficients of the ARMA filter; (s) represents a band-limited white noise process.

In Fig.(7.1) the target spectrum (Eq.(7.40)) is shown, whereas in Fig.(7.2) the one estimated by Eq.(7.39) is plotted. To this aim, for each realization generated using Eq.(7.43), wavelet coefficients for each scale and position are calculated and a mean value over all the realizations corresponding to these discrete scale and time position values is computed. In this manner, a total number of 500 time histories are produced with a duration $(T_o = 18.9\,\mathrm{sec})$. The Nyquist frequency is chosen to be $(\omega_{Nyq} = 50 rad/\mathrm{sec})$.

As far as the calculation of the wavelet coefficients is considered, a computationally efficient algorithm, which takes advantage of the fast Fourier transform (FFT) scheme, can be found in Newland (1997, 1999a, 1999b). In fact, in Newland (1993b) comparisons with Mallat's pyramid algorithm (Mallat, 1989) include cases where the FFT-based algorithm appears more efficient. Furthermore, it is obvious that by changing the values of (m) and (n) there is a

compromise between time and frequency resolution. The value $(n-m=5)$ is chosen to be used in the ensuing analysis. In Fig.(7.3) the target and the estimated EPS are plotted at two time instants $(t=5.7\sec)$ and $(t=15.7\sec)$. It can be readily seen that the two EPS are in good agreement with each other.

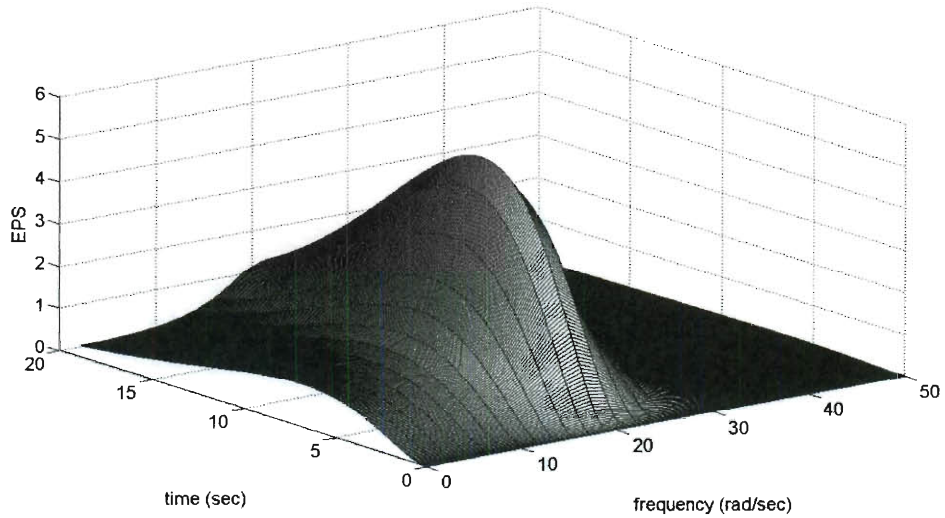

Fig.(7.1). Target time-modulated Kanai-Tajimi power spectrum: $(a=0.1, b=0.2)$ and $(\omega_g = 20 rad/\sec, \zeta_g = 0.24, S_1 = 1)$.

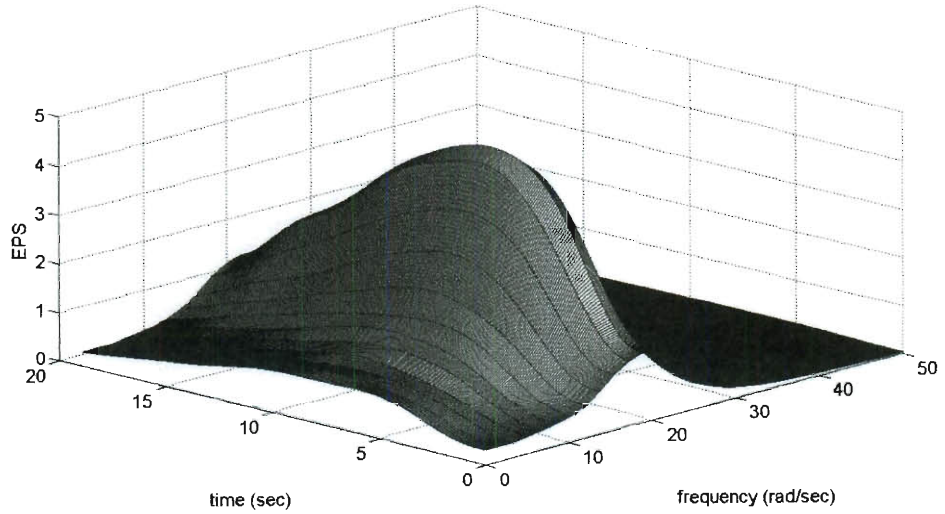

Fig.(7.2). Time-modulated Kanai-Tajimi power spectrum estimate using MCS (500 realizations): $(a=0.1, b=0.2)$ and $(\omega_g = 20 rad/\sec, \zeta_g = 0.24, S_1 = 1)$.

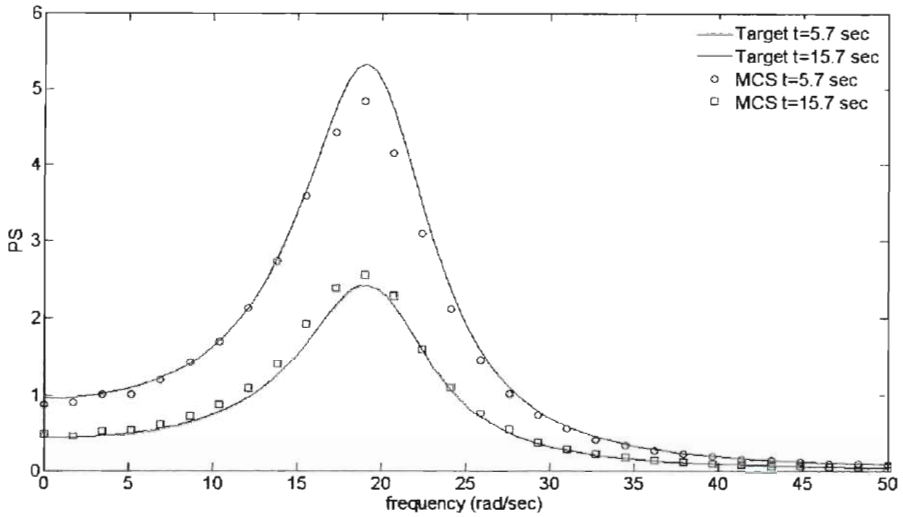

Fig.(7.3). Time-modulated Kanai-Tajimi power spectrum at $(t = 5.7\,\text{sec})$ and $(t = 15.7\,\text{sec})$. Comparison between MCS data (500 realizations) and the target spectrum: $(a = 0.1, b = 0.2)$ and $(\omega_g = 20 rad/\text{sec}, \zeta_g = 0.24, S_1 = 1)$.

7.3.3 Non-Separable EPS estimation application

Next the proposed approach is applied for the non-separable spectrum of the form

$$S(\omega,t) = S_2\left(\frac{\omega}{5\pi}\right)^2 e^{-0.15t} t^2 e^{-\left(\frac{\omega}{5\pi}\right)^2 t}, \quad t \geq 0, \quad -\infty < \omega < \infty, \tag{7.44}$$

where $(S_2 = 1)$, is considered next. This spectrum (Fig.(7.4)) comprises some of the predominant features of seismic shaking, such as decreasing of the dominant frequency with time (Liu, 1970; Spanos and Solomos, 1983). Realization records compatible with Eq.(7.44) are produced using the concept of spectral representation of a stochastic process (Shinozuka and Jan, 1972; Shinozuka and

Deodatis, 1988; Liang et al., 2007). In Fig.(7.5) the EPS estimate using Eq.(7.39) is plotted. In Fig.(7.6) the target and the EPS estimate are plotted at two time instants $(t = 1.6\,\text{sec})$ and $(t = 4.1\,\text{sec})$. The two EPS are in good agreement verifying the reliability of the generalized harmonic wavelet-based EPS estimation approach in cases of physically realistic versions of EPS with time-varying frequency content.

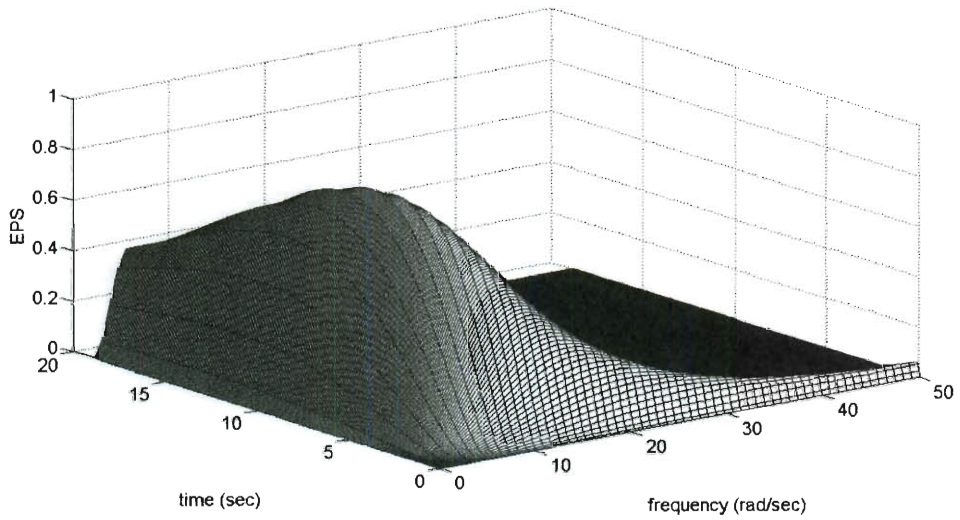

Fig.(7.4). Non-separable evolutionary power spectrum $(S_2 = 1)$.

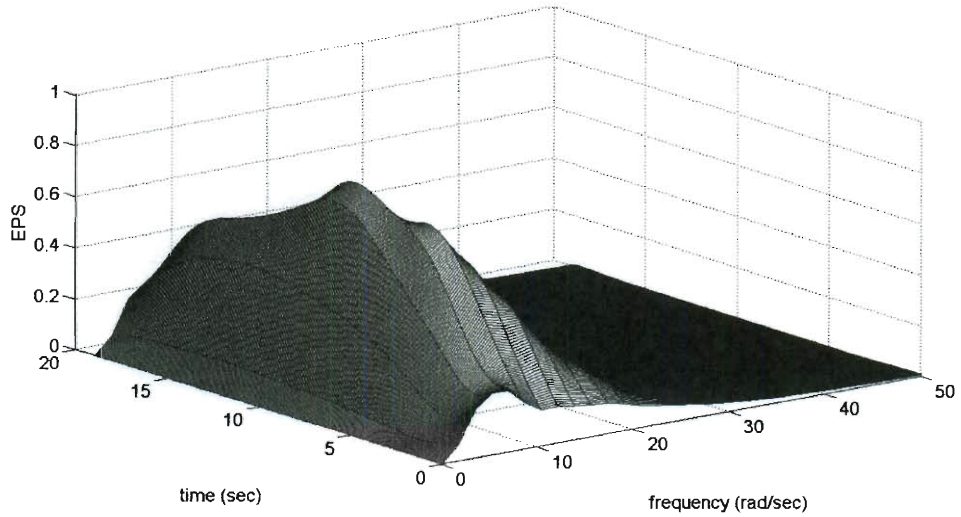

Fig.(7.5). Non-separable evolutionary power spectrum $(S_2 = 1)$ estimate using MCS (500 realizations).

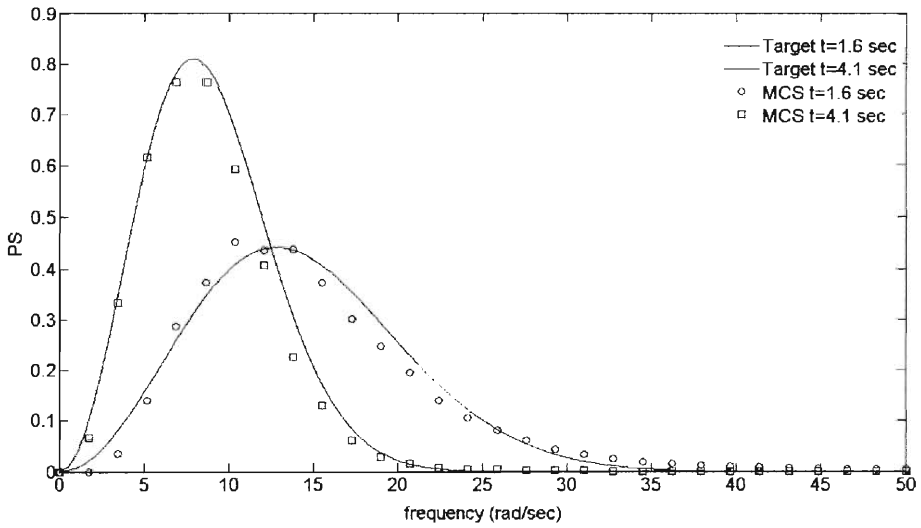

Fig.(7.6). Non-separable power spectrum $(S_2 = 1)$ at $(t = 1.6\,\text{sec})$ and $(t = 4.1\,\text{sec})$. Comparison between MCS data (500 realizations) and the target spectrum.

7.4 Excitation-response EPS relationship for a linear system

7.4.1 Linear response EPS determination

Wavelet-based representations of realizations of stochastic processes have naturally led to the problem of determining wavelet-based system excitation-response relationships. Early attempts towards this direction include the work by Basu and Gupta (1998, 2000) where the determination of the response of a linear single-degree-of-freedom system subject to wavelet-specified seismic excitation was attempted. Excitation-response relationships for linear multi-degree-of-freedom systems were developed in Basu and Gupta (1997) and in Tratskas and Spanos (2003).

Note that the aforementioned literature deals with the wavelet representation of realizations of stochastic processes or, in other words, with representing deterministic functions. In fact, as it has been pointed out in Priestley (1996), unless a rigorous mathematical background model exists for representing non-stationary stochastic processes via wavelets, questions are raised concerning any kind of wavelet-based time-dependent spectral analysis.

In this section, relying on the rigorous LSW process representation of non-stationary stochastic processes developed in section 7.2 and on the orthogonality properties of the components of the proposed representation, excitation-response EPS relationships are derived for a linear system for each time and frequency band. It is shown that since the approach possesses inherently the element of time-dependence the linear system can be time-variant in general.

In this context, consider a linear single-degree-of-freedom system whose motion is governed by the differential equation

$$\ddot{x}+2\zeta_0\omega_0\dot{x}+\omega_0^2 x=w(t), \tag{7.45}$$

where (ζ_0) is the ratio of critical damping; (ω_0) is the natural frequency; and $(w(t))$ represents a zero-mean non-stationary stochastic process possessing an EPS $S(\omega,t)$. Utilizing next the representations of Eqs.(7.11) and (7.20) both for the response and for the excitation processes Eq.(7.45) becomes

$$\sum_{(m,n)}\sum_{k}\ddot{x}_{(m,n),k}+2\zeta_0\omega_0\sum_{(m,n)}\sum_{k}\dot{x}_{(m,n),k}+\omega_0^2\sum_{(m,n)}\sum_{k}x_{(m,n),k}=\sum_{(m,n)}\sum_{k}w_{(m,n),k}, \tag{7.46}$$

where

$$\begin{aligned}x_{(m,n),k}(t)=A_{(m,n),k}\cos\left(\omega_{c,(m,n),k}\left(t-\frac{kT_0}{n-m}\right)\right)+\ldots\\ B_{(m,n),k}\sin\left(\omega_{c,(m,n),k}\left(t-\frac{kT_0}{n-m}\right)\right),\end{aligned} \tag{7.47}$$

and

$$\begin{aligned}w_{(m,n),k}(t)=C_{(m,n),k}\cos\left(\omega_{c,(m,n),k}\left(t-\frac{kT_0}{n-m}\right)\right)+\ldots\\ D_{(m,n),k}\sin\left(\omega_{c,(m,n),k}\left(t-\frac{kT_0}{n-m}\right)\right).\end{aligned} \tag{7.48}$$

Considering next the orthogonality conditions of monochromatic functions leads to

$$\int_{\frac{kT_0}{n-m}}^{\frac{(k+1)T_0}{n-m}}\cos\left(\omega_{c,(m,n),k}\left(t-\frac{kT_0}{n-m}\right)\right)\cos\left(\omega_{c,(i,j),l}\left(t-\frac{lT_0}{j-i}\right)\right)dt=\begin{cases}\dfrac{1}{2}\dfrac{T_0}{n-m}, & \begin{matrix}m=i,\\ n=j,\\ k=l\end{matrix}\\ 0, & otherwise\end{cases}, \tag{7.49}$$

$$\int_{\frac{kT_0}{n-m}}^{\frac{(k+1)T_0}{n-m}} \sin\left(\omega_{c,(m,n),k}\left(t-\frac{kT_0}{n-m}\right)\right)\sin\left(\omega_{c,(i,j),l}\left(t-\frac{lT_0}{j-i}\right)\right)dt=\begin{cases}\dfrac{1}{2}\dfrac{T_o}{n-m}, & \begin{matrix}m=i,\\ n=j,\\ k=l\end{matrix}\\ 0, & otherwise\end{cases}, \quad (7.50)$$

and

$$\int_{\frac{kT_0}{n-m}}^{\frac{(k+1)T_0}{n-m}} \cos\left(\omega_{c,(m,n),k}\left(t-\frac{kT_0}{n-m}\right)\right)\sin\left(\omega_{c,(i,j),l}\left(t-\frac{lT_0}{j-i}\right)\right)dt=0. \quad (7.51)$$

Substituting Eqs.(7.47-7.48) into Eq.(7.46) and exploiting Eqs.(7.49-7.51) yields (see also Spanos et al., 2002, Failla et al., 2003, Spanos et al., 2011)

$$\begin{cases}-(\omega_{c,(m,n),k})^2 A_{(m,n),k}+2\zeta_0\omega_0(\omega_{c,(m,n),k})B_{(m,n),k}+\omega_0^2 A_{(m,n),k}=C_{(m,n),k}\\ -(\omega_{c,(m,n),k})^2 B_{(m,n),k}-2\zeta_0\omega_0(\omega_{c,(m,n),k})A_{(m,n),k}+\omega_0^2 B_{(m,n),k}=D_{(m,n),k}\end{cases}. \quad (7.52)$$

Manipulating further Eq.(7.52) yields

$$A_{(m,n),k}^2+B_{(m,n),k}^2=\frac{C_{(m,n),k}^2+D_{(m,n),k}^2}{\left[\omega_0^2-(\omega_{c,(m,n),k})^2\right]^2+\left[(\omega_{c,(m,n),k})2\zeta_0\omega_0\right]^2}. \quad (7.53)$$

Applying the expectation operator and considering Eq.(7.22), Eq.(7.53) becomes

$$S_{(m,n),k}^x=\frac{S_{(m,n),k}^w}{\left[\omega_0^2-(\omega_{c,(m,n),k})^2\right]^2+\left[(\omega_{c,(m,n),k})2\zeta_0\omega_0\right]^2}. \quad (7.54)$$

Note that this excitation-response EPS relationship (Eq.(7.54)), valid in the intervals $(m\Delta\omega\le\omega<n\Delta\omega)$ and $\left(\frac{k}{n-m}T_o\le t<\frac{k+1}{n-m}T_o\right)$, resembles the celebrated spectral input-output relationship of the linear stationary analysis. This should be expected since the above analysis relies on the LSW process representation of Eq.(7.9).

7.4.2 Linear time-invariant system application

To assess the accuracy of Eq.(7.54) a linear oscillator of the form of Eq.(7.45) is considered, where $(\omega_0 = 10 rad/\sec, \zeta = 0.1)$. In Fig.(7.7) the response EPS estimated by Monte Carlo simulation (MCS) is shown. A time-modulated Kanai-Tajimi spectrum is chosen for the excitation EPS (Eq.(7.40)) possessing the values $(a = 0.1, b = 0.3, \omega_g = 30 rad/\sec, \zeta_g = 0.01)$. In Fig.(7.8) the response EPS is determined according to Eq.(7.50). In Fig.(7.9) the EPS (Eq.(7.54)) is compared with MCS data for different time instants confirming the accuracy of the approach.

Further, the response EPS of the linear oscillator $(\omega_0 = 10 rad/\sec, \zeta = 0.1)$ under the non-separable spectrum $(S_2 = 1)$ is computed next. In Figs.(7.10) and (7.11) the MCS estimation and the approximate response EPS are shown respectively. In Fig.(7.12) the computed EPS is compared with MCS data for different time instants, confirming the accuracy of the proposed approach.

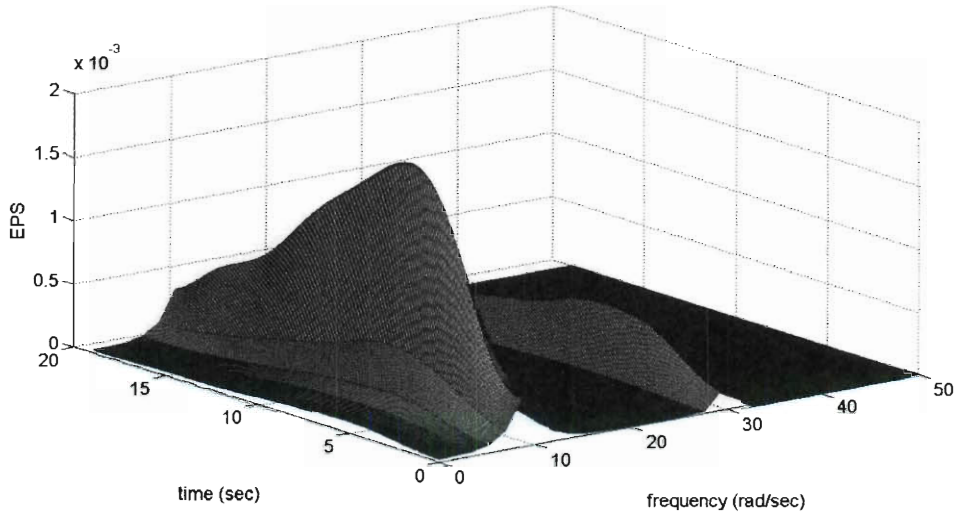

Fig.(7.7). Response EPS of a linear oscillator $(\omega_0 = 10 rad/\sec, \zeta = 0.1)$ under a time-modulated Kanai-Tajimi spectrum $(a = 0.1, b = 0.3, \omega_g = 30 rad/\sec, \zeta_g = 0.01)$. MCS estimation (500 realizations).

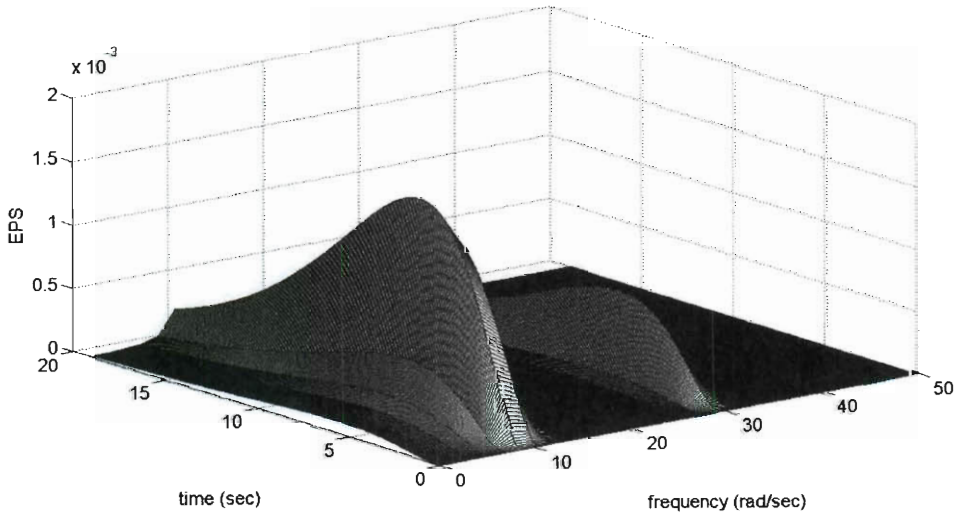

Fig.(7.8). Response EPS of a linear oscillator $(\omega_0 = 10 rad/\sec, \zeta = 0.1)$ under a time-modulated Kanai-Tajimi spectrum $(a = 0.1, b = 0.3, \omega_g = 30 rad/\sec, \zeta_g = 0.01)$. Analytical approach.

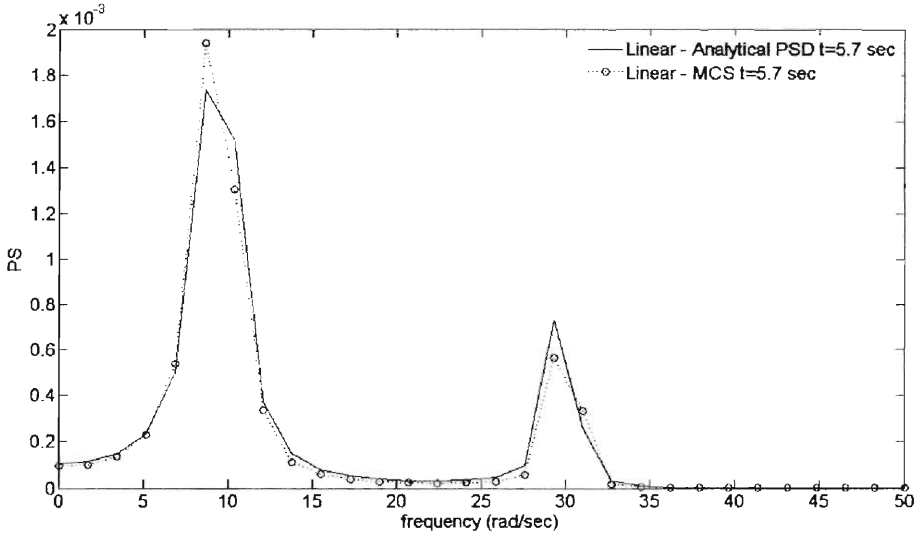

Fig.(7.9). Response EPS of a linear oscillator $(\omega_0 = 10 rad/\sec, \zeta = 0.1)$ at $(t = 5.7\sec)$ and $(t = 15.7\sec)$ under a time-modulated Kanai-Tajimi spectrum $(a = 0.1, b = 0.3, \omega_g = 30 rad/\sec, \zeta_g = 0.01)$. Comparison between MCS data (500 realizations) and the analytical approach.

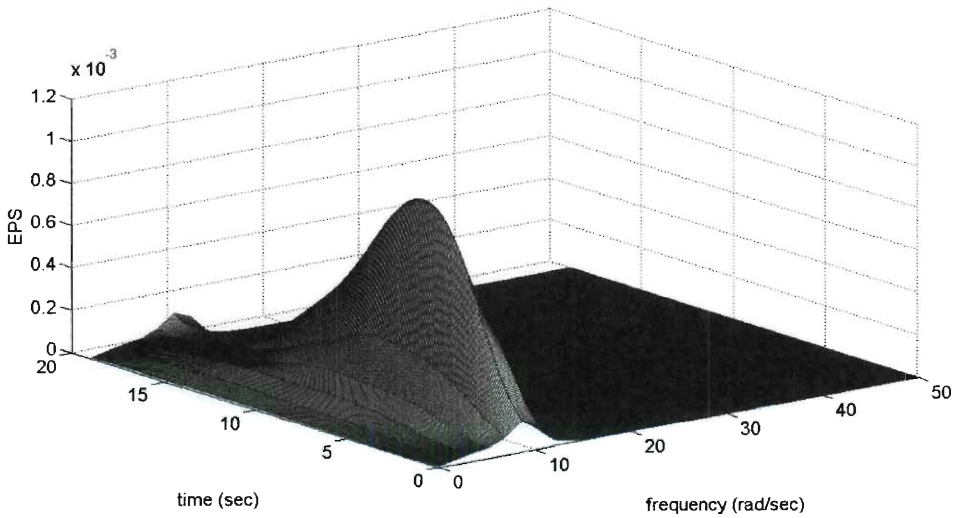

Fig.(7.10). Response EPS of a linear oscillator $(\omega_0 = 10 rad/\sec, \zeta = 0.1)$ under a non-separable evolutionary spectrum $(S_2 = 1)$. MCS estimation (500 realizations).

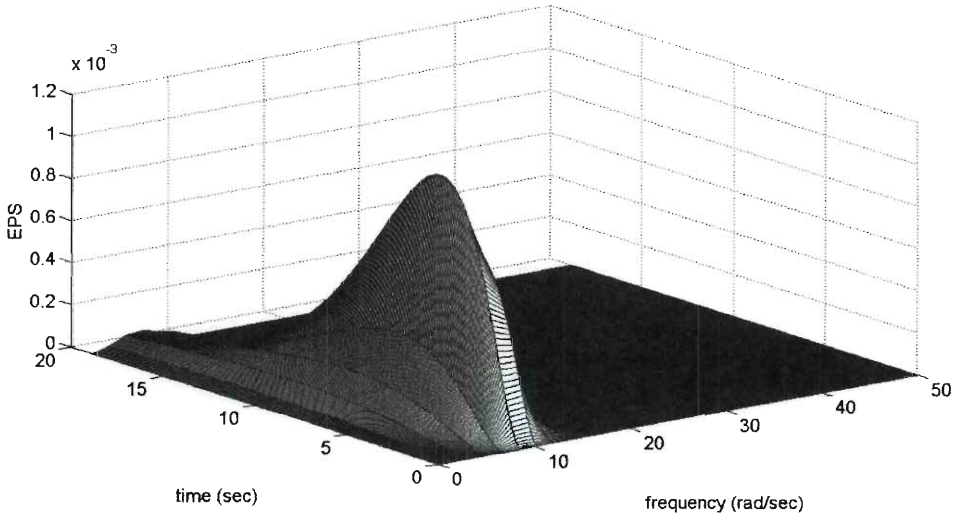

Fig.(7.11). Response EPS of a linear oscillator $(\omega_0 = 10 rad/\sec, \zeta = 0.1)$ under a non-separable evolutionary spectrum $(S_2 = 1)$. Analytical approach.

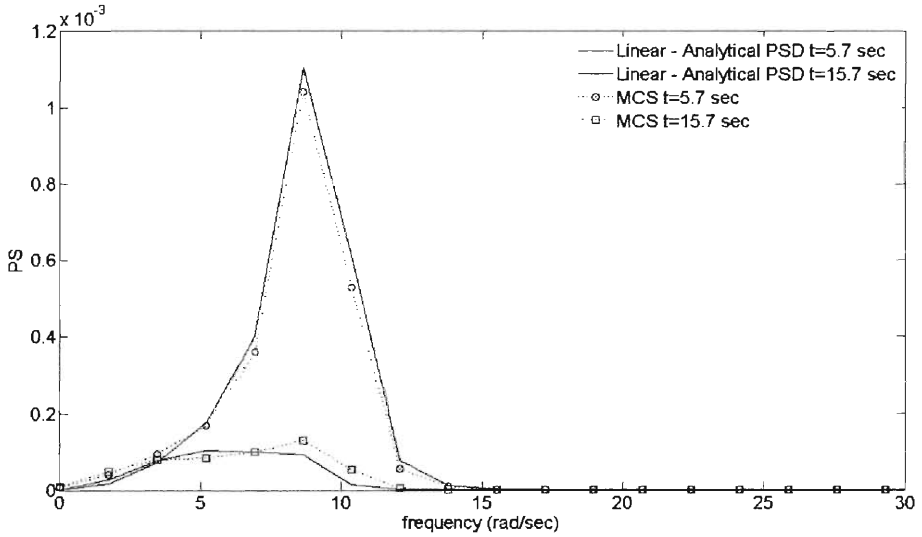

Fig.(7.12). Response EPS of a linear oscillator $(\omega_0 = 10 rad/\sec, \zeta = 0.1)$ at $(t = 5.7 \sec)$ and $(t = 15.7 \sec)$ under a non-separable evolutionary spectrum $(S_2 = 1)$. Comparison between MCS data (500 realizations) and the analytical approach.

7.4.3 Linear time-variant system application

Examining Eq.(7.54) it is readily seen that it represents an input-output spectral relationship, valid in non-overlapping time and frequency intervals. This observation suggests that the proposed approach can perform satisfactorily in cases of linear time-variant (LTV) systems, since it inherently possesses the element of time dependence. Consider next the following equation of motion of a Mathieu type oscillator

$$\ddot{x}+2\zeta_0\omega_0\dot{x}+\omega^2(t)x=w(t), \tag{7.55}$$

where

$$\omega^2(t)=\omega_0^2\left(1-\frac{3}{10}\cos(0.5t)\right), \tag{7.56}$$

where $(\omega_0=10 rad/\sec, \zeta=0.1)$. In this case it is assumed that all the parameters of the problem are such that the system has a stable response in a stochastic sense (e.g. Ibrahim, 1985). The response EPS of a Mathieu oscillator is calculated using the non-separable excitation EPS (Eq.(7.44)). The MCS estimation (Fig.(7.13)) appears to be in quite good agreement with the approximate approach (Fig.(7.14)). Comparisons of the EPS with MCS data at distinct time instants (Fig.(7.15)) further support the reliability of Eq.(7.54).

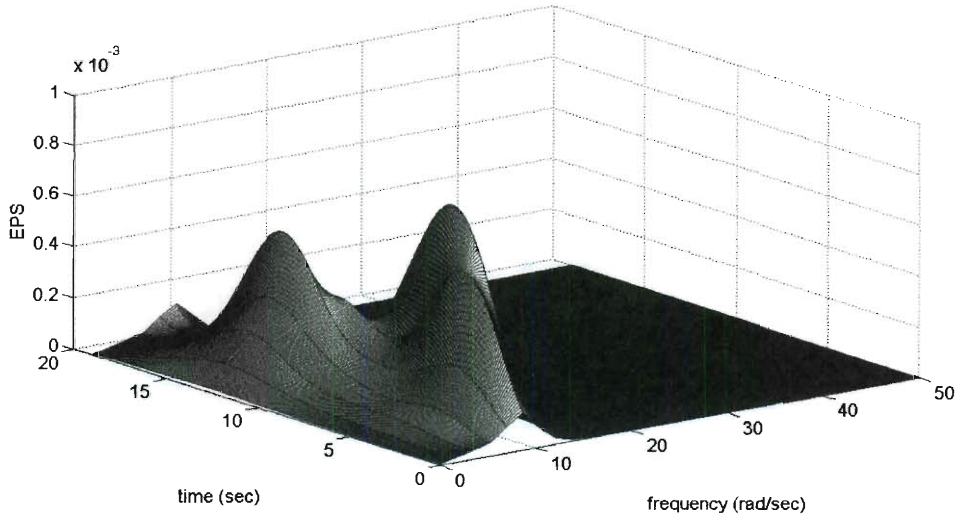

Fig.(7.13). Response EPS of a Mathieu oscillator $(\omega_0 = 10 rad/\sec, \zeta = 0.1)$ under a non-separable evolutionary spectrum $(S_2 = 1)$. MCS estimation (500 realizations).

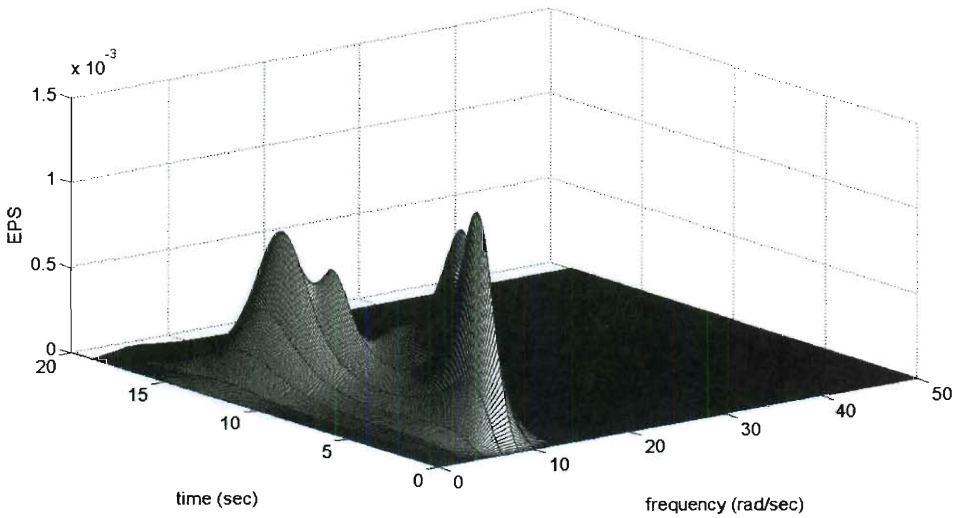

Fig.(7.14). Response EPS of a Mathieu oscillator $(\omega_0 = 10 rad/\sec, \zeta = 0.1)$ under a non-separable evolutionary spectrum $(S_2 = 1)$. Analytical approach.

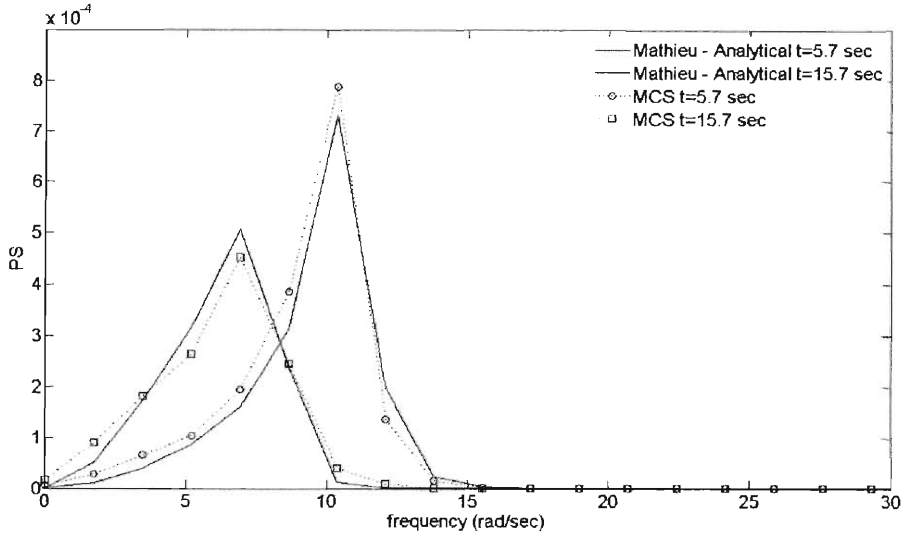

Fig.(7.15). Response EPS of a Mathieu oscillator $(\omega_0 = 10 rad/\sec, \zeta = 0.1)$ at $(t = 5.7\sec)$ and $(t = 15.7\sec)$ under a non-separable evolutionary spectrum $(S_2 = 1)$. Comparison between MCS data (500 realizations) and the analytical approach.

7.5 Harmonic wavelets based statistical linearization

7.5.1 Nonlinear response EPS determination

Early attempts towards developing a linearization approach include the work by Basu and Gupta (1999a) who developed and applied a linearization approach for the evaluation of the response of a sliding foundation (Basu und Gupta, 1999b) and for the response determination of a Duffing oscillator (Basu and Gupta, 2001).

The aforementioned approach yields equivalent linear elements essentially averaged over the different wavelet scales leading to a LTV system. As in the case of a linear system, the aforementioned literature on linearization approaches

deals with deterministic functions and not with stochastic processes. In this section, relying on the LSW representation developed in section 7.2 a statistical linearization approach is developed. In this regard, the equivalent stiffness and damping elements corresponding to the specific frequency and time band are employed to evaluate the response EPS.

Consider next a nonlinear single-degree-of-freedom system whose motion is governed by the differential equation

$$\ddot{x}+2\zeta_0\omega_0\dot{x}+\omega_0^2 x+\varepsilon h[x,\dot{x}]=w(t), \tag{7.57}$$

where (ε) denotes the degree of nonlinearity; and $(h[x,\dot{x}])$ is an arbitrary nonlinear function which depends on the response displacement and velocity. Replacing next the nonlinear system of Eq.(7.57) with the equivalent linear

$$\ddot{x}+2\zeta_{eq}\omega_{eq}\dot{x}+\omega_{eq}^2 x=w(t), \tag{7.58}$$

the difference between Eq.(7.57) and Eq.(7.58) is

$$Er=\varepsilon h[x,\dot{x}]+\left(2\zeta_0\omega_0-2\zeta_{eq}\omega_{eq}\right)\dot{x}+\left(\omega_0^2-\omega_{eq}^2\right)x. \tag{7.59}$$

To define equivalent linear elements $\left(\omega_{eq,(m,n),k}^2\right)$ and $\left(2\zeta_{eq,(m,n),k}\omega_{eq,(m,n),k}\right)$ corresponding to the intervals $(m\Delta\omega\le\omega<n\Delta\omega)$ and $\left(\frac{k}{n-m}T_o\le t<\frac{k+1}{n-m}T_o\right)$ the representations of Eqs.(7.11) and (7.20), and the orthogonality conditions (Eqs.(7.49-7.51)) are employed. Thus, requiring the error to be zero and applying a Galerkin scheme (e.g. Spanos et al., 2002), the error (Er) is projected on the functions $\left(x_{(m,n),k}\right)$ and $\left(\dot{x}_{(m,n),k}\right)$ yielding

$$\varepsilon\int_{\frac{kT_0}{n-m}}^{\frac{(k+1)T_0}{n-m}} h[\sum_{(m,n)}\sum_{k} x_{(m,n),k}, \sum_{(m,n)}\sum_{k} \dot{x}_{(m,n),k}]x_{(m,n),k}dt + \ldots$$
$$\left(2\zeta_0\omega_0 - 2\zeta_{eq,(m,n),k}\omega_{eq,(m,n),k}\right)\int_{\frac{kT_0}{n-m}}^{\frac{(k+1)T_0}{n-m}}\left(\sum_{(m,n)}\sum_{k}\dot{x}_{(m,n),k}\right)x_{(m,n),k}dt + \ldots \tag{7.60}$$
$$\left(\omega_0^2 - \omega_{eq,(m,n),k}^2\right)\int_{\frac{kT_0}{n-m}}^{\frac{(k+1)T_0}{n-m}}\left(\sum_{(m,n)}\sum_{k}x_{(m,n),k}\right)x_{(m,n),k}dt = 0,$$

and

$$\varepsilon\int_{\frac{kT_0}{n-m}}^{\frac{(k+1)T_0}{n-m}} h[\sum_{(m,n)}\sum_{k} x_{(m,n),k}, \sum_{(m,n)}\sum_{k} \dot{x}_{(m,n),k}]\dot{x}_{(m,n),k}dt + \ldots$$
$$\left(2\zeta_0\omega_0 - 2\zeta_{eq,(m,n),k}\omega_{eq,(m,n),k}\right)\int_{\frac{kT_0}{n-m}}^{\frac{(k+1)T_0}{n-m}}\left(\sum_{(m,n)}\sum_{k}\dot{x}_{(m,n),k}\right)\dot{x}_{(m,n),k}dt + \ldots \tag{7.61}$$
$$\left(\omega_0^2 - \omega_{eq,(m,n),k}^2\right)\int_{\frac{kT_0}{n-m}}^{\frac{(k+1)T_0}{n-m}}\left(\sum_{(m,n)}\sum_{k}x_{(m,n),k}\right)\dot{x}_{(m,n),k}dt = 0,$$

respectively. Considering Eq.(7.20), the orthogonality conditions (Eqs.(7.49-7.51)), and taking expectations Eqs.(7.60-7.61) become

$$\varepsilon E\left(\int_{\frac{kT_0}{n-m}}^{\frac{(k+1)T_0}{n-m}} h[\sum_{(m,n)}\sum_{k} x_{(m,n),k}, \sum_{(m,n)}\sum_{k} \dot{x}_{(m,n),k}]x_{(m,n),k}dt\right) + \ldots$$
$$\left(\omega_0^2 - \omega_{eq,(m,n),k}^2\right)\left(\frac{T_0}{n-m}\right)E\left(x_{(m,n),k}^2\right) = 0, \tag{7.62}$$

and

$$\varepsilon E\left(\int_{\frac{kT_0}{n-m}}^{\frac{(k+1)T_0}{n-m}} h[\sum_{(m,n)}\sum_{k} x_{(m,n),k}, \sum_{(m,n)}\sum_{k} \dot{x}_{(m,n),k}]\dot{x}_{(m,n),k}dt\right) + \ldots$$
$$\left(2\zeta_0\omega_0 - 2\zeta_{eq,(m,n),k}\omega_{eq,(m,n),k}\right)\left(\frac{T_0}{n-m}\right)E\left(\dot{x}_{(m,n),k}^2\right) = 0, \tag{7.63}$$

or, equivalently

$$\omega^2_{eq,(m,n),k} = \omega^2_0 + \varepsilon \frac{E\left(\int_{\frac{kT_0}{n-m}}^{\frac{(k+1)T_0}{n-m}} h[\sum_{(m,n)}\sum_{k} x_{(m,n),k}, \sum_{(m,n)}\sum_{k} \dot{x}_{(m,n),k}] x_{(m,n),k} dt \right)}{\left(\frac{T_0}{n-m}\right) E\left(x^2_{(m,n),k}\right)}, \tag{7.64}$$

and

$$2\zeta_{eq,(m,n),k}\omega_{eq,(m,n),k} = 2\zeta_0\omega_0 + \ldots$$
$$\varepsilon \frac{E\left(\int_{\frac{kT_0}{n-m}}^{\frac{(k+1)T_0}{n-m}} h[\sum_{(m,n)}\sum_{k} x_{(m,n),k}, \sum_{(m,n)}\sum_{k} \dot{x}_{(m,n),k}] \dot{x}_{(m,n),k} dt \right)}{\left(\frac{T_0}{n-m}\right) E\left(\dot{x}^2_{(m,n),k}\right)}. \tag{7.65}$$

Note that the equivalent elements (Eqs.(7.64-7.65)) are treated as frequency and time dependent. In other words, Eqs.(7.64-7.65) are valid in the intervals $\left(m\Delta\omega \le \omega < n\Delta\omega\right)$ and $\left(\frac{k}{n-m}T_o \le t < \frac{k+1}{n-m}T_o\right)$. Obviously, the evaluation of the equivalent stiffness and damping elements depends on the response statistics. Thus, additional spectral input-output relationships must be considered to yield a system of simultaneous nonlinear equations which can be solved iteratively. To this aim, the spectral excitation-response relationship Eq.(7.54) is invoked which becomes

$$S^x_{(m,n),k} = \frac{S^w_{(m,n),k}}{\left[\omega^2_{eq,(m,n),k} - (\omega_{c,(m,n),k})^2\right]^2 + \left[(\omega_{c,(m,n),k}) 2\zeta_{eq,(m,n),k}\omega_{eq,(m,n),k}\right]^2}. \tag{7.66}$$

It can be readily seen that for each translation (time) level (k), the unknowns $\left(\omega^2_{eq,(m,n),k}\right)$, $\left(2\zeta_{eq,(m,n),k}\omega_{eq,(m,n),k}\right)$ and $\left(S^x_{(m,n),k}\right)$ can be obtained by solving Eqs.(7.64-7.66) and considering Eqs.(7.32-7.33). To this aim, an iterative scheme is adopted. Initial values are assumed for the unknowns $\left(\omega^2_{eq,(m,n),k}\right)$ and

$\left(2\zeta_{eq,(m,n),k}\omega_{eq,(m,n),k}\right)$. Then, $\left(S^{x}_{(m,n),k}\right)$ is evaluated using Eq.(7.66). This value is used in Eqs.(7.64-7.65) to calculate the equivalent stiffness and damping elements. The iterative scheme is repeated until convergence is reached.

Note that the proposed statistical linearization approach can be the basis for performing a joint time-frequency response analysis. It is readily applicable for both separable and non-separable excitation EPS circumventing any pre-processing treatments commonly used in alternative linearization approaches.

7.5.2 Duffing oscillator application

To assess the accuracy of the approach, a Duffing oscillator of the form

$$\ddot{x}+2\zeta_0\omega_0\dot{x}+\omega_0^2x+\varepsilon\omega_0^2x^3=w(t),\quad \varepsilon>0, \tag{7.67}$$

is considered. Applying Eqs. (7.64-7.65) yields

$$2\zeta_{eq,(m,n),k}\omega_{eq,(m,n),k}=2\zeta_0\omega_0, \tag{7.68}$$

and

$$\omega^2_{eq,(m,n),k}=\omega_0^2+\varepsilon\omega_0^2\frac{E\left(x^4_{(m,n),k}\right)+3\sum\limits_{(i,j),i\neq m,j\neq n}E\left(x^2_{(m,n),k}\right)E\left(x^2_{(i,j),k}\right)}{E\left(x^2_{(m,n),k}\right)}, \tag{7.69}$$

or, equivalently

$$\omega^2_{eq,(m,n),k}=\omega_0^2+\varepsilon\omega_0^2\left(\frac{E\left(x^4_{(m,n),k}\right)}{E\left(x^2_{(m,n),k}\right)}+3\sum_{(i,j),i\neq m,j\neq n}E\left(x^2_{(i,j),k}\right)\right). \tag{7.70}$$

Considering next the standard Gaussian assumption for the response processes, Eq.(7.70) reduces to

$$\omega_{eq,(m,n),k}^2 = \omega_0^2 \left(1 + \varepsilon 3 \sum_{(m,n)} E\left(x_{(m,n),k}^2 \right) \right). \tag{7.71}$$

The parameters values $\left(\omega_0 = 10 rad/\sec, \zeta = 0.1, \varepsilon = 10\right)$ are chosen for the Duffing oscillator of Eq.(7.67). The response EPS of the Duffing oscillator is calculated using the non-separable excitation EPS of Eq.(7.44). The MCS estimation (Fig.(7.16)) appears to be in good agreement with the approximate approach (Fig.(7.17)) even for this high degree of nonlinearity. Comparisons of the EPS with MCS data at distinct time instants (Fig.(7.18)) confirm the above claim.

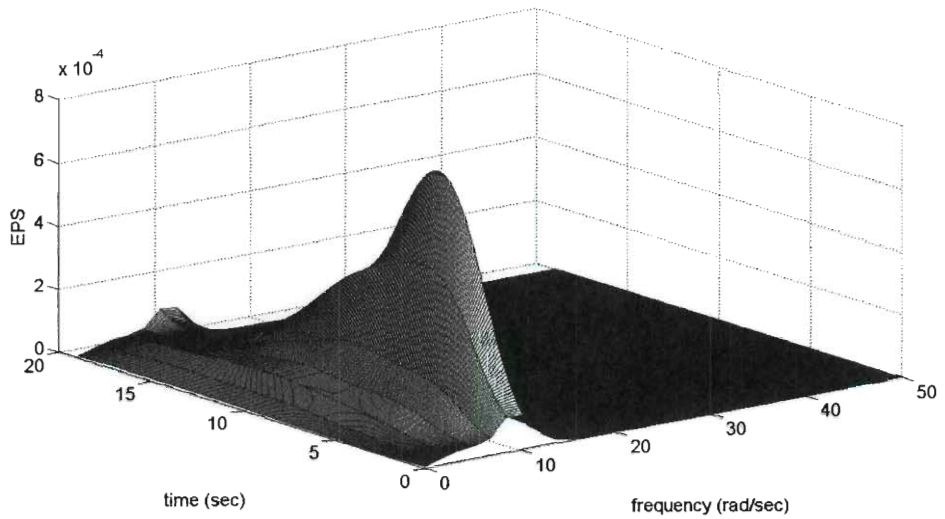

Fig.(7.16). Response EPS of a Duffing oscillator $\left(\omega_0 = 10 rad/\sec, \zeta = 0.1, \varepsilon = 10\right)$ under a non-separable evolutionary spectrum $\left(S_2 = 1\right)$. MCS estimation (500 realizations).

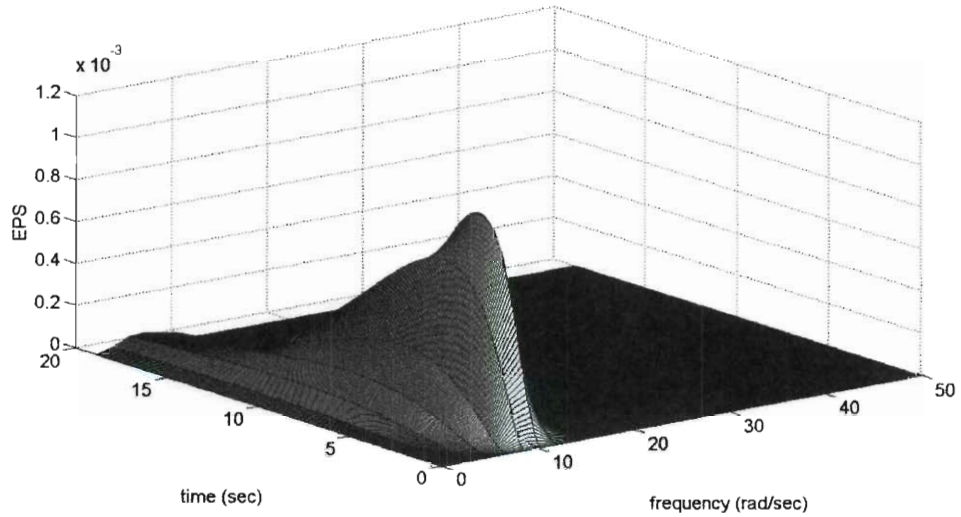

Fig.(7.17). Response EPS of a Duffing oscillator $(\omega_0 = 10 rad/\sec, \zeta = 0.1, \varepsilon = 10)$ under a non-separable evolutionary spectrum $(S_2 = 1)$. Analytical approach.

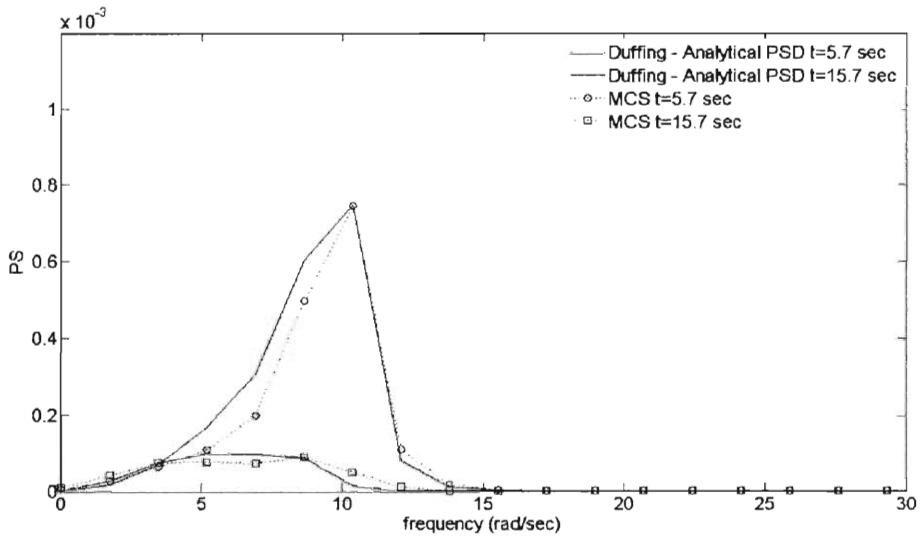

Fig.(7.18). Response EPS of a Duffing oscillator $(\omega_0 = 10 rad/\sec, \zeta = 0.1, \varepsilon = 10)$ at $(t = 5.7 \sec)$ and $(t = 15.7 \sec)$ under a non-separable evolutionary spectrum $(S_2 = 1)$. Comparison between MCS data (500 realizations) and the analytical approach.

7.5.3 Linear-plus-cubic damping oscillator application

To assess the accuracy of the approach when damping nonlinearities are considered, an oscillator possessing linear plus cubic damping of the form

$$\ddot{x}+2\zeta_0\omega_0\dot{x}+\omega_0^2x+\varepsilon 2\zeta_0\omega_0\dot{x}^3=w(t),\quad \varepsilon>0, \tag{7.72}$$

is studied next. Applying Eqs. (7.64-7.65) yields

$$2\zeta_{eq,(m,n),k}\omega_{eq,(m,n),k}=2\zeta_0\omega_0+\ldots \\ \varepsilon 2\zeta_0\omega_0\frac{E\left(\dot{x}^4_{(m,n),k}\right)+3\sum\limits_{(i,j),i\neq m,j\neq n}E\left(\dot{x}^2_{(m,n),k}\right)E\left(\dot{x}^2_{(i,j),k}\right)}{E\left(\dot{x}^2_{(m,n),k}\right)}, \tag{7.73}$$

and

$$\omega^2_{eq,(m,n),k}=\omega_0^2. \tag{7.74}$$

Considering once more the standard Gaussian assumption for the response processes, Eq.(7.73) reduces to

$$2\zeta_{eq,(m,n),k}\omega_{eq,(m,n),k}=2\zeta_0\omega_0\left(1+\varepsilon 3\sum_{(m,n)}E\left(\dot{x}^2_{(m,n),k}\right)\right). \tag{7.75}$$

To assess the reliability of the approach for the damping nonlinearity, the response EPS of the oscillator (Eq.(7.72)) is calculated using the non-separable excitation EPS (Eq.(7.44)). The values $\left(\omega_0=10rad/\sec,\zeta=0.1,\varepsilon=1\right)$ are chosen. Despite the high degree of nonlinearity, the MCS estimation (Fig.(7.19)) appears to be in good agreement with the approximate approach (Fig.(7.20)). The above claim is confirmed by comparisons of the EPS at distinct time instants (Fig.(7.21)).

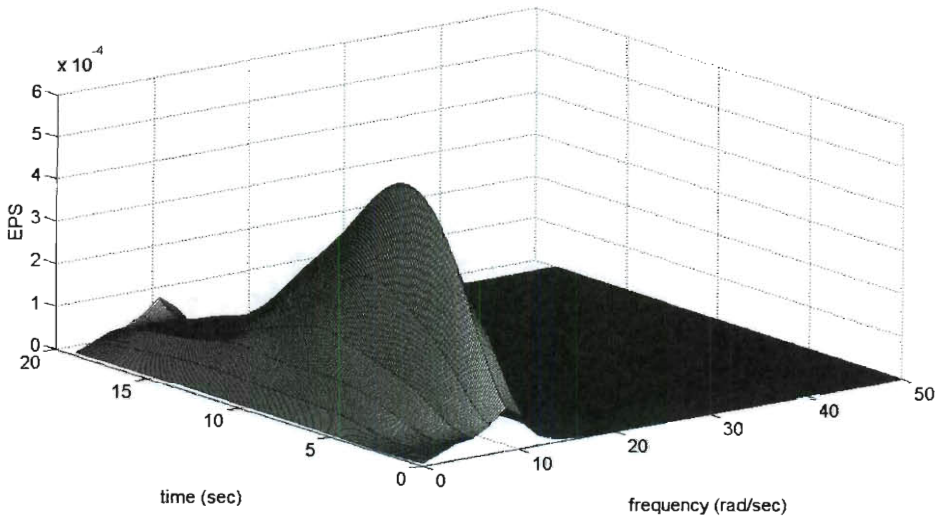

Fig.(7.19). Response EPS of a Linear-plus-cubic damping oscillator $(\omega_0 = 10 rad/\sec, \zeta = 0.1, \varepsilon = 1)$ under a non-separable evolutionary spectrum $(S_2 = 1)$. MCS estimation (500 realizations).

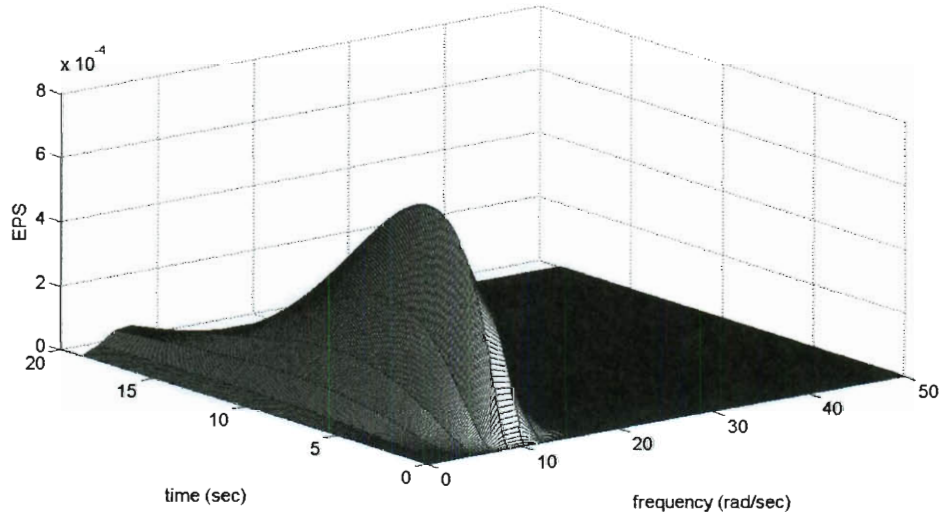

Fig.(7.20). Response EPS of a Linear-plus-cubic damping oscillator $(\omega_0 = 10 rad/\sec, \zeta = 0.1, \varepsilon = 1)$ under a non-separable evolutionary spectrum $(S_2 = 1)$. Analytical approach.

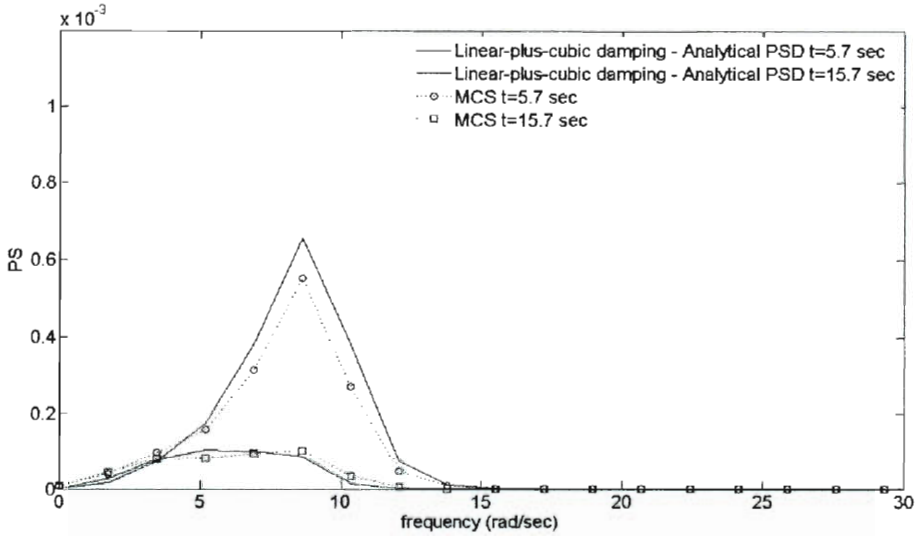

Fig.(7.21). Response EPS of a Linear-plus-cubic damping oscillator $(\omega_0 = 10 rad/\sec, \zeta = 0.1, \varepsilon = 1)$ at $(t = 5.7\sec)$ and $(t = 15.7\sec)$ under a non-separable evolutionary spectrum $(S_2 = 1)$. Comparison between MCS data (500 realizations) and the analytical approach.

Chapter 8

Harmonic wavelets based statistical linearization of the Bouc-Wen hysteretic model

8.1 Preliminary remarks

Structural systems can exhibit nonlinear inelastic behavior with restoring forces depending on the time history of the response under severe earthquake excitation. This memory-dependent relationship between force and deformation is generally described in the literature by the term hysteresis. A mathematical description of various existing models of hysteresis can be found in Macki et al. (1993). As expected, several research attempts have focused on determining response statistics of hysteretic oscillators under evolutionary excitation (e.g. Kougioumtzoglou and Spanos, 2009).

The introduction of the smooth and versatile Bouc-Wen hysteretic model (Bouc, 1967; Wen, 1976) was followed by its successful application to numerous structural dynamics related fields. For instance, the Bouc-Wen model has been used for base-isolation studies (e.g. Lin et al., 1989) and for the response analysis of soil deposits (e.g. Pires, 1996). One of the reasons for the popularity of the model, besides its versatility in efficiently capturing a wide range of hysteretic behaviors, is the feasibility of explicitly computing equivalent linear elements. Specifically, a statistical linearization method (e.g. Roberts and Spanos, 2003) was proposed by Wen (1980) where closed form expressions were derived for the

equivalent linear elements of the Bouc-Wen model. The method exhibited improved accuracy in comparison to earlier attempts which involved the assumption of a narrow-band response (e.g. Wen, 1976). Further, the model was extended to account for structural degradation (Baber and Wen, 1981), pinching effects (Foliente et al., 1996), and asymmetric hysteresis (Dobson et al., 1997; Song and Der Kiureghian, 2006). A detailed presentation of the applications and the extensions of the Bouc-Wen model can be found in review papers and books, such as the ones by Wen (1986, 1989), Ikhouane and Rodellar (2007) and Ismail et al. (2009).

Further, statistical linearization based algorithms for the analysis of the Bouc-Wen model were discussed in Faravelli et al. (1998) from a mathematically rigorous point of view. Ma et al. (2004) suggested that certain parameters of the model are insensitive, and thus a significant simplification of the model is possible. In Yang et al. (1991) the chaotic behavior of the model was studied and the potential relevance to stochastic analyses was discussed. Alternative approaches include the work by Park (1992), where empirical coefficients were obtained from intensive Monte Carlo simulations, and the work by Schueller et al. (1994) where a numerical method was proposed in the general framework of finite element modeling with any constitutive hysteretic model. In Noori et al. (1995) the stochastic averaging method was applied to derive first-passage and stationary response statistics, whereas in Davoodi and Noori (1990) a non-Gaussian closure method was applied to compute second and higher order response moments.

Further, modifications of the conventional statistical linearization method to enhance its performance include the work by Hurtado and Barbat (1996, 2000) who adopted a combination of Dirac and Gauss probability density functions (PDFs). In this manner, the bounded nature of the nonlinear restoring force was taken into account. Iwankiewicz and Nielsen (1992) applied a statistical linearization method to study the response of a Bouc-Wen system under Poisson distributed random pulses. Further, Wen and Eliopoulos (1994) applied the statistical linearization method for response analysis of inelastic structures under a realistic non-stationary excitation with time-varying frequency content.

Focusing on the response analysis of hysteretic structures under evolutionary excitation it can be seen that a wavelet-based formulation is capable of performing a joint time-frequency response analysis. In this chapter, the harmonic wavelets based statistical linearization method, developed in chapter 7, is extended to perform a joint time-frequency response analysis of a Bouc-Wen hysteretic oscillator subject to stochastic evolutionary excitation. Specifically, relying on a mathematically rigorous approach to modeling non-stationary processes (Nason et al., 2000; Triantafyllopoulos and Nason, 2009) excitation-response relationships are derived for each time and frequency band in the form of a nonlinear system of equations. Solving the nonlinear system in an iterative manner for each time and frequency interval yields the response EPS. Pertinent Monte Carlo simulation data are included.

8.2 Mathematical formulation

8.2.1 Harmonic wavelets

In this section the main concepts related to EPS estimation and representation of non-stationary stochastic processes by harmonic wavelets are presented in a concise manner.

A harmonic wavelet of (m,n) scale and (k) position in time attains a representation in the frequency domain of the form (Newland, 1994)

$$\Psi^{G}_{(m,n),k}(\omega)=\begin{cases}\dfrac{1}{(n-m)\Delta\omega}e^{-i\frac{\omega kT_o}{n-m}}, & m\Delta\omega\le\omega<n\Delta\omega\\ 0, & otherwise\end{cases}, \tag{8.1}$$

where (m), (n) and (k) are considered to be positive integers and

$$\Delta\omega=\frac{2\pi}{T_o}, \tag{8.2}$$

where (T_o) is the signal total time duration. The inverse Fourier transform of Eq.(8.1) gives the time-domain representation of the wavelet which is equal to

$$\psi^{G}_{(m,n),k}(t)=\frac{e^{in\Delta\omega\left(t-\frac{kT_0}{n-m}\right)}-e^{im\Delta\omega\left(t-\frac{kT_0}{n-m}\right)}}{i(n-m)\Delta\omega\left(t-\frac{kT_0}{n-m}\right)}. \tag{8.3}$$

Newland (1994) showed that a collection of harmonic wavelets spanning adjacent non-overlapping intervals at different scales forms an orthogonal basis. The continuous generalized harmonic wavelet transform (GHWT) is further defined as

$$W^{G,f}_{(m,n),k}=\frac{n-m}{T_o}\int_{-\infty}^{\infty}f(t)\overline{\psi^{G}_{(m,n),k}(t)}dt, \tag{8.4}$$

and projects any finite energy signal $(f(t))$ on this wavelet basis. In Eq.(8.4) the bar over a symbol represents complex conjugation.

Further, taking into account the time-frequency representation capabilities of the wavelet transform it is natural to consider a representation of a random process $(f(t))$ in the form

$$f(t)=\sum_{(m,n)}\sum_{k} f_{(m,n),k}(t), \tag{8.5}$$

where $\left(f_{(m,n),k}(t)\right)$ represents the process at scale (m,n) and translation (k) defined in the intervals $(m\Delta\omega \le \omega_l < n\Delta\omega)$ and $\left(\frac{k}{n-m}T_o \le t < \frac{k+1}{n-m}T_o\right)$. In chapter 7 a spectral representation involving harmonics of random amplitudes was developed for the process $\left(f_{(m,n),k}(t)\right)$ based on the concept of locally stationary wavelet (LSW) processes introduced by Nason et al. (2000). In fact, it was shown that

$$\begin{aligned} f^{RA}_{(m,n),k}(t) = A_{(m,n),k}\cos\left(\omega_{c,(m,n),k}\left(t-\frac{kT_0}{n-m}\right)\right)+\ldots \\ B_{(m,n),k}\sin\left(\omega_{c,(m,n),k}\left(t-\frac{kT_0}{n-m}\right)\right). \end{aligned} \tag{8.6}$$

Note that this representation is defined in the intervals $(m\Delta\omega \le \omega_l < n\Delta\omega)$ and $\left(\frac{k}{n-m}T_o \le t < \frac{k+1}{n-m}T_o\right)$ with

$$\omega_{c,(m,n),k} = \frac{(n+m)\Delta\omega}{2}, \tag{8.7}$$

and $\left(A_{(m,n),k}\right)$, $\left(B_{(m,n),k}\right)$ representing statistically independent random variables with mean value equal to zero and variance equal to

$$E\left(A^2_{(m,n),k}\right)=E\left(B^2_{(m,n),k}\right)=2S^{ff}_{(m,n),k}\left(n-m\right)\Delta\omega\,. \tag{8.8}$$

In Eq.(8.8) $\left(S^{ff}_{(m,n),k}\right)$ represents the EPS of the process (f), assumed to have constant value in the intervals $\left(m\Delta\omega\le\omega_l<n\Delta\omega\right)$ and $\left(\frac{k}{n-m}T_o\le t<\frac{k+1}{n-m}T_o\right)$. Alternatively, a spectral representation of $\left(f_{(m,n),k}(t)\right)$ involving harmonics of constant amplitudes and of random phases can be cast in the form

$$f^{RP}_{(m,n),k}(t)=\sqrt{4S^{ff}_{(m,n),k}\left(n-m\right)\Delta\omega}\cos\left(\omega_{c,(m,n),k}\left(t-\frac{kT_0}{n-m}\right)+\phi_{(m,n),k}\right), \tag{8.9}$$

where $\left(\phi_{(m,n),k}\right)$ are independent random variables following a uniform distribution over the interval $[0,2\pi]$. Further, it was shown in chapter 7 that the EPS $\left(S^{ff}_{(m,n),k}\right)$ can be estimated by the equation

$$S_{ff}(\omega_i,t_i)=S^{ff}_{(m,n),k}=\frac{E\left[\left|W^{G,f}_{(m,n),k}\right|^2\right]}{\left(n-m\right)\Delta\omega},\quad m\Delta\omega\le\omega_i<n\Delta\omega,\quad \frac{kT_o}{n-m}\le t_i<\frac{(k+1)T_o}{n-m}. \tag{8.10}$$

Similarly, the cross EPS $\left(S^{fg}_{(m,n),k}\right)$ of two stochastic processes (f) and (g) can be estimated as

$$S_{fg}(\omega_i,t_i)=S^{fg}_{(m,n),k}=\frac{E\left[W^{G,f}_{(m,n),k}\overline{W^{G,g}_{(m,n),k}}\right]}{\left(n-m\right)\Delta\omega},\quad m\Delta\omega\le\omega_i<n\Delta\omega,\quad \frac{kT_o}{n-m}\le t_i<\frac{(k+1)T_o}{n-m}. \tag{8.11}$$

In fact, in chapter 7 Eq.(8.10) was used to obtain estimates not only for separable but non-separable in time and frequency EPS as well.

Considering next Eq.(8.6) and reviewing some of the properties it implies it can be readily seen that

$$E\left(f^{RA}_{(m,n),k}(t)\right)=E\left(\dot{f}^{RA}_{(m,n),k}(t)\right)=E\left(\ddot{f}^{RA}_{(m,n),k}(t)\right)=0, \tag{8.12}$$

and

$$E\left(f^{RA}_{(m,n),k}(t)\dot{f}^{RA}_{(m,n),k}(t)\right)=E\left(\dot{f}^{RA}_{(m,n),k}(t)\ddot{f}^{RA}_{(m,n),k}(t)\right)=0, \tag{8.13}$$

where the symbol $\left(E(.)\right)$ represents the expectation operator. Further, utilizing Eq.(8.8) and manipulating yields

$$E\left(\left(f^{RA}_{(m,n),k}(t)\right)^2\right)=2S^{ff}_{(m,n),k}\left(n-m\right)\Delta\omega. \tag{8.14}$$

Similarly,

$$E\left(\left(\dot{f}^{RA}_{(m,n),k}(t)\right)^2\right)=2\omega^2_{c,(m,n),k}S^{ff}_{(m,n),k}\left(n-m\right)\Delta\omega, \tag{8.15}$$

$$E\left(\left(\ddot{f}^{RA}_{(m,n),k}(t)\right)^2\right)=2\omega^4_{c,(m,n),k}S^{ff}_{(m,n),k}\left(n-m\right)\Delta\omega, \tag{8.16}$$

and

$$E\left(f^{RA}_{(m,n),k}(t)\ddot{f}^{RA}_{(m,n),k}(t)\right)=-2\omega^2_{c,(m,n),k}S^{ff}_{(m,n),k}\left(n-m\right)\Delta\omega. \tag{8.17}$$

8.2.2 Nonlinear response EPS determination

In this section, a statistical linearization method is developed for the Bouc-Wen hysteretic oscillator for each time and frequency interval. Specifically, the associated equation of motion of the single-degree-of-freedom system reads

$$\ddot{x}+2\zeta_0\omega_0\dot{x}+a\omega_0^2x+\left(1-a\right)\omega_0^2z=w(t), \tag{8.18}$$

where (ζ_0) is the ratio of critical damping; (ω_0) is the natural frequency of the corresponding linear oscillator; $(w(t))$ represents a Gaussian, zero-mean non-stationary random process possessing an evolutionary broad-band power spectrum, $S(\omega,t)$; and (a) represent the "rigidity ratio" and can be viewed as a form of post-yield to pre-yield stiffness ratio. In the Bouc-Wen model the additional state (z) is related to the displacement (x) by the differential equation

$$\dot{z} = -\gamma|\dot{x}|z|z|^{n-1} - \beta\dot{x}|z|^n + A\dot{x}, \tag{8.19}$$

where the constant parameters (γ), (β), (A) and (n) are capable of representing a wide range of hysteresis loops, including softening and hardening behaviors. Utilizing next the representations of Eqs.(8.5) and (8.6) for the excitation and response processes yields

$$x(t) = \sum_{(m,n)} \sum_{k} x_{(m,n),k}(t), \tag{8.20}$$

$$z(t) = \sum_{(m,n)} \sum_{k} z_{(m,n),k}(t), \tag{8.21}$$

and

$$w(t) = \sum_{(m,n)} \sum_{k} w_{(m,n),k}(t), \tag{8.22}$$

where

$$\begin{aligned} x_{(m,n),k}(t) = A_{(m,n),k} \cos\left(\omega_{c,(m,n),k}\left(t - \frac{kT_0}{n-m}\right)\right) + \ldots \\ B_{(m,n),k} \sin\left(\omega_{c,(m,n),k}\left(t - \frac{kT_0}{n-m}\right)\right), \end{aligned} \tag{8.23}$$

$$z_{(m,n),k}(t) = C_{(m,n),k}\cos\left(\omega_{c,(m,n),k}\left(t-\frac{kT_0}{n-m}\right)\right)+\ldots$$
$$D_{(m,n),k}\sin\left(\omega_{c,(m,n),k}\left(t-\frac{kT_0}{n-m}\right)\right), \tag{8.24}$$

and

$$w_{(m,n),k}(t) = E_{(m,n),k}\cos\left(\omega_{c,(m,n),k}\left(t-\frac{kT_0}{n-m}\right)\right)+\ldots$$
$$F_{(m,n),k}\sin\left(\omega_{c,(m,n),k}\left(t-\frac{kT_0}{n-m}\right)\right). \tag{8.25}$$

A common assumption involved in the classical statistical linearization approaches dictates that the processes $(\dot{x})$ and (z) are jointly Gaussian (e.g. Wen, 1980; Roberts and Spanos, 2003). Adopting this assumption for the processes $\left(\dot{x}_{(m,n),k}\right)$ and $\left(z_{(m,n),k}\right)$ yields

$$E\left(\dot{x}_{(m,n),k}z_{(m,n),k}\right) = \rho_{\dot{x}_{(m,n),k},z_{(m,n),k}}\sqrt{E\left(\dot{x}^2_{(m,n),k}\right)E\left(z^2_{(m,n),k}\right)}, \tag{8.26}$$

or, equivalently,

$$E\left(\dot{x}_{(m,n),k}z_{(m,n),k}\right) = \rho_{\dot{x}_{(m,n),k},z_{(m,n),k}}\,2\omega_{c,(m,n),k}\left(n-m\right)\Delta\omega\sqrt{S^{\dot{x}\dot{x}}_{(m,n),k}S^{zz}_{(m,n),k}}, \tag{8.27}$$

where Eqs.(8.14-8.15) have been considered; and $\left(\rho_{\dot{x}_{(m,n),k},z_{(m,n),k}}\right)$ represents the correlation coefficient of the processes $\left(\dot{x}_{(m,n),k}\right)$ and $\left(z_{(m,n),k}\right)$. Employing next the representations of Eqs.(8.23-8.24) and manipulating yields

$$
\begin{aligned}
&E\left(\dot{x}_{(m,n),k}z_{(m,n),k}\right)=\omega_{c,(m,n),k}\left(E\left(B_{(m,n),k}D_{(m,n),k}\right)-E\left(A_{(m,n),k}C_{(m,n),k}\right)\right)\\
&\times\sin\left(\omega_{c,(m,n),k}\left(t-\frac{kT_0}{n-m}\right)\right)\cos\left(\omega_{c,(m,n),k}\left(t-\frac{kT_0}{n-m}\right)\right)+\ldots\\
&\omega_{c,(m,n),k}E\left(B_{(m,n),k}C_{(m,n),k}\right)\cos^2\left(\omega_{c,(m,n),k}\left(t-\frac{kT_0}{n-m}\right)\right)-\ldots\\
&\omega_{c,(m,n),k}E\left(A_{(m,n),k}D_{(m,n),k}\right)\sin^2\left(\omega_{c,(m,n),k}\left(t-\frac{kT_0}{n-m}\right)\right).
\end{aligned}
\tag{8.28}
$$

Further, for $\left(E\left(\dot{x}_{(m,n),k}z_{(m,n),k}\right)\right)$ to be time-independent, in accordance with Eq.(8.27), the relationships

$$E\left(B_{(m,n),k}D_{(m,n),k}\right)=E\left(A_{(m,n),k}C_{(m,n),k}\right), \tag{8.29}$$

and

$$E\left(B_{(m,n),k}C_{(m,n),k}\right)=-E\left(A_{(m,n),k}D_{(m,n),k}\right), \tag{8.30}$$

are invoked. Then, Eq.(8.28) becomes

$$E\left(\dot{x}_{(m,n),k}z_{(m,n),k}\right)=\omega_{c,(m,n),k}E\left(B_{(m,n),k}C_{(m,n),k}\right). \tag{8.31}$$

Similarly, utilizing Eqs.(8.23-8.24) and (8.29-8.30) and manipulating yields

$$E\left(x_{(m,n),k}z_{(m,n),k}\right)=E\left(A_{(m,n),k}C_{(m,n),k}\right), \tag{8.32}$$

and

$$E\left(\dot{x}_{(m,n),k}\dot{z}_{(m,n),k}\right)=\omega_{c,(m,n),k}^2E\left(A_{(m,n),k}C_{(m,n),k}\right). \tag{8.33}$$

Employing next the representations of Eqs.(8.20-8.22) Eq.(8.19) becomes

$$
\begin{aligned}
&\sum_{(m,n)}\sum_{k}\ddot{x}_{(m,n),k}+2\zeta_0\omega_0\sum_{(m,n)}\sum_{k}\dot{x}_{(m,n),k}+a\omega_0^2\sum_{(m,n)}\sum_{k}x_{(m,n),k}+\ldots\\
&(1-a)\omega_0^2\sum_{(m,n)}\sum_{k}z_{(m,n),k}=\sum_{(m,n)}\sum_{k}w_{(m,n),k}.
\end{aligned}
\tag{8.34}
$$

Further, considering the orthogonality conditions of monochromatic functions leads to

$$\int_{\frac{kT_0}{n-m}}^{\frac{(k+1)T_0}{n-m}} \cos\left(\omega_{c,(m,n),k}\left(t-\frac{kT_0}{n-m}\right)\right)\cos\left(\omega_{c,(i,j),l}\left(t-\frac{lT_0}{j-i}\right)\right)dt=\begin{cases}\frac{1}{2}\frac{T_0}{n-m}, & m=i,\ n=j,\ k=l\\ 0, & otherwise\end{cases} \quad (8.35)$$

$$\int_{\frac{kT_0}{n-m}}^{\frac{(k+1)T_0}{n-m}} \sin\left(\omega_{c,(m,n),k}\left(t-\frac{kT_0}{n-m}\right)\right)\sin\left(\omega_{c,(i,j),l}\left(t-\frac{lT_0}{j-i}\right)\right)dt=\begin{cases}\frac{1}{2}\frac{T_0}{n-m}, & m=i,\ n=j,\ k=l\\ 0, & otherwise\end{cases} \quad (8.36)$$

and

$$\int_{\frac{kT_0}{n-m}}^{\frac{(k+1)T_0}{n-m}} \cos\left(\omega_{c,(m,n),k}\left(t-\frac{kT_0}{n-m}\right)\right)\sin\left(\omega_{c,(i,j),l}\left(t-\frac{lT_0}{j-i}\right)\right)dt=0. \quad (8.37)$$

Substituting Eqs.(8.23-8.25) into Eq.(8.34) and exploiting Eqs.(8.35-8.37) yields (see also Spanos et al. 2011)

$$\begin{cases}-(\omega_{c,(m,n),k})^2 A_{(m,n),k}+2\zeta_0\omega_0(\omega_{c,(m,n),k})B_{(m,n),k}+a\omega_0^2 A_{(m,n),k}+\ldots\\ (1-a)\omega_0^2 C_{(m,n),k}=E_{(m,n),k},\\ -(\omega_{c,(m,n),k})^2 B_{(m,n),k}-2\zeta_0\omega_0(\omega_{c,(m,n),k})A_{(m,n),k}+a\omega_0^2 B_{(m,n),k}+\ldots\\ (1-a)\omega_0^2 D_{(m,n),k}=F_{(m,n),k}.\end{cases} \quad (8.38)$$

Manipulating further Eq.(8.38) yields

$$\begin{aligned}&\left(A_{(m,n),k}^2+B_{(m,n),k}^2\right)\left[\left(a\omega_0^2-\omega_{c,(m,n),k}^2\right)^2+\left(2\zeta_0\omega_0\omega_{c,(m,n),k}\right)^2\right]+\ldots\\ &\left(C_{(m,n),k}^2+D_{(m,n),k}^2\right)\left[\omega_0^4\left(1-2a+a^2\right)\right]+\ldots\\ &\left(A_{(m,n),k}C_{(m,n),k}+B_{(m,n),k}D_{(m,n),k}\right)\left[2a\omega_0^4(1-a)-2\omega_{c,(m,n),k}^2\omega_0^2(1-a)\right]+\ldots\\ &\left(B_{(m,n),k}C_{(m,n),k}-A_{(m,n),k}D_{(m,n),k}\right)\left[4\zeta_0\omega_0^3(1-a)\omega_{c,(m,n),k}\right]=E_{(m,n),k}^2+F_{(m,n),k}^2,\end{aligned} \quad (8.39)$$

and taking into account Eqs.(8.8), (8.14), and (8.29-8.33) yields

$$
\begin{aligned}
&E\left(x_{(m,n),k}^2\right)\left[\left(a\omega_0^2-\omega_{c,(m,n),k}^2\right)^2+\left(2\zeta_0\omega_0\omega_{c,(m,n),k}\right)^2\right]+\ldots\\
&E\left(z_{(m,n),k}^2\right)\left[\omega_0^4\left(1-2a+a^2\right)\right]+\ldots\\
&E\left(x_{(m,n),k}z_{(m,n),k}\right)\left[2a\omega_0^4\left(1-a\right)-2\omega_{c,(m,n),k}^2\omega_0^2\left(1-a\right)\right]+\ldots\\
&E\left(\dot{x}_{(m,n),k}z_{(m,n),k}\right)\left[4\zeta_0\omega_0^3\left(1-a\right)\right]=E\left(w_{(m,n),k}^2\right).
\end{aligned}
\tag{8.40}
$$

Replacing next the nonlinear system of Eqs.(8.18-8.19) with an equivalent linear (e.g. Roberts and Spanos, 2003) of the form

$$M\underline{\ddot{y}}+\left(C+C_e\right)\underline{\dot{y}}+\left(K+K_e\right)\underline{y}=\underline{W}(t), \tag{8.41}$$

the error is defined as

$$\underline{Er}=\underline{g}(\underline{y},\underline{\dot{y}})-C_{eq}\underline{\dot{y}}-K_{eq}\underline{y}, \tag{8.42}$$

where

$$\underline{y}=\begin{pmatrix}x\\z\end{pmatrix}, \tag{8.43}$$

$$M=\begin{bmatrix}1&0\\0&0\end{bmatrix}, \tag{8.44}$$

$$C=\begin{bmatrix}2\zeta_0\omega_0&0\\0&1\end{bmatrix}, \tag{8.45}$$

$$K=\begin{bmatrix}a\omega_0^2&\left(1-a\right)\omega_0^2\\0&0\end{bmatrix}, \tag{8.46}$$

$$\underline{W}(t)=\begin{pmatrix}w(t)\\0\end{pmatrix}, \tag{8.47}$$

and

$$\underline{g}(\underline{y},\underline{\dot{y}})=\begin{pmatrix}0\\\gamma\left|\dot{x}\right|z\left|z\right|^{n-1}+\beta\dot{x}\left|z\right|^n-A\dot{x}\end{pmatrix}. \tag{8.48}$$

Next, to define equivalent linear elements matrices $\left(C_{e,(m,n),k}\right)$ and $\left(K_{e,(m,n),k}\right)$ corresponding to the intervals $\left(m\Delta\omega \le \omega < n\Delta\omega\right)$ and $\left(\frac{k}{n-m}T_o \le t < \frac{k+1}{n-m}T_o\right)$, the representations of Eqs.(8.5-8.6), and the orthogonality conditions (Eqs.(8.35-8.37)) are employed. Thus, requiring the error to be zero and applying a Galerkin scheme (e.g. Failla et al., 2003), the error $\left(\underline{Er}\right)$ is projected on the vector $\left(\underline{\hat{y}}_{(m,n),k} = \left[\underline{y}_{(m,n),k}, \underline{\dot{y}}_{(m,n),k}\right]^T\right)$ yielding (see also Roberts and Spanos, 2003)

$$\int_{\frac{kT_0}{n-m}}^{\frac{(k+1)T_0}{n-m}} g_i(\underline{y},\underline{\dot{y}})\underline{\hat{y}}_{(m,n),k}\,dt = \int_{\frac{kT_0}{n-m}}^{\frac{(k+1)T_0}{n-m}} \left(\underline{\hat{y}}_{(m,n),k}\underline{\hat{y}}^T\right)\begin{bmatrix}\underline{k}_{ei,(m.n),k}^T \\ \underline{c}_{ei,(m.n),k}^T\end{bmatrix} dt, \quad i=1,2, \tag{8.49}$$

where $\left(\underline{k}_{ei,(m.n),k}\right)$ and $\left(\underline{c}_{ei,(m.n),k}\right)$ are the i-th rows of the matrices $\left(K_{e,(m,n),k}\right)$ and $\left(C_{e,(m,n),k}\right)$, respectively. Considering Eq.(8.6), the orthogonality conditions (Eqs.(8.35-8.37)), and taking expectations Eq.(8.49) yields

$$\int_{\frac{kT_0}{n-m}}^{\frac{(k+1)T_0}{n-m}} E\left(g_i(\underline{y},\underline{\dot{y}})\underline{\hat{y}}_{(m,n),k}\right)dt = \left(\frac{T_0}{n-m}\right)E\left(\underline{\hat{y}}_{(m,n),k}\underline{\hat{y}}_{(m,n),k}^T\right)\begin{bmatrix}\underline{k}_{ei,(m.n),k}^T \\ \underline{c}_{ei,(m.n),k}^T\end{bmatrix}, \quad i=1,2. \tag{8.50}$$

Further, assuming the case where $\left(n=1\right)$ and adopting a polynomial approximation for the function $\left(g(\underline{y},\underline{\dot{y}})\right)$ yields

$$\underline{g}(\underline{y},\underline{\dot{y}}) = \begin{pmatrix} 0 \\ \gamma\dot{x}^2 z + \beta\dot{x}z^2 - A\dot{x}\end{pmatrix}. \tag{8.51}$$

Then, utilizing Eq.(8.51) and manipulating Eq.(8.50) the equivalent linear elements can be approximated by

$$k_{eq,(m,n),k} = \gamma\sum_{(m,n)} E\left(\dot{x}_{(m,n),k}^2\right) + 2\beta\sum_{(m,n)} E\left(\dot{x}_{(m,n),k}z_{(m,n),k}\right), \tag{8.52}$$

and

$$c_{eq,(m,n),k} = 2\gamma \sum_{(m,n)} E\left(\dot{x}_{(m,n),k} z_{(m,n),k}\right) + \beta \sum_{(m,n)} E\left(z^2_{(m,n),k}\right) - A, \tag{8.53}$$

and the equivalent linear elements matrices are given by the equations

$$C_{e,(m,n),k} = \begin{bmatrix} 0 & 0 \\ c_{eq,(m,n),k} & 0 \end{bmatrix}, \tag{8.54}$$

and

$$K_{e,(m,n),k} = \begin{bmatrix} 0 & 0 \\ 0 & k_{eq,(m,n),k} \end{bmatrix}, \tag{8.55}$$

Further, multiplying the equivalent linear counterpart of Eq.(8.19) with $\left(z_{(m,n),k}\right)$, taking expectations, and relying on the independence of the random amplitude variables yields

$$E\left(\dot{x}_{(m,n),k} z_{(m,n),k}\right) = -\frac{k_{eq,(m,n),k}}{c_{eq,(m,n),k}} E\left(z^2_{(m,n),k}\right). \tag{8.56}$$

Furthermore, multiplying the equivalent linear counterpart of Eq.(8.19) with $\left(\dot{z}_{(m,n),k}\right)$ and employing Eqs.(8.13-8.15) leads to the equation

$$E\left(\dot{x}_{(m,n),k} \dot{z}_{(m,n),k}\right) = -\frac{1}{c_{eq,(m,n),k}} \omega^2_{c,(m,n),k} E\left(z^2_{(m,n),k}\right). \tag{8.57}$$

Considering next Eqs.(8.32-8.33) and (8.57) yields

$$E\left(x_{(m,n),k} z_{(m,n),k}\right) = -\frac{1}{c_{eq,(m,n),k}} E\left(z^2_{(m,n),k}\right). \tag{8.58}$$

Multiplying the equivalent linear counterpart of Eq.(8.19) with $\left(\dot{x}_{(m,n),k}\right)$, employing Eqs.(8.13-8.15) and considering Eqs.(8.23-8.24) and (8.56-8.57) leads to the equation

$$E\left(x^2_{(m,n),k}\right)=\frac{k^2_{eq,(m,n),k}+\omega^2_{c,(m,n),k}}{c^2_{eq,(m,n),k}\omega^2_{c,(m,n),k}}E\left(z^2_{(m,n),k}\right). \tag{8.59}$$

It can be seen that Eq.(8.40) together with Eqs.(8.52-8.53), (8.56) and (8.58-8.59) form a nonlinear system of equations in the intervals $\left(m\Delta\omega\le\omega<n\Delta\omega\right)$ and $\left(\frac{k}{n-m}T_o\le t<\frac{k+1}{n-m}T_o\right)$ which is solved iteratively in the following (e.g. Roberts and Spanos, 2003) to compute the response EPS.

8.3 Numerical examples

To assess the accuracy of the proposed approach Monte Carlo simulations are performed considering both separable and non-separable excitations. For each Monte Carlo simulation an ensemble size of 500 realizations is used, whereas the parameters values $\left(A=1,\beta=0.5,\gamma=0.5,\omega_0=10,\zeta_0=0.1\right)$ are chosen for the Bouc-Wen oscillator. The total time duration of each realization is equal to $\left(T_o=18.9\sec\right)$, whereas the Nyquist frequency is chosen to be $\left(\omega_{Nyq}=50rad/\sec\right)$. As far as the EPS estimation is considered, for the calculation of the wavelet coefficients a computationally efficient algorithm is employed which takes advantage of the fast Fourier transform (FFT) scheme (e.g. Newland, 1993; Newland, 1997). Further it is clear that by changing the values of (m) and (n) a compromise is introduced between time and frequency resolution. The value $\left(n-m=5\right)$ is chosen to be used in the ensuing analysis.

8.3.1 Time-modulated Kanai-Tajimi excitation EPS

In the case of a separable random process the EPS of the excitation is assumed in the form

$$S(\omega,t)=|g(t)|^2 S_v(\omega), \tag{8.60}$$

where $(g(t))$ is a slowly varying time-dependent modulating function; and $(S_v(\omega))$ is the power spectrum of a stationary process $(v(t))$. In the case of a time-modulated Kanai-Tajimi (Kanai, 1957; Tajimi, 1960) spectrum Eq.(8.60) is defined as in section 7.3.2. Time histories compatible with $S(\omega,t)$ are produced by using Eq.(7.43).

In Fig.(8.1) the Kanai-Tajimi excitation EPS is shown, whereas Figs.(8.2-8.4) demonstrate response related EPS data for the case where $(a=0.01)$. This relatively high value of the parameter represents a nearly elasto-plastic system. In Fig.(8.2) the response EPS of process (x) is computed according to the statistical linearization method and compared to the MCS based estimations for different time instants. Equivalent response EPS results are shown in Figs.(8.3-8.4) for the process (z) and the process $(\dot{x})$, respectively. It can be readily seen that the harmonic wavelet-based statistical linearization performs satisfactorily. It is noted, however, that the developed method fails to capture the response EPS frequency content of the process (x) for $(\omega=0)$. This drift component of the response of the process (x) has been observed in the literature for elasto-plastic systems and attempts have been made to extend the statistical linearization method to predict this phenomenon (e.g. Bouc and Boussaa, 2002). In the context

of the herein developed wavelet-based statistical linearization one expects it to perform in a similar fashion to the conventional linearization considering the similarities in the development of the two methods. In fact, in the case of the Gaussian assumption drift cannot be reproduced satisfactorily by the conventional statistical linearization method (e.g. Park, 1992; Hurtado and Barbat, 2000) verifying the aforementioned argument.

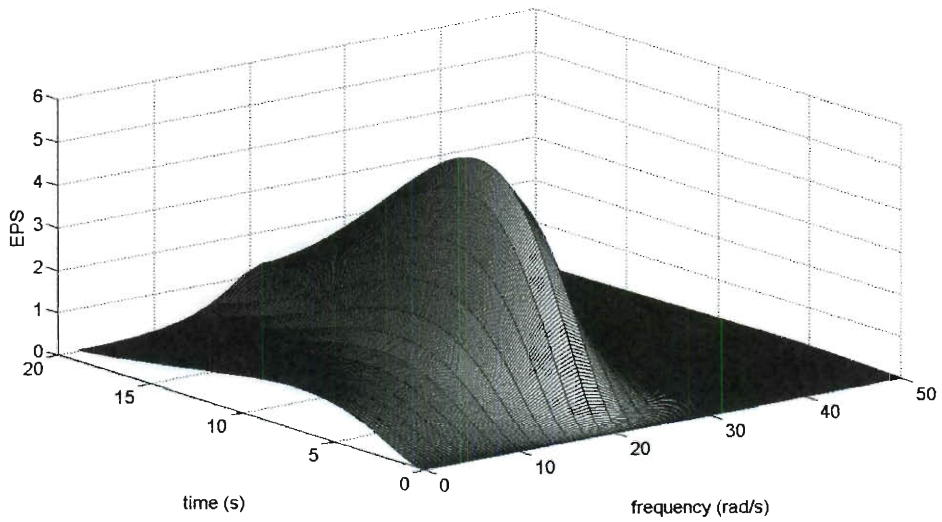

Fig.(8.1). Time-modulated Kanai-Tajimi EPS: $(c = 0.1, b = 0.2)$ and $(\omega_g = 20 rad/\sec, \zeta_g = 0.24, S_1 = 1)$.

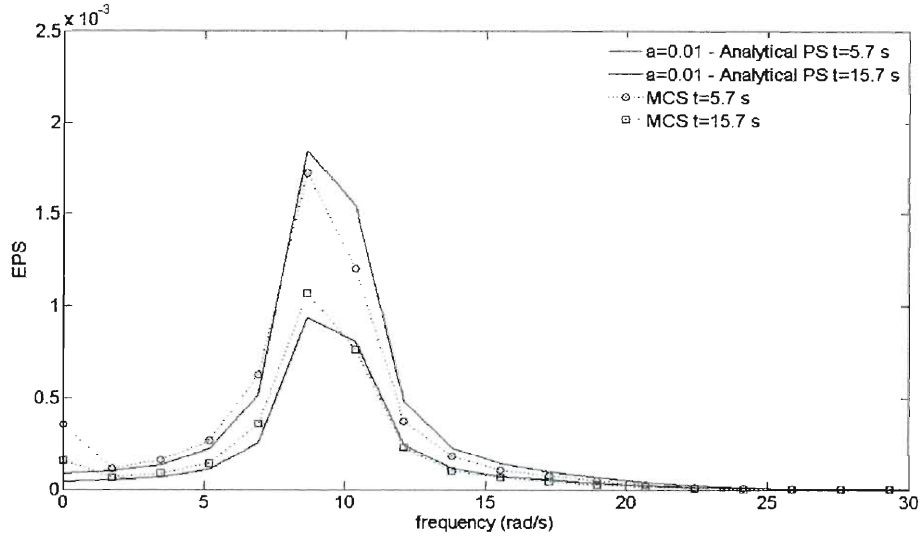

Fig.(8.2). Response EPS (x) of a Bouc-Wen oscillator $(a=0.01, \omega_0=10 rad/\sec, \zeta=0.1)$ at $(t=5.7\sec)$ and $(t=15.7\sec)$ under a time-modulated Kanai-Tajimi spectrum $(c=0.1, b=0.2, \omega_g=20 rad/\sec, \zeta_g=0.24, S_1=1)$. Comparison between MCS data (500 realizations) and the analytical approach.

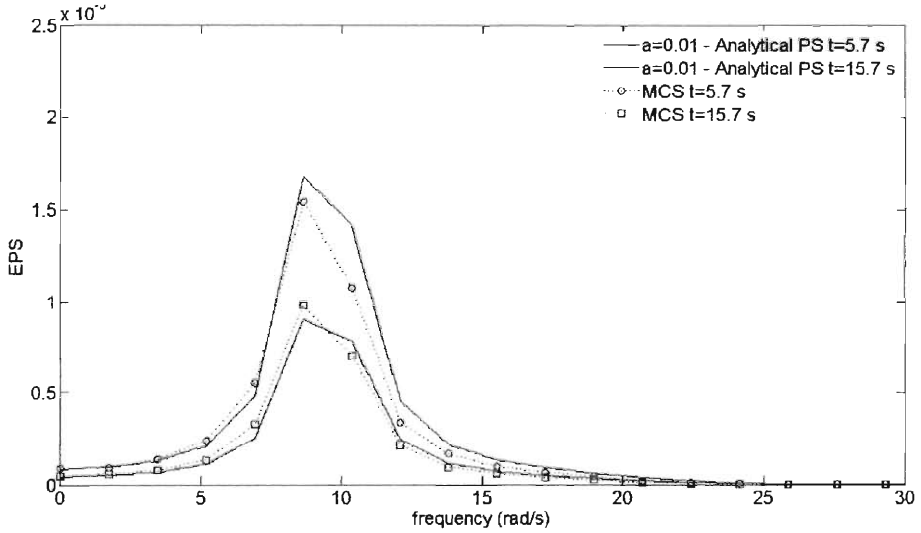

Fig.(8.3). Response EPS (z) of a Bouc-Wen oscillator $(a=0.01, \omega_0=10 rad/\sec, \zeta=0.1)$ at $(t=5.7\sec)$ and $(t=15.7\sec)$ under a time-modulated Kanai-Tajimi spectrum $(c=0.1, b=0.2, \omega_g=20 rad/\sec, \zeta_g=0.24, S_1=1)$. Comparison between MCS data (500 realizations) and the analytical approach.

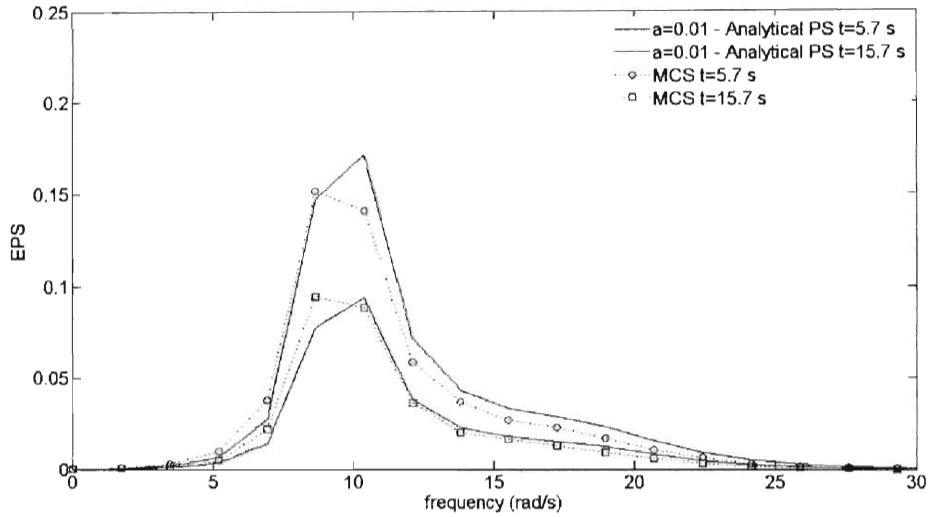

Fig.(8.4). Response EPS $(\dot{x})$ of a Bouc-Wen oscillator $(a=0.01, \omega_0=10 rad/\sec, \zeta=0.1)$ at $(t=5.7\sec)$ and $(t=15.7\sec)$ under a time-modulated Kanai-Tajimi spectrum $(c=0.1, b=0.2, \omega_g=20 rad/\sec, \zeta_g=0.24, S_1=1)$. Comparison between MCS data (500 realizations) and the analytical approach.

8.3.2 Non-separable excitation EPS

Next, the response EPS of the Bouc-Wen oscillator under the non-separable spectrum of the form

$$S(\omega,t)=S_2\left(\frac{\omega}{5\pi}\right)^2 e^{-0.15t}t^2 e^{-\left(\frac{\omega}{5\pi}\right)^2 t}, \quad t\geq 0, \quad -\infty<\omega<\infty, \tag{8.61}$$

where $(S_2=10)$ is computed. This spectrum (Fig.(8.5)) comprises some of the main characteristics of ground excitation, such as decreasing of the dominant frequency with time (e.g. Liu, 1970; Spanos and Solomos, 1983). Sample paths compatible with Eq.(8.61) are produced using the concept of spectral representation of a stochastic process (e.g. Liang et al., 2007). Specifically, the equation

$$w(t)=\sum_{k=1}^{m}\sqrt{4S(k\Delta\omega,t)\Delta\omega}\cos\left(\left(k\Delta\omega\right)t+\theta_k\right) \tag{8.62}$$

is used, in which $\left(m=400,\Delta\omega=\omega_{Nyq}/m\right)$; and $\left(\theta_k\right)$ is a phase angle uniformly distributed over the interval $\left(0,2\pi\right)$.

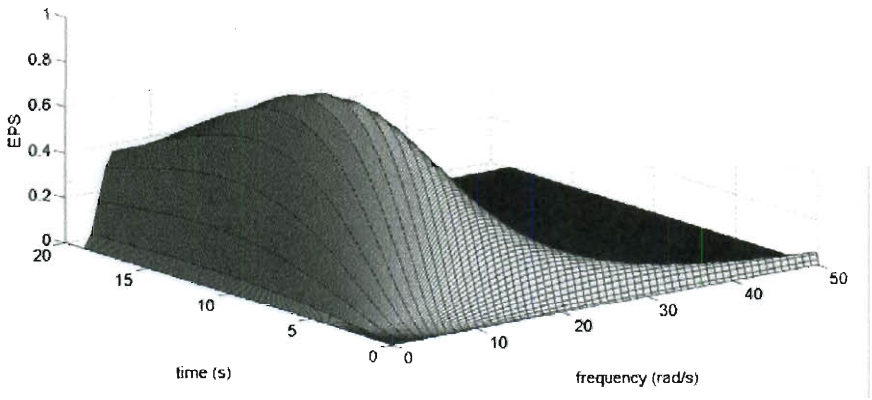

Fig.(8.5). Non-separable evolutionary excitation spectrum $\left(S_2=10\right)$

Figs.(8.6-8.8) demonstrate response related EPS data for the case where $\left(a=0.01\right)$. In Fig.(8.6) the response EPS of process $\left(x\right)$ is computed according to the statistical linearization method and compared to the MCS based estimations for different time instants. Equivalent response EPS results are shown in Figs.(8.7-8.8) for the process $\left(z\right)$ and the process $\left(\dot{x}\right)$, respectively. It can be readily seen that the harmonic wavelet-based statistical linearization performs satisfactorily. Following a similar behavior as in the case of the time-modulated Kanai-Tajimi EPS the method fails to reproduce the drift component of the response process $\left(x\right)$.

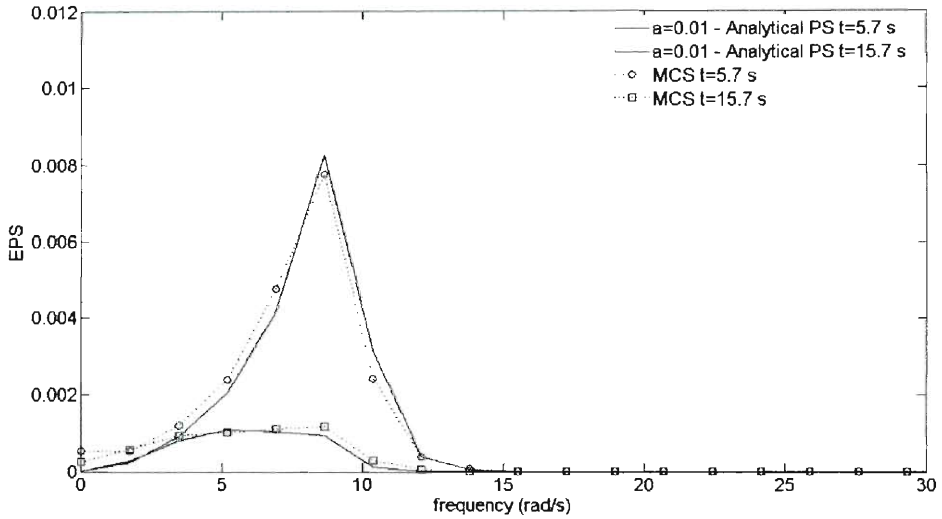

Fig.(8.6). Response EPS (x) of a Bouc-Wen oscillator $(a=0.01, \omega_0=10 rad/\sec, \zeta=0.1)$ at $(t=5.7\sec)$ and $(t=15.7\sec)$ under a non-separable evolutionary spectrum $(S_2=10)$. Comparison between MCS data (500 realizations) and the analytical approach.

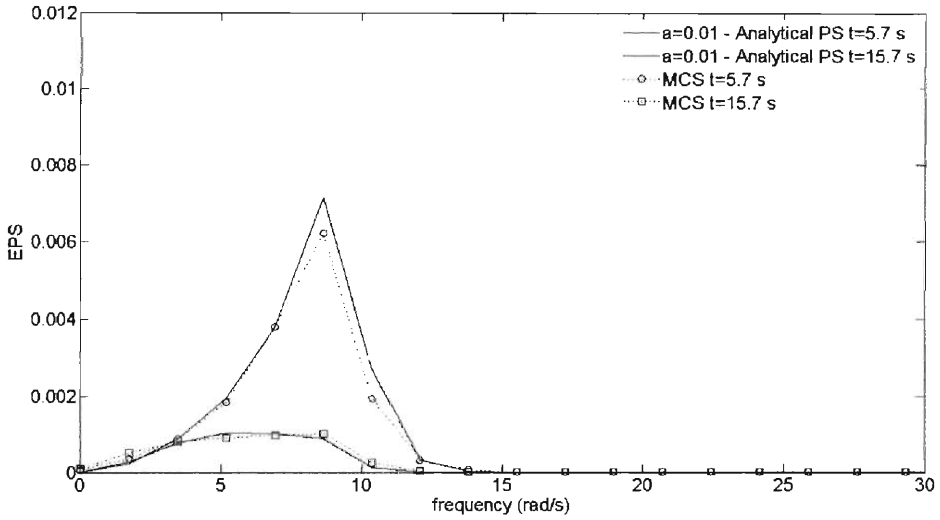

Fig.(8.7). Response EPS (z) of a Bouc-Wen oscillator $(a=0.01, \omega_0=10 rad/\sec, \zeta=0.1)$ at $(t=5.7\sec)$ and $(t=15.7\sec)$ under a non-separable evolutionary spectrum $(S_2=10)$. Comparison between MCS data (500 realizations) and the analytical approach.

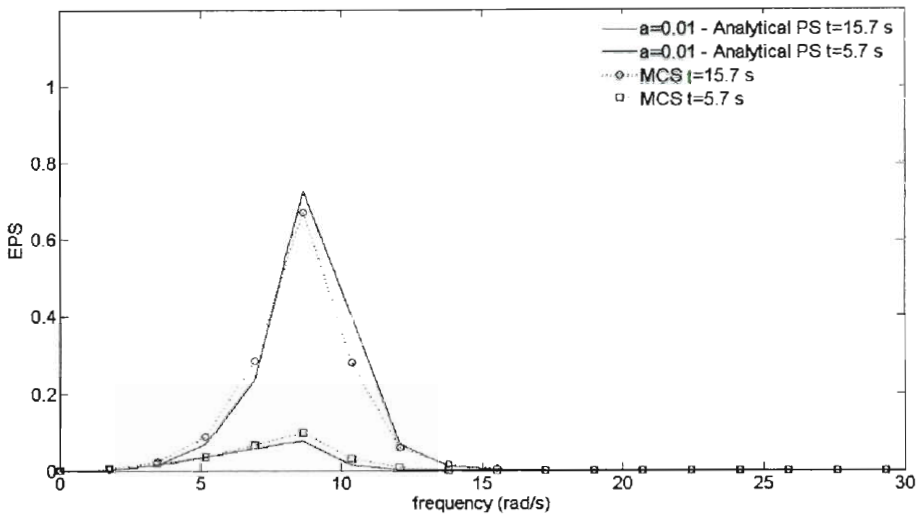

Fig.(8.8). Response EPS $(\dot{x})$ of a Bouc-Wen oscillator $(a = 0.01, \omega_0 = 10 rad/\sec, \zeta = 0.1)$ at $(t = 5.7\sec)$ and $(t = 15.7\sec)$ under a non-separable evolutionary spectrum $(S_2 = 10)$. Comparison between MCS data (500 realizations) and the analytical approach.

Chapter 9

An identification approach for nonlinear time-variant structural systems via harmonic wavelets

9.1 Preliminary remarks

Most mechanical or structural systems can exhibit nonlinear and time-varying behavior when subjected to severe excitations, such as earthquakes. The need to identify the damage in an early stage and to assure the safety and functionality of the structure has made structural health monitoring (SHM) an important research field (e.g. Farrar and Worden, 2007). It can be readily seen that for the purpose of SHM reliable identification approaches are necessary to quantify successfully the nonlinear time-varying behavior of the structures.

As far as identification of linear systems is concerned, several approaches have been developed over the past decades. For instance, time domain methods (e.g. Hac and Spanos, 1990) have exhibited satisfactory performance even for cases of short data records or incomplete knowledge of the system input. Further, the random decrement method (RDM), introduced by Cole (1971, 1973) in a heuristic manner, has received attention from many researchers. It succeeds in estimating the auto-correlation function of stochastically excited linear systems. Rigorous treatment of the RDM can be found in references such as Spanos and Zeldin (1998) and Minko et al. (2007).

In terms of nonlinear system identification various interesting approaches have been developed such as the ones based on the Volterra-Wiener (VW) representation theory (Bedrosian and Rice, 1971; Schetzen, 1980; Rugh, 1981; Jones, 2007; Franz and Schoelkopf, 2006). The VW approach has been used also in conjunction with neural networks for the identification of hysteretic systems (Pei et al., 2004). Nevertheless, the VW approach requires significant computational effort and appears unattractive for multi-degree-of-freedom (MDOF) systems. Further, discrete time nonlinear autoregressive moving average models with exogenous input (NARMAX) are often preferred for practical nonlinear system identification from experimental data (e.g. Rahrooh and Shepard, 2009).

An alternative approach utilizes a representation of the nonlinear restoring forces as a set of parallel linear sub-systems. As a result, the identification of a nonlinear system can be achieved by adopting a multiple-input/single-output (MISO) linear system analysis approach (Rice and Fitzpatrick, 1988; Bendat et al., 1992; Bendat et al., 1995; Bendat, 1998) and by utilizing measured stationary excitation-response data. Several marine/offshore system identification applications have followed based on the aforementioned reverse MISO approach. For instance, Spanos and Lu (1995) addressed the nonlinearity induced by the structure-environment interaction in marine applications, whereas identification of MDOF moored structures was performed by Raman et al. (2005) and by Panneer Selvam et al. (2006). In Zeldin and Spanos (1998) the MISO approach was examined from a novel perspective and was shown that it can be interpreted as a

Gram-Schmidt kind of orthogonal decomposition. A more detailed presentation of nonlinear system identification techniques can be found in review articles, such as the ones by Nowak (2002) and by Kerschen et al. (2006).

From another perspective, wavelet-based identification approaches (e.g. Kijeswki and Kareem, 2003; Spanos and Failla, 2005) appear promising in detecting the evolutionary features of structures (e.g. degradation) and can result in effective SHM (e.g. Hou et al., 2006). Early attempts on wavelet-based identification approaches include the work by Staszewski (1998) based on the ridges and skeletons of the wavelet transform. In the same context, Ta and Lardies (2006) used the ridges and skeletons of the continuous wavelet transform to identify weak nonlinearities and estimate their values. Kitada (1998) expressed the tangent stiffness of the structural system as a series expansion of wavelets and employed a least-squares approach to determine the coefficients. Lamarque et al. (2000) introduced a wavelet-based formula similar to the logarithmic decrement formula to estimate damping. Sone et al. (2004) developed an identification approach for linear systems based on the wavelet transform of acceleration measurements. Ghanem and Romeo (2000) presented a wavelet-Galerkin approach for identification of linear time-variant (LTV) systems. The approach was also applied to nonlinear system identification (Ghanem and Romeo, 2001). In Chakraborty et al. (2006) the modal parameters of a linear MDOF system were identified using a modified Littlewood-Paley (LP) wavelet basis function. The same wavelet basis function was used in Basu et al. (2008) to perform an on-line identification of the stiffness of LTV systems. More recent advancements include

the work by Chen et al. (2009) and by Chang and Shi (2009). The former utilized the Morlet wavelet transform for identification of linear systems, whereas the latter focused on identification of hysteretic systems.

In this chapter a generalization of the reverse MISO identification approach is proposed based on the harmonic wavelet transform. The nonlinear system is expressed as a combination of linear sub-systems in the wavelet domain. For this purpose, time and frequency dependent generalized harmonic wavelet-based frequency response functions (GHW-FRFs) are defined and a conditioning procedure is used to de-correlate the inputs of the equivalent MISO system. In this regard, the approach can address cases of nonlinear systems with time-varying parameters by utilizing non-stationary excitation-response data. The non-stationary excitation can be non-Gaussian in general with an arbitrary evolutionary power spectrum (EPS). Various examples of linear and nonlinear time-variant structural systems are used to demonstrate the accuracy of the approach. The reliability of the approach is verified also for the case of signals corrupted by noise.

9.2 Identification approach

9.2.1 Harmonic wavelet-based input-output relationships

Consider a single-degree-of-freedom (SDOF) linear time-variant (LTV) system whose motion is governed by the differential equation

$$\ddot{x} + C(t)\dot{x} + K(t)x = w(t), \tag{9.1}$$

where (C) represents the time-varying damping; (K) represents the time-varying stiffness; and $(w(t))$ denotes a zero-mean non-stationary excitation. Applying the GHWT on both sides of Eq.(9.1) yields

$$W^G_{(m,n),k}[\ddot{x}]+W^G_{(m,n),k}[C(t)\dot{x}]+W^G_{(m,n),k}[K(t)x]=W^G_{(m,n),k}[w]. \tag{9.2}$$

Further, assuming that the damping and stiffness elements are slowly-varying in time, and thus, approximately constant over the compact support of the harmonic wavelet in the time domain, Eq.(9.2) becomes

$$W^G_{(m,n),k}[\ddot{x}]+C_k W^G_{(m,n),k}[\dot{x}]+K_k W^G_{(m,n),k}[x]=W^G_{(m,n),k}[w], \tag{9.3}$$

where (C_k, K_k) represent the values of the damping and stiffness elements in the (k) translation (time) interval. Focusing next on the GHWT of the function $(\dot{x})$ and applying integration by parts yields

$$W^G_{(m,n),k}[\dot{x}]=\frac{n-m}{T_o}\left[x(t)\overline{\psi^G_{(m,n),k}}(t)\right]_{-\infty}^{\infty}-\frac{n-m}{T_o}\int_{-\infty}^{\infty}x(t)\frac{d\overline{\psi^G_{(m,n),k}}(t)}{dt}dt. \tag{9.4}$$

Taking into account the compact support of the harmonic wavelet in the time domain, Eq.(9.4) becomes

$$W^G_{(m,n),k}[\dot{x}]=-\frac{n-m}{T_o}\int_{-\infty}^{\infty}x(t)\frac{d\overline{\psi^G_{(m,n),k}(t)}}{dt}dt. \tag{9.5}$$

Further, considering Eq.(7.3) and observing that

$$\int_{m\Delta\omega}^{n\Delta\omega}e^{i\omega\left(t-\frac{kT_0}{n-m}\right)}d\omega=\frac{e^{in\Delta\omega\left(t-\frac{kT_0}{n-m}\right)}-e^{im\Delta\omega\left(t-\frac{kT_0}{n-m}\right)}}{i(n-m)\Delta\omega\left(t-\frac{kT_0}{n-m}\right)}(n-m)\Delta\omega, \tag{9.6}$$

yields

$$\int_{m\Delta\omega}^{n\Delta\omega} e^{i\omega\left(t-\frac{kT_0}{n-m}\right)} d\omega = \psi^G_{(m,n),k}(t)\left((n-m)\Delta\omega\right). \tag{9.7}$$

Assuming next that the frequency band $[m\Delta\omega, n\Delta\omega]$ is small enough Eq.(9.7) can be recast in the form

$$\psi^G_{(m,n),k}(t) = e^{i\omega_{c,(m,n),k}\left(t-\frac{kT_0}{n-m}\right)}, \tag{9.8}$$

where

$$\omega_{c,(m,n),k} = \frac{(n+m)\Delta\omega}{2}. \tag{9.9}$$

Combining Eqs.(9.5) and (9.8) and manipulating yields

$$W^G_{(m,n),k}[\dot{x}] = i\omega_{c,(m,n),k}\frac{n-m}{T_o}\int_{-\infty}^{\infty} x(t)\overline{\psi^G_{(m,n),k}(t)}dt, \tag{9.10}$$

or, equivalently

$$W^G_{(m,n),k}[\dot{x}] = i\omega_{c,(m,n),k} W^G_{(m,n),k}[x]. \tag{9.11}$$

Applying a similar analysis for the GHWT of the function $(\ddot{x})$ yields

$$W^G_{(m,n),k}[\ddot{x}] = -\omega^2_{c,(m,n),k} W^G_{(m,n),k}[x]. \tag{9.12}$$

Taking into account Eqs.(9.11-9.12) Eq.(9.3) becomes

$$W^G_{(m,n),k}[x]\left(-\omega^2_{c,(m,n),k} + i\omega_{c,(m,n),k}C_k + K_k\right) = W^G_{(m,n),k}[w]. \tag{9.13}$$

Applying complex conjugation to Eq.(9.13) yields

$$\overline{W^G_{(m,n),k}}[x]\left(-\omega^2_{c,(m,n),k} - i\omega_{c,(m,n),k}C_k + K_k\right) = \overline{W^G_{(m,n),k}}[w]. \tag{9.14}$$

Combining Eqs.(9.13-9.14) and taking expectations results in

$$E\left[\left|W^G_{(m,n),k}[x]\right|^2\right] = \frac{1}{\left(K_k - \omega^2_{c,(m,n),k}\right)^2 + \left(\omega_{c,(m,n),k}C_k\right)^2} E\left[\left|W^G_{(m,n),k}[w]\right|^2\right]. \tag{9.15}$$

Considering next Eq.(9.15), and taking into account Eq.(7.39) yields

$$S^{xx}_{(m,n),k} = \frac{1}{\left(K_k - \omega^2_{c,(m,n),k}\right)^2 + \left(\omega_{c,(m,n),k} C_k\right)^2} S^{ww}_{(m,n),k}. \tag{9.16}$$

It can be readily seen that Eq.(9.16) resembles the celebrated spectral input-output relationship of the linear stationary random vibration theory. Eq.(9.16) can be viewed as an equivalent relationship in the harmonic wavelet domain. This suggests defining the GHW-FRF as

$$H^G_{(m,n),k} = \left(-\omega^2_{c,(m,n),k} + i\omega_{c,(m,n),k} C_k + K_k\right)^{-1}. \tag{9.17}$$

Note that the GHW-FRF is defined in the intervals $\left(m\Delta\omega \le \omega < n\Delta\omega\right)$ and $\left(\frac{k}{n-m}T_o \le t < \frac{k+1}{n-m}T_o\right)$, or, in other words, it is frequency and time dependent. Utilizing next Eq.(9.17), Eq.(9.16) can take the equivalent form (see also ch. 7)

$$S^{xx}_{(m,n),k} = \left|H^G_{(m,n),k}\right|^2 S^{ww}_{(m,n),k}. \tag{9.18}$$

Further, multiplying Eq.(9.13) with $\left(\overline{W^G_{(m,n),k}[w]}\right)$ and taking expectations yields

$$E\left[W^G_{(m,n),k}[x]\overline{W^G_{(m,n),k}[w]}\right] = H^G_{(m,n),k} E\left[\left|W^G_{(m,n),k}[w]\right|^2\right], \tag{9.19}$$

or, equivalently

$$S^{xw}_{(m,n),k} = H^G_{(m,n),k} S^{ww}_{(m,n),k}, \tag{9.20}$$

where Eq.(8.11) has been considered. Ultimately, harmonic wavelets based auto- and cross-spectral input-output relationships can be derived and will be used in the ensuing analysis to develop the harmonic wavelet-based reverse MISO identification approach.

9.2.2 Harmonic wavelets based reverse MISO identification

Consider a nonlinear SDOF system whose motion is governed by the differential equation

$$\ddot{u}+C(t)\dot{u}+K(t)u+h[u,\dot{u}]=w(t), \tag{9.21}$$

where $(h[u,\dot{u}])$ is an arbitrary nonlinear function which depends on the response displacement and velocity. In the following, it is assumed that the nonlinear function $(h[u,\dot{u}])$ can be expressed as a superposition of zero-memory nonlinear transformations and linear sub-systems (e.g. Zeldin and Spanos, 1998). Specifically,

$$h[u,\dot{u}]=\sum_{l=1}^{M} A_l\left(\frac{d}{dt}\right)p_l(u), \tag{9.22}$$

where (A_l) represents polynomial functions; (p_l) represents zero-memory nonlinear transformations; and (M) accounts for the total number of base functions used in the representation of the nonlinear restoring force $(h[u,\dot{u}])$. The terms (u) and (p_l) associated with the unknown structural parameters are interpreted as the inputs (x_l) of the MISO system. Then, the composed MISO system can be described by the equation

$$\sum_{l=1}^{s} A_l\left(\frac{d}{dt}\right)x_l(t)+n(t)=w(t), \tag{9.23}$$

where (s) denotes the total number of the input variables used in the equivalent MISO representation of the nonlinear structural system; and $(n(t))$ accounts for possible extraneous noise. Note that in the developed MISO problem formulation

the traditional input/output roles of the excitation/response quantities have been reversed (see also Bendat et al., 2002). Applying next the GHWT on both sides of Eq.(9.23) yields

$$\sum_{l=1}^{s} A^{G}_{l,(m,n),k} W^{G}_{(m,n),k}[x_l] + W^{G}_{(m,n),k}[n] = W^{G}_{(m,n),k}[w]. \tag{9.24}$$

It can be readily seen that the unknowns in the system identification problem consist of the different $\left(A^{G}_{i,(m,n),k}\right)$ GHW-FRFs. In the following, extensively used stationary random data MISO analysis techniques for identification of linear FRFs (e.g. Bendat, 1998), are properly adapted and extended for the case of GHW-FRFs.

Obviously, the number of multiple inputs (s) depends on the nature of the nonlinearity term $(h[x,\dot{x}])$. Without loss of generality, and for simplicity, assume that the nonlinear system under consideration can be described by the reverse two-input/single output model of Fig.(9.1).

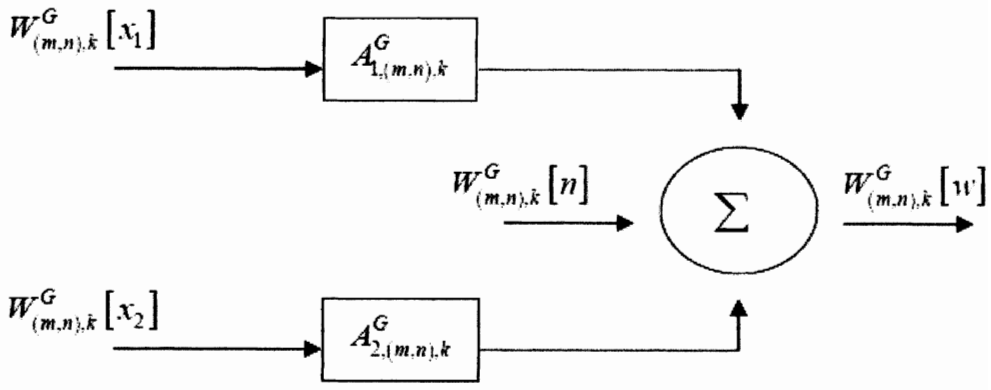

Fig.(9.1). Two-input/single output linear model in the harmonic wavelet domain.

Then, Eq.(9.24) becomes

$$A^{G}_{1,(m,n),k}W^{G}_{(m,n),k}[x_1]+A^{G}_{2,(m,n),k}W^{G}_{(m,n),k}[x_2]+W^{G}_{(m,n),k}[n]=W^{G}_{(m,n),k}[w], \tag{9.25}$$

where $\left(A^{G}_{1,(m,n),k}\right)$ is simply the reciprocal of the linear GHW-FRF of Eq.(9.17), namely

$$A^{G}_{1,(m,n),k}=\left(H^{G}_{(m,n),k}\right)^{-1}. \tag{9.26}$$

Note that in the MISO model of Fig.(9.1) $\left(W^{G}_{(m,n),k}[x_1]\right)$ and $\left(W^{G}_{(m,n),k}[x_2]\right)$ represent, in general, correlated inputs. In Bendat (1998) techniques are described to replace the original set of correlated inputs with a new set of uncorrelated inputs determined by using conditioned power spectra (PS) (see also Rice and Fitzpatrick, 1988; Spanos and Lu, 1995). The generalization of the therein described techniques to the case of time and frequency dependent harmonic wavelet-based EPS is rather straightforward. Specifically, Fig.(9.1) can be replaced by the equivalent MISO model of Fig.(9.2) with new uncorrelated inputs $\left(W^{G}_{(m,n),k}[z_1]\right)$ and $\left(W^{G}_{(m,n),k}[z_2]\right)$ passing through new linear systems $\left(L^{G}_{1,(m,n),k}\right)$ and $\left(L^{G}_{2,(m,n),k}\right)$.

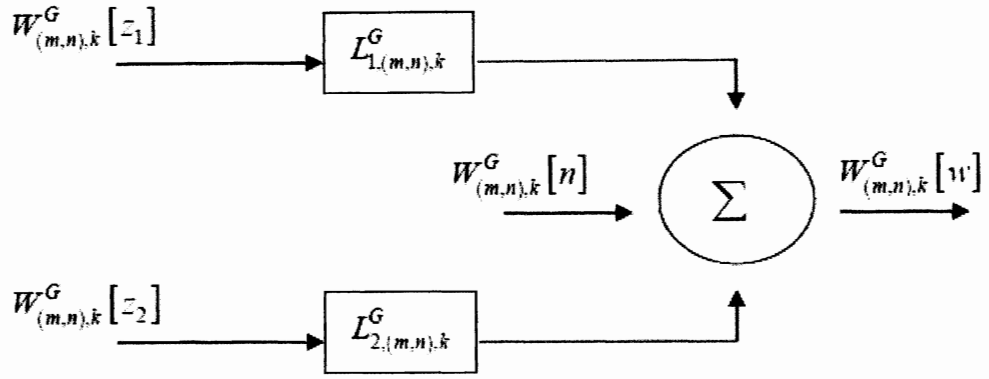

Fig.(9.2). Equivalent two-input/single output linear model in the harmonic wavelet domain with uncorrelated inputs.

The relationship between Figs.(9.1-9.2) is given by the equations

$$A^G_{2,(m,n),k} = L^G_{2,(m,n),k}, \tag{9.27}$$

and

$$A^G_{1,(m,n),k} = L^G_{1,(m,n),k} - A^G_{2,(m,n),k}\frac{S^{x_1x_2}_{(m,n),k}}{S^{x_1x_1}_{(m,n),k}}, \tag{9.28}$$

where

$$L^G_{2,(m,n),k} = \frac{S^{x_2w}_{(m,n),k} - \dfrac{S^{x_1w}_{(m,n),k}}{S^{x_1x_1}_{(m,n),k}} S^{x_2x_1}_{(m,n),k}}{S^{x_2x_2}_{(m,n),k} - \dfrac{\left|S^{x_1x_2}_{(m,n),k}\right|^2}{S^{x_1x_1}_{(m,n),k}}}, \tag{9.29}$$

and

$$L^G_{1,(m,n),k} = \frac{S^{x_1w}_{(m,n),k}}{S^{x_1x_1}_{(m,n),k}}. \tag{9.30}$$

Further, it is of interest in the analysis of MISO linear systems to calculate coherence functions as indicators of the modeling error. They provide information

about the "goodness-of-fit" of the model subject to the measured data. Note that this kind of quantitative information is not readily applicable in alternative time-domain identification approaches. In this context, the generalized harmonic wavelets based coherence function (GHW-CF) is defined as

$$\left(\gamma^{G,y_1:y_2}_{(m,n),k}\right)^2 = \frac{\left|S^{y_1y_2}_{(m,n),k}\right|^2}{S^{y_1y_1}_{(m,n),k}S^{y_2y_2}_{(m,n),k}}, \tag{9.31}$$

whereas the generalized harmonic wavelet-based cumulative coherence function (GHW-CCF) is defined as

$$\left(\gamma^{G,w:x}_{(m,n),k}\right)^2 = \left(\gamma^{G,w:z_1}_{(m,n),k}\right)^2 + \left(\gamma^{G,w:z_2}_{(m,n),k}\right)^2, \tag{9.32}$$

and can be viewed as a measure of the adequacy of the developed model with respect to the measured excitation and response quantities at the frequency and time intervals $\left(m\Delta\omega \le \omega < n\Delta\omega\right)$ and $\left(\frac{k}{n-m}T_o \le t < \frac{k+1}{n-m}T_o\right)$.

9.3 Numerical examples

In the numerical applications following, the non-separable spectrum of the form

$$S(\omega,t) = S_1\left(\frac{\omega}{5\pi}\right)^2 e^{-0.15t}t^2e^{-\left(\frac{\omega}{5\pi}\right)^2 t}, \quad t \ge 0, \quad -\infty < \omega < \infty, \tag{9.33}$$

where $\left(S_1 = 50\right)$, is considered to produce the excitation realizations. This spectrum (Fig.(9.3)) comprises some of the main characteristics of seismic shaking, such as decreasing of the dominant frequency with time (Liu, 1970; Spanos and Solomos, 1983). Sample paths compatible with Eq.(9.33) are

produced using the concept of spectral representation of a stochastic process. In this regard, a representation of the non-stationary process $\left(z_{non}(t)\right)$ takes the form (e.g. Spanos and Zeldin, 1998; Liang et al., 2007)

$$z_{non}(t) = \sum_{n=0}^{N-1} \sqrt{4S_{z_{non}}(n\Delta\omega, t)\Delta\omega}\cos\left((n\Delta\omega)t + \phi_n\right), \tag{9.34}$$

where $\left(\phi_0, \phi_1, ...\phi_{N-1}\right)$ are independent random phases following a uniform distribution over the interval $[0, 2\pi]$; and $\left(S_{z_{non}}(\omega, t)\right)$ is the evolutionary power spectrum (EPS) of the non-stationary process $\left(z_{non}(t)\right)$.

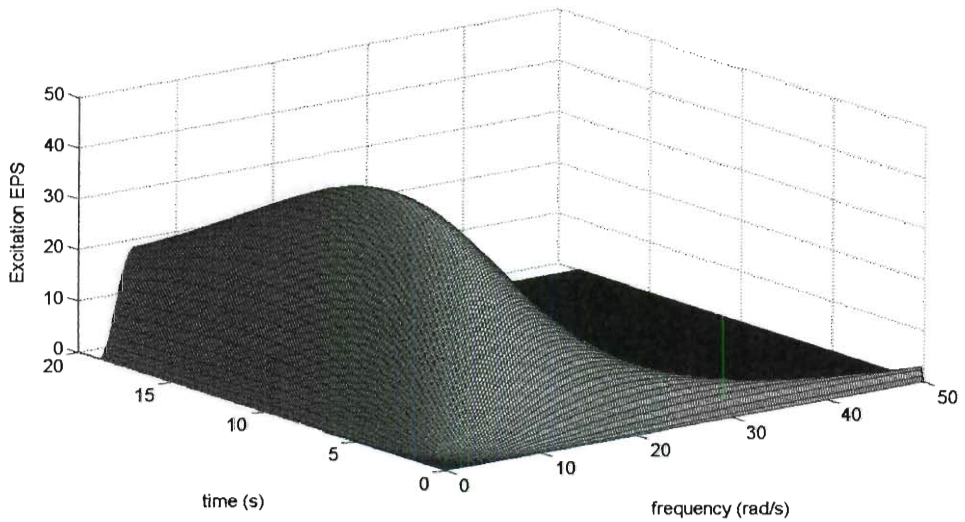

Fig.(9.3). Non-separable evolutionary excitation spectrum $\left(S_1 = 50\right)$.

As far as the calculation of the wavelet coefficients is concerned, a computationally efficient algorithm, which takes advantage of the fast Fourier transform (FFT) scheme, can be found in Newland (1997, 1999). Further, a standard 4th order Runge-Kutta numerical integration scheme is utilized for the

solution of the governing nonlinear equations of motion. Also, the effect of noise is taken into consideration. Specifically, Gaussian white noise is added to simulate the measurement noise corresponding to signal-to-noise ratio equal to 40 dB; that is the standard deviation of the added white noise is equal to 10% of the standard deviation of the corresponding signal.

9.3.1 LTV system with abrupt stiffness variation

First, an LTV system with abrupt stiffness variation is considered to demonstrate the efficiency of the approach with respect to linear problems. The time-varying system parameters of Eq.(9.21) are chosen such that

$$C(t) = 2, \tag{9.35}$$

$$K(t) = \begin{cases} 100, & 0 \le t < 6 \\ 80, & t \ge 6 \end{cases}, \tag{9.36}$$

and

$$h[u, \dot{u}] = 0. \tag{9.37}$$

The above defined system can be viewed as a realistic representation of the case of sudden loss of stiffness due to a severe earthquake event. In Fig.(9.4) the squared modulus of the estimated GHW-FRF is plotted for different time instants and compared to the theoretical values. In Fig.(9.5) the GHW-CCF, plotted for various time instants, supports the validity of the estimated model since it is quite close to unity over a wide frequency range. In fact, the frequency domain where the GHW-CCF is close to unity extends well beyond the natural frequency of the associated LTV system. Further, the time-varying parameters have been estimated by utilizing the real and imaginary parts of the GHW-FRF of Eq.(9.26).

Specifically, it is seen that the value of the stiffness (K_k) is equal to the real part of $\left(A^G_{1,(m,n),k}\right)$ for the case of $\left(\omega_{c,(m,n),k}=0\right)$. Further, the damping (C_k) is estimated as the ratio of the imaginary part of $\left(A^G_{1,(m,n),k}\right)$ over the corresponding frequency $\left(\omega_{c,(m,n),k}\right)$. The stiffness and damping estimates are plotted in Figs.(9.6) and (9.7), respectively. Comparisons with the target values show a satisfactory degree of accuracy. Obviously, the accuracy of the estimates deteriorates in the presence of noise, as expected. Nevertheless, the approach captures successfully the time-varying behavior of the system.

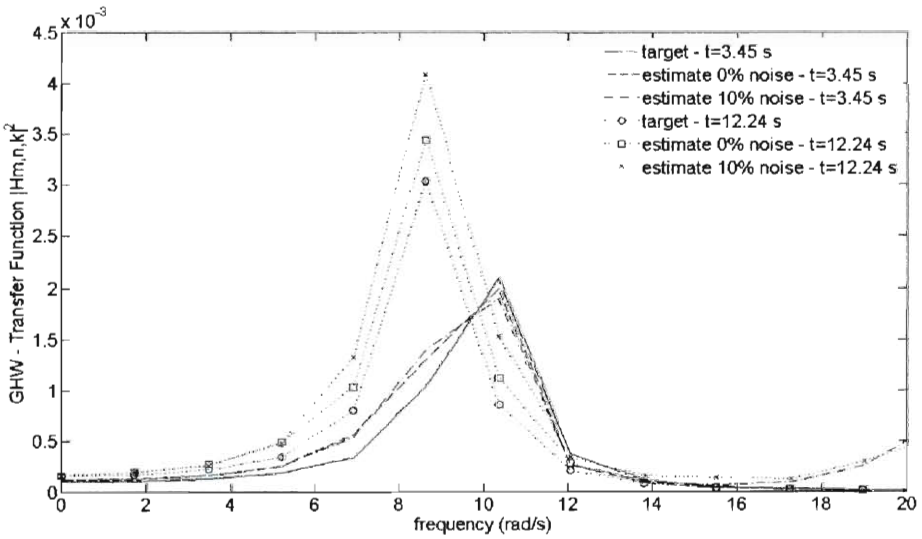

Fig.(9.4). Comparison between the target value of the squared modulus of the GHW-FRF and estimates derived from noiseless and noise corrupted data at different time instants.

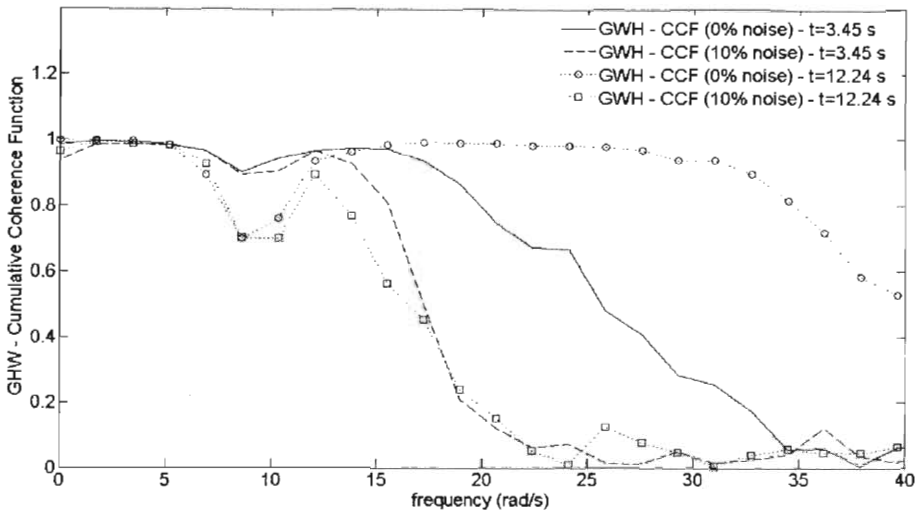

Fig.(9.5). Estimates of the GHW-CCF derived from noiseless and noise corrupted data at different time instants.

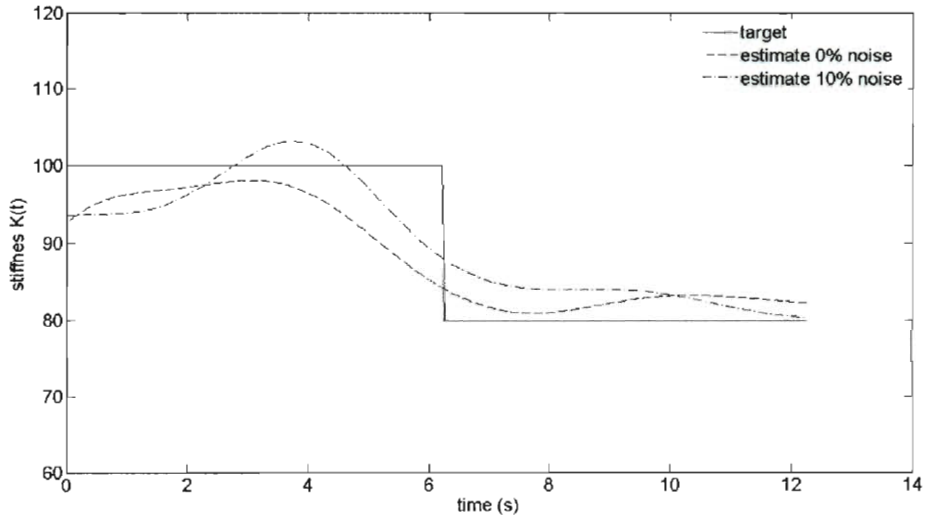

Fig.(9.6). Comparison between the target value of the stiffness and estimates derived from noiseless and noise corrupted data.

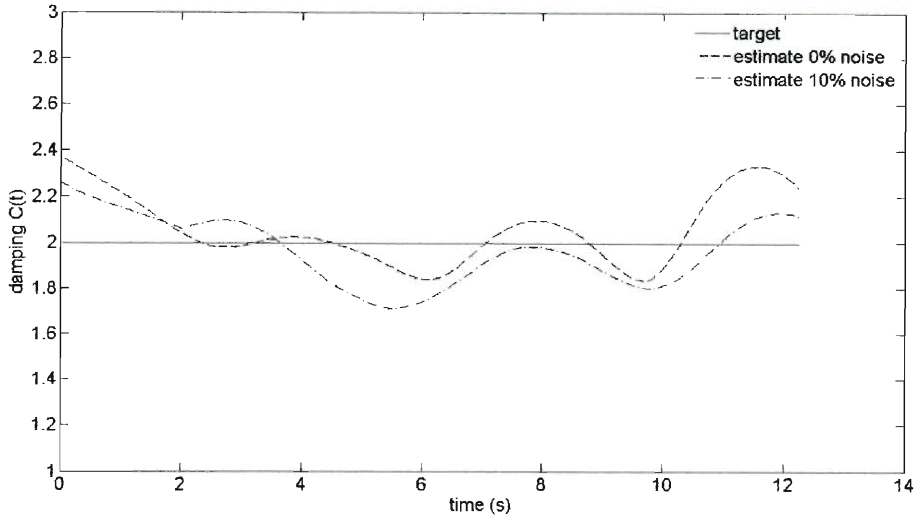

Fig.(9.7). Comparison between the target value of the damping and estimates derived from noiseless and noise corrupted data.

9.3.2 Duffing oscillator with time-varying parameters

A Duffing oscillator with smoothly time-varying parameters is considered next to demonstrate the efficiency of the approach to address nonlinear systems. The parameters of the system of Eq.(9.21) become

$$C(t) = 2 + 0.01t^2, \tag{9.38}$$

$$K(t) = 100 - 0.1t^2, \tag{9.39}$$

and

$$h[u, \dot{u}] = \varepsilon K(t) u^3, \tag{9.40}$$

where (ε) represents the nonlinearity magnitude with value equal to $(\varepsilon = 1)$. The smoothly varying stiffness and damping quantities can provide a realistic model of a degrading structure during a seismic event, whereas the Duffing form of the nonlinearity can model reasonably the behavior of a structure subjected to

pounding by an adjacent structure during seismic shaking (e.g. Wolf and Skrikerud, 1980).

The squared modulus of the estimated GHW-FRF is plotted in Fig.(9.8) and compared to the theoretical values for different time instants. In Fig.(9.9) it is seen that the GHW-CCF is close to unity over a wide frequency range. The stiffness, damping and nonlinearity magnitude estimates are plotted in Figs.(9.10), (9.11) and (9.12), respectively. It can be readily seen that the nonlinearity magnitude (ε) is equal to the real part of $\left(A^{G}_{2,(m,n),k}\right)$. It is calculated as the mean of the values of $\left(A^{G}_{2,(m,n),k}\right)$ over the frequency range where the GHW-CCF is close to unity. The developed approach captures successfully the time-varying character of the parameters values even in the presence of noise.

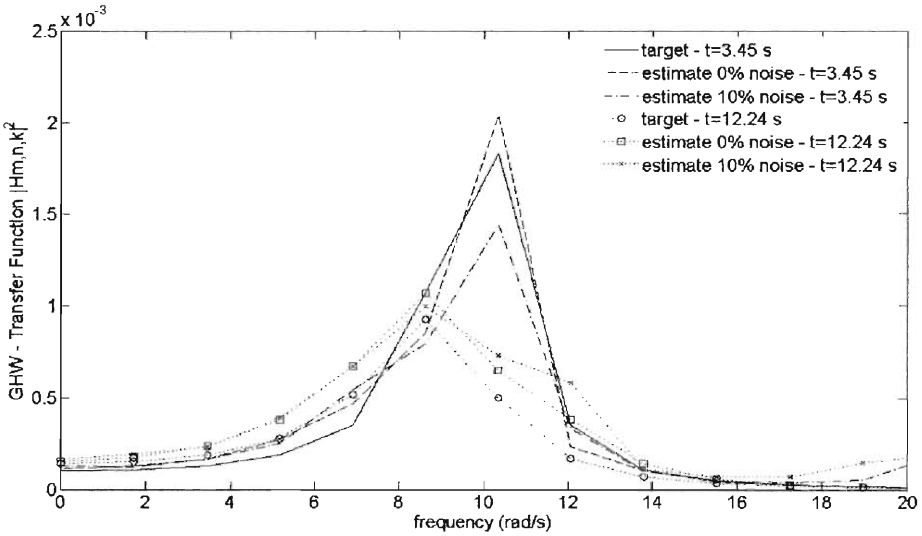

Fig.(9.8). Comparison between the target value of the squared modulus of the GHW-FRF and estimates derived from noiseless and noise corrupted data at different time instants.

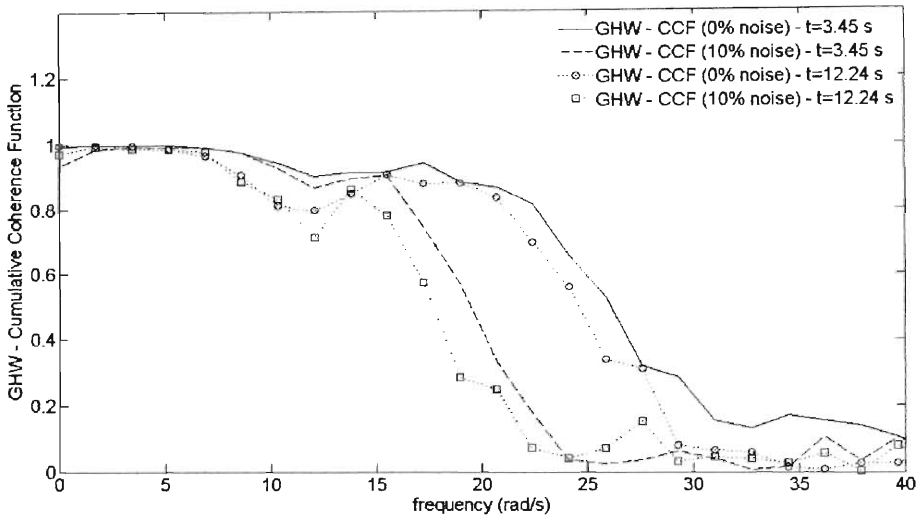

Fig.(9.9). Estimates of the GHW-CCF derived from noiseless and noise corrupted data at different time instants.

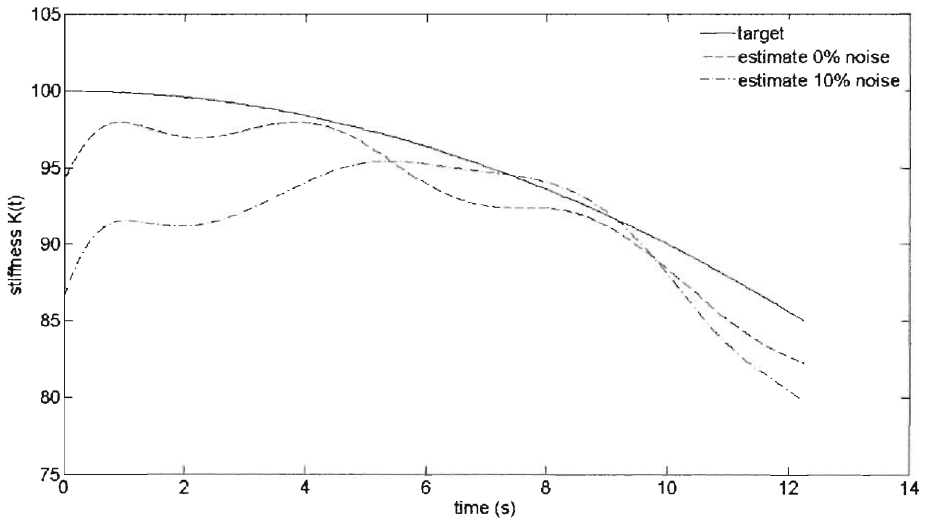

Fig.(9.10). Comparison between the target value of the stiffness and estimates derived from noiseless and noise corrupted data.

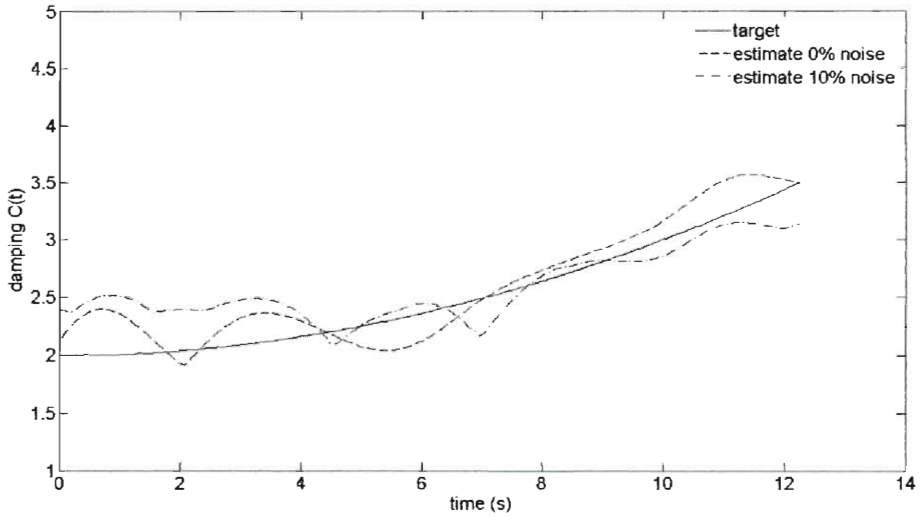

Fig.(9.11). Comparison between the target value of the damping and estimates derived from noiseless and noise corrupted data.

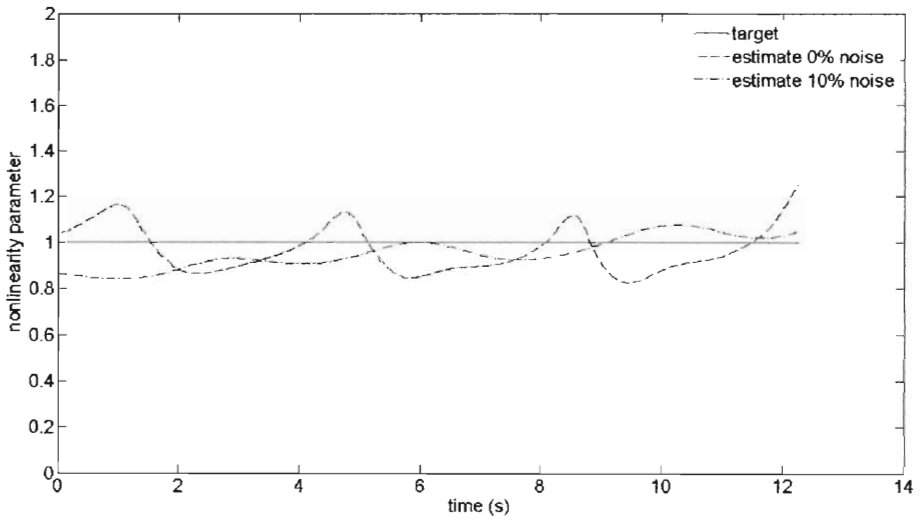

Fig.(9.12). Comparison between the target value of the nonlinearity magnitude (ε) and estimates derived from noiseless and noise corrupted data.

9.3.3 Mathieu oscillator with nonlinear damping

A Mathieu kind of oscillator with smoothly nonlinear damping is considered next to demonstrate the efficiency of the approach in treating damping nonlinearities. The parameters of the system of Eq.(9.21) are chosen such that

$$C(t)=2, \tag{9.41}$$

$$K(t)=100-30\cos(0.5t), \tag{9.42}$$

and

$$h[u,\dot{u}]=\left(\gamma C(t)\frac{1}{3}\frac{d}{dt}\right)u^3, \tag{9.43}$$

where (γ) represents the nonlinearity magnitude with value equal to $(\gamma=1)$. In Fig.(9.13) the squared modulus of the estimated GHW-FRF is plotted and compared to the theoretical values for different time instants. In Fig.(9.14) it is shown that the GHW-CCF is close to unity over a wide frequency range. The stiffness, damping and nonlinearity magnitude estimates are plotted in Figs.(9.15), (9.16) and (9.17), respectively. Specifically, the nonlinearity magnitude (γ) is equal to the imaginary part of $\left(A^{G}_{2,(m,n),k}\right)$ divided by the term $\left(C(t)\frac{1}{3}\omega_{c,(m,n),k}\right)$. It is determined as the mean value over the frequency range where the GHW-CCF is close to unity. The developed approach manages to capture successfully the time-varying character of the parameters values even in the presence of noise. Comparisons with the target values show a satisfactory degree of accuracy even for the case of noise corrupted data.

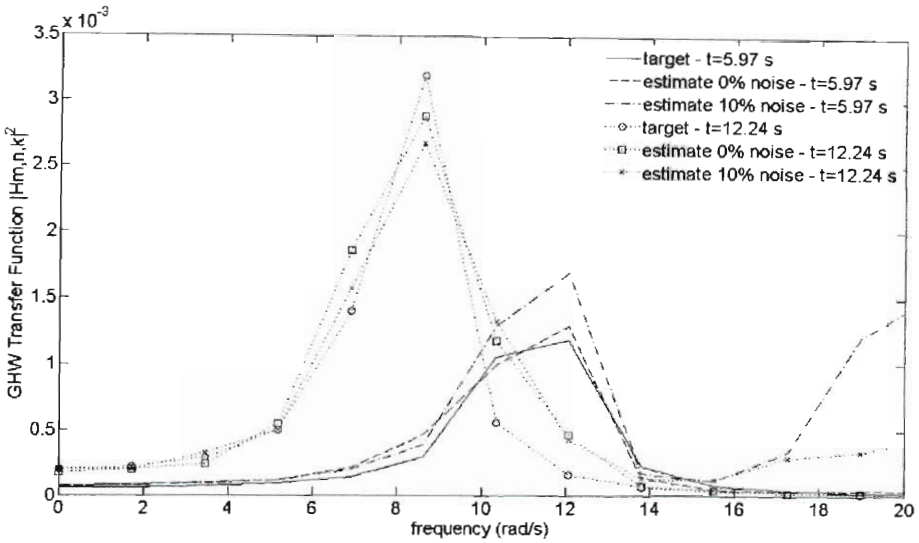

Fig.(9.13). Comparison between the target value of the squared modulus of the GHW-FRF and estimates derived from noiseless and noise corrupted data at different time instants.

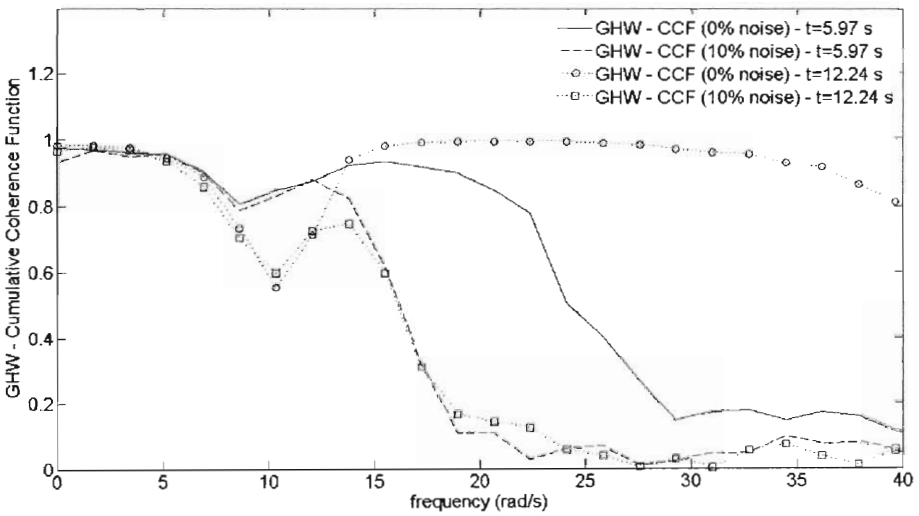

Fig.(9.14). Estimates of the GHW-CCF derived from noiseless and noise corrupted data at different time instants.

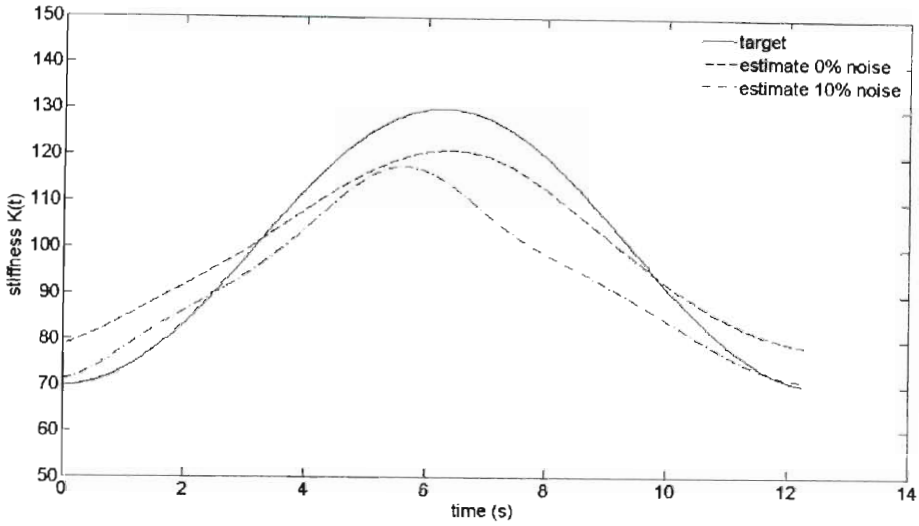

Fig.(9.15). Comparison between the target value of the stiffness and estimates derived from noiseless and noise corrupted data.

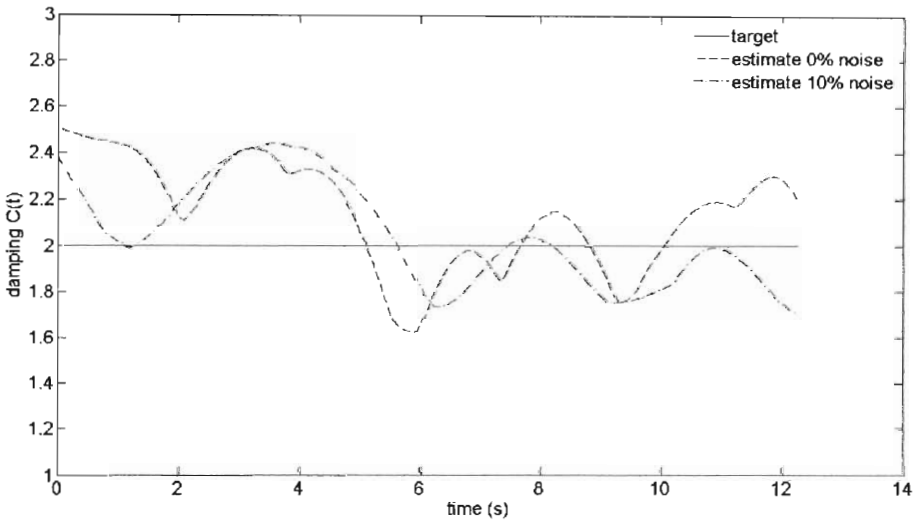

Fig.(9.16). Comparison between the target value of the damping and estimates derived from noiseless and noise corrupted data.

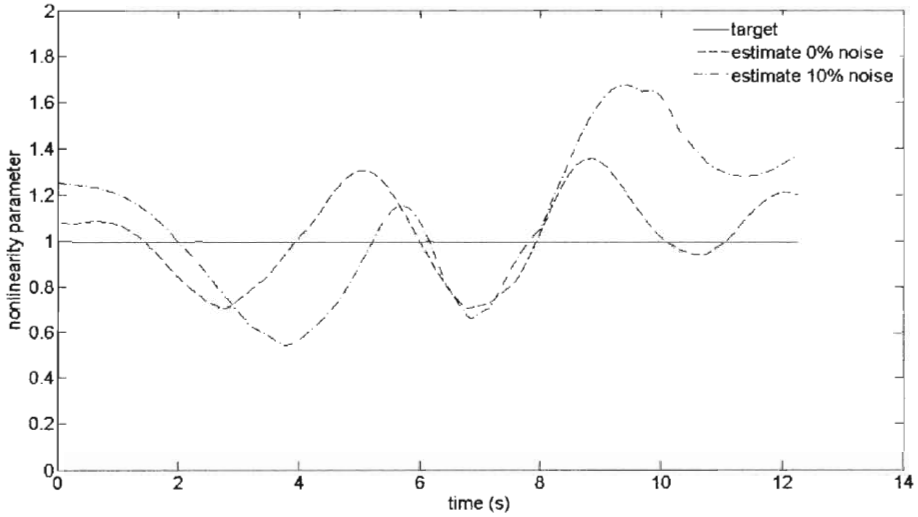

Fig.(9.17). Comparison between the target value of the nonlinearity magnitude (γ) and estimates derived from noiseless and noise corrupted data.

Chapter 10

Concluding remarks

In this chapter, the main conclusions associated with the analytical formulations and the numerical results of this thesis are presented and discussed. Also, suggestions for further development of the proposed methods are outlined.

In chapter 2 a formula which estimates the PSD of the stochastic response of nonlinear systems has been considered. The formula, which is based on the notion of conditional PSD, has been widely used in computing, with remarkable reliability, the response PSDs of a wide range of stochastically excited nonlinear oscillators. Despite the popularity and the versatility of the approach, its mathematical legitimacy has been based so far on arguments of limited rigor. In this regard, an effort to provide a concrete proof has been made in this chapter by utilizing spectral representations both for the excitation and the response processes of the nonlinear system; this has been done in conjunction with an equivalent linear approximation of the original system. Further, exploiting the orthogonality properties of the monochromatic functions which are involved in the expansions has led to a straightforward verification of the formula. Furthermore, an intuitive interpretation of the concept of the conditional PSD has been included. Specifically, it has been shown that the nonlinear response PSD can be viewed as a sum of the PSDs which correspond to equivalent amplitude

dependent linear systems. The necessity of invoking for the system response not only stationarity but ergodicity as well has been pointed out.

In chapter 3 an approximate analytical approach based on the concepts of statistical linearization and of stochastic averaging has been developed for determining the evolutionary stochastic response of MDOF nonlinear systems. Specifically, a system dimension reduction approach, which utilizes the concept of an effective LTV SDOF system associated with each degree of freedom, has yielded the non-stationary response amplitude PDF corresponding to each degree of freedom. Further, the approach can be applied in conjunction with recently developed design spectrum based analyses to obtain peak response estimates without resorting to numerical integration of the nonlinear equations of motion. Numerical examples have included a 2-DOF shear building model with stiffness and damping nonlinearities, as well as a 2-DOF shear building model endowed with the Bouc-Wen hysteretic model. Pertinent Monte Carlo simulations have verified the accuracy and reliability of the approach even for cases of excitations possessing non-separable EPS. Thus, it has been shown that the approach can be readily applied for cases of physically realistic excitations without resorting to pre-processing treatments, such as pre-filtering, commonly used in alternative linearization schemes. Future work may include adaptation/generalization of stochastic system dimension reduction methods, originally developed for theoretical/statistical physics applications to realistic response behavior prediction and reliability assessment of large-scale complex systems of engineering interest. Potential applications may vary from the study of MDOF nonlinear (hysteretic)

systems and of interdependent civil infrastructure systems to the stochastic analysis of (nano)materials with random properties.

In chapter 4 a numerical Wiener PIS approach has been applied to derive response and first-passage statistics of nonlinear oscillators subject to evolutionary broad-band stochastic excitation. Specifically, relying on the Markov properties of the response process and on a discrete version of the C-K relation, response envelope and first-passage statistics have been derived for the Van der Pol, the Duffing and the Preisach oscillators. The deviation of the excitation process from Gaussian white noise and the effect it has on the Markovian character of the response process leads to questions regarding the validity of the C-K equation. Nevertheless, it has been shown that the Wiener PIS approach yields quite accurate and reliable results for different excitation and nonlinearity levels.

In chapter 5 a numerical Wiener PIS approach has been developed to examine the behavior of the response amplitude process and to derive first-passage PDF estimates for a softening Duffing oscillator under stochastic excitation. In the context of nonlinear stochastic dynamics, the Duffing oscillator with softening nonlinearity has been so far treated in a manner which has disregarded important aspects of the analysis, such as considering the unbounded behavior the response process experiences when the restoring force acquires negative values. In chapter 5, relying on a discrete version of the C-K equation and introducing a special form for the conditional PDF, a rigorous treatment of the subject has been provided. First-passage PDFs have been computed and

compared to pertinent Monte Carlo simulations. Further, the proposed approach has been applied to determine the capsizing probability of a ship under physically realistic non-white wave excitations. Different levels of nonlinearity magnitude and of barrier value have been considered to demonstrate the reliability and accuracy of the approach.

In chapter 6 the potential of the analytical Wiener path integral to address certain engineering mechanics problems has been demonstrated. In this manner, non-stationary response statistics of a broad class of nonlinear oscillators, namely oscillators with nonlinear damping, have been determined. Specifically, relying on stochastic averaging and on statistical linearization a first order SDE governing the evolution of the response amplitude envelope has been established. Further, it has been shown that a variational formulation utilizing the concept of the most probable path and considering the drift and diffusion coefficients of the stochastic differential equation has yielded an approximate solution for the Wiener path integral. A Van der Pol, a Rayleigh, and a linear-plus-cubic damping oscillators have been considered to demonstrate the versatility and the satisfactory level of accuracy the method exhibits. Compared to the existing alternative numerical PIS approaches, the proposed approach appears considerably more efficient computationally since there is no need to advance the solution in short time steps only. Future work may include the generalization of the Wiener path integral method to determine the response PDF of nonlinear/hysteretic MDOF systems under evolutionary stochastic excitation. It constitutes a reliable and computationally efficient alternative for general system uncertainty quantification

and risk/reliability assessment. Further, because of its versatility the approach facilitates greatly the efficient design of mechanical/structural systems. Potential applications include aerospace, marine/offshore, and earthquake engineering, as well as wind energy harvesting (e.g. efficient wind turbine design).

In chapter 7 a novel harmonic wavelets based statistical linearization approach has been proposed for determining the EPS of the response of nonlinear oscillators under evolutionary stochastic excitation. The approach has been developed in conjunction with the family of harmonic wavelets. Specifically, relying on the properties of the generalized harmonic wavelet and exploiting the concept of a locally stationary wavelet-based representation of stochastic processes, a process corresponding to a specific scale and translation level has been defined. In this context, first an EPS estimation approach has been presented in conjunction with the proposed process representation and has been applied in estimating both separable and non-separable EPS; and thus demonstrating the capacity of the approach to capture successfully the time-varying frequency content of a complex non-stationary stochastic phenomenon. Next, focusing on the case of a linear system and relying on the orthogonality properties of the developed representation an excitation-response EPS relationship has been derived. This is valid both for linear time-invariant and linear time-variant systems. Finally, for the statistical linearization approach excitation-response relationships have been obtained by employing the novel concept of wavelet scale (frequency) and wavelet translation level (time) dependent equivalent stiffness and damping elements. The resulting nonlinear system of equations has been

solved in an iterative manner to determine the response EPS. Thus, a joint time-frequency response analysis has been achieved. Pertinent Monte Carlo simulations have demonstrated the reliability of the approach both for damping and stiffness nonlinearities.

In chapter 8 the harmonic wavelets based statistical linearization method developed in chapter 7 has been extended to evaluate the response EPS of the Bouc-Wen hysteretic oscillator under non-stationary stochastic excitation.

In chapter 9 a harmonic wavelet-based identification approach has been developed for nonlinear systems with time-varying parameters. Specifically, relying on measured excitation-response (non-stationary) data, and on the localization properties of the generalized harmonic wavelet transform the time-dependent GHW-FRFs have been identified by a conditioning procedure. They have been further utilized to determine the time-varying parameters of the associated system. This has been done in conjunction with an extension of the well-established reverse MISO spectral identification approach to the harmonic wavelet domain. It can be viewed as a generalization of the approach to address cases of non-stationary measured data and of nonlinear time-variant systems. The reliability of the identification approach, a prerequisite for effective SHM, has been demonstrated for a number of linear and nonlinear time-variant structural systems, even for the case of noise corrupted data. Future work may include the development of an efficient/robust structural system parameters identification method via (harmonic) wavelets and (stochastic) neural networks, and, eventually, of an effective structural health monitoring process. Based on the localization

properties of the (harmonic) wavelets and on the extrapolation capabilities of the (stochastic) neural networks it can be a reliable method for fault/damage detection and, ultimately, for quantification of civil infrastructure sustainability.

References

Agrawal O. P., 1998. Application of wavelets in modeling stochastic dynamic systems, *Journal of Vibration and Acoustics, vol. 120: 763-769.*

Arnold L., 1974. *Stochastic Differential Equations: Theory and Applications.* New York: Wiley.

Arnold L., Chuesov I., Ochs G., 2004. Stability and Capsizing of ships in random sea – a survey, *Nonlinear Dynamics, vol. 36: 135-179.*

Au S. K., 2009. Importance sampling for elasto-plastic systems using adapted process with deterministic control, *International Journal of Non-Linear Mechanics, vol. 44: 190-199.*

Baber T. T., Wen Y. K., 1981. Random vibration of hysteretic degrading systems, *Journal of Engineering Mechanics Division, vol. 107: 1069-1087.*

Bach A., Durr D., Stawicki B., 1977. Functionals of paths of a diffusion process and the Onsager-Machlup function, *Zeitschrift fur Physik B, vol. 26: 191-193.*

Bach A., Durr D., Korsch H. J., 1978. Derivation of quasideterministic Fokker-Planck dynamics, *Physics Letters, vol. 68A: 5-8.*

Basu B., Gupta V. K., 1997. Non-stationary seismic response of MDOF systems by wavelet transform, *Earthquake Engineering and Structural Dynamics, vol. 26: 1243-1258.*

Basu B., Gupta V. K., 1998. Seismic response of SDOF systems by wavelet modeling of non-stationary processes, *Journal of Engineering Mechanics, vol. 124: 1142-1150.*

Basu B., Gupta V.K., 1999a. On equivalent linearization using wavelet transform, *Journal of Vibration and Acoustics, vol. 121: 429-432.*

Basu B., Gupta V. K., 1999b. Wavelet-based analysis of the non-stationary response of a slipping foundation, *Journal of Sound and Vibration, vol. 222: 547-563.*

Basu B., Gupta V. K., 2000. Stochastic seismic response of single-degree-of-freedom systems through wavelets, *Engineering Structures, vol. 22: 1714-1722.*

Basu B., Gupta V. K., 2001. Wavelet-based stochastic seismic response of a Duffing oscillator, *Journal of Sound and Vibration, vol. 245: 251-260.*

Basu B., Nagarajaiah S., Chakraborty A., 2008. Online identification of linear time-varying stiffness of structural systems by wavelet analysis, *Structural Health Monitoring, vol. 7: 21-36.*

Bedrosian E., Rice S. O., 1971. The output properties of Volterra systems (Nonlinear systems with memory) driven by harmonic and Gaussian Inputs, *Proceedings of the IEEE, vol. 59: 1688-1707.*

Belenky V. L., Sevastianov N. B., 2007. *Stability and safety of ships: Risk of capsizing*, The Society of Naval Architects and Marine Engineers, 2nd Edition.

Bellizzi S., Defilippi M., 2003. Nonlinear mechanical systems identification using linear systems with random parameters, *Mechanical Systems and Signal Processing, 17: 203-210.*

Bendat J. S., Piersol A. G., 1971. *Random data: Analysis and measurement procedures*, New York, Wiley-Interscience.

Bendat J. S., Palo P. A., Coppolini R. N., 1992. A general identification technique for nonlinear differential equations of motion, *Probabilistic Engineering Mechanics, vol. 7: 43-61.*

Bendat J. S., Palo P. A., Coppolini R. N., 1995. Identification of physical parameters with memory in nonlinear systems, *International Journal of Non-Linear Mechanics, vol. 30: 841-860.*

Bendat J. S., 1998. *Nonlinear systems, techniques and applications*, New York, Wiley-Interscience.

Bertotti G., Mayergoyz I. D. (eds), 2003a. *The science of hysteresis, vol. I: Mathematical modeling and applications*, Elsevier.

Bertotti G., Mayergoyz I. D. (eds), 2003b. *The science of hysteresis, vol. III: Hysteresis in materials*, Elsevier.

Bouc R., 1967. Forced vibration of mechanical system with hysteresis, *Proceedings of 4th Conference on Nonlinear Oscillation, Prague.*

Bouc R., 1994. The power spectral density of response for a strongly nonlinear random oscillator, *Journal of Sound and Vibration, 175: 317-331.*

Bouc R., Boussaa D., 2002. Drifting response of hysteretic oscillators to stochastic excitation, *International Journal of Non-Linear Mechanics, vol. 37: 1397-1406.*

Brennan M. J., Kovacic I., Carrella A., Waters T. P., 2008. On the jump-up and jump-down frequencies of the Duffing oscillator, *Journal of Sound and Vibration, vol. 318: 1250-1261.*

Brush S. G., 1961. Functional integrals and statistical physics, *Reviews of Modern Physics, vol. 33: 79-92.*

Cai G. Q., Lin Y. K., 1998. Reliability of nonlinear structural frame under seismic excitation, *Journal of Engineering Mechanics, vol. 124: 852-856.*

Caughey T. K., Stumpf H. J., 1961. Transient response of a dynamic system under random excitation, *Journal of Applied Mechanics, vol. 28: 563-566.*

Caughey T. K., 1963. Equivalent linearization techniques, *Journal of the Acoustical Society of America, 35: 1706-1711.*

Chaichian M., Demichev A., 2001. *Path integrals in Physics, vol. I, stochastic processes and quantum mechanics*, Institute of Physics Publishing, Bristol and Philadelphia.

Chakraborty A., Basu B., Mitra M., 2006. Identification of modal parameters of a mdof system by modified L-P wavelet packets, *Journal of Sound and Vibration, vol. 295: 827-837.*

Chakraborty A., Basu B., 2008. Non-stationary response analysis of long span bridges under spatially varying differential support motions using continuous wavelet transform", *Journal of Engineering Mechanics, vol. 134: 155-162.*

Chandrashekhar S., 1943. Stochastic problems in physics and astronomy, *Rev. Mod. Phys. 15(1): 1-89.* Reprinted in *Selected Papers on Noise and Stochastic Processes*, N. Wax, ed. 1954. New York, Dover: 1-91.

Chang C-C., Shi Y., 2009. Identification of time-varying hysteretic structures using wavelet multiresolution analysis, *International Journal of Non-Linear Mechanics, doi:10.1016/j.ijnonlinmec.2009.08.009.*

Chen S-L., Liu J-J., Lai H-C., 2009. Wavelet analysis for identification of damping ratios and natural frequencies, *Journal of Sound and Vibration, doi:10.1016/j.jsv.2009.01.029.*

Clough R. W., Penzien J., 1993. *Dynamics of structures,* New York: McGraw-Hill.

Cole H. A., 1971. Failure detection of a space shuttle wing flutter model by random decrement, *NASA report TM X-62041.*

Cole H. A., 1973. On-line failure detection and damping measurement of aerospace structures by random decrement signatures, *NASA report CR-2205.*

Conte J. P., Peng B. F., 1996. An explicit closed-form solution for linear systems subjected to non-stationary random excitation, *Probabilistic Engineering Mechanics, 11: 37-50.*

Cramer H., Leadbetter M. R., 1967. *Stationary and related stochastic processes*, Wiley, New York.

Crandall S. H., ed., 1958. *Random vibration*, vol. I.Cambridge, MA: MIT Press.

Crandall S. H., ed., 1963. *Random vibration*, vol. II.Cambridge, MA: MIT Press.

Crandall S. H., Mark W. D., 1963. *Random vibration in mechanical systems*. New York: Academic Press.

Dahlhaus R., 1997. Fitting time series models to non-stationary processes, *The Annals of Statistics, vol. 25: 1-37.*

Dalzell J., 1978. A note on the form of ship roll damping, *Journal of Ship Research, vol. 22: 178-185.*

Daubechies I., 1992. *Ten lectures on wavelets*, SIAM, Philadelphia.

Davoodi H., Noori M., 1990. Extension of an Ito-based general approximation technique for random vibration of a BBW general hysteresis model, part II: non-Gaussian analysis, *Journal of Sound and Vibration, vol. 140: 319-339.*

Dekker H., 1976. Time-local Gaussian processes, path integrals and nonequilibrium nonlinear diffusion, *Physica, vol. 85A: 363-373.*

Dekker H., 1977. A functional Stieltjes measure and generalized diffusion processes, *Physica, vol. 87A: 419-425.*

Di Paola M., Elishakoff I., 1996. Non-stationary response of linear systems under stochastic Gaussian and non-Gaussian excitation: a brief overview of recent results, *Chaos, Solitons and Fractals, vol. 7: 961-971.*

Di Paola M., Santoro R., 2008. Path integral solution for nonlinear system enforced by Poisson white noise, *Probabilistic Engineering Mechanics, vol. 23: 164-169.*

Dobson S., Noori M., Hou Z., Dimentberg M., Baber T. T., 1997. Modeling and random vibration analysis of SDOF systems with asymmetric hysteresis, *International Journal of Non-Linear Mechanics, vol. 32: 669-680.*

Durr D., Bach A., 1977. The Onsager-Machlup function as Lagrangian for the most probable path of a diffusion process, *Communications in Mathematical Physics, vol. 60: 153-170.*

Durr D., Bach A., 1979. Application of the Onsager-Machlup function to nonlinear diffusion processes, *Zeitschrift fur Physik B, vol. 32: 413-417.*

Eckley I. A., Nason G. P., Treloar R. L., 2010. Locally stationary wavelet fields with application to the modeling and analysis of image texture, *Applied Statistics, vol. 59: 595-616.*

Elishakoff I. E., 1999. *Probabilistic theory of structures*. New York: Dover Publications.

Ewing G. M., 1985. *Calculus of variations with applications*, Dover, New York.

Failla G., Spanos P. D., Di Paola M., 2003. Response power spectrum of multi-degree-of-freedom nonlinear systems by a Galerkin technique, *Journal of Applied Mechanics, vol. 70: 708-714.*

Falkoff D., 1958. Statistical theory of irreversible processes Part I. Integral over fluctuation path formulation, *Annals of Physics, vol. 4: 325-346.*

Fang T., Li J. Q., Sun M. N., 2002. A universal solution for evolutionary random response problems, *Journal of Sound and Vibration, vol. 253: 909-916.*

Faravelli L., Casciati F., Singh M. P., 1988. Stochastic equivalent linearization algorithms and their applicability to hysteretic systems, *Meccanica, vol. 23: 107-112.*

Farrar C. R., Worden K., 2007. An introduction to structural health monitoring, *Phil. Trans. R. Soc. A, vol. 365: 303-315.*

Feller W., 1954. Diffusion processes in one dimension, *Transactions of the American Mathematical Society, vol. 77: 1-31.*

Feng G. M., Wang B., Lu Y. F., 1992. Path integral, functional method, and stochastic dynamical systems, *Probabilistic Engineering Mechanics, vol. 7: 149-157.*

Feynman R. P., 1948. Space-time approach to non-relativistic quantum mechanics, *Reviews of Modern Physics, vol. 20: 367-387.*

Feynman R. P., Hibbs A. R., 1965. *Quantum mechanics and path integrals*, McGraw-Hill, New York.

Foliente G. C., Singh M. P., Noori M. N., 1996. Equivalent linearization of generally pinching hysteretic degrading systems, *Earthquake Engineering and Structural Dynamics, vol. 25: 611-629.*

Franz M. O., Schoelkopf B., 2006. A unifying view for Wiener and Volterra theory and polynomial kernel regression, *Neural Computation, vol. 18: 3097-3118.*

Froude W., 1861. On the rolling of ships, *Transactions of the Institute of Naval Architects, vol. 11: 180-229.*

Gamerman D., 2006. *Markov Chain Monte Carlo: a stochastic simulation for Bayesian interference*, Taylor and Francis.

Gardiner C. W., 1985. *Handbook for Stochastic Methods for Physics, Chemistry and the Natural Sciences*, Springer-Verlag, Berlin, Heidelberg, New York.

Gelfand I. M., Yaglom A. M., 1960. Integration in functional spaces and its applications in quantum physics, *Journal of Mathematical Physics, vol. 1: 48-69.*

Ghanem R., Romeo F., 2000. A wavelet-based approach for the identification of linear time-varying dynamical systems, *Journal of Sound and Vibration, vol. 234: 555-576.*

Ghanem R., Romeo F., 2001. A wavelet-based approach for model and parameter identification of nonlinear systems, *International Journal of Non-Linear Mechanics, vol. 36: 835-859.*

Giaralis A., Spanos P. D., 2009. Wavelet-based response spectrum compatible synthesis of accelerograms - Eurocode application (EC8), *Soil Dynamics and Earthquake Engineering, vol. 29: 219-235.*

Giaralis A., Spanos P. D., 2010. Effective linear damping and stiffness coefficients of nonlinear systems for design spectrum based analysis, *Soil Dynamics and Earthquake Engineering, vol. 30: 798-810.*

Gihman I. F., Skorohod A. V., 1972. *Stochastic differential equations*, Springer-Verlag, Berlin, Heidelberg, New York.

Gihman I. F., Skorohod A. V., 1975. *The Theory of Stochastic Processes*, vol. II, Springer-Verlag, Berlin, Heidelberg, New York.

Goto H., Iemura H., 1973. Linearization Techniques for Earthquake Response of Simple Hysteretic Structures, *Proceedings of the Japaneese Society of Civil Engineering, Vol.212: 109-119.*

Graham R., 1977. Path integral formulation of general diffusion processes, *Zeitschrift fur Physik B, vol. 26: 281-290.*

Grigoriu M., 1990. Applications of diffusion models to reliability analysis of Daniels systems, *Structural Safety, vol. 7: 219-228.*

Grigoriu M., 1993. Spectral representation method in simulation, *Probabilistic Engineering Mechanics, 8: 75-90.*

Grigoriu M., 2002. *Stochastic calculus, applications in science and engineering*, Birkhauser, Boston.

Grossmann A., Morlet J., 1984. Decomposition of Hardy functions into square integrable wavelets of constant shape, *SIAM Journal on Mathematical Analysis, vol. 15: 723-736.*

Gupta I. D., Trifunac M. D., 2000. A note on the nonstationarity of seismic response of structures, *Engineering Structures, vol. 23: 1567-1577.*

Hac A., Spanos P. D., 1990. Time domain method for parameter system identification, *Journal of Vibration and Acoustics, vol. 112: 281-287.*

Haken H., 1976. Generalized Onsager-Machlup function and classes of path integral solutions of the Fokker-Planck equation and the master equation, *Zeitschrift fur Physik B, vol. 24: 321-326.*

Hammond J. K., 1968. On the response of single and multidegree of freedom systems to non-stationary random excitations, *Journal of Sound and Vibration, vol. 7: 393-416.*

Hammond J. K., 1973. Evolutionary spectra in random vibration, *Journal of the Royal Statistical Society, vol. 35: 167-188.*

Hasselmann K., Ross D. B., Mueller P., Sell W., 1976. A parametric wave prediction model, *Journal of Physical Oceanography, vol. 6: 200-228.*

Horsthemke W., Bach A., 1975. Onsager-Machlup function for one dimensional nonlinear diffusion processes, *Zeitschrift fur Physik B, vol. 22: 189-192.*

Hou Z., Hera A., Shinde A., 2006. Wavelet-based structural health monitoring of earthquake excited structures, *Computer-Aided Civil and Infrastructure Engineering, vol. 21: 268-279.*

Hsieh S. R., Troesch A. W., Shaw S. W., 1994. A nonlinear probabilistic method for predicting vessel capsizing in random beam seas, *Proc. R. Soc. Lond. A, vol. 446: 195-211.*

Huang G., Chen X., 2009. Wavelets-based estimation of multivariate evolutionary spectra and its application to non-stationary downburst winds, *Engineering Structures, doi:10.1016/j.enstruct.2008.12.010.*

Hurtado J. E., Barbat A. H., 1996. Improved stochastic linearization method using mixed distributions, *Structural Safety, vol. 18: 49-62.*

Hurtado J. E., Barbat A. H., 2000. Equivalent linearization of the Bouc-Wen hysteretic model, *Engineering Structures, vol. 22: 1121-1132.*

Hussaini N. Y., 1996. *Wavelets: theory and applications*, Oxford University Press.

Ibrahim R. A., 1985. *Parametric Random Vibration*, Dover Publications.

Ibrahim R. A., Ghalhoub N. G., Falzarano J., 2007. Interaction of ships and ocean structures with ice loads and stochastic ocean waves, *Applied Mechanics Review, vol. 60: 246-289.*

Ikhouane F., Rodellar J., 2007. *Systems with hysteresis: analysis, identification and control using the Bouc-Wen model*, John Wiley and Sons.

Iourtchenko D., Mo E., Naess A., 2008. Reliability of strongly nonlinear single degree of freedom dynamic systems by the path integration method, *Journal of Applied Mechanics, vol. 75: 061016-1-061016-8.*

Ismail M., Ikhouane F., Rodellar J., 2009. The hysteresis Bouc-Wen model, a survey, *Archives of Computational Methods in Engineering, vol. 16: 161-188.*

Iwankiewicz R., Nielsen S. R. K., 1992. Dynamic response of hysteretic systems to Poisson-distributed pulse trains, *Probabilistic Engineering Mechanics, vol. 7: 135-148.*

Jangid R. S., Datta T. K., 1999. Evaluation of the methods for response analysis under non-stationary excitation, *Shock and Vibration, vol. 6: 285-297.*

Jiang C., Troesch A. W., Shaw S. W., 2000. Capsize criteria for ship models with memory-dependent hydrodynamics and random excitation, *Phil. Trans. R. Soc. Lond. A, vol. 358: 1761-1791.*

Jones J. C. P., 2007. Simplified computation of the Volterra frequency response functions of nonlinear systems, *Mechanical Systems and Signal Processing, vol. 21: 1452-1468.*

Jumarie G., 2007. Path integral for the probability of the trajectories generated by fractional dynamics subject to Gaussian white noise, *Applied Mathematics Letters, vol. 20: 846-852.*

Kac M., 1949. On distributions of certain Wiener functionals, *Transactions of the American Mathematical Society, vol. 65: 1-13.*

Kanai K., 1957. Semi-empirical formula for the seismic characteristics of the ground, *University of Tokyo, Bulletin of Earthquake Research Institute.*

Keinert F., 2004. *Wavelets and multiwavelets*, Chapman and Hall.

Kerschen G., Worden K., Vakakis A., Golinval J-C., 2006. Past, present and future of nonlinear system identification in structural dynamics, *Mechanical Systems and Signal Processing, vol. 20: 505-592.*

Kijewski T., Kareem A., 2003. Wavelet transform for system identification in civil engineering, *Computer-Aided Civil and Infrastructure Engineering, vol. 18: 339-355.*

Kitada Y., 1998. Identification of nonlinear structural dynamic systems using wavelets, *Journal of Engineering Mechanics, vol. 124: 1059-1066.*

Kleinert H., 2009. *Path integrals in quantum mechanics, statistics, polymer physics, and financial market*, online version.

Koornwinder T. H., 1998. *Wavelets: An elementary treatment of theory and applications*, World Scientific.

Kougioumtzoglou I. A., 2009. *Response and first-passage statistics of nonlinear structural models under evolutionary stochastic loads*, M.Sc. Thesis, Department of Civil and Environmental Engineering, Rice University, Houston.

Kougioumtzoglou I. A., Spanos P. D., 2009. An approximate approach for nonlinear system response determination under evolutionary stochastic excitation, *Current Science, Indian Academy of Sciences, vol. 97: 1203-1211.*

Kovaleva A., 2009. An exact solution of the first-exit time problem for a class of structural systems, *doi:10.1016/j.probengmech.2009.01.002.*

Kree P., Soize C., 1986. *Mathematics of random phenomena: random vibrations of mechanical structures*, Kluwer Academic.

Krenk S., Roberts J. B., 1999. Local similarity in nonlinear random vibration, *Journal of Applied Mechanics, ASME, vol. 66: 225-235.*

Ktena A., Fotiadis D. I., Spanos P. D., Massalas C. V., 2001. A Preisach model identification procedure and simulation of hysteresis in ferromagnets and shape memory alloys, *Physica B, vol. 306: 84-90.*

Lam H. F., Ng C. T., 2008. A probabilistic method for the detection of obstructed cracks of beam-type structures using spatial wavelet transform, *Probabilistic Engineering Mechanics, vol. 23: 237-245.*

Lamarque C-H., Pernot S., Cuer A., 2000. Damping identification in multi-degree-of-freedom systems via a wavelet-logarithmic decrement - Part 1: Theory, *Journal of Sound and Vibration, vol. 235: 361-374.*

Langouche F., Roekaerts D., Tirapegui E., 1979. Functional integrals and the Fokker-Planck equation, *Il Nuovo Cimento, vol. 53B: 135-159.*

Li J., Chen J., 2009. *Stochastic dynamics of structures,* J. Wiley and Sons.

Liang J., Chaudhuri S. R., Shinozuka M., 2007. Simulation of non-stationary stochastic processes by spectral representation, *Journal of Engineering Mechanics, vol. 133: 616-627.*

Lin Y. K., 1967. *Probabilistic theory of structural dynamics.* New York: McGraw-Hill.

Lin Y. K., Cai G. Q., 1995. *Probabilistic structural dynamics: advanced theory and applications.* McGraw-Hill, New York.

Lin B. C., Tadjbakhsh I. G., Papageorgiu A. S., Ahmadi G., 1989. Response of base-isolated building to random excitations described by the Clough-Penzien spectral model, *Earthquake Engineering and Structural Dynamics, vol. 18: 49-62.*

Lin J., Zhang W., Williams F. W., 1994. Pseudo-excitation algorithm for nonstationary random seismic responses, *Engineering Structures, vol. 16: 270-276.*

Lin H., Yim S. C. S., 1996. Nonlinear rocking motions. II: Overturning under random excitations, *Journal of Engineering Mechanics, vol. 122: 728-735.*

Liu S. C., 1970. Evolutionary power spectral density of strong-motion earthquakes, *Bulletin of the Seismological Society of America, vol. 60: 891-900.*

Lu C. H., Evan-Iwanowski R. M., 1994. The nonstationary effects on a softening Duffing oscillator, *Mechanics Research Communications, vol. 21: 555-564.*

Lutes L. D., Sarkani S., 2004. *Random vibrations: analysis of structural and mechanical systems*, Elsevier.

Ma F., Zhang H., Bockstedte A., Foliente G. C., Paevere P., 2004. Parameter analysis of the differential model of hysteresis, *Journal of Applied Mechanics, vol. 71: 342-349.*

Macki J. W., Nistri P., Zecca P., 1993. Mathematical models for hysteresis, *SIAM Review, vol. 35: 94-123.*

Mallat S., 1989. A theory for multi-resolution signal decomposition: the wavelet representation, *I.E.E.E. Transactions on Pattern Analysis and Machine Intelligence, vol. 11: 674-693.*

Mallat S., 1999. *A wavelet tour of signal processing*, Academic Press, San Diego.

Mamontov E., Naess A., 2009. An analytical-numerical method for fast evaluation of probability densities for transient solutions of nonlinear Ito's stochastic differential equations, *International Journal of Engineering Science, vol. 47: 116-130.*

Mayergoyz I. D., 2003. *Mathematical models of hysteresis and their applications*, Elsevier.

Mayergoyz I. D., Dimian M., 2005. Stochastic aspects of hysteresis, *Journal of Physics: Conference Series, vol. 22: 139-147.*

McWilliam S., Knappett D. J., Fox C. H. J., 2000. Numerical solution of the stationary FPK equation using Shannon wavelets, *Journal of Sound and Vibration, vol. 232: 405-430.*

Miles R. N., 1989. An approximate solution for the spectral response of Duffing's oscillator with random input, *Journal of Sound and Vibration, 132: 43-49.*

Miles R. N., 1993. Spectral response of a bilinear oscillator, *Journal of Sound and Vibration, 163: 319-326.*

Miller L. A., 2005. Structural dynamics and resonance in plants with nonlinear stiffness, *Journal of Theoretical Biology, vol. 234: 511-524.*

Minko I. D. M., Bernard P., Fogli M., 2007. Asymptotic analysis of the random decrement, *Probabilistic Engineering Mechanics, vol. 22: 250-256.*

Muscolino G., Ricciardi G., Vasta M., 1997. Stationary and Non-Stationary probability density function for non-linear oscillators, *International Journal of Non-Linear Mechanics, vol. 32: 1051-1064.*

Mukherjee S., Gupta V.K., 2002. Wavelet-based generation of spectrum-compatible time-histories, *Soil Dynamics and Earthquake Engineering, vol. 22: 799-804.*

Naess A., Johnsen J. M., 1993. Response statistics of nonlinear, compliant offshore structures by the path integral solution method, *Probabilistic Engineering Mechanics, vol. 8: 91-106.*

Naess A., Moe V., 1996. Stationary and non-stationary random vibration of oscillators with bilinear hysteresis, *Int. J. Non-Linear Mech., 31: 553-562.*

Naess A., Moe V., 2000. Efficient path integration methods for nonlinear dynamic systems, *Probabilistic Engineering Mechanics, vol.15: 221-231.*

Naess A., Iourtchenko D., Batsevych O., 2010. Relability of systems with randomly varying parameters by the path integration method, *Probabilistic Engineering Mechanics, doi:10.1016/j.probengmech.2010.05.005.*

Nagarajaiah S., Basu B., 2010. Output only modal identification and structural damage detection using time frequency and wavelet techniques, *Earthquake Engineering and Engineering Vibration, vol. 8: 583-605.*

Nason G. P., von Sachs R., Kroisand G., 2000. Wavelet processes and adaptive estimation of evolutionary wavelet spectra, *Journal of the Royal Statistical Society, vol. 62: 271-292.*

Nason G. P., 2008. *Wavelet methods in statistics with R.*, Springer.

Nayfeh A. H., Sanchez N. E., 1989. Bifurcations in a forced softening Duffing oscillator, *Int. J. Non-Linear Mech., 24: 483-497.*

Newland D. E., 1993a. *An introduction to random vibrations, spectral and wavelet analysis*, 3rd Edition, Dover, New York.

Newland D. E., 1993b. Harmonic wavelet analysis, *Proceedings of the Royal Society of London A, vol. 443: 203-225.*

Newland D. E., 1994a. Wavelet analysis of vibration, Part I: Theory, *Journal of Vibration and Acoustics, vol. 116: 409-425.*

Newland D. E., 1994b. Harmonic and musical wavelets, *Proceedings of the Royal Society London A, vol. 444: 605-620.*

Newland D. E., 1997. Practical signal analysis: Do wavelets make any difference?, *Proceedings of 16th ASME Biennial Conference on Vibration and Noise, Sacramento.*

Newland D. E., 1999a. Ridge and phase identification in the frequency analysis of transient signals by harmonic wavelets, *Journal of Vibration and Acoustics, vol. 121: 149-155.*

Newland D. E., 1999b. Harmonic wavelets in vibrations and acoustics, *Philosophical Transactions of the Royal Society of London, vol. 357: 2607-2625.*

Newland D. E., Butler G. D., 2000. Application of time-frequency analysis to transient data from centrifuge earthquake testing, *Shock and Vibration, vol. 7: 195-202.*

Ni Y. Q., Ying Z. G., Ko J. M., 2002. Random response analysis of Preisach hysteretic systems with symmetric weight distribution, *Journal of Applied Mechanics, vol. 69: 171-178.*

Nigam, N. C., 1983. *Introduction to Random Vibrations.* MIT Press Series in Structural Mechanics.

Nocedal J., Wright S. J., 2006. *Numerical Optimization*, New York, Springer.

Noori M., Dimentberg M., Hou Z., Christodoulidou R., Alexandrou A., 1995. First-passage study and stationary response analysis of a BWB hysteresis model using quasi-conservative stochastic averaging method, *Probabilistic Engineering Mechanics, vol. 10: 161-170.*

Nowak R. D., 2002. Nonlinear system identification, *Circuits systems signal processing, vol. 21: 109-122.*

Oksendal B., 2003. *Stochastic Differential Equations: An Introduction with Applications,* Springer, 6th edition.

Olsen A. I., Naess A., 2007. An importance sampling procedure for estimating failure probabilities of non-linear dynamic systems subjected to random noise, *International Journal of Non-Linear Mechanics, 42: 848-863.*

Ombao H., Raz J., von Sachs R., Guo W., 2002. The SLEX model of a non-stationary random process, *Annals of the Institute of Statistical Mathematics, vol. 54: 171-200.*

Onsager L., Machlup S., 1953. Fluctuations and irreversible processes, *Physical Review, vol. 91: 1505-1515.*

Paneer Selvam R., Bhattacharyya S. K., 2006. System identification of a coupled two DOF moored floating body in random ocean waves, *Journal of Offshore Mechanics and Arctic Engineering, vol. 128: 191-202.*

Park Y. J., 1992. Equivalent linearization for seismic responses. I: Formulation and error analysis, *Journal of Engineering Mechanics, vol. 118: 2207-2226.*

Pei J. S., Smyth A. W., Kosmatopoulos E. B., 2004. Analysis and modification of Volterra/Wiener neural networks for the adaptive identification of nonlinear hysteretic dynamic systems, *Journal of Sound and Vibration, vol. 275: 693-718.*

Phoon K. K., Huang S. P., Quek S. T., 2002. Implementation of Karhunen-Loeve expansion for simulation using a wavelet-Galerkin scheme, *Probabilistic Engineering Mechanics, vol. 17: 293-303.*

Pichler L., Pradlwarter H. J., 2008. Evolution of probability densities in the phase space for reliability analysis of nonlinear structures, *doi:10.1016/j.strusafe.2008.09.002.*

Pierson W. J., Moskowitz L., 1964. A proposed spectral form for fully developed wind seas based on the similarity theory of S. A. Kitaigorodskii, *Journal of Geophysical Research, vol. 69: 5181-5190.*

Pires J. A., 1996. Stochastic seismic response analysis of soft soil sites, *Nuclear Engineering and Design, vol. 160: 363-377.*

Pirrotta A., Santoro R., 2010. Probabilistic response of nonlinear systems under combined normal and Poisson white noise via path integral method, *Probabilistic Engineering Mechanics, doi:10.1016/j.probengmech.2010.06.003.*

Preumont A., 1994. *Random vibration and spectral analysis*, Kluwer Academic.

Priestley M. B., 1965. Evolutionary spectra and non-stationary processes, *Journal of the Royal Statistical Society, vol. 27: 204-237.*

Priestley M. B., 1967. Power spectral analysis of non-stationary random processes, *Journal of Sound and Vibration, vol. 6: 86-97.*

Priestley M. B., 1988. *Non-linear and non-stationary time series analysis,* Academic Press, San Diego.

Priestley M. B., 1996. Wavelets and time-dependent spectral analysis, *Journal of time series analysis, vol. 17: 85-103.*

Priestley M. B., Tong H., 1973. On the analysis of bivariate non-stationary processes, *Royal Statistical Society, vol. 35: 153-166.*

Proppe C., Pradlwarter H.J., Schueller G. I., 2003. "Equivalent linearization and Monte Carlo simulation in stochastic dynamics", *Probabilistic Engineering Mechanics, vol. 18: 1-15.*

Qian S., 2002. *Introduction to time-frequency and wavelet transforms*, Prentice Hall, New Jersey.

Radunovic D. P., 2009. *Wavelets: from math to practice*, Springer.

Rahrooh A., Shepard S., 2009. Identification of nonlinear systems using NARMAX model, *Nonlinear Analysis, doi:10.1016/j.na.2009.01.150.*

Raman S., Yim S. C. S., Palo P. A., 2005. Nonlinear model for sub- and super-harmonic motions of a MDOF moored structure, Part 1 – System identification, *Journal of Offshore Mechanics and Arctic Engineering, vol. 127: 283-290.*

Reinhall P. G., Miles R. N., 1989. Effect of damping and stiffness on the random vibration of nonlinear periodic plates, *Journal of Sound and Vibration, 132: 33-42.*

Rice S. O., 1944. *Mathematical analysis of random noise*, Bell Syst. Tech. J. 23: 282-332; 24: 46-156. Reprinted in *Selected Papers on Noise and Stochastic Processes*, N. Wax, ed. 1954. New York, Dover: 133-249.

Rice H. J., Fitzpatrick J. A., 1988. A generalized technique for spectral analysis of nonlinear systems, *Mechanical Systems and Signal Processing, vol. 2: 195-207.*

Risken H., 1984. *The Fokker-Planck Equation, Methods of solution and Applications*, Springer-Verlag.

Roberts J. B., Spanos P. D., 1986. Stochastic Averaging: An Approximate Method of Solving Random Vibration Problems, *International Journal of Non-Linear Mechanics, vol. 21: 111-134.*

Roberts J. B., 1986a. Response of an oscillator with nonlinear damping and a softening spring to non-white excitation, *Probabilistic Engineering Mechanics, 1: 40-48.*

Roberts J. B., 1986b. First-Passage probabilities for randomly excited systems: Diffusion Methods, *Probabilistic Engineering Mechanics, 1: 66-81.*

Roberts J. B., Vasta M., 2000. Markov modeling and stochastic identification for nonlinear ship rolling in random waves, *Phil. Trans. R. Soc. Lond. A, vol. 358: 1917-1941.*

Roberts J. B., Spanos P. D., 2003. *Random Vibration and Statistical Linearization.* New York: Dover Publications.

Robson J. D., 1963. *An introduction to random vibration.* Edinburgh: University Press.

Rocandelli M., 1989. Langevin formulation of quantum mechanics, *Il Nuovo Cimento, vol. 11: 73-99.*

Roy R. V., 1997. Asymptotic analysis of first-passage problems, *International Journal of Non-Linear Mechanics, 32: 173-186.*

Rubinstein R. Y., 1981. *Simulation and the Monte Carlo method*, Wiley.

Rubinstein R. Y., Kroese D. P., 2008. *Simulation and the Monte Carlo method*, Wiley.

Rubino G., Tuffin B. (eds), 2009. *Rare event simulation using Monte Carlo methods*, J. Wiley and Sons.

Rucka M., Wilde K., 2006. Application of continuous wavelet transform in vibration based damage detection method for beams and plates, *Journal of Sound and Vibration, vol. 297: 536-550.*

Rudinger F., Krenk S., 2003a. Spectral density of oscillator with bilinear stiffness and white noise excitation, *Probabilistic Engineering Mechanics, 18: 215-222.*

Rudinger F., Krenk S., 2003b. Spectral density of an oscillator with power law damping excited by white noise, *Journal of Sound and Vibration, 261: 365-371.*

Rugh W. J., 1981. *Nonlinear system theory: The Volterra/Wiener approach*, The John Hopkins University Press, Baltimore, MD.

Schenk C. A., Pradlwarter H. J., Schueller G. I., 2005. Non-stationary response of large, non-linear finite element systems under stochastic loading, *Computers and Structures, vol. 83: 1086-1102.*

Schetzen M., 1980. *The Volterra and Wiener theories of nonlinear systems*, John Wiley and Sons.

Schueller G. I., Pandey M. D., Pradlwarter H. J., 1994. Equivalent linearization (EQL) in engineering practice for aseismic design, *Probabilistic Engineering Mechanics, vol. 9: 95-102.*

Schueller G. I. (ed.), 1997. A state-of-the-art report on computational stochastic mechanics, *Probabilistic Engineering Mechanics, vol. 12: 197-321.*

Schueller G. I., Spanos P. D. (eds), 2000. Monte Carlo simulation: proceedings of the International Conference on Monte Carlo simulation, Principality of Monaco.

Schulman L. S., 1981. *Techniques and applications of path integration*, Wiley, New York.

Senjanovic I., Cipric G., Parunov J., 2000. Survival analysis of fishing vessels rolling in rough seas, *Phil. Trans. R. Soc. Lond. A, vol. 358: 1943-1965.*

Sesselberg M., Petruccione F., 1993. An improved algorithm for the estimation of the mean first-passage time of ordinary stochastic differential equations, *Computer Physics Communications, vol. 74: 247-255.*

Shinozuka M., Jan C. M., 1972. Digital simulation of random processes and its applications, *Journal of Sound and Vibration, 25: 111-128.*

Shinozuka M., Deodatis G., 1988. Stochastic process models for earthquake ground motion, *Probabilistic Engineering Mechanics, vol. 3: 114-123.*

Shinozuka M., Deodatis G., 1991. Simulation of stochastic processes by spectral representation, *Applied Mechanics Reviews, vol. 44, no4: 191-203.*

Shinozuka M., Deodatis G., 1996. Simulation of multi-dimensional Gaussian fields by spectral representation, *Applied Mechanics Reviews, vol. 49, no1: 29-53.*

Smyth A.W., Masri S. F., 2002. Non-stationary response of nonlinear systems using equivalent linearization with a compact analytical form of the excitation process, *Probabilistic Engineering Mechanics, vol. 17: 97-108.*

Socha L., 2005. Linearization in analysis of nonlinear stochastic systems: Recent results-Part I: Theory, *Applied Mechanics Reviews, 58: 178-205.*

Socha L., 2008. *Linearization methods for stochastic dynamic systems*, Lecture Notes in Physics, 730, Springer.

Soize C., 1995. Stochastic linearization method with random parameters for SDOF nonlinear dynamical systems: prediction and identification procedures, *Probabilistic Engineering Mechanics, 10: 143-152.*

Solnes J., 1997. *Stochastic processes and random vibrations: theory and engineering applications*, J. Wiley and Sons.

Sone A., Hata H., Masuda A., 2004. Identification of structural parameters using the wavelet transform of acceleration measurements, *Journal of Pressure Vessel Technology, vol. 126: 128-133.*

Song J., Der Kiureghian A., 2006. Generalized Bouc-Wen model for highly asymmetric hysteresis, *Journal of engineering mechanics, vol. 132: 610-618.*

Soong T. T., 1973. *Random Differential Equations in Science and Engineering*, Academic Press New York and London.

Soong T. T., Grigoriu M., 1993. *Random Vibration of Mechanical and Structural Systems*, Prentice Hall, New Jersey.

Spanos P. D., Chen T. W., 1980. Response of a dynamic system to flow-induced load, *International Journal of Non-Linear Mechanics, vol. 15: 115-116.*

Spanos P. D., Lutes L. D., 1980. Probability of response to evolutionary process, *Journal of Engineering Mechanics, vol. 106: 213-224.*

Spanos P. D., Solomos G. P., 1983. Markov approximation to transient vibration, *Journal of Engineering Mechanics, vol. 109: 1134-1150.*

Spanos P. D., 1983. ARMA algorithms for ocean wave modeling, *Journal of Energy Resources Technology, vol. 105: 300-309.*

Spanos P. D., Mignolet M. P., 1986. Z-transform modeling of p-m wave spectrum, *Journal of Engineering Mechanics, vol. 112: 745-759.*

Spanos P. D., Donley M., Roesset J., 1987. Evolutionary power spectrum estimation of September 19, 1985 Mexico earthquake accelerograms, *Proceedings of the U. S. – Japan Seminar on Stochastic Approaches in Earthquake Engineering, Boca Raton, FL, Springer-Verlag, vol. 32: 322-333.*

Spanos P. D., Lu R., 1995. Nonlinear system identification in offshore structural reliability, *Journal of Offshore Mechanics and Arctic Engineering, vol. 117: 171-177.*

Spanos P. D., Zeldin B. A., 1998. Monte Carlo treatment of random fields: A broad perspective, *Applied Mechanics Reviews, vol. 51, no3: 219-237.*

Spanos P. D., Di Paola M., Failla G., 2002. A Galerkin approach for power spectrum determination of nonlinear oscillators, *Meccanica, vol. 37: 51-65.*

Spanos P.D., Cacciola P., Muscolino G., 2004a. Stochastic averaging of Preisach hysteretic systems, *Journal of Engineering Mechanics, vol. 130: 1257-1267.*

Spanos P. D., Cacciola P., Red-Horse J., 2004b. Random vibration of SMA systems via Preisach formalism, *Nonlinear Dynamics, vol. 36: 405-419.*

Spanos P. D., Failla G., 2004. Evolutionary spectra estimation using wavelets, *Journal of Engineering Mechanics, vol. 130, 952-960.*

Spanos P. D., Tezcan J., Tratskas P., 2005. Stochastic processes evolutionary spectrum estimation via harmonic wavelets, *Computer Methods in Applied Mechanics and Engineering, vol. 194: 1367-1383.*

Spanos P. D., Failla G., 2005. Wavelets: Theoretical concepts and vibrations related applications, *The Shock and Vibration Digest, vol. 37: 359-375.*

Spanos P. D., Failla G., Santini A., Pappatico M., 2006. Damage detection in Euler-Bernoulli beams via spatial wavelet analysis, *Structural Control and Health Monitoring, vol. 13: 472-487.*

Spanos P. D., Sofi A., Di Paola M., 2007. Non-stationary response envelope probability densities of nonlinear oscillators, *Journal of Applied Mechanics, vol. 74: 315-324.*

Spanos P. D., Kougioumtzoglou I. A., Soize C., 2011. On the determination of the power spectrum of randomly excited oscillators via stochastic averaging: An alternative perspective, *Probabilistic Engineering Mechanics, vol. 26: 10-15.*

Spyrou K. J., Thomson J. M. T., 2000. The nonlinear dynamics of ship motions: a field overview and some recent developments, *Phil. Trans. R. Soc. Lond. A, vol. 358: 1735-1760.*

Staszewski W. J., 1998. Identification of nonlinear systems using multi-scale ridges and skeletons of the wavelet transform, *Journal of Sound and Vibration, vol. 214: 639-658.*

Stratonovich R. L., 1971. *Sel. Transl. Math. Stat. Prob.* vol. 10: 273.

Sun W. J., Kareem A., 1989. Response of MDOF systems to nonstationary random excitation, *Engineering Structures, vol. 11: 83-91.*

Surendran S., Lee S. K., Sohn K. H., 2007. Simplified model for predicting the onset of parametric rolling, *Ocean Engineering, vol. 34: 630-637.*

Szemplinska – Stupnicka W., 1988. Bifurcations of harmonic solution leading to chaotic motion in the softening type Duffing oscillator, *Int. J. Non-Linear Mech., 23: 257-277.*

Ta M-N., Lardies J., 2006. Identification of weak nonlinearities on damping and stiffness by the continuous wavelet transform, *Journal of Sound and Vibration, vol. 293: 16-37.*

Tajimi H., 1960. A statistical method for determining the maximum response of a building structure during an earthquake, *Proceedings of the 2nd World Conference on Earthquake Engineering, Tokyo and Kyoto, Japan.*

Taylan M., 1999. Solution of the nonlinear roll model by a generalized asymptotic method, *Ocean Engineering, vol. 26: 1169-1181.*

Taylan M., 2000. The effect of nonlinear damping and restoring in ship rolling, *Ocean Engineering, vol. 27: 921-932.*

Tisza L., Manning I., 1957. Fluctuations and irreversible processes, *Physical Review, vol. 105: 1695-1705.*

To C. W. S., 2000. *Nonlinear Random Vibration, Analytical Techniques and Applications*, Swets & Zeitlinger B. V., Lisse the Netherlands.

To C. W. S., Chen Z., 2008. First-passage time of nonlinear ship rolling in narrow band non-stationary random seas, *Journal of Sound and Vibration, vol. 309: 197-209.*

Tootkaboni M., Graham-Brady L., 2010. Stochastic direct integration schemes for dynamic systems subjected to random excitations, *Probabilistic Engineering Mechanics, vol. 25: 163-171.*

Tratskas P., Spanos P. D., 2003. Linear multi-degree-of-freedom system stochastic response by using the harmonic wavelet transform, *Journal of Applied Mechanics, vol. 70: 724-731.*

Triantafyllopoulos K., Nason G. P., 2009. A note on state space representations of locally stationary wavelet time series, *Statistics and Probability Letters, vol. 79: 50-54.*

Trifunac M. D., 1971. Response envelope spectrum and interpretation of strong earthquake ground motion, *Bulletin of the Seismological Society of America, vol. 61: 343-356.*

Vidakovic B., 1999. *Statistical modeling by wavelets*, Wiley.

Virgin L., Cartee L. A., 1991. A note on the escape from a potential well, *Int. J. Non-Linear Mech., 26: 449-452.*

Von Wagner U., 2004. Nonlinear longitudinal vibrations of non-slender piezoceramic rods, *International Journal of Non-Linear Mechanics, vol. 39: 673-688.*

Wang Y., Ying Z. G., Zhu W. Q., 2009a. Stochastic averaging of energy envelope of Preisach hysteretic systems, *Journal of Sound and Vibration, 321: 976-993.*

Wang Y., Ying Z. G., Zhu W. Q., 2009b. Nonlinear stochastic optimal control of Preisach hysteretic systems, *Probabilistic Engineering Mechanics, vol. 24: 255-264.*

Wehner M. F., Wolfer W. G., 1983a. Numerical evaluation of path-integral solutions to Fokker-Planck equations, *Physical Review A, vol. 27: 2663-2670.*

Wehner M. F., Wolfer W. G., 1983b. Numerical evaluation of path-integral solutions to Fokker-Planck equations. II. Restricted stochastic processes, *Physical Review A, vol. 28: 3003-3011.*

Wehner M. F., Wolfer W. G., 1987. Numerical evaluation of path-integral solutions to Fokker-Planck equations. III. Time and functionally dependent coefficients, *Physical Review A, vol. 35: 1795-1801.*

Welch P.D, 1967. The Use of Fast Fourier Transform for the Estimation of Power Spectra: A Method Based on Time Averaging Over Short, Modified Periodograms, *IEEE Trans. Audio Electroacoustics, vol. AU-15: 70-73.*

Wen Y. K., 1976. Method for random vibration of hysteretic systems, *Journal of the Engineering Mechanics Division, vol. 102: 249-263.*

Wen Y. K., 1980. Equivalent linearization for hysteretic systems under random excitation, *Journal of Applied Mechanics, vol. 47: 150-154.*

Wen Y. K., 1986. Stochastic response and damage analysis of inelastic structures, *Probabilistic Engineering Mechanics, vol. 1: 49-57.*

Wen Y. K., 1989. Methods of random vibration for inelastic structures, *Applied Mechanics Reviews, vol. 42: 39-52.*

Wen Y. K., Eliopoulos D., 1994. Method for non-stationary random vibration of inelastic structures, *Probabilistic Engineering Mechanics, vol. 9: 115-123.*

Wiegel F. W., 1975. Path integral methods in statistical mechanics, *Physics Reports, vol. 16: 57-114.*

Wiener N., 1930. Generalized harmonic analysis, *Acta Mathematica, vol. 55: 117-258.*

Wolf J. P., Skrikerud P. E., 1980. Mutual pounding of adjacent structures during earthquakes, *Nuclear Engineering and Design, vol. 57: 253-275.*

Xie W. X., Xu W., Cai L., Path integration of the Duffing-Rayleigh oscillator subject to harmonic and stochastic excitations, *Applied Mathematics and Computation, vol. 171: 870-884.*

Yang C. Y., Cheng A. H-D., Roy R. V., 1991. Chaotic and stochastic dynamics for a nonlinear structural system with hysteresis and degradation, *Probabilistic Engineering Mechanics, vol. 6: 193-203*

Young R. K., 1993. *Wavelet theory and its applications*, Kluwer Academic.

Yu J. S., Cai G. Q., Lin Y. K., 1997. A new path integration procedure based on Gauss-Legendre scheme, *Int. J. Non-Linear Mech., 32: 759-768.*

Yu Y., Shenoi R. A., Zhu H., Xia L., 2006. Using wavelet transforms to analyze nonlinear ship rolling and heave-roll coupling, *Ocean Engineering, vol. 33: 912-926.*

Zembaty Z., 1988. A note on non-stationary stochastic response and strong motion duration, *Earthquake Engineering and Structural Dynamics, vol. 16: 1189-1200.*

Zhu W. Q., 1988. Stochastic averaging methods in random vibration, *Applied Mechanics Reviews, vol. 41: 189-199.*

Zhu W. Q., 1996. Recent developments and applications of the stochastic averaging method in random vibration, *Applied Mechanics Reviews, vol. 49: 72-80.*